TECHNISCHE UNIVERSITÄT
BERGAKADEMIE FREIBERG
The University of Resources. Since 1765.

A Theory for the Homogenisation Towards Micromorphic Media and its Application to Size Effects and Damage

By the Faculty of Mechanical, Process and Energy Engineering
of the Technische Universität Bergakademie Freiberg

approved

Thesis

to attain the academic degree of

habilitierter Doktor-Ingenieur
(Dr.-Ing. habil.)

submitted by **Dr.-Ing. Geralf Hütter**

born on the December 10, 1984 in Dresden

Submitted at: January 16, 2018

Assessors: Prof. Dr. Ing. Samuel Forest
Prof. Dipl.-Ing. Björn Kiefer, Ph.D.
Prof. Dr.-Ing. habil. Paul Steinmann

Date of the award: Freiberg, February 12, 2019

Abstract

The classical Cauchy-Boltzmann theory of continuum mechanics requires that the dimension, over which macroscopic gradients occur, are much larger than characteristic length scales of the microstructure. For this reason, the classical continuum theory comes to its limits for very small specimens or if material degradation leads to a localisation of deformations into bands, whose width is determined by the microstructure itself. Deviations from the predictions of the classical theory of continuum mechanics are referred to as size effects.

It is well-known, that generalised continuum theories can describe size effects in principle. Especially micromorphic theories gain increasing popularity due its favorable numerical implementation. However, the formulation of the additionally necessary constitutive equations is a problem. For linear-elastic behavior, the number of material parameters increases considerably compared to the classical theory. The experimental determination of these parameters is thus very difficult. For nonlinear and history-dependent processes, even the qualitative structure of the constitutive equations can hardly be assessed solely on base of phenomenological considerations. Homogenisation methods are a promising approach to solve this problem.

The present thesis starts with a critical review on the classical theory of homogenisation and the approaches on micromorphic homogenisation which are available in literature. On this basis, a theory is developed for the homogenisation of a classical Cauchy-Boltzmann continuum at the microscale towards a micromorphic continuum at the macroscale. In particular, the micro-macro-relations are specified for all macroscopic kinetic and kinematic field quantities. On the microscale, the corresponding boundary-value problem is formulated, whereby kinematic, static or periodic boundary conditions can be used. No restrictions are imposed on the material behavior, i. e. it can be linear or nonlinear. The special cases of the micropolar theory (Cosserat theory), microstrain theory and microdilatational theorie are considered.

The proposed homogenisation method is demonstrated for several examples. The simplest example is the uniaxial case, for which the exact solution can be specified. Furthermore, the micromorphic elastic properties of a porous, foam-like material are estimated in closed form by means of Ritz' method with a cubic ansatz. A comparison with partly available exact solutions and FEM solutions indicates a qualitative and quantitative agreement of sufficient accuracy. For the special cases of micropolar and microdilatational theory, the material parameters are specified in the established nomenclature from literature. By means of these material parameters the size effect of an elastic foam structure is investigated and compared with corresponding results from literature.

Furthermore, micromorphic damage models for quasi-brittle and ductile failure are presented. Quasi-brittle damage is modelled by propagation of microcracks. For the ductile mechanism, Gurson's limit-load approach on the microscale is extended by microdilatational terms. A finite-element implementation shows, that the damage model exhibits h-convergence even in the softening regime and that it thus can describe localisation.

Zusammenfassung

Die klassische Cauchy-Boltzmann-Kontinuumstheorie setzt voraus, dass die Abmessungen, über denen makroskopische Gradienten auftreten, sehr viele größer sind als charakteristische Längenskalen der Mikrostruktur. Aus diesem Grund stößt die klassische Kontinuumstheorie bei sehr kleinen Proben ebenso an ihre Grenzen wie bei Schädigungsvorgängen, bei denen die Deformationen in Bändern lokalisieren, deren Breite selbst von der Längenskalen der Mikrostruktur bestimmt wird. Abweichungen von Vorhersagen der klassischen Kontinuumstheorie werden als Größeneffekte bezeichnet.

Es ist bekannt, dass generalisierte Kontinuumstheorien Größeneffekte prinzipiell beschreiben können. Insbesondere mikromorphe Theorien erfreuen sich auf Grund ihrer vergleichsweise einfachen numerischen Implementierung wachsender Beliebtheit. Ein großes Problem stellt dabei die Formulierung der zusätzlich notwendigen konstitutiven Gleichungen dar. Für linear-elastisches Verhalten steigt die Zahl der Materialparameter im Vergleich zur klassischen Theorie stark an, was deren experimentelle Bestimmung sehr schwierig macht. Bei nichtlinearen und lastgeschichtsabhängigen Prozessen lässt sich selbst die qualitative Struktur der konstitutiven Gleichungen ausschließlich auf Basis phänomenologischer Überlegungen kaum erschließen. Homogenisierungsverfahren stellen einen vielversprechenden Ansatz dar, um dieses Problem zu lösen.

Die vorliegende Arbeit gibt zunächst einen kritischen Überblick über die klassische Theorie der Homogenisierung sowie die im Schriftum verfügbaren Ansätze zur mikromorphen Homogenisierung. Auf dieser Basis wird eine Theorie zur Homogenisierung eines klassischen Cauchy-Boltzmann-Kontinuums auf Mikroebene zu einem mikromorphen Kontinuum auf der Makroebene entwickelt. Insbesondere werden Mikro-Makro-Relationen für alle makroskopischen kinetischen und kinematischen Feldgrößen angegebenen. Auf der Mikroebene wird das entsprechende Randwertproblem formuliert, wobei kinematische, statische oder periodische Randbedingungen verwendet werden können. Das Materialverhalten unterliegt keinen Einschränkungen, d. h., dass es sowohl linear als auch nichtlinear sein kann. Die Sonderfälle der mikropolaren Theorie (Cosserat-Theorie), Mikrodehnungstheorie und mikrodilatationalen Theorie werden erarbeitet.

Das vorgeschlagene Homogenisierungsverfahren wird für eine Reihe von Beispielen demonstriert. Als einfachstes Beispiel dient der einachsige Fall, für den die exakte Lösung angegebenen werden kann. Weiterhin werden die mikromorphen, elastischen Eigenschaften eines porösen, schaumartigen Materials mittels des Ritz-Verfahrens mit einem kubischen Ansatz in geschlossener Form abgeschätzt. Ein Vergleich mit teilweise verfügbaren exakten Lösungen sowie FEM-Lösungen weist eine qualitative und quantitative Übereinstimmung hinreichender Genauigkeit aus. Für die Sonderfälle mikropolaren und mikrodilatationalen Theorien werden die Materialparameter in der im Schriftum üblichen Nomenklatur angegebenen. Mittels dieser Materialparameter wird der Größeneffekt in einer elastischen Schaumstruktur untersucht und mit entsprechenden Ergebnissen aus dem Schrifttum verglichen.

Desweiteren werden mikromorphe Schädigungsmodelle für quasi-sprödes und duktiles Versagen vorgestellt. Quasi-spröde Schädigung wird durch das Wachstum von Mikrorissen modelliert. Für den duktilen Mechanismus wird der Ansatz von Gurson einer Grenzlastanalyse auf Mikroebene um mikrodilatationale Terme erweitert. Eine Finite-Elemente-Implementierung zeigt, dass das Schädigungsmodell auch im Entfestigungsbereich h-Konvergenz aufweist und die Lokalisierung beschreiben kann.

Preface

The research presented within this thesis was carried out during my time at the Chair of Applied Mechanics – Solid Mechanics at the TU Bergakademie Freiberg from 2013 until 2017 and was partly published in journal articles [1–4]. First of all, I would like to thank Prof. Dr. rer. nat. habil. Meinhard Kuna and Prof. Dipl.-Ing. Björn Kiefer, Ph. D., for granting the freedom to work at this personal research project and for encouraging me taking steps towards my individual development in research and teaching. All colleagues at the chair contributed to an inspiring atmosphere. In particular, I am deeply indebted to Dr.-Ing. Stephan Roth for the common efforts on the efficient implementation and usage of user-defined finite elements of in Abaqus for coupled problems.

My first contact with the micromorphic theory was a plenary lecture “Mechanics of Generalized Continua and Heterogeneous Materials” held by Prof. Samuel Forest at the GAMM conference 2010 in Karlsruhe. This illustrative lecture motivated me to study this theory in detail. I am also very grateful to Dr.-Ing. Jörg Brummund who was always available for helpful discussions on any kinds of fundamentals of mechanics. In addition, I like to acknowledge the commitment of the students Rostyslav Skrypnyk and Vincent von Oertzen who supported my research as student assistants. Furthermore, I am very grateful to the reviewers of this thesis for spending their time on it. Finally, I would like to thank my family for their support, in particular my wife Sylvia.

Contents

1. Introduction

Classical theories of continuum mechanics can only be applied when the macroscopic wavelengths of relevant field quantities are much larger than the characteristic microstructural dimensions, a limitation manifested already in the lack of an intrinsic length scale in such continuum theories. However, in many engineering problems this condition is not fulfilled, e. g. for micro and nanodevices or at a crack tip, see Fig. 1.1. Material degradation due to damage mechanisms finally leads to a localization of the deformations in narrow bands. In reality, the width of such bands is determined by length scales of the microstructure like the distance of voids, grains or atomic defects. Classical continuum theories do not possess an internal length scale and can thus not describe such localization phenomena adequately. Corresponding finite element simulations exhibit a spurious mesh dependency.

In principle, generalized continuum theories can overcome these limitations. Among the generalized theories of continuum mechanics, micromorphic theory of Eringen and Mindlin [7–10] has an outstanding role since it incorporates many others like the Cosserat theory or strain gradient theory as special cases. For a recent review and a comprehensive classification the reader is referred to [11, 12]. Phenomenologically, it is well-established how such theories can be constructed based on macroscopic thermodynamic considerations and/or the principle of virtual powers. Thereby, additional, generalized stresses occur which appear in additional balance equations [8, 13–16]. This requires to formulate respective additional constitutive relations and to identify the corresponding constitutive parameters.

For linear-elastic behavior of isotropic material, the limited number of additional material parameters may be determined by regression of size effects in real or numerical experiments. This method has been successfully applied in particular for the Cosserat theory which possesses four non-classical parameters, see e. g. [5, 17–30]. However, Lakes [20] argued that this method can hardly be adopted to other micromorphic theories with more non-classical parameters.

Also highly non-linear and history-dependent classical constitutive laws were generalized heuristically by linear and reversible approaches for the generalized stress measures (i. e. quadratic ansatzes in the thermodynamic potentials) for simplicity, e. g. [14, 15]. This applies in particular to damage models and phase field models. Though, this approach is questionable as argued recently in [31, 32]. In particular, the formulation and interpretation of the additionally necessary boundary conditions is problematic. Ehlers and Volk [33] incorporated non-classical stress measures heuristically also in the yield condition.

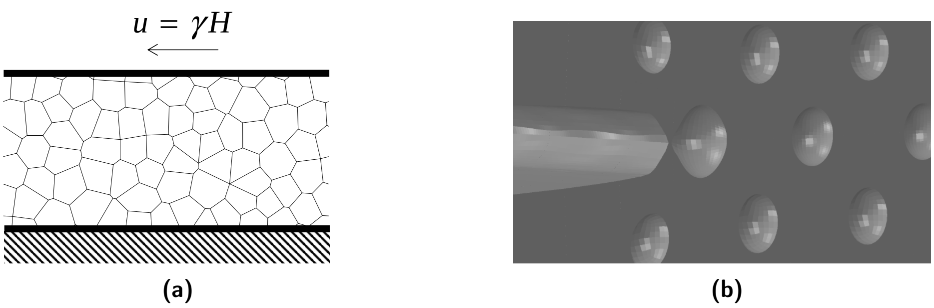

Fig. 1.1.: Gradients over microstructure dimensions: (a) shearing of thin layer of foam (from [5]), (b) void growth at a crack tip (from [6])

Homogenisation of the heterogeneous microstructure offers a solution to this problem. Regarding classical continuum mechanics, the homogenisation procedure, whereby the macroscopic stresses and strains are defined as the volume averages of their microscopic counterparts and can be prescribed via corresponding boundary conditions at the microscale, is established already for decades [34, 35]. For the so-called couple stress theory (constrained Cosserat theory) the additional boundary conditions of bending-type were specified more or less intuitively as well [36, 37], in particular if the continuum theory at the microscale has rotational degrees of freedom [27, 38–43] as it is the case for plates, beams and rigid particles. Independent of each other, Gologanu et al. [44] and Kouznetsova et al. [45] proposed theories for the homogenisation of a Cauchy-Boltzmann continuum at the microscale towards a strain gradient continuum at the macroscale. These authors extended Hill's kinematic boundary conditions by additional quadratic terms and derived a suitable micro-macro relation for the corresponding double stress.

However, for the homogenisation from a Cauchy continuum at the microscale towards an unconstrained micromorphic continuum at the macroscale the definition of the macroscopic quantities and the formulation of respective boundary conditions at the microscale turned out to be problematic. Eringen [7, 8] derived the governing macroscopic balance equations via a spatial averaging procedure. Unfortunately, Eringen did neither formulate kinematic relations between microscopic and macroscopic kinematic quantities nor did he formulate a boundary-value problem at the microscale. Forest and Sab [46, 47] provided explicit integral expressions for the relations between microscopic and macroscopic kinematic quantities of micromorphic theories. However, it turned out to be a problem that the expressions for the generalized deformation measures could not be transformed to surface integrals and thus, in contrast to classical homogenisation, not be prescribed by boundary conditions at the microscale. For this reason polynomial expressions were identified according to several strategies that fulfill the integral expressions identically and attempts were made to characterize additional "fluctuation" fields [47–50]. The drawback of this approach is that no boundary value problem could strictly be formulated at the microscale.

The scope of the present thesis is to formulate a consistent theory for the homogenisation of a Cauchy-Boltzmann continuum at the microscale towards a micromorphic continuum at the macroscale and to demonstrate it for certain examples.

The present works is organized as follows: Section 2 reviews in detail both Hill's classical theory of homogenisation as well as the aforementioned approaches to extend it towards strain gradient and micromorphic theories. Section 3 presents an approach to formulate kinetic and kinematic micro-macro relations of an unconstrained micromorphic theory. A boundary-value problem is formulated at the microscale whose solution yields the micromorphic constitutive relation for the macroscale. This boundary value problem is solved exactly and approximately in Section 4 for linear-elastic material. Section (5) is dedicated to the development and application of constitutive models for quasi-brittle and ductile damage within the micromorphic framework. Finally, certain general aspects of the micromorphic theory of homogenisation are discussed in Section 6 before Section 7 closes with a summary.

The notation within the present contribution is adopted from Forest and Sab [47], i. e. scalars, vectors and tensors of second, third and forth order are denoted by a, $\underline{\mathbf{b}}$, $\underset{\sim}{\mathbf{c}}$, $\underset{\sim}{\underline{\mathbf{d}}}$ and $\underset{\approx}{\mathbf{e}}$, respectively. Single, double and threefold contractions are written as $\cdot$, $:$ and $\vdots$, respectively, and are computed from left to right, i. e. $\underset{\sim}{\underline{\mathbf{d}}} \vdots \underset{\sim}{\underline{\mathbf{e}}} = d_{ijk}e_{ijk}$. In particular, $\underset{\sim}{\mathbf{I}}$ and $\underset{\sim}{\epsilon}$ denote the second order identity tensor and the permutation tensor, respectively. The operator $((\circ))^{\mathrm{T}}$ denotes the complete transposition of all indices of a tensor. For a second order tensor this is done by the forth order transposing tensor $\underset{\approx}{\mathbf{I}}_{\mathrm{T}}$ as $\underset{\sim}{\mathbf{c}}^{\mathrm{T}} = \underset{\approx}{\mathbf{I}}_{\mathrm{T}} : \underset{\sim}{\mathbf{c}}$. Analogously, a symmetrization tensor $\underset{\approx}{\mathbf{I}}_{\mathrm{S}}$ is introduced as $\operatorname{sym} \underset{\sim}{\mathbf{c}} = \frac{1}{2}(\underset{\sim}{\mathbf{c}} + \underset{\sim}{\mathbf{c}}^{\mathrm{T}}) = \underset{\approx}{\mathbf{I}}_{\mathrm{S}} : \underset{\sim}{\mathbf{c}}$. The symbols $\underline{\mathbf{x}}$ and $\underline{\mathbf{X}}$ refer to the location vectors at the microscale and macroscale, respectively. The nabla operator is $\underline{\nabla}$ whose subscript ($\underline{\nabla}_{\underline{\mathbf{X}}}$ or $\underline{\nabla}_{\underline{\mathbf{x}}}$) specifies, whether it is computed with respect to $\underline{\mathbf{X}}$ or $\underline{\mathbf{x}}$. The material time derivate is denoted by a dot $(\dot{(\circ)})$.

2. Literature review: Micromorphic theory and strain-gradient theory

2.1. Variational approach

2.1.1. Cauchy-Boltzmann continuum

For a classical Cauchy-Boltzmann continuum, the balances of linear and angular momentum read

$$\underline{\nabla}_{\underline{\mathbf{X}}} \cdot \underset{\sim}{\mathbf{\Sigma}} + \rho \underline{\mathbf{f}} - \rho \underline{\dot{\mathbf{V}}} = 0 \tag{2.1}$$

$$\underset{\sim}{\mathbf{\Sigma}} = \underset{\sim}{\mathbf{\Sigma}}^{\mathrm{T}} , \tag{2.2}$$

in the domain $\underline{\mathbf{X}} \in \Omega_{\underline{\mathbf{X}}}$ respectively. Therein, the symbols $\underline{\mathbf{V}}$, $\underset{\sim}{\mathbf{\Sigma}}$ and $\underline{\mathbf{f}}$ refer to the macroscopic values of velocity, Cauchy stress and specific volumetric forces, respectively. Equations (2.1) (2.2) together with traction or displacement boundary conditions

$$\underline{\mathbf{N}} \cdot \underset{\sim}{\mathbf{\Sigma}} = \underline{\mathbf{t}} \qquad \text{on } \partial\Omega_t \tag{2.3}$$

$$\underline{\mathbf{U}} = \underline{\bar{\mathbf{U}}} \qquad \text{on } \partial\Omega_u \tag{2.4}$$

and a suitable material law, describe an initial boundary value problem for the fields of displacements $\underline{\mathbf{U}}(\underline{\mathbf{X}}, t)$ or velocities $\underline{\mathbf{V}}(\underline{\mathbf{X}}, t) = \underline{\dot{\mathbf{U}}}$, respectively. An *equivalent* weak form of Eqs. (2.1)–(2.3) is obtained by requiring

$$0 = \delta\mathcal{L} = \delta\mathcal{W}_{\text{int}} - \delta\mathcal{W}_{\text{ext}} + \delta\mathcal{K} \tag{2.5}$$

with

$$\delta\mathcal{W}_{\text{int}} = \int\limits_{\Omega_{\underline{\mathbf{X}}}} \underset{\sim}{\mathbf{\Sigma}} : \delta\underset{\sim}{\mathbf{E}} \, \mathrm{d}V \qquad \text{with} \qquad \delta\underset{\sim}{\mathbf{E}} = \frac{1}{2}\left(\underline{\nabla}_{\underline{\mathbf{X}}} \delta\underline{\mathbf{U}} + \delta\underline{\mathbf{U}} \otimes \underline{\nabla}_{\underline{\mathbf{X}}}\right) \tag{2.6}$$

$$\delta\mathcal{W}_{\text{ext}} = \int\limits_{\Omega_{\underline{\mathbf{X}}}} \rho \underline{\mathbf{f}} \cdot \delta\underline{\mathbf{U}} \, \mathrm{d}V + \int\limits_{\partial\Omega_t} \underline{\bar{\mathbf{t}}} \cdot \delta\underline{\mathbf{U}} \, \mathrm{d}S \tag{2.7}$$

$$\delta\mathcal{K} = \int\limits_{\Omega_{\underline{\mathbf{X}}}} \rho \underline{\dot{\mathbf{V}}} \cdot \delta\underline{\mathbf{U}} \, \mathrm{d}V \tag{2.8}$$

for all kinematically admissible test functions $\delta\underline{\mathbf{U}}(\underline{\mathbf{X}})$. Equation 2.5 is also known as *principle of virtual power*. In this context, the test function $\delta\underline{\mathbf{U}}(\underline{\mathbf{X}})$ is also termed field of virtual displacements or of virtual velocities, respectively.

If the stresses $\underset{\sim}{\mathbf{\Sigma}}$ and external loadings $\underline{\mathbf{f}}$ and $\underline{\bar{\mathbf{t}}}$ have variational potentials, i. e., if the material is hyperelastic and the loading is conservative, then Eq. (2.5) corresponds to the stationarity condition of a variation problem (Hamilton's principle of stationary action).

In the static case $\delta\mathcal{K} = 0$ it corresponds to the *minimum of the elastic energy*

$$\mathcal{W} \xrightarrow{\underline{\mathbf{U}}(\underline{\mathbf{X}})} \text{Min.} \tag{2.9}$$

with

$$\mathcal{W}_{\text{int}} = \int_{\Omega_{\underline{\mathbf{X}}}} \overline{W}_{\text{int}}(\underline{\nabla}_{\underline{\mathbf{X}}}\underline{\mathbf{U}})\, \mathrm{d}V\,. \tag{2.10}$$

The strain energy density $\overline{W}_{\text{int}}$ must depend only on objective parts of the displacement gradient $\underline{\nabla}_{\underline{\mathbf{X}}}\underline{\mathbf{U}}$. In a theory of infinitesimal deformations this is the symmetric part $\underset{\sim}{\mathbf{E}} = 1/2(\underline{\nabla}_{\underline{\mathbf{X}}}\underline{\mathbf{U}} + \underline{\mathbf{U}} \otimes \underline{\nabla}_{\underline{\mathbf{X}}})$.

2.1.2. Second gradient theory / Strain gradient theory

Toupin [51] allowed the strain energy density

$$\overline{W}_{\text{int}} = \overline{W}_{\text{int}}(\underset{\sim}{\mathbf{E}}, \underset{\approx}{\mathbf{K}}^{\nabla\nabla U}) \tag{2.11}$$

to depend additionally on the *second displacement gradient*[1]

$$\underset{\approx}{\mathbf{K}}^{\nabla\nabla U} = \underline{\nabla}_{\underline{\mathbf{X}}}\underline{\mathbf{U}} \otimes \underline{\nabla}_{\underline{\mathbf{X}}}\,. \tag{2.12}$$

In this context, the Cauchy-Boltzmann theory is often referred to as first gradient theory. Toupin "postulate[d] as a necessary condition of equilibrium" for the second gradient theory that the stationarity condition $\delta\mathcal{W} = 0$ remains valid. Thus, the variation of the internal work becomes

$$\delta\mathcal{W}_{\text{int}} = \int_{\Omega_{\underline{\mathbf{X}}}} \bar{\underset{\sim}{\sigma}} : \delta\underset{\sim}{\mathbf{E}} + \underset{\approx}{\mathbf{M}}^{\nabla\nabla U} \vdots \delta\underset{\approx}{\mathbf{K}}^{\nabla\nabla U}\, \mathrm{d}V \tag{2.13}$$

wherein the classical stress and the "double stress" are

$$\bar{\underset{\sim}{\sigma}} = \operatorname{sym}\left(\frac{\partial\overline{W}_{\text{int}}}{\partial\underset{\sim}{\mathbf{E}}}\right), \qquad \underset{\approx}{\mathbf{M}}^{\nabla\nabla U} = \frac{\partial\overline{W}_{\text{int}}}{\partial\underset{\approx}{\mathbf{K}}^{\nabla\nabla U}}\,, \tag{2.14}$$

respectively. In this context, Toupin incorporated additional volume and surface terms with $\delta\underline{\nabla}_{\underline{\mathbf{X}}}\underline{\mathbf{U}}$ to the virtual external work $\delta\mathcal{W}_{\text{ext}}$ in Eq. (2.7). The corresponding Euler-Lagrange equations to $\delta\mathcal{W} = 0$ are the equilibrium condition

$$\underline{\nabla}_{\underline{\mathbf{X}}} \cdot \underset{\sim}{\mathbf{\Sigma}} + \rho\underline{\mathbf{f}} = 0 \tag{2.15}$$

with

$$\underset{\sim}{\mathbf{\Sigma}} = \bar{\underset{\sim}{\sigma}} - \underset{\approx}{\mathbf{M}}^{\nabla\nabla U} \cdot \underline{\nabla}_{\underline{\mathbf{X}}} \tag{2.16}$$

and boundary conditions which shall not be discussed here. Toupin [51] referred to $\bar{\underset{\sim}{\sigma}}$ as "Cauchy stress" due to the analogy of Eq. (2.14) with the corresponding relation of the classical theory. However, Eq. (2.15) shows that the Cauchy theorem (2.3) does not apply to $\bar{\underset{\sim}{\sigma}}$ but to $\underset{\sim}{\mathbf{\Sigma}}$ defined according to Eq. 2.16. That is why the author prefers to refer to $\bar{\underset{\sim}{\sigma}}$ and $\underset{\sim}{\mathbf{\Sigma}}$ as *internal stress* and *external stress*, respectively. Mostly, $\underset{\sim}{\mathbf{\Sigma}}$ is eliminated by inserting Eq. (2.16) into Eq. (2.15).

Mindlin [10] extended the approach of Toupin to the dynamic case by incorporating additional quadratic terms in $\underline{\nabla}_{\underline{\mathbf{X}}}\underline{\mathbf{V}}$ to the kinetic energy $\mathcal{K}$ postulating, analogously to Toupin, that Hamilton's principle and thus the principle of virtual power (2.5) still hold.

[1] Note that the sequence of indices for non-classical measures of deformation and respective stress measures differs throughout literature on the topic. Here, a definition is adopted which will be favorable for a comparison with micromorphic theories.

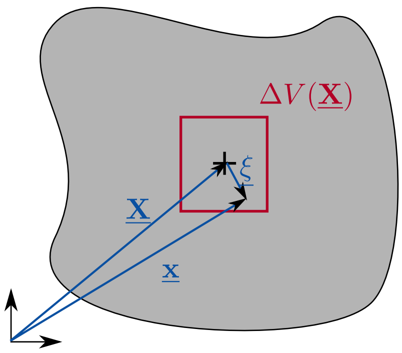

Fig. 2.1.: Micromorphic continuum

Mindlin [10, 52] pointed also out that the 18 components of the second gradient $\underset{\approx}{\mathbf{K}}^{\nabla\nabla U} = \underline{\nabla}_{\mathbf{X}}\underline{\mathbf{U}} \otimes \underline{\nabla}_{\mathbf{X}}$ can be related to the 18 components *strain gradient* $\underline{\nabla}_{\mathbf{X}}\underset{\sim}{\mathbf{E}}$ tensor according to

$$K^{\nabla\nabla U}_{ijk} = U_{j,ik} = E_{ij,k} + E_{kj,i} - E_{kj,i} \,. \tag{2.17}$$

Thus, he proposed an alternative, equivalent form ("Form II") to Eq. (2.11) ("Form I") as

$$\overline{W}_{\text{int}} = \overline{W}_{\text{int}}(\underset{\sim}{\mathbf{E}}, \underline{\nabla}_{\mathbf{X}}\underset{\sim}{\mathbf{E}}) \,. \tag{2.18}$$

which implies to define a double stress work-conjugate to $\underline{\nabla}_{\mathbf{X}}\underset{\sim}{\mathbf{E}}$ as

$$\underset{\approx}{\mathbf{M}}^{\nabla E} = \frac{\partial \overline{W}_{\text{int}}}{\partial \underline{\nabla}_{\mathbf{X}}\underset{\sim}{\mathbf{E}}} \,. \tag{2.19}$$

Consequently, the Euler-Lagrange equation (2.16) becomes

$$\underset{\sim}{\mathbf{\Sigma}} = \underset{\sim}{\bar{\sigma}} - \underset{\approx}{\mathbf{M}}^{\nabla E} \cdot \underline{\nabla}_{\mathbf{X}} \,. \tag{2.20}$$

For completeness it shall be mentioned that Mindlin also proposed a third form in which the gradient of the rotation is separated in order to draw a reference to Koiter's couple stress theory.

2.1.3. Micromorphic theory

Mindlin [10] proposed a theory of elasticity "with micro-structure". It is based on the idea that a "micro-medium" $\Delta V(\underline{\mathbf{X}})$ is attached to each macroscopic material point $\underline{\mathbf{X}}$, compare Fig. 2.1, and that "micro-displacements can be expressed ... as an approximation ... [up to the] linear term of the series"

$$\underline{\mathbf{u}} = \underline{\mathbf{U}} + \underset{\sim}{\chi} \cdot (\underline{\mathbf{x}} - \underline{\mathbf{X}}) \,. \tag{2.21}$$

The "micro-deformation" $\underset{\sim}{\chi}$ is "homogeneous in the micro-medium" $\Delta V(\underline{\mathbf{X}})$ "and non-homogeneous in the macro-medium" $\underline{\mathbf{X}} \in \Omega_{\underline{\mathbf{X}}}$.

Based on this idea, he specified the kinetic energy as

$$\mathcal{K} = \int\limits_{\Omega_{\underline{\mathbf{X}}}} \left\langle \frac{1}{2}\rho\dot{\underline{\mathbf{u}}} \cdot \dot{\underline{\mathbf{u}}} \right\rangle_V \,\mathrm{d}V \tag{2.22}$$

with the average over the "micro-volume" denoted as

$$\langle(\circ)\rangle_V = \frac{1}{\Delta V(\underline{\mathbf{X}})} \int\limits_{\Delta V(\underline{\mathbf{X}})} (\circ)(\underline{\mathbf{x}}) \,\mathrm{d}V \,. \tag{2.23}$$

Inserting the microscopic relation (2.21) to Eq. (2.22) yields

$$\mathcal{K} = \int\limits_{\Omega_{\underline{\mathbf{X}}}} \frac{1}{2}\overline{\rho}\dot{\underline{\mathbf{U}}} \cdot \dot{\underline{\mathbf{U}}} + \frac{1}{2}\left(\dot{\underset{\sim}{\chi}} \cdot \underset{\sim}{\mathbf{G}}_{\rho} \cdot \dot{\underset{\sim}{\chi}}^{\mathrm{T}}\right) : \underset{\sim}{\mathbf{I}} \,\mathrm{d}V \tag{2.24}$$

whereby the macroscopic density and the tensor of microinertia were identified as

$$\overline{\rho} = \langle\rho\rangle_V\,, \qquad \underset{\sim}{\mathbf{G}}_{\rho} = \left\langle\rho\underline{\xi}\otimes\underline{\xi}\right\rangle_V \tag{2.25}$$

Furthermore, it was assumed that $\left\langle\rho\underline{\xi}\right\rangle_V = 0$, i. e. the macroscopic location is defined as the center of mass (barycenter)

$$\underline{\mathbf{X}} = \frac{1}{\overline{\rho}}\left\langle\rho\underline{\mathbf{x}}\right\rangle_V\,. \tag{2.26}$$

In view of the microscopic interpretation of $\underset{\sim}{\chi}$ according to Eq. (2.21), Mindlin specified the following objective measures of deformation (for infinitesimal deformations)

- classical strain $\underset{\sim}{\mathbf{E}}$
- "relative deformation" $\underset{\sim}{\mathbf{e}} = \underline{\mathbf{U}} \otimes \underline{\nabla}_{\underline{\mathbf{X}}} - \underset{\sim}{\chi}$
- "micro-deformation gradient" $\underset{\approx}{\underline{\mathbf{K}}} = \underline{\nabla}_{\underline{\mathbf{X}}}\underset{\sim}{\chi}$

which the strain energy density is postulated to depend on[2]:

$$\overline{W}_{\mathrm{int}} = \overline{W}_{\mathrm{int}}(\underset{\sim}{\mathbf{E}}, \underset{\sim}{\mathbf{e}}, \underset{\approx}{\underline{\mathbf{K}}}) \tag{2.27}$$

Thus, the variation of the strain energy becomes

$$\delta\mathcal{W}_{\mathrm{int}} = \int\limits_{\Omega_{\underline{\mathbf{X}}}} \underset{\sim}{\bar{\sigma}} : \delta\underset{\sim}{\mathbf{E}} + \underset{\sim}{\mathbf{s}} : \delta\underset{\sim}{\mathbf{e}} + \underset{\approx}{\underline{\mathbf{M}}} \vdots \delta\underset{\approx}{\underline{\mathbf{K}}} \,\mathrm{d}V\,. \tag{2.28}$$

with stress measures defined as

$$\underset{\sim}{\bar{\sigma}} = \mathrm{sym}\left(\frac{\partial\overline{W}_{\mathrm{int}}}{\partial\underset{\sim}{\mathbf{E}}}\right), \qquad \underset{\sim}{\mathbf{s}} = \frac{\partial\overline{W}_{\mathrm{int}}}{\partial\underset{\sim}{\mathbf{e}}}\,, \qquad \underset{\approx}{\underline{\mathbf{M}}} = \frac{\partial\overline{W}_{\mathrm{int}}}{\partial\underset{\approx}{\underline{\mathbf{K}}}}\,. \tag{2.29}$$

With kinetic energy and strain energy density given by Eqs. (2.24) and (2.27), the Hamilton principle yields the "variational equations of motion"

$$\underline{\nabla}_{\underline{\mathbf{X}}} \cdot \left(\underset{\sim}{\bar{\sigma}} + \underset{\sim}{\mathbf{s}}^{\mathrm{T}}\right) + \overline{\rho}\underline{\mathbf{f}} - \overline{\rho}\ddot{\underline{\mathbf{U}}} = 0\,, \tag{2.30}$$

$$\underline{\nabla}_{\underline{\mathbf{X}}} \cdot \underset{\approx}{\underline{\mathbf{M}}} + \underset{\sim}{\mathbf{s}} - \ddot{\underset{\sim}{\chi}} \cdot \underset{\sim}{\mathbf{G}}_{\rho} = 0\,. \tag{2.31}$$

Comparing Eq. (2.30) with Eq. (2.15) shows that the external stress can be identified as

$$\underset{\sim}{\mathbf{\Sigma}} = \underset{\sim}{\bar{\sigma}} + \underset{\sim}{\mathbf{s}}^{\mathrm{T}}\,. \tag{2.32}$$

Thus, Eq. (2.31) may be interpreted that the difference $\underset{\sim}{\mathbf{s}}$ between external stress $\underset{\sim}{\mathbf{\Sigma}}$ and internal stress $\underset{\sim}{\bar{\sigma}}$, and higher order body forces $\underset{\sim}{\mathbf{m}}$, are the sources of double stresses $\underset{\approx}{\underline{\mathbf{M}}}$ and higher order inertia. The magnitude of the latter depends on the second moment of inertia $\underset{\sim}{\mathbf{G}}_{\rho}$. Eringen coined the term "micromorphic theory" for this theory.

Mindlin pointed out that a second gradient theory is obtained when $\underset{\sim}{\mathbf{e}} = 0$ is enforced, i. e.

$$\underset{\sim}{\chi} = \underline{\mathbf{U}} \otimes \underline{\nabla}_{\underline{\mathbf{X}}}\,. \tag{2.33}$$

However, Eq. (2.33) is not the only opportunity for obtaining a second gradient theory as will be discussed in section 3.6.1.

[2] Corresponding Lagrangian deformation measures were given already by Truesdell and Toupin [53]

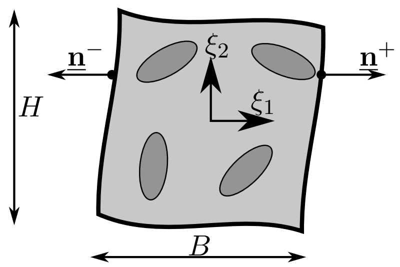

Fig. 2.2.: Microscopic volume element with periodic boundary conditions

2.1.4. Method of virtual power

Mindlin and Toupin constructed their generalized continuum theories by firstly postulating that the strain energy density $\overline{W}_{\text{int}}$ depends on additional *objective measures* of deformation, Eqs. (2.11), (2.18) and (2.27), and that the kinetic energy $\mathcal{K}$ may depend on additional quantities (but not explicitly on time). Secondly, they postulated that the Hamilton's principle of least action, corresponding to the principle of minimum elastic energy in the static case, does apply. Mathematically, this principle forms a variational problem. According to Noether's theorem, both postulates have the consequence that, in absence of external volume contributions, the *linear momentum*, *angular momentum* and *mechanical energy* are conserved quantities.

However, already for the Cauchy-Boltzmann continuum it is known that no action functional can be constructed for general irreversible material laws (so that the mechanical energy is no conserved quantity). In order to address irreversible material behavior in generalized continuum theories, Germain [13] generalized the variational approach of Mindlin and Toupin to the "method of virtual power". In this method, the stationarity condition

$$0 = \delta\mathcal{L} = \delta\mathcal{W}_{\text{int}} - \delta\mathcal{W}_{\text{ext}} + \delta\mathcal{K} \tag{2.34}$$

is postulated to hold irrespective of the existence of an action functional for arbitrary values of the *virtual* fields. Germain formulated the requirement that $\delta\mathcal{W}_{\text{int}}$ and $\delta\mathcal{K}$ need to be objective. Based on the structure of $\delta\mathcal{W}_{\text{int}}$, respective terms may be incorporated into the virtual external work $\delta\mathcal{W}_{\text{ext}}$, both as volume and surface contributions.

For the second gradient and micromorphic theories under consideration, this means that not the functional dependencies of the strain energy density $\overline{W}_{\text{int}}$ are postulated but directly the virtual internal work of $\delta\mathcal{W}_{\text{int}}$ according to Eqs. (2.13) and (2.28), respectively. Finally, the same balance equations (2.15)–(2.16), (2.20) and (2.30)–(2.31), respectively, are obtained as with the variational approach of Mindlin and Toupin, which now, however, allow to formulate irreversible material laws.

Today, the method of virtual power is the established way to derive the balance equations for generalised continuum theories, e. g. [11, 44, 45, 54–58]. A review of the method was given by Maugin [59]. Hellinger [60] traced the method back to Lagrange, pointing out, however, both its universality as well as its purely axiomatic nature.

2.2. Homogenisation approaches

2.2.1. Classical theory of homogenisation

In the classical theory of homogenisation by Hill [34], the macroscopic values of stress $\underset{\sim}{\mathbf{\Sigma}}$ and strain $\underset{\sim}{\mathbf{E}}$ are defined as volume averages of their microscopic counterparts $\underset{\sim}{\sigma}$ and $\underset{\sim}{\varepsilon}$, respectively, over a microscopic volume element $\Delta V(\underline{\mathbf{X}})$ (Fig. 2.2)

$$\underset{\sim}{\boldsymbol{\Sigma}} = \langle \underset{\sim}{\sigma} \rangle_V \,, \tag{2.35}$$

$$\underset{\sim}{\mathbf{E}} = \langle \underset{\sim}{\varepsilon} \rangle_V \,. \tag{2.36}$$

Furthermore, it is required that the macroscopic value of mechanical power is identical to the microscopic average:

$$\underset{\sim}{\boldsymbol{\Sigma}} : \dot{\underset{\sim}{\mathbf{E}}} = \langle \underset{\sim}{\sigma} : \dot{\underset{\sim}{\varepsilon}} \rangle_V \tag{2.37}$$

This requirement is known as *Hill-Mandel condition* or *condition of macro-homogeneity*.

Boundary conditions

In order to compute the macroscopic quantities $\underset{\sim}{\mathbf{E}}$ and $\underset{\sim}{\boldsymbol{\Sigma}}$, a boundary value problems needs to be formulated which determines the microscopic fields of $\underset{\sim}{\varepsilon}(\underline{\mathbf{x}})$ and $\underset{\sim}{\sigma}(\underline{\mathbf{x}})$ at each microscopic point $\underline{\mathbf{x}} \in \Delta V(\underline{\mathbf{X}})$.

Thus, in addition to the standard equilibrium conditions and the strain-displacement relation

$$\underline{\nabla}_{\underline{\mathbf{x}}} \cdot \underset{\sim}{\sigma} = 0 \text{ and } \underset{\sim}{\sigma} = \underset{\sim}{\sigma}^{\mathrm{T}} \tag{2.38}$$

$$\underset{\sim}{\varepsilon} = \frac{1}{2}(\underline{\nabla}_{\underline{\mathbf{x}}}\underline{\mathbf{u}} + \underline{\mathbf{u}} \otimes \underline{\nabla}_{\underline{\mathbf{x}}}) \tag{2.39}$$

suitable boundary conditions have to be formulated which ensure that the micro-macro relations (2.35)–(2.37) are satisfied. For this purpose, these relations are transformed to surface integrals over the boundary $\partial\Delta V(\underline{\mathbf{X}})$ of the volume element ΔV by means of the divergence theorem together with Eqs. (2.38)–(2.39):

$$\underset{\sim}{\boldsymbol{\Sigma}} = \frac{1}{\Delta V} \oint_{\partial\Delta V} \underline{\xi} \otimes \underline{\mathbf{n}} \cdot \underset{\sim}{\sigma} \,\mathrm{d}S \,, \tag{2.40}$$

$$\underset{\sim}{\mathbf{E}} = \frac{1}{2\Delta V} \oint_{\partial\Delta V} \underline{\mathbf{n}} \otimes \underline{\mathbf{u}} + \underline{\mathbf{n}} \otimes \underline{\mathbf{u}} \,\mathrm{d}S \,, \tag{2.41}$$

$$\underset{\sim}{\boldsymbol{\Sigma}} : \dot{\underset{\sim}{\mathbf{E}}} = \frac{1}{\Delta V} \oint_{\partial\Delta V} \underline{\mathbf{n}} \cdot \underset{\sim}{\sigma} \cdot \dot{\underline{\mathbf{u}}} \,\mathrm{d}S \,. \tag{2.42}$$

Therein, $\underline{\xi} = \underline{\mathbf{x}} - \underline{\mathbf{X}}$ refers to the location of a point at the microscale relative to the macroscopic position $\underline{\mathbf{X}}$ as shown in Figs. 2.1 and 2.2. When using the divergence theorem, it was assumed that neither the displacement field $\underline{\mathbf{u}}(\underline{\mathbf{x}})$ nor the stress field $\underset{\sim}{\sigma}(\underline{\mathbf{x}})$ exhibit jumps.

The first approach is to satisfy (2.40) directly by *static boundary conditions*

$$\underline{\mathbf{n}} \cdot \underset{\sim}{\sigma} = \underline{\mathbf{n}} \cdot \underset{\sim}{\boldsymbol{\Sigma}} \qquad \text{on } \partial\Delta V(\underline{\mathbf{X}}) \,. \tag{2.43}$$

In this case, the external loads $\underset{\sim}{\boldsymbol{\Sigma}}$ of the volume element has to be self-equilibrating which requires

$$\underset{\sim}{\boldsymbol{\Sigma}}^{\mathrm{T}} = \underset{\sim}{\boldsymbol{\Sigma}} \tag{2.44}$$

in accordance with Eqs. (2.35) and $(2.38)_2$. The static boundary condition (2.43) can be inserted to the Hill-Mandel condition (2.42). Using Eqs. (2.41) and (2.44), it turns out that Eq. (2.42) is satisfied by static boundary conditions.

Alternatively, *kinematic boundary conditions*

$$\underline{\mathbf{u}} = \underline{\xi} \cdot \underset{\sim}{\mathbf{E}} \qquad \text{on } \partial\Delta V(\underline{\mathbf{X}}) \tag{2.45}$$

can be imposed which satisfy the kinematic micro-macro relation (2.41) a priori. The kinematic boundary condition (2.45) can be inserted to the Hill-Mandel condition (2.42) showing that the latter is fulfilled by Eq. (2.40) for the macroscopic stress.

Periodic boundary conditions allow *fluctuations* $\Delta\underline{\mathbf{u}}(\underline{\mathbf{x}})$ in additions to the linear mapping (2.45):

$$\underline{\mathbf{u}} = \underset{\sim}{\xi} \cdot \underset{\approx}{\mathbf{E}} + \Delta\underline{\mathbf{u}}(\underline{\mathbf{x}}) \qquad \text{on } \partial\Delta V(\underline{\mathbf{X}})\,. \tag{2.46}$$

In order to satisfy the micro-macro relation (2.41) for the strain it is required that

$$\oint\limits_{\partial\Delta V} \Delta\underline{\mathbf{u}} \otimes \underline{\mathbf{n}} + \underline{\mathbf{n}} \otimes \Delta\underline{\mathbf{u}}\,\mathrm{d}S = 0\,. \tag{2.47}$$

This requirement is fulfilled by any periodic fluctuation field

$$\Delta\underline{\mathbf{u}}(\underset{\sim}{\xi}^+) = \Delta\underline{\mathbf{u}}(\underset{\sim}{\xi}^-) \tag{2.48}$$

with $\underset{\sim}{\xi}^+$ and $\underset{\sim}{\xi}^-$ being the locations (relative to the center $\underline{\mathbf{X}}$) of "homologous" points at the boundary $\partial\Delta V(\underline{\mathbf{X}})$ with opposite normal directions $\underline{\mathbf{n}}^+ = -\underline{\mathbf{n}}^-$. Equations (2.46) and (2.48) can be used to eliminate $\Delta\underline{\mathbf{u}}$ yielding

$$\underline{\mathbf{u}}(\underset{\sim}{\xi}^+) - \underline{\mathbf{u}}(\underset{\sim}{\xi}^-) = \left(\underset{\sim}{\xi}^+ - \underset{\sim}{\xi}^-\right) \cdot \underset{\approx}{\mathbf{E}} \qquad \text{on } \partial\Delta V(\underline{\mathbf{X}})\,. \tag{2.49}$$

For a rectangular volume element as shown in Fig. 2.1,Eq. (2.49) becomes[3]

$$\begin{aligned} \underline{\mathbf{u}}(\xi_1, H/2) - \underline{\mathbf{u}}(\xi_1, -H/2) &= B\underline{\mathbf{b}}_1 \cdot \underset{\approx}{\mathbf{E}} \qquad \forall \xi_1 \in [-B/2, B/2]\,, \\ \underline{\mathbf{u}}(B/2, \xi_2) - \underline{\mathbf{u}}(-B/2, \xi_2) &= H\underline{\mathbf{b}}_2 \cdot \underset{\approx}{\mathbf{E}} \qquad \forall \xi_2 \in [-H/2, H/2] \end{aligned} \tag{2.50}$$

wherein $\underline{\mathbf{b}}_1$ and $\underline{\mathbf{b}}_2$ refer to the unit base vectors of the coordinate system $\xi_1 - \xi_2$. However, neither (2.49) nor its special case (2.50) define a complete set of boundary conditions for the PDE (2.38)–(2.39) at the microscale.

For complete description of the boundary value problem, equilibrium condition (2.38) is written in variational form

$$\mathcal{L} = \langle W \rangle_V - \frac{1}{\Delta V} \int\limits_{\partial\Delta V^+} \underset{\sim}{\lambda}(\underset{\sim}{\xi}^+) \cdot \left[\underline{\mathbf{u}}^+ - \underline{\mathbf{u}}^- - \left(\underset{\sim}{\xi}^+ - \underset{\sim}{\xi}^-\right) \cdot \underset{\approx}{\mathbf{E}}\right] \mathrm{d}S \xrightarrow{\underline{\mathbf{u}}(\underset{\sim}{\xi}), \underset{\sim}{\lambda}(\underset{\sim}{\xi}^+)} \text{Min.}\,. \tag{2.51}$$

Therein, the Lagrange multiplier $\underset{\sim}{\lambda}(\underset{\sim}{\xi}^+)$ as a function of location $\underset{\sim}{\xi}^+$ enforces constraint (2.49) requiring that the boundary $\partial\Delta V$ is parametrized adequately as $\underset{\sim}{\xi}^+ \in \partial\Delta V^+(\underline{\mathbf{X}})$ and $\underset{\sim}{\xi}^- = \underset{\sim}{\xi}^-(\underset{\sim}{\xi}^+)$. The Euler-Lagrange equations to the variational problem (2.51) are (2.38) in the domain $\underset{\sim}{\xi} \in \Delta V$ as well as constraint (2.49) together with boundary conditions

$$\begin{aligned} \underline{\mathbf{n}} \cdot \underset{\approx}{\sigma} &= \underset{\sim}{\lambda}(\underset{\sim}{\xi}) \qquad \text{on } \partial\Delta V^+(\underline{\mathbf{X}})\,, \\ \underline{\mathbf{n}} \cdot \underset{\approx}{\sigma} &= -\underset{\sim}{\lambda}(\underset{\sim}{\xi}) \qquad \text{on } \partial\Delta V^-(\underline{\mathbf{X}})\,. \end{aligned} \tag{2.52}$$

The stationarity condition $\delta\mathcal{L} = 0$ of (2.51) can be generalized to hold also for irreversible material behavior at the microscale corresponding then to the weak form (principle of virtual power) with the same result (2.52). Obviously, periodic boundary conditions yield anti-periodic traction boundary conditions (2.52) which do, in contrast to static boundary conditions (2.43), depend on the location $\underset{\sim}{\xi}$ and are part of the solution. Inserting (2.52) to (2.40) yields a macroscopic stress

$$\underset{\approx}{\mathbf{\Sigma}} = \frac{1}{\Delta V} \int\limits_{\partial\Delta V^+} \underset{\sim}{\lambda}(\underset{\sim}{\xi}^+) \otimes \left(\underset{\sim}{\xi}^+ - \underset{\sim}{\xi}^-\right) \mathrm{d}S\,. \tag{2.53}$$

It can be verified easily that Eqs. (2.49) and (2.53) satisfy the Hill-Mandel condition (2.42).

[3]Note that Eq. (2.50) is not the only possible choice of homologous points, though the established one.

Large Deformations

Eulerian description In the current configuration (*Eulerian description*), equilibrium conditions (2.38) still hold for the Cauchy stress $\underset{\sim}{\sigma}$. Consequently, definition (2.35) of the macroscopic Cauchy stress $\underset{\sim}{\boldsymbol{\Sigma}}$ and its surface representation (2.40) remain valid if the integrals are computed over the current domain of the microscopic volume element. This applies also to the static boundary condition (2.43). However, in a Eulerian description spatial derivative and and material time derivative $(\dot{\circ})$ do not commute when computing the strain rate $\dot{\underset{\sim}{\varepsilon}}$ for the Hill-Mandel condition (2.37). Thus, the latter has to be written with respect to the velocities $\underline{\mathbf{v}}$ directly as

$$\left\langle \underset{\sim}{\sigma} : \underset{\sim}{\mathbf{d}} \right\rangle_V = \underset{\sim}{\boldsymbol{\Sigma}} : \underset{\sim}{\mathbf{D}} \qquad \text{with} \qquad \underset{\sim}{\mathbf{d}} = \frac{1}{2}(\underline{\nabla}_{\underline{\mathbf{x}}}\underline{\mathbf{v}} + \underline{\mathbf{v}} \otimes \underline{\nabla}_{\underline{\mathbf{x}}}) \tag{2.54}$$

The macroscopic rate of deformation becomes

$$\underset{\sim}{\mathbf{D}} = \left\langle \underset{\sim}{\mathbf{d}} \right\rangle_V = \frac{1}{2\Delta V} \oint\limits_{\partial \Delta V} \underline{\mathbf{n}} \otimes \underline{\mathbf{v}} + \underline{\mathbf{n}} \otimes \underline{\mathbf{v}} \,\mathrm{d}S\,. \tag{2.55}$$

Consequently, the kinematic boundary condition (2.45) has to be formulated also with respect to the velocities as

$$\underline{\mathbf{v}} = \underline{\xi} \cdot \underset{\sim}{\mathbf{D}} \qquad\qquad \text{on } \partial\Delta V(\underline{\mathbf{X}})\,. \tag{2.56}$$

Analogously, periodic boundary conditions (2.49) remain possible if they are formulated with respect to $\underline{\mathbf{v}}$ and $\underset{\sim}{\mathbf{D}}$, respectively, requiring that opposite points with $\underline{\mathbf{n}}^+ = -\underline{\mathbf{n}}^-$ are identified in the current configuration.

Lagrangian description In a Lagrangeian description the macroscopic deformation gradient $\bar{\underset{\sim}{\mathbf{F}}}$ and the first Piola-Kirchhoff stress $\underset{\sim}{\boldsymbol{\Sigma}}^{\mathrm{PK}}$ are defined as averages of their microscopic counterparts with respect to the reference configuration $\underline{\mathbf{x}}_0 \in \Delta V_0(\underline{\mathbf{X}}_0)$ [35]

$$\underset{\sim}{\boldsymbol{\Sigma}}^{\mathrm{PK}} = \left\langle \underset{\sim}{\sigma}^{\mathrm{PK}} \right\rangle_{V_0}\,, \tag{2.57}$$

$$\bar{\underset{\sim}{\mathbf{F}}} = \left\langle \underset{\sim}{\mathbf{F}} \right\rangle_{V_0}\,. \tag{2.58}$$

The equilibrium conditions and the kinematic relation at the microscale are

$$\underline{\nabla}_{\underline{\mathbf{x}}_0} \cdot \underset{\sim}{\sigma}^{\mathrm{PK}} = 0 \text{ and } \underset{\sim}{\mathbf{F}} \cdot \underset{\sim}{\sigma}^{\mathrm{PK}} = \underset{\sim}{\sigma}^{\mathrm{PK}^{\mathrm{T}}} \cdot \underset{\sim}{\mathbf{F}}^{\mathrm{T}} \tag{2.59}$$

$$\underset{\sim}{\mathbf{F}} = \underline{\mathbf{x}}_0 \otimes \underline{\nabla}_{\underline{\mathbf{x}}_0} = \underset{\sim}{\mathbf{I}} + \underline{\mathbf{u}} \otimes \underline{\nabla}_{\underline{\mathbf{x}}_0}\,. \tag{2.60}$$

The Hill-Mandel condition reads

$$\underset{\sim}{\boldsymbol{\Sigma}}^{\mathrm{PK}} : \dot{\bar{\underset{\sim}{\mathbf{F}}}}^{\mathrm{T}} = \left\langle \underset{\sim}{\sigma}^{\mathrm{PK}} : \dot{\underset{\sim}{\mathbf{F}}}^{\mathrm{T}} \right\rangle_V\,. \tag{2.61}$$

Consequently, static boundary conditions

$$\underline{\mathbf{n}} \cdot \underset{\sim}{\sigma}^{\mathrm{PK}} = \underline{\mathbf{n}} \cdot \underset{\sim}{\boldsymbol{\Sigma}}^{\mathrm{PK}} \qquad\qquad \text{on } \partial\Delta V_0(\underline{\mathbf{X}}_0)\,. \tag{2.62}$$

have to be specified with respect to the first Piola-Kirchhoff stress or kinematic boundary conditions in terms of the deformation gradient

$$\underline{\mathbf{x}} = \bar{\underset{\sim}{\mathbf{F}}} \cdot \underline{\mathbf{x}}_0 \qquad\qquad \text{on } \partial\Delta V_0(\underline{\mathbf{X}}_0)\,. \tag{2.63}$$

Both type of boundary conditions satisfies the Hill-Mandel relation (2.37). Evaluating the total angular momentum $0 = \int\limits_{\partial\Delta V_0} \underline{\mathbf{x}} \times (\underline{\mathbf{n}} \cdot \underset{\sim}{\sigma}^{\mathrm{PK}})\,\mathrm{d}S$ of ΔV yields

$$\bar{\underset{\sim}{\mathbf{F}}} \cdot \underset{\sim}{\boldsymbol{\Sigma}}^{\mathrm{PK}} = \underset{\sim}{\boldsymbol{\Sigma}}^{\mathrm{PK}^{\mathrm{T}}} \cdot \bar{\underset{\sim}{\mathbf{F}}}^{\mathrm{T}} \tag{2.64}$$

as macroscopic counterpart to Eq. $(2.59)_2$ both for static and kinematic boundary conditions (2.62) and (2.63), respectively.

Remarks

An important issue for homogenisation is the choice the volume element ΔV. In classical homogenisation, it is required that the volume element ΔV needs to be "representative". According to Hill [34], this means that it "(a) is structurally entirely typical of the whole mixture on average, and (b) contains a sufficient number of inclusions for the apparent overall moduli to be effectively independent of the surface values of traction and displacement, so long as these values are 'macroscopically uniform'."

For a regular microstructure, condition (b) can be satisfied by applying periodic boundary conditions to a unit volume element. Applying static boundary conditions on such a unit volume element lead to lower-bounds of the stiffness, kinematic boundary conditions to upper bounds. If ΔV encompasses a sufficient number of unit volumes, the effect of the type of boundary conditions vanishes.

Another issue was pointed out by Gologanu et al. [44]: "The classical Hill-Mandel approach to homogenisation does not say anything about the existence of such a thing as the 'macroscopic velocity', from which the 'macroscopic strain rate' should derive. It is only when the homogenisation procedure is completed (i. e., the macroscopic constitutive equations fully defined) and microscopic quantities henceforth forgotten that one introduces the heuristic assumption that the 'macroscopic strain rate', as defined through homogenisation, can be identified with the symmetric part of the (macroscopic) gradient of some 'macroscopic velocity'.". The macroscopic velocity is not objective which is why it does not need to be transferred to the microscale (in contrast to e. g. the temperature in thermal homogenisation problems). Analogously, the assumption that the macroscopic stress satisfies the same balance equation $\underline{\nabla}_{\underline{\mathbf{X}}} \cdot \underset{\sim}{\mathbf{\Sigma}} = 0$ as its counterpart on the microscale is heuristic as well.

In view of the envisaged application to porous media, it shall be mentioned that the kinematic micro-macro relation (2.41) requires that the microscopic displacement field $\underline{\mathbf{u}}(\underline{\mathbf{x}})$ is defined on the complete boundary $\partial\Delta V$ of the volume element. This requirement is critical e. g. for open-cell foams. Kinematic boundary conditions (2.45) can be employed in such cases, the displacement field is just defined even in the intersection of the pores with $\partial\Delta V$. However, static boundary conditions cannot be used in such cases as the pores cannot carry the non-vanishing surface tractions. Periodic boundary conditions are used in such cases under the pragmatic assumption that the fluctuations $\Delta\underline{\mathbf{u}}$ vanish at the intersection of the pores with $\partial\Delta V$ [61].

2.2.2. Strain-gradient theory by Gologanu, Kouznetsova et al.

Kinematic boundary conditions

The classical kinematic boundary condition (2.45) and (2.56), respectively, of the microscopic volume element is linear with respect to the location. For constructing a homogenisation towards a macroscopic strain-gradient theory, Gologanu et al. [44] added a quadratic term to the kinematic boundary conditions

$$\underline{\mathbf{v}} = \underset{\sim}{\mathbf{A}} \cdot \underline{\mathbf{x}} + \frac{1}{2}\underset{\approx}{\mathbf{B}} : (\underline{\mathbf{x}}\underline{\mathbf{x}}) \qquad \text{on } \partial\Delta V(\underline{\mathbf{X}}) \tag{2.65}$$

in a velocity formulation with respect to the current configuration. Inserting this approach to the definition (2.55) of the macroscopic rate of deformation yields

$$D_{ij} = A_{(ij)} + \frac{1}{2}\left(B_{ijk} + B_{jik}\right)\langle x_k \rangle_V \ . \tag{2.66}$$

Upon defining the macroscopic location as geometric center of the microscopic volume element

$$\underline{\mathbf{X}} = \langle \underline{\mathbf{x}} \rangle_V \tag{2.67}$$

the gradient of the rate of deformation can be computed from Eq. (2.66) as

$$\frac{\partial D_{ij}}{\partial X_k} = \frac{1}{2}\left(B_{ijk} + B_{jik}\right) . \tag{2.68}$$

By means of a cyclic permutation with respect to i, j, and k, Eq. (2.68) can be solved for $\underset{\approx}{\underline{\mathbf{B}}}$ as $B_{ijk} = D_{ij,k} + D_{ki,j} - D_{jk,i}$, compare Eq. (2.17).

Generalized Hill-Mandel lemma In classical theory of homogenisation, the kinetic and kinematic micro-macro relations (2.35)–(2.36) are specified and boundary conditions needed to identified which satisfy the Hill-Mandel *condition* (2.54). In contrast, for the homogisation approach towards a macroscopic strain-gradient theory by Gologanu et al. [44], the kinematic boundary condition (2.65) is formulated ad hoc and the corresponding kinetic micro-macro relations for stress measures have to be identified. For this purpose, the average mechanical power from the left-hand side of Eq. (2.54) is firstly transformed to a surface integral using local equilibrium conditions (2.38). Inserting kinematic boundary condition (2.65) and eliminating $\underset{\sim}{\mathbf{A}}$ and $\underset{\approx}{\underline{\mathbf{B}}}$ by Eqs. (2.66)and (2.68) yields

$$\begin{aligned} \left\langle \underset{\sim}{\sigma} : \underset{\sim}{\mathbf{d}} \right\rangle_V &= \frac{1}{\Delta V} \oint\limits_{\partial \Delta V} \underline{\mathbf{n}} \cdot \underset{\sim}{\sigma} \cdot \underline{\mathbf{v}} \, \mathrm{d}S \\ &= \left\langle \underset{\sim}{\sigma} \right\rangle_V : \underset{\sim}{\mathbf{D}} + \left\langle \underline{\xi} \otimes \underset{\sim}{\sigma} \right\rangle_V \vdots \left(\nabla_{\underline{\mathbf{X}}} \underset{\sim}{\mathbf{D}} \right) . \end{aligned} \tag{2.69}$$

wherein $\underline{\xi} = \underline{\mathbf{x}} - \underline{\mathbf{X}}$, cmp. Fig. 2.1. From Eq. (2.69), the macroscopic stresses can be identified as

$$\bar{\underset{\sim}{\sigma}} = \left\langle \underset{\sim}{\sigma} \right\rangle_V = \frac{1}{\Delta V} \oint\limits_{\partial \Delta V} \underline{\mathbf{x}} \otimes \underline{\mathbf{n}} \cdot \underset{\sim}{\sigma} \, \mathrm{d}S \tag{2.70}$$

$$\underset{\approx}{\underline{\mathbf{M}}}^{\nabla E} = \left\langle \underline{\xi} \otimes \underset{\sim}{\sigma} \right\rangle_V = \frac{1}{2\Delta V} \oint\limits_{\partial \Delta V} \underline{\xi} \otimes \underline{\mathbf{n}} \cdot \underset{\sim}{\sigma} \otimes \underline{\xi} + \underline{\xi} \otimes \underline{\xi} \otimes \underline{\mathbf{n}} \cdot \underset{\sim}{\sigma} - \underline{\mathbf{n}} \cdot \underset{\sim}{\sigma} \otimes \underline{\xi} \otimes \underline{\xi} \, \mathrm{d}S \tag{2.71}$$

so that the generalized Hill-Mandel lemma (2.69) becomes

$$\left\langle \underset{\sim}{\sigma} : \underset{\sim}{\mathbf{d}} \right\rangle_V = \bar{\underset{\sim}{\sigma}} : \underset{\sim}{\mathbf{D}} + \underset{\approx}{\underline{\mathbf{M}}}^{\nabla E} \vdots \left(\nabla_{\underline{\mathbf{X}}} \underset{\sim}{\mathbf{D}} \right) . \tag{2.72}$$

Macroscopic velocity Additionally, a relation between $\underset{\sim}{\mathbf{D}}$ and the velocity $\underline{\mathbf{V}}$ is required for formulating a boundary value problem on the macroscale. In classical theory of homogenisation, this relationship is postulated. Instead, Gologanu et al. [44] defined $\underline{\mathbf{V}}(\underline{\mathbf{X}})$ "in an admittedly somewhat artificial manner" as the average over the surface $\partial \Delta V(\underline{\mathbf{X}})$

$$\underline{\mathbf{V}} = \langle \underline{\mathbf{v}} \rangle_{\partial \Delta V} \tag{2.73}$$

in order to be able to insert the kinematic boundary condition (2.65). Doing so and writing $\underline{\mathbf{x}} = \underline{\mathbf{X}} + \underline{\xi}$ yields

$$\underline{\mathbf{V}} = \underset{\sim}{\mathbf{A}} \cdot \underline{\mathbf{X}} + \frac{1}{2} \underset{\approx}{\underline{\mathbf{B}}} : (\underline{\mathbf{X}}\underline{\mathbf{X}}) + \frac{1}{2} \underset{\approx}{\underline{\mathbf{B}}} : \langle \underline{\xi}\underline{\xi} \rangle_{\partial \Delta V} \tag{2.74}$$

under condition that $\left\langle \underline{\xi} \right\rangle_{\partial \Delta V} = 0$ which is valid for "simple shapes..., for instance ellipsoidal or parallelepipedic" $\Delta V(\underline{\mathbf{X}})$. If the second geometric moment $\left\langle \underline{\xi}\underline{\xi} \right\rangle_{\partial \Delta V}$ of the surface does not depend on $\underline{\mathbf{X}}$, then the symmetric part of the gradient of the macroscopic velocity Eq. (2.73) coincides with $\underset{\sim}{\mathbf{D}}$ in Eq. (2.66)

$$\frac{1}{2}\left(V_{i,j} + V_{j,i}\right) = A_{(ij)} + \frac{1}{2}\left(B_{ijk} + B_{jik}\right) X_k = D_{ij} . \tag{2.75}$$

Having thus identified $\underset{\sim}{\mathbf{A}}$ and $\underset{\approx}{\mathbf{B}}$ as the first and second gradients of the macroscopic velocity field allows to write the kinematic boundary condition (2.65) as

$$\underline{\mathbf{v}} = \underline{\mathbf{V}}_0(\underline{\mathbf{X}}) + \underline{\xi} \cdot \left(\underline{\nabla_{\mathbf{X}}\mathbf{V}}\right) + \frac{1}{2}(\underline{\xi\xi}) : \left(\underline{\nabla_{\mathbf{X}}\nabla_{\mathbf{X}}\mathbf{V}}\right) \qquad \text{on } \partial\Delta V(\underline{\mathbf{X}}) \tag{2.76}$$

with $\underline{\mathbf{V}}_0(\underline{\mathbf{X}}) = \underline{\mathbf{X}} \cdot (\underline{\nabla_{\mathbf{X}}\mathbf{V}}(\underline{\mathbf{X}})) - \frac{1}{2}(\underline{\mathbf{XX}}) : (\underline{\nabla_{\mathbf{X}}\nabla_{\mathbf{X}}\mathbf{V}}(\underline{\mathbf{X}}))$.

Furthermore, Gologanu et al. [44] pointed out that the kinematic boundary condition (2.65) or (2.76), respectively, contains a rigid body motion which is why not all components of the $\underset{\approx}{\mathbf{M}}$ are independent of each other.

Gologanu et al. employed the method of virtual power to derive the macroscopic equilibrium conditions, see section 2.1.4.

Periodic boundary conditions by Kouznetsova et al.

Kouznetsova et al. [45, 56][4] motivated the kinematic boundary condition (2.76) as a Taylor expansion and incorporated additionally a fluctuation field

$$\underline{\mathbf{v}} = \underline{\xi} \cdot \left(\underline{\nabla_{\mathbf{X}}\mathbf{V}}\right) + \frac{1}{2}(\underline{\xi\xi}) : \left(\underline{\nabla_{\mathbf{X}}\nabla_{\mathbf{X}}\mathbf{V}}\right) + \Delta\underline{\mathbf{v}}(\underline{\xi}) \qquad \text{on } \partial\Delta V(\underline{\mathbf{X}}) \tag{2.77}$$

in analogy to the classic homogenisation (2.46). As in classical theory, it has to be ensured that the fluctuations $\Delta\underline{\mathbf{v}}$ do not contribute to the macroscopic deformations. For the classical term with $\underline{\nabla_{\mathbf{X}}\mathbf{V}}$, the kinematic micro-macro relation (2.55) can be satisfied by requiring $\Delta\underline{\mathbf{v}}$ to be periodic

$$\Delta\underline{\mathbf{v}}(\underline{\xi}^+) = \Delta\underline{\mathbf{v}}(\underline{\xi}^-)\,. \tag{2.78}$$

Regarding the second macroscopic velocity gradient $\underline{\nabla_{\mathbf{X}}\nabla_{\mathbf{X}}\mathbf{V}}$, Kouznetsova provided only an implicit micro-macro relation

$$0 = \oint\limits_{\partial\Delta V} (\underline{\mathbf{n}} \otimes \underline{\mathbf{x}} + \underline{\mathbf{x}} \otimes \underline{\mathbf{n}}) \otimes \Delta\underline{\mathbf{v}}\,\mathrm{d}S\,. \tag{2.79}$$

The classical condition of periodicity (2.78) does not satisfy Eq. (2.79) ad hoc. For instance, for a rectangular microscopic volume element $\Delta V(\underline{\mathbf{X}})$ as shown in Fig. 2.2, Eq. (2.79) implies the additional requirements

$$\int\limits_{-H/2}^{H/2} \Delta\underline{\mathbf{v}}\left(\xi_1 = \frac{B}{2}, \xi_2\right) \mathrm{d}\xi_2 = 0\,, \qquad \int\limits_{-B/2}^{B/2} \Delta\underline{\mathbf{v}}\left(\xi_1, \xi_2 = \frac{H}{2}\right) \mathrm{d}\xi_1 = 0\,. \tag{2.80}$$

A kinematic micro-macro relation for the second gradient $\underline{\nabla_{\mathbf{X}}\nabla_{\mathbf{X}}\mathbf{V}}$ can be obtained by eliminating $\Delta\underline{\mathbf{v}}$ from Eq. (2.79) by Eq. (2.77). Sorting for microscopic and macroscopic quantities yields

$$\delta_{ij}G_{mn}V_{k,mn} + G_{jm}V_{k,im} + G_{im}V_{k,jm} = \frac{1}{\Delta V} \oint\limits_{\partial\Delta V} (n_i\xi_j + n_j\xi_i)\,v_k\,\mathrm{d}S \tag{2.81}$$

whereby, the second geometric moment of the microscopic volume element ΔV was defined as

$$\underset{\sim}{\mathbf{G}} = \left\langle \underline{\xi} \otimes \underline{\xi} \right\rangle_V\,. \tag{2.82}$$

[4] Apparently, Kouznetsova et al. did not take note of the previous work of Gologanu et al. Kouznetsova et el. chose a Lagrangian description which is adapted here to an Eulerian one for comparison with the aforementioned theory of Gologanu et al.

At first glimpse, the components of Eq. (2.81) provide 18 linear equations (symmetry w. r. t. i and j) for the 18 independent components of the second velocity gradient $\underline{\nabla_{\mathbf{X}}}\underline{\nabla_{\mathbf{X}}}\underline{\mathbf{V}}$ in the 3D case or eight equations for eight components in the 2D case, respectively. However, a close look at Eq. (2.81) shows that a *superimposed rigid-body translation* $\underline{\mathbf{v}} \to \overline{\underline{\mathbf{v}}} = \underline{\mathbf{v}} + \underline{\mathbf{v}}_0$ affects its right-hand side whereas its left-hand side is invariant with respect to such a rigid translation. It has to be concluded that the kinematic micro-macro relations (2.81) or (2.79), respectively, are *not objective*. This fact is closely related to the finding of Gologanu et al. [44] that the corresponding kinematic boundary condition (2.76), or (2.77) with $\Delta\underline{\mathbf{v}} = 0$, respectively, contains a rigid-body translation.

Irrespective of this problem, a generalized Hill-Mandel conditions is obtained as

$$\begin{aligned}\langle \underset{\sim}{\sigma} : \underset{\sim}{\mathbf{d}} \rangle_V =& \frac{1}{\Delta V} \oint\limits_{\partial \Delta V} \underline{\mathbf{n}} \cdot \underset{\sim}{\sigma} \cdot \underline{\mathbf{v}} \, \mathrm{d}S \\ =& \frac{1}{\Delta V} \oint\limits_{\partial \Delta V} \underline{\xi} \otimes \underline{\mathbf{n}} \cdot \underset{\sim}{\sigma} \, \mathrm{d}S : \underline{\nabla_{\mathbf{X}}}\underline{\mathbf{V}}(\underline{\mathbf{X}}) + \frac{1}{2\Delta V} \oint\limits_{\partial \Delta V} \underline{\xi} \otimes \underline{\xi} \otimes \underline{\mathbf{n}} \cdot \underset{\sim}{\sigma} \, \mathrm{d}S \,\vdots\, \big(\underline{\nabla_{\mathbf{X}}}\underline{\nabla_{\mathbf{X}}}\underline{\mathbf{V}}\big) \\ &+ \frac{1}{\Delta V} \oint\limits_{\partial \Delta V} \underline{\mathbf{n}} \cdot \underset{\sim}{\sigma} \cdot \Delta\underline{\mathbf{v}}(\underline{\xi}) \, \mathrm{d}S \,. \end{aligned} \tag{2.83}$$

whereby the symbols

$$\underset{\sim}{\underline{\mathbf{L}}} = \underline{\nabla_{\mathbf{X}}}\underline{\mathbf{V}}, \qquad \underset{\approx}{\underline{\mathbf{L}}}^{\nabla\nabla U} = \underline{\nabla_{\mathbf{X}}}\underline{\mathbf{V}} \otimes \underline{\nabla_{\mathbf{X}}} \tag{2.84}$$

for the first and second (Eulerian) velocity gradient, respectively, have been introduced.

Under the condition that the fluctuations $\Delta\underline{\mathbf{v}}$ do not contribute to the power

$$\oint\limits_{\partial \Delta V} \underline{\mathbf{n}} \cdot \underset{\sim}{\sigma} \cdot \Delta\underline{\mathbf{v}}(\underline{\xi}) \, \mathrm{d}S = 0 \,, \tag{2.85}$$

the macroscopic stress and double stress

$$\bar{\underset{\sim}{\sigma}} = \frac{1}{\Delta V} \oint\limits_{\partial \Delta V} \underline{\xi} \otimes \underline{\mathbf{n}} \cdot \underset{\sim}{\sigma} \, \mathrm{d}S = \langle \underset{\sim}{\sigma} \rangle_V \tag{2.86}$$

$$\underset{\approx}{\underline{\mathbf{M}}}^{\nabla\nabla U} = \frac{1}{2\Delta V} \oint\limits_{\partial \Delta V} \underline{\xi} \otimes (\underline{\mathbf{n}} \cdot \underset{\sim}{\sigma}) \otimes \underline{\xi} \, \mathrm{d}S = \frac{1}{2} \langle \underline{\xi}\underset{\sim}{\sigma} + \underset{\sim}{\sigma}\underline{\xi} \rangle_V \tag{2.87}$$

can be identified, which are work-conjugate to $\underset{\sim}{\underline{\mathbf{L}}}$ and $\underset{\approx}{\underline{\mathbf{L}}}^{\nabla\nabla U}$, respectively. The definition of the double stresses (2.71) and (2.87) can be converted consistently into each other and correspond to Mindlin's forms II and I, respectively.

Objective definition of the macroscopic deformations The problem, that the kinematic micro-macro relation (2.81) is not objective, can be solved by incorporating an additional rigid translation $\underline{\mathbf{V}}(\underline{\mathbf{X}})$ in the velocity field at the boundary

$$\underline{\mathbf{v}} = \underline{\mathbf{V}}(\underline{\mathbf{X}}) + \underline{\xi} \cdot \big(\underline{\nabla_{\mathbf{X}}}\underline{\mathbf{V}}\big) + \frac{1}{2}(\underline{\xi}\underline{\xi}) : \big(\underline{\nabla_{\mathbf{X}}}\underline{\nabla_{\mathbf{X}}}\underline{\mathbf{V}}\big) + \Delta\underline{\mathbf{v}}(\underline{\xi}) \qquad \text{on } \partial\Delta V(\underline{\mathbf{X}}) \tag{2.88}$$

corresponding firstly to a strict Taylor expansion and secondly exactly to the kinematic boundary condition (2.76) of Gologanu et al. for vanishing fluctuations $\Delta\underline{\mathbf{v}} = 0$. Eliminating again the fluctuations from the requirement (2.79) using Eq. (2.88), the kinematic micro-macro relation (2.81) becomes

$$2\delta_{ij}V_k + \delta_{ij}G_{mn}V_{k,mn} + G_{jm}V_{k,im} + G_{im}V_{k,jm} = \frac{1}{\Delta V}\oint\limits_{\partial\Delta V} (n_i\xi_j + n_j\xi_i)\, v_k \,\mathrm{d}S \tag{2.89}$$

$$= 2\delta_{ij}\langle v_k\rangle_V + \langle \xi_j v_{k,i} + \xi_i v_{k,j}\rangle_V \,. \tag{2.90}$$

For Eq. (2.90) to be consistent for arbitrary imposed rigid-body translations, the macroscopic velocity is defined as volume average of its microscopic counterpart

$$\underline{\mathbf{V}} = \langle \underline{\mathbf{v}} \rangle_V \;, \tag{2.91}$$

in contrast to definition (2.73) of Gologanu et al. Consequently, Eq. 2.90 becomes

$$\delta_{ij}G_{mn}V_{k,mn} + G_{jm}V_{k,im} + G_{im}V_{k,jm} = \langle \xi_j v_{k,i} + \xi_i v_{k,j}\rangle_V \,. \tag{2.92}$$

and provides an objective (implicit) kinematic micro-macro relation for the second gradient $V_{k,ij}$. The trace of Eq. (2.92) with respect to i and j yields

$$(2+n)G_{mn}V_{k,mn} = 2\langle \xi_i v_{k,i}\rangle_V \tag{2.93}$$

wherein $n = \delta_{ii}$ is the dimension of space. This result can be inserted to Eq. (2.92) yielding

$$G_{jm}V_{k,im} + G_{im}V_{k,jm} = \langle \xi_j v_{k,i} + \xi_i v_{k,j}\rangle_V - \frac{2}{2+n}\delta_{ij}\langle \xi_p v_{k,p}\rangle_V \,. \tag{2.94}$$

In the very most cases of practical relevance, the geometric moment $\underset{\sim}{\mathbf{G}}$ is a spherical tensor $\underset{\sim}{\mathbf{G}} = G\underset{\sim}{\mathbf{I}}$ and Eq. (2.94) becomes an explicit expression for the second velocity gradient. Note that the right-hand sides of Eqs. (2.92) or (2.94), respectively, cannot be transformed completely to surface integrals and thus not be prescribed solely by boundary conditions. Rather, the constraint Eq. (2.91) with respect to the macroscopic velocity remains as a volume term. The Hill-Mandel condition (2.83) and the derived definition (2.87) of the hyperstress are not affected by introducing $\underline{\mathbf{V}}$ in Eq. (2.88). The macroscopic velocity gradient is defined as $\underline{\nabla}_{\underline{\mathbf{X}}}\underline{\mathbf{V}} = \left\langle \underline{\nabla}_{\underline{\mathbf{x}}}\underline{\mathbf{v}} \right\rangle_V$ as in the classical theory (2.55) (where mostly only the symmetric part is transferred).

Static boundary conditions

In analogy to the kinematic boundary conditions (2.65), Mühlich et al. [62] proposed to amend the classical static boundary conditions (2.43) by an additional term which is linear with respect to the location $\underline{\mathbf{x}}$

$$\underline{\mathbf{n}}\cdot\underset{\sim}{\sigma} = \underline{\mathbf{n}}\cdot\underset{\sim}{\mathbf{R}} + \underline{\mathbf{n}}\cdot\underset{\approx}{\mathbf{T}}\cdot\underline{\mathbf{x}} \qquad \text{on } \partial\Delta V(\underline{\mathbf{X}})\,. \tag{2.95}$$

The definition (2.40) of the macroscopic stress $\bar{\underset{\sim}{\sigma}}$, which is recovered in the strain gradient theory in Eqs. (2.70) and (2.86), respective, shows that $\underset{\sim}{\mathbf{R}}$ can be identified as $\bar{\underset{\sim}{\sigma}}$.

Mühlich et al. argued that according to the reasoning of Gologanu et al. [44] (as outlined in section 2.2.2), then $\underset{\approx}{\mathbf{T}}$ in Eq. (2.95) needs to be identified as the gradient of $\bar{\underset{\sim}{\sigma}}$. Thus, the static boundary condition (2.95) would be suitable only for a stress gradient theory (compare [63]). This argumentation would apply also to the justification of an extended boundary condition as Taylor series by Kouznetsova [56] as outlined in section 2.2.2.

Kaczmarczyk et al. [64] claimed to provide "formulation . . . allowing any type of RVE boundary conditions (e. g. displacement, traction, periodic)" for the homogenisation towards a second gradient theory. Having switched "to matrix–vector notation, after FE discretization of the RVE", these authors presented a "generalized form of the RVE boundary conditions" with some matrices which connect nodal forces and displacements. However, neither in continuum form nor for the FEM discretization, do they provide formulae but only sketches and (vague) discussions. The sketches indicate a linear variation of the tractions at the boundary, analogous to Eq. (2.95). Furthermore, Kaczmarczyk et al. referred to the micro-macro relations (2.86) and (2.87) for $\underset{\sim}{\bar{\sigma}}$ and $\underset{\approx}{\underline{\mathbf{M}}}^{\nabla\nabla U}$, respectively. Thus, it may be assumed that their procedure would be to determine $\underset{\sim}{\mathbf{R}}$ and $\underset{\approx}{\underline{\mathbf{T}}}$ in (2.95) from the kinetic micro-macro relations (2.86) and (2.87). Again, Eq. (2.86) would yield $\underset{\sim}{\mathbf{R}} = \underset{\sim}{\bar{\sigma}}$. Equation (2.87) would yield 18 linear equations for the 18 independent components of $\underset{\approx}{\underline{\mathbf{M}}}^{\nabla\nabla U}$. However, such a procedure conflicts with the cited reasoning of Mühlich et al. [62].

Remarks

Anyway, it can be concluded that the homogenisation theory of Gologanu, Kouznetsova et al. is a consistent extension of the classical theory of homogenisation. A boundary-value problem is formulated at the microscale whose solution, either analytical or numerical, leads to macroscopic constitutive equations for the strain-gradient theory. It has been applied successfully e. g. in [56, 61, 62, 65]. However, the numerical implementation of a strain-gradient theory is not trivial due to its continuity requirements and related boundary conditions, in particular at edges, e. g. [66].

2.2.3. Micromorphic theory by Eringen

With the variational approach or by the method of virtual power, the macroscopic balance equations are derived from functionals which are formulated axiomatically. In contrast, Eringen et al. [7, 8] presented an approach to obtain the macroscopic balance equations by averaging the established balance equations at the microscale.

Average theorem for balance laws

Consider a general balance equation at the microscale of type

$$\frac{D}{Dt}\int_{\Omega} \rho\varphi_m \, \mathrm{d}V = \oint_{\partial\Omega} \underline{\mathbf{n}} \cdot \underline{\psi}_a \, \mathrm{d}S + \int_{\Omega} \rho\psi_m \, \mathrm{d}V \tag{2.96}$$

with φ_m, ψ_m and $\underline{\psi}_a$ and being the densities of storage, sources and flux, respectively, in a continuum of mass density ρ. The global balance (2.96) can be localized as usual to

$$\rho\dot{\varphi}_m = \underline{\nabla}_{\underline{\mathbf{x}}} \cdot \underline{\psi}_a + \rho\psi_m \text{ in } \Omega\,. \tag{2.97}$$

Thereby, use was made of the balance of mass. According to Eringen [7, 8] macroscopic counterparts to these balance equations are obtained by dividing the domain Ω into small but *finite* volumes $\Delta V(\underline{\mathbf{X}})$ as sketched in Fig. 2.1 for each of which Eq. (2.96) is valid. Finally, the sum of those many elements is approximated as integrals over the macroscopic domain

$\underline{\mathbf{X}} \in \Omega_{\underline{\mathbf{X}}}$ (with boundary $\partial\Omega_{\underline{\mathbf{X}}}$ whose normal is $\underline{\mathbf{N}}$). For the flux terms, this procedure is written as

$$\begin{aligned}\int\limits_{\Omega} \underline{\nabla}_{\mathbf{x}} \cdot \underline{\psi}_a \,\mathrm{d}V &= \oint\limits_{\partial\Omega} \underline{\mathbf{n}} \cdot \underline{\psi}_a \,\mathrm{d}S = \sum_K \int\limits_{\Delta A_K} \underline{\mathbf{n}} \cdot \underline{\psi}_a \,\mathrm{d}S \quad \text{with } \Delta A_K := \partial\Omega \cap \Delta V_K \\ &= \sum_K \underbrace{\frac{1}{\Delta A_K} \int\limits_{\Delta A_K} \underline{\mathbf{n}} \cdot \underline{\psi}_a \,\mathrm{d}S}_{:=\underline{\mathbf{N}}\cdot\left\langle\underline{\psi}_a\right\rangle_\Delta} \Delta A_K \approx \oint\limits_{\partial\Omega_{\underline{\mathbf{X}}}} \underline{\mathbf{N}} \cdot \left\langle \underline{\psi}_a \right\rangle_\Delta \,\mathrm{d}S = \int\limits_{\Omega_{\underline{\mathbf{X}}}} \underline{\nabla}_{\mathbf{X}} \cdot \left\langle \underline{\psi}_a \right\rangle_\Delta \mathrm{d}V\end{aligned} \tag{2.98}$$

whereas for the source (and storage) terms it reads

$$\int\limits_{\Omega} \rho\varphi_m \mathrm{d}V = \sum_L \int\limits_{\Delta V_L} \rho\varphi_m \mathrm{d}V \qquad = \sum_L \underbrace{\frac{1}{\Delta V_L} \int\limits_{\Delta V_L} \rho\varphi_m \mathrm{d}V}_{:=\langle\rho\varphi_m\rangle_V} \Delta V_L \approx \int\limits_{\Omega_{\underline{\mathbf{X}}}} \langle\rho\varphi_m\rangle_V \,\mathrm{d}V \tag{2.99}$$

Finally, a macroscopic balance law

$$\frac{D}{Dt} \int\limits_{\Omega} \langle\rho\varphi_m\rangle_V \;\mathrm{d}V = \oint\limits_{\partial\Omega_{\underline{\mathbf{X}}}} \underline{\mathbf{N}} \cdot \left\langle \underline{\psi}_a \right\rangle_\Delta \;\mathrm{d}S + \int\limits_{\Omega_{\underline{\mathbf{X}}}} \langle\rho\psi_m\rangle_V \;\mathrm{d}V \tag{2.100}$$

is obtained with an equivalent local version

$$\langle\rho\dot{\varphi}_m\rangle_V = \underline{\nabla}_{\mathbf{X}} \cdot \left\langle \underline{\psi}_a \right\rangle_\Delta + \langle\rho\psi_m\rangle_V \;. \tag{2.101}$$

Comparing Eq. (2.101) with the average of balance (2.97) shows that finally the approximation of Eringen

$$\left\langle \underline{\nabla}_{\mathbf{x}} \cdot \underline{\psi}_a \right\rangle_V \approx \left\langle \underline{\psi}_a \right\rangle_\Delta \tag{2.102}$$

is to replace the average of the divergence of the flux by the "surface operator" $\langle(\circ)\rangle_\Delta$ applied to the flux. Unfortunately, to the author's knowledge, neither Eringen nor any other source in literature provided yet an explicit definition of the surface operator.

Microscopic balance laws of Cauchy-Boltzmann continuum

The Cauchy continuum at the microscale is described by the following balance equations:

$$\begin{aligned}
&\text{Energy:} && \rho\dot{\Phi} + \frac{1}{2}\rho\left(\underline{\mathbf{v}} \cdot \underline{\mathbf{v}}\right)^{\cdot} = \underline{\nabla}_{\mathbf{x}} \cdot \left(\underset{\sim}{\sigma} \cdot \underline{\mathbf{v}}\right) - \underline{\nabla}_{\mathbf{x}} \cdot \underline{\mathbf{q}} + \rho\underline{\mathbf{f}} \cdot \underline{\mathbf{v}} && (2.103)\\
&\text{Entropy:} && \rho\dot{\eta} + \underline{\nabla}_{\mathbf{x}} \cdot \underline{\mathbf{h}} \geq 0 && (2.104)\\
&\text{Linear momentum:} && \underline{\nabla}_{\mathbf{x}} \cdot \underset{\sim}{\sigma} + \rho\underline{\mathbf{f}} - \rho\dot{\underline{\mathbf{v}}} = 0 && (2.105)\\
&\text{Angular momentum:} && \underset{\approx}{\epsilon} : \underset{\sim}{\sigma} = 0 && (2.106)
\end{aligned}$$

whereby use was made already of the balance of mass. In these equations, Φ and η are the specific intrinsic energy and entropy, respectively. Furthermore, $\underline{\mathbf{v}}$, $\underset{\sim}{\sigma}$ and $\underline{\mathbf{f}}$ denote the velocity, stress and body force, respectively. The symbols $\underline{\mathbf{q}}$ and $\underline{\mathbf{h}}$ refer to the fluxes of heat and entropy, respectively.

Approximation of microscopic velocity field

For a micromorphic continuum of degree one, the microscopic velocity field $\underline{\mathbf{v}}(\underline{\mathbf{x}})$ is approximated by a polynomial of order one:

$$\tilde{\underline{\mathbf{v}}} = \underline{\mathbf{V}}(\underline{\mathbf{X}}) + \underset{\sim}{\mathbf{L}}^{\chi}(\underline{\mathbf{X}}) \cdot (\underline{\mathbf{x}} - \underline{\mathbf{X}}) \tag{2.107}$$

with the macroscopic velocity $\underline{\mathbf{V}}$ and a rate of microdeformation $\underset{\sim}{\mathbf{L}}^{\chi}$. Special cases of (2.107) are the Cosserat (micropolar) continuum with $\underset{\sim}{\mathbf{L}}^{\chi} = -\underline{\mathbf{\Omega}}^{\chi} \cdot \underset{\approx}{\epsilon}$ so that $\underline{\mathbf{\Omega}}^{\chi}(\underline{\mathbf{X}})$ is a microrate of rotation or the microdilatational continuum with $\underset{\sim}{\mathbf{L}}^{\chi} = \frac{1}{3}\dot{\chi}^{\mathrm{v}}\underset{\sim}{\mathbf{I}}$. In this context, the Cauchy continuum with $\underset{\sim}{\mathbf{L}}^{\chi} = 0$ can be seen as a micromorphic continuum of order zero.

Macroscopic balance laws

According to section 2.2.3, the microscopic balance laws of the Cauchy continuum from section 2.2.3 yield the following macroscopic counterparts:

Linear and Angular Momentum The microscopic balance of linear momentum (2.105) yields

$$0 = \nabla_{\underline{\mathbf{X}}} \cdot \underbrace{\langle \underset{\sim}{\sigma} \rangle_{\Delta}}_{=:\underset{\sim}{\mathbf{\Sigma}}} + \underbrace{\langle \rho \underline{\mathbf{f}} \rangle_{V}}_{=:\bar{\rho}\bar{\underline{\mathbf{f}}}} - \bar{\rho}\dot{\underline{\mathbf{V}}} \tag{2.108}$$

and allows to define the macroscopic values $\underset{\sim}{\mathbf{\Sigma}}$ and $\underline{\mathbf{f}}$ of (extrinsic) stress and body force, respectively. In (2.108), the approximation (2.107) of the velocity field was inserted for the inertia term and the barycentric definition (2.26) of $\underline{\mathbf{X}}$ was employed with macroscopic mass density $\bar{\rho}$ defined as volume average according to Eq. (2.25).

Berglund [67] employed the classical definition (2.40) of the macroscopic stress $\underset{\sim}{\mathbf{\Sigma}}$ in (2.108), though without addressing the double stresses or the surface operator in general.

Furthermore, a macroscopic counterpart of the balance of linear momentum weighted with the distance $\underline{\xi} = \underline{\mathbf{x}} - \underline{\mathbf{X}}$ will be needed for the energy balance. With respect to the linear approximation (2.107) of the velocity field, this might be interpreted as a Galerkin approach. The balance of linear momentum (2.105) weighted by $\underline{\mathbf{x}}$ can be written as

$$\nabla_{\underline{\mathbf{x}}} \cdot \left(\underset{\sim}{\sigma} \otimes \underline{\mathbf{x}}\right) - \underset{\sim}{\sigma}^{\mathrm{T}} + \rho\underline{\mathbf{f}} \otimes \underline{\mathbf{x}} - \rho\dot{\underline{\mathbf{v}}} \otimes \underline{\mathbf{x}} = 0 \tag{2.109}$$

and thus exhibits also the structure of a balance equation (2.97) so that the average theorem (2.101) can be applied to obtain a macroscopic counterpart. Upon subtraction of Eq. (2.108) weighted by the macroscopic location $\underline{\mathbf{X}}$ (and written in a form as Eq. (2.109)) and inserting again Eq. (2.107) for the inertia term, one obtains

$$0 = \nabla_{\underline{\mathbf{X}}} \cdot \underbrace{\langle \underset{\sim}{\sigma} \otimes (\underline{\mathbf{x}} - \underline{\mathbf{X}}) \rangle_{\Delta}}_{=:\underset{\approx}{\underline{\mathbf{M}}}} + \underbrace{\langle \underset{\sim}{\sigma} \rangle_{\Delta}^{\mathrm{T}}}_{=\underset{\sim}{\mathbf{\Sigma}}^{\mathrm{T}}} - \underbrace{\langle \underset{\sim}{\sigma}^{\mathrm{T}} \rangle_{V}}_{=:\bar{\underset{\sim}{\sigma}}^{\mathrm{T}}} + \underbrace{\langle \rho\underline{\mathbf{f}} \otimes (\underline{\mathbf{x}} - \underline{\mathbf{X}}) \rangle_{V}}_{=:\bar{\rho}\underset{\sim}{\mathbf{m}}} - \dot{\underset{\sim}{\mathbf{L}}}^{\chi} \cdot \underbrace{\langle \rho\underline{\xi} \otimes \underline{\xi} \rangle_{V}}_{=:\underset{\sim}{\mathbf{G}}_{\rho}} \tag{2.110}$$

The balance of angular momentum (2.106) yields the symmetry of the macroscopic intrinsic stress

$$0 = \underset{\approx}{\epsilon} : \bar{\underset{\sim}{\sigma}}\,. \tag{2.111}$$

The macroscopic counterpart to (2.106) weighted with $\underline{\xi}$ does not yield additional information.

Equations (2.108), (2.110) and (2.111) have identical structure as Eqs. (2.29), (2.30) and (2.31) of Mindlin (except higher order body forces $\underset{\sim}{\mathbf{m}}$ which could be incorporated easily in Mindlin's approach). The comparison shows that the internal stress $\bar{\underset{\sim}{\sigma}}$ corresponds to the volume average of the microscopic stress. The external stress $\underset{\sim}{\mathbf{\Sigma}}$ and the double stress $\underset{\approx}{\underline{\mathbf{M}}}$ are defined via the surface operator.

Eq. (2.111) can be also inserted in the skew-symmetric part of (2.110):

$$0 = \nabla_{\underline{\mathbf{X}}} \cdot \underset{\approx}{\underline{\mathbf{M}}} : \underset{\approx}{\underline{\epsilon}} - \underset{\sim}{\mathbf{\Sigma}} : \underset{\approx}{\underline{\epsilon}} + \bar{\rho}\underset{\sim}{\mathbf{m}} : \underset{\approx}{\underline{\epsilon}} - \dot{\underset{\sim}{\mathbf{L}}}^{\chi} \cdot \underset{\sim}{\mathbf{G}}_{\rho} : \underset{\approx}{\underline{\epsilon}} \tag{2.112}$$

The term $\underset{\sim}{\mathbf{\Sigma}} : \underset{\approx}{\underline{\epsilon}}$ on the right-hand side can be transformed to storage and divergence parts as in classical continuum mechanics so that, in absence of body forces and moments, (2.112) as the skew-symmetric part of (2.110) has conservation type and can, in analogy to classical continuum mechanics, also be interpreted as macroscopic balance of angular momentum (as usually done in Cosserat theory, cf. Section 3.6.2).

Energy and Entropy The averaged microscopic energy balance (2.103) becomes

$$\underbrace{\left\langle \rho\dot{\Phi}\right\rangle_V}_{=:\bar{\rho}\dot{\bar{\Phi}}} + \frac{1}{2}\left\langle \rho\left(\underline{\mathbf{v}}\cdot\underline{\mathbf{v}}\right)^{\bullet}\right\rangle_V = \nabla_{\underline{\mathbf{X}}} \cdot \langle \underset{\sim}{\sigma} \cdot \underline{\mathbf{v}}\rangle_\Delta - \nabla_{\underline{\mathbf{X}}} \cdot \underbrace{\langle \underline{\mathbf{q}}\rangle_\Delta}_{=:\underline{\mathbf{Q}}} + \langle \rho \underline{\mathbf{f}} \cdot \underline{\mathbf{v}}\rangle_V \tag{2.113}$$

and allows to introduce the macroscopic values $\overline{\Phi}$ and $\underline{\mathbf{Q}}$ of specific intrinsic energy and heat flux, respectively. Replacing the local velocity field $\underline{\mathbf{v}}(\underline{\mathbf{x}})$ by its approximation (2.107) and inserting the definitions of the macroscopic stress measures yields

$$\bar{\rho}\dot{\bar{\Phi}} + \frac{1}{2}\bar{\rho}\left(\underline{\mathbf{V}}\cdot\underline{\mathbf{V}}\right)^{\bullet} + \frac{1}{2}\underset{\sim}{\mathbf{G}}_{\rho} : \left(\underset{\sim}{\mathbf{L}}^{\chi\mathrm{T}} \cdot \underset{\sim}{\mathbf{L}}^{\chi}\right)^{\bullet} = \nabla_{\underline{\mathbf{X}}} \cdot \left(\underset{\sim}{\mathbf{\Sigma}} \cdot \underline{\mathbf{V}} + \underset{\approx}{\underline{\mathbf{M}}} : \underset{\sim}{\mathbf{L}}^{\chi}\right) - \nabla_{\underline{\mathbf{X}}} \cdot \underline{\mathbf{Q}} + \bar{\rho}\underline{\mathbf{f}} \cdot \underline{\mathbf{V}} + \bar{\rho}\underset{\sim}{\mathbf{m}} : \underset{\sim}{\mathbf{L}}^{\chi} \tag{2.114}$$

The balance of internal energy is obtained by applying the product rule and inserting the balances of momenta (2.108), (2.110) and (2.111) as

$$\begin{aligned} \bar{\rho}\dot{\bar{\Phi}} &= \underset{\sim}{\mathbf{\Sigma}} : \nabla_{\underline{\mathbf{X}}}\underline{\mathbf{V}} + \left(\underset{\sim}{\bar{\sigma}}^{\mathrm{T}} - \underset{\sim}{\mathbf{\Sigma}}^{\mathrm{T}}\right) : \underset{\sim}{\mathbf{L}}^{\chi} + \underset{\approx}{\underline{\mathbf{M}}} \vdots \nabla_{\underline{\mathbf{X}}}\underset{\sim}{\mathbf{L}}^{\chi} - \nabla_{\underline{\mathbf{X}}} \cdot \underline{\mathbf{Q}} \\ &= \underset{\sim}{\bar{\sigma}} : \underset{\sim}{\mathbf{D}} + \underbrace{\left(\underset{\sim}{\mathbf{\Sigma}}^{\mathrm{T}} - \underset{\sim}{\bar{\sigma}}\right)}_{=\underset{\sim}{\mathbf{s}}} : \underset{\sim}{\mathbf{L}}^{e} + \underset{\approx}{\underline{\mathbf{M}}} \vdots \underset{\approx}{\underline{\mathbf{L}}}^{K} - \nabla_{\underline{\mathbf{X}}} \cdot \underline{\mathbf{Q}}\,. \end{aligned} \tag{2.115}$$

Therein, the Eulerian rates of deformation $\underset{\sim}{\mathbf{D}} = \operatorname{sym}(\nabla_{\underline{\mathbf{X}}}\underline{\mathbf{V}})$, $\underset{\sim}{\mathbf{L}}^{e} = \underline{\mathbf{V}} \otimes \nabla_{\underline{\mathbf{X}}} - \underset{\sim}{\mathbf{L}}^{\chi}$ and $\underset{\approx}{\underline{\mathbf{L}}}^{K} = \nabla_{\underline{\mathbf{X}}}\underset{\sim}{\mathbf{L}}^{\chi}$ have been introduced. For infinitesimal deformations, they coincide with the rates of Mindlin's measures of deformation $\underset{\sim}{\mathbf{D}} = \dot{\underset{\sim}{\mathbf{E}}}$, $\underset{\sim}{\mathbf{L}}^{e} = \dot{\underset{\sim}{\mathbf{e}}}$, $\underset{\approx}{\underline{\mathbf{L}}}^{K} = \dot{\underset{\approx}{\underline{\mathbf{K}}}}$ so that Eq. (2.115) recovers Mindlin's expression for the work for the isothermal and reversible case, compare in particular Eq. (2.28) in Section 2.1.3. Equation (2.115) can also be written as

$$\bar{\rho}\dot{\bar{\Phi}} = \underset{\sim}{\mathbf{\Sigma}} : \underset{\sim}{\mathbf{L}}^{e\mathrm{T}} + \underset{\sim}{\bar{\sigma}} : \operatorname{sym}\left(\underset{\sim}{\mathbf{L}}^{\chi}\right) + \underset{\approx}{\underline{\mathbf{M}}} \vdots \underset{\approx}{\underline{\mathbf{L}}}^{K} - \nabla_{\underline{\mathbf{X}}} \cdot \underline{\mathbf{Q}}\,. \tag{2.116}$$

This shows that that $\underset{\sim}{\mathbf{L}}^{\chi\mathrm{s}} := \operatorname{sym}\left(\underset{\sim}{\mathbf{L}}^{\chi}\right)$ and $\underset{\sim}{\mathbf{L}}^{e\mathrm{T}}$ are the work-conjugate deformation measures to $\underset{\sim}{\bar{\sigma}}$ and $\underset{\sim}{\mathbf{\Sigma}}$ as favored by Eringen and Suhubi [9].

The microscopic entropy balance (2.104) yields its macroscopic counterpart of identical structure

$$\underbrace{\langle \rho\dot{\eta}\rangle_V}_{:=\bar{\rho}\dot{S}} + \nabla_{\underline{\mathbf{X}}} \cdot \underbrace{\langle \underline{\mathbf{h}}\rangle_\Delta}_{:=\underline{\mathbf{H}}} \geq 0 \tag{2.117}$$

defining the macroscopic values S and $\underline{\mathbf{H}}$ of specific entropy and flux of entropy, respectively.

Remarks

The problem is that, to the author's best knowledge, neither Eringen nor other researchers provided yet an explicit definition of the surface operator $\langle\!\langle(\circ)\rangle\!\rangle_\Delta$ which occurs for every flux-like quantity. Kinematic micro-macro relations were specified by Eringen neither.

2.2.4. Average field theory by Forest et al.

Kinematics

In order to address kinematic micro-macro relations for a micromorphic theory, Forest and Sab [46, 47] distinguished between the *actual* displacement field $\underline{\mathbf{u}}(\underline{\mathbf{x}})$ at the microscale and its macroscopic *approximation* $\underline{\tilde{\mathbf{u}}}(\underline{\mathbf{X}}, \underline{\mathbf{x}})$. For the latter, Forest et al. adopted the linear approach of Mindlin and Eringen, Eqs. (2.21) and (2.107), respectively,

$$\underline{\tilde{\mathbf{u}}} = \underline{\mathbf{U}}(\underline{\mathbf{X}}) + \underset{\sim}{\chi}(\underline{\mathbf{X}}) \cdot (\underline{\mathbf{x}} - \underline{\mathbf{X}}) \,. \tag{2.118}$$

The macroscopic displacement $\underline{\mathbf{U}}(\underline{\mathbf{X}})$ and the microdeformation $\underset{\sim}{\chi}(\underline{\mathbf{X}})$ are defined from the postulate that the error between this approximation and the true microscopic field $\underline{\mathbf{u}}(\underline{\mathbf{x}})$ is minimized in a quadratic sense over a microstructural volume element $\Delta V(\underline{\mathbf{X}})$:

$$\left\langle \|\underline{\mathbf{u}}(\underline{\mathbf{x}}) - \underline{\tilde{\mathbf{u}}}\|^2 \right\rangle_V \xrightarrow{\underline{\mathbf{U}}, \underset{\sim}{\chi}} \min. \tag{2.119}$$

If $\underline{\mathbf{X}}$ is defined as the location of the geometric center of ΔV, i. e.

$$\underline{\mathbf{X}} = \langle \underline{\mathbf{x}} \rangle_V \ . \tag{2.120}$$

then the optimization problem (2.119) yields [46]

$$\underline{\mathbf{U}}(\underline{\mathbf{X}}) = \langle \underline{\mathbf{u}} \rangle_V \tag{2.121}$$

$$\underset{\sim}{\chi}(\underline{\mathbf{X}}) = \langle \underline{\mathbf{u}}(\underline{\mathbf{x}}) \otimes (\underline{\mathbf{x}} - \underline{\mathbf{X}}) \rangle_V \cdot \underset{\sim}{\mathbf{G}}^{-1} \tag{2.122}$$

with $\underset{\sim}{\mathbf{G}}$ referring again to the second geometric moment of ΔV, Eq. (2.82).

Both, in the macroscopic theory of Mindlin, section 2.1.3, and in the microscopic theory of Eringen, section 2.2.3, the gradients of the macroscopic quantities $\underline{\mathbf{U}}(\underline{\mathbf{X}})$ and $\underset{\sim}{\chi}(\underline{\mathbf{X}})$, or of the respective velocities, appear as measures of deformation.

These macroscopic gradients of the integrals in (2.121) and (2.121) defined by the average operator (2.23) can be computed by the Leibniz integral rule (Reynolds transport theorem)

$$\frac{\mathrm{d}\,\langle(\circ)(\underline{\mathbf{x}}, \underline{\mathbf{X}})\rangle_V}{\mathrm{d}X_j} = \left\langle \frac{\partial((\circ))}{\partial x_j} + \frac{\partial((\circ))}{\partial X_j} \right\rangle_V . \tag{2.123}$$

Therein, it was assumed that the size ΔV does not depend on $\underline{\mathbf{X}}$. Applying the average theorem (2.123) to Eqs. (2.121) and (2.121) yields

$$\underline{\nabla_{\underline{\mathbf{X}}} \mathbf{U}} = \left\langle \underline{\nabla_{\underline{\mathbf{x}}} \mathbf{u}} \right\rangle_V \tag{2.124}$$

$$\underset{\sim}{\underline{\mathbf{K}}} = \underline{\nabla_{\underline{\mathbf{X}}}} \underset{\sim}{\chi} = \left\langle \underline{\nabla_{\underline{\mathbf{x}}} \mathbf{u}} \otimes \underline{\xi} \right\rangle_V \cdot \underset{\sim}{\mathbf{G}}^{-1} = \left[\frac{1}{\Delta V} \oint\limits_{\Delta V(\underline{\mathbf{X}})} \underline{\mathbf{n}}\underline{\mathbf{u}}\underline{\xi} \,\mathrm{d}S \right] \cdot \underset{\sim}{\mathbf{G}}^{-1} - \underset{\approx}{\mathbf{I}}_{\mathrm{T}} : \left(\langle \underline{\mathbf{u}} \rangle_V \, \underset{\sim}{\mathbf{G}}^{-1} \right) \tag{2.125}$$

$$K_{ijk} = \frac{\partial \chi_{jk}}{\partial X_i} = \left\langle \frac{\partial u_j}{\partial x_i} \xi_m \right\rangle_V G^{-1}_{mk} = \left[\frac{1}{\Delta V} \oint\limits_{\Delta V(\underline{\mathbf{X}})} u_j \xi_m n_i \,\mathrm{d}S \right] G^{-1}_{mk} - \langle u_j \rangle_V \, G^{-1}_{ik} \,.$$

Therein, $\underset{\approx}{\mathbf{I}}_{\mathrm{T}}$ is the transposing forth order tensor defined as $\underset{\sim}{\mathbf{a}}^{\mathrm{T}} = \underset{\approx}{\mathbf{I}}_{\mathrm{T}} : \underset{\sim}{\mathbf{a}}$. For Eq. (2.125) it was assumed that the geometric moment $\underset{\sim}{\mathbf{G}}$ does not depend on $\underline{\mathbf{X}}$. The symmetric part of Eq. (2.124) coincides with Hill's definition (2.36) of the macroscopic strain in the classical theory of homogenisation.

Note that the kinematic micro-macro relations (2.121), (2.122), (2.125) for $\underline{\mathbf{U}}$, $\underset{\sim}{\chi}$ and $\underset{\sim}{\underline{\mathbf{K}}}$, respectively, cannot be converted completely to surface integrals. Although the macroscopic displacement $\underline{\mathbf{U}} = \langle \underline{\mathbf{u}} \rangle_V$ itself is mostly of minor interest, it remains as volume term in Eq. (2.125). This term is necessary for Eq. (2.125) to be objective, compare section 2.2.2. Comparing in particular Eq. (2.125) with Eq. (2.94) shows that the modified micro-macro relation (2.94) for the second gradient $\underset{\sim}{\underline{\mathbf{K}}}^{\nabla\nabla U} = \underline{\nabla}_{\underline{\mathbf{X}}} \underline{\mathbf{u}} \otimes \underline{\nabla}_{\underline{\mathbf{X}}}$ contains certain components of $\underset{\sim}{\underline{\mathbf{K}}}$ from relation (2.125). However, $\underset{\sim}{\underline{\mathbf{K}}}^{\nabla\nabla U}$ is symmetric whereas $\underset{\sim}{\underline{\mathbf{K}}}$ does not exhibit any symmetry ad hoc.

Polynomial approach

Forest et al. [47, 68, 69] extended the quadratic ansatz (2.65) of Gologanu et al. [44] by a cubic term (with coefficients $\underset{\approx}{\mathbf{D}}$) and fluctuations $\Delta\underline{\mathbf{v}}(\underline{\xi})$

$$\underline{\mathbf{u}} = \underline{\mathbf{A}} + \underset{\sim}{\mathbf{B}} \cdot \underline{\xi} + \underset{\sim}{\underline{\mathbf{C}}} : (\underline{\xi}\underline{\xi}) + \underset{\approx}{\mathbf{D}} \vdots (\underline{\xi}\underline{\xi}\underline{\xi}) + \Delta\underline{\mathbf{u}}(\underline{\xi}) \tag{2.126}$$

in order to homogenize a Cauchy-Boltzmann continuum at the microscale towards a micromorphic continuum at the macroscale. Later, even a quartic term was amendend [68]. However, certain kinematic micro-macro relations cannot be transformed to surface integrals as mentioned already. This means that the microdeformation $\underset{\sim}{\chi}$ and a certain part of $\underset{\sim}{\underline{\mathbf{K}}}$ cannot be prescribed by kinematic boundary conditions.

For that reason, several authors, e. g. [47, 50, 68, 70], assumed a polynomial displacement field (2.126) in the *complete volume element* $\underline{\xi} \in \Delta V(\underline{\mathbf{X}})$ and inserted it to the kinematic micro-macro relations (2.121), (2.122), (2.124) and (2.125). This are four tensorial equations for the four tensors $\underline{\mathbf{U}}$, $\underset{\sim}{\chi}$, $\underline{\nabla}_{\underline{\mathbf{X}}} \underline{\mathbf{U}}$ and $\underset{\sim}{\underline{\mathbf{K}}}$. However, the coefficient tensors $\underline{\mathbf{A}}$, $\underset{\sim}{\mathbf{B}}$, $\underset{\sim}{\underline{\mathbf{C}}}$, $\underset{\approx}{\mathbf{D}}$ have 60 independent components which contribute to $\underline{\mathbf{v}}(\underline{\xi})$ in (2.126) compared to 48 independent coefficients of the macroscopic kinematic quantities $\underline{\mathbf{U}}$, $\underset{\sim}{\chi}$, $\underline{\nabla}_{\underline{\mathbf{X}}} \underline{\mathbf{U}}$ and $\underset{\sim}{\underline{\mathbf{K}}}$. Thus, even without fluctuations $\Delta\underline{\mathbf{v}}(\underline{\xi}) = 0$, the coefficient tensors cannot be determined uniquely. Mostly, certain coefficients were fixed more or less arbitrarily *ad hoc* to a certain value in order to solve the under-determined system of equations for $\underline{\mathbf{A}}$, $\underset{\sim}{\mathbf{B}}$, $\underset{\sim}{\underline{\mathbf{C}}}$, $\underset{\approx}{\mathbf{D}}$ (and eventually coefficients of quartic terms). Similarly, a piecewise linear approach with fixed coefficients was employed in several studies [67, 71–74].

Having identified these coefficients in terms of $\underline{\mathbf{U}}$, $\underset{\sim}{\chi}$, $\underline{\nabla}_{\underline{\mathbf{X}}} \underline{\mathbf{U}}$ and $\underset{\sim}{\underline{\mathbf{K}}}$, attempts were presented were the polynomial field (2.126) was prescribed either only at the boundary $\underline{\xi} \in \partial\Delta V$ or in the complete volume element $\underline{\xi} \in \Delta V(\underline{\mathbf{X}})$. In both cases, the internal work $\left\langle \underset{\sim}{\sigma} : \dot{\underset{\sim}{\varepsilon}} \right\rangle_V$ can be evaluated and used to define the work conjugate stress measures by means of a generalized Hill-Mandel condition

$$\left\langle \underset{\sim}{\sigma} : \dot{\underset{\sim}{\varepsilon}} \right\rangle_V = \bar{\underset{\sim}{\sigma}} : \dot{\underset{\sim}{\mathbf{E}}} + \underset{\sim}{\mathbf{s}} : \dot{\underset{\sim}{\mathbf{e}}} + \underset{\sim}{\underline{\mathbf{M}}} \vdots \dot{\underset{\sim}{\underline{\mathbf{K}}}} \tag{2.127}$$

motivated by the macroscopic virtual work (2.28). In Eq. (2.127) it was assumed that the fluctuations $\Delta\underline{\mathbf{u}}(\underline{\xi})$, if considered, do not contribute to the work. A number of attempts was presented to characterize potential symmetry properties of $\Delta\underline{\mathbf{u}}(\underline{\xi})$ which shall not be discussed here.

If a polynomial field like (2.126) is prescribed only at the boundary $\underline{\xi} \in \partial\Delta V$ as done e. g. in [69, 70, 75], a boundary value problem is formulated at the microscale together with the equilibrium condition $\underline{\nabla}_{\underline{\mathbf{x}}} \cdot \underset{\sim}{\sigma} = 0$ in ΔV (and an adequate description of $\Delta\underline{\mathbf{v}}$). This boundary value problem problem contains the classical homogenisation as a special case.

However, the non-classical kinematic micro-macro relations (2.121) and (2.125) are in general not satisfied. In this sense, the micromorphic homogenisation with polynomial boundary conditions is inconsistent. In contrast, if the polynomial field (2.126) is prescribed in the complete volume element $\underline{\xi} \in \Delta V$, then also the non-classical kinematic micro-macro relations can be satisfied. If the non-classical terms are absent, the approach corresponds to a Taylor-Voigt estimate which is known to yield only very rough upper bound estimates. In both cases, the indeterminacy of the cubic coefficients of (2.126) is problematic.

Minimal loading conditions

As alternative to the polynomial approach to micromorphic homogenisation, Jänicke and Steeb [76] proposed the "minimal loading conditions" concept. The idea is to prescribe the kinematic micro-macro relations (2.121), (2.122), (2.124) and (2.125) as only global constraints at the micro-scale in a displacement-based FE^2 formulation.

In the present contribution, the corresponding boundary-value problem at the micro-scale shall be formulated. Firstly, hyperelastic material is considered at the micro-scale. In this case, the boundary-value problem can be formulated equivalently in variational form by the principle of minimum strain energy. The kinematic micro-macro relations are implemented by Lagrange multipliers as only constraints:

$$
\begin{aligned}
\mathcal{L} = \langle W \rangle_V + \underline{\lambda}^U \cdot \left(\underline{\mathbf{U}} - \langle \underline{\mathbf{u}} \rangle_V\right) + \underset{\sim}{\lambda}^{\nabla U} : \left(\underline{\nabla}_{\mathbf{X}} \underline{\mathbf{U}} - \left\langle \underline{\nabla}_{\mathbf{x}} \underline{\mathbf{u}} \right\rangle_V \right) + \\
+ \underset{\sim}{\lambda}^{\chi} : \left(\underset{\sim}{\chi} - \left\langle \underline{\mathbf{u}} \otimes \underline{\xi} \right\rangle_V \cdot \underset{\sim}{\mathbf{G}}^{-1} \right) + \underset{\approx}{\lambda}^{K} \vdots \left[\underset{\approx}{\underline{\mathbf{K}}} - \left\langle \underline{\nabla}_{\mathbf{x}} \underline{\mathbf{u}} \otimes \underline{\xi} \right\rangle_V \cdot \underset{\sim}{\mathbf{G}}^{-1} \right] \to \text{Min.}\,,
\end{aligned}
\tag{2.128}
$$

The stationarity conditions are the kinematic micro-macro relations (2.121), (2.122), (2.124) and (2.125) as well as

$$
0 = \delta\mathcal{L} = \left\langle \underset{\sim}{\sigma} : \delta\underset{\sim}{\varepsilon} \right\rangle_V - \underline{\lambda}^U \cdot \langle \delta\underline{\mathbf{u}} \rangle_V - \underset{\sim}{\lambda}^{\nabla U} : \left\langle \underline{\nabla}_{\mathbf{x}} \delta\underline{\mathbf{u}} \right\rangle_V - \underset{\sim}{\lambda}^{\chi} : \left\langle \delta\underline{\mathbf{u}}\underline{\xi} \right\rangle_V \cdot \underset{\sim}{\mathbf{G}}^{-1} - \underset{\approx}{\lambda}^{K} \vdots \left\langle \underline{\nabla}_{\mathbf{x}} \delta\underline{\mathbf{u}}\underline{\xi} \right\rangle_V \cdot \underset{\sim}{\mathbf{G}}^{-1}\,.
\tag{2.129}
$$

Equation (2.129) holds for all kinematically admissible trial fields $\delta\underline{\mathbf{u}}(\underline{\mathbf{x}})$. Among those fields is the actual velocity yield $\underline{\mathbf{v}}(\underline{\mathbf{x}})$. Inserting it together with the kinematic micro-macro relations (2.121), (2.122), (2.124) and (2.125) yields

$$
\left\langle \underset{\sim}{\sigma} : \dot{\underset{\sim}{\varepsilon}} \right\rangle_V = \underline{\lambda}^U \cdot \dot{\underline{\mathbf{U}}} + \underset{\sim}{\lambda}^{\nabla U} : \underline{\nabla}_{\mathbf{X}} \dot{\underline{\mathbf{U}}} + \underset{\sim}{\lambda}^{\chi} : \dot{\underset{\sim}{\chi}} + \underset{\approx}{\lambda}^{K} \vdots \dot{\underset{\approx}{\underline{\mathbf{K}}}}\,.
\tag{2.130}
$$

Interpreting Eq. (2.130) as a generalized Hill-Mandel lemma, it turns out that the Lagrange multipliers $\underline{\lambda}^U$, $\underset{\sim}{\lambda}^{\nabla U}$, $\underset{\sim}{\lambda}^{\chi}$ and $\underset{\approx}{\lambda}^{K}$ are the work-conjugate measures to the kinematic quantities $\underline{\mathbf{U}}$, $\underline{\nabla}_{\mathbf{X}}\underline{\mathbf{U}}$, $\underset{\sim}{\chi}$ and $\underset{\approx}{\underline{\mathbf{K}}}$, respectively. Favorably, Eq. (2.130) is written in terms of the objective deformation measures $\underset{\sim}{\mathbf{E}}$, $\underset{\sim}{\mathbf{e}}$ and $\underset{\approx}{\underline{\mathbf{K}}}$ as

$$
\left\langle \underset{\sim}{\sigma} : \dot{\underset{\sim}{\varepsilon}} \right\rangle_V = \left[\underset{\sim}{\lambda}^{\nabla U} + \underset{\sim}{\lambda}^{\chi} \right] : \dot{\underset{\sim}{\mathbf{E}}} - \underset{\sim}{\lambda}^{\chi} : \dot{\underset{\sim}{\mathbf{e}}} + \underset{\approx}{\lambda}^{K} \vdots \dot{\underset{\approx}{\underline{\mathbf{K}}}} + \underline{\lambda}^U \cdot \dot{\underline{\mathbf{U}}} + \left[\underset{\sim}{\lambda}^{\nabla U} + \underset{\sim}{\lambda}^{\chi\mathrm{T}} \right] : \underset{\sim}{\mathbf{W}}
\tag{2.131}
$$

A comparison with the macroscopic internal work in Eq. (2.28) reveals that the Lagrange multipliers are related to the macroscopic stress measures as

$$
\bar{\underset{\sim}{\sigma}} = \operatorname{sym}\left(\underset{\sim}{\lambda}^{\nabla U} + \underset{\sim}{\lambda}^{\chi} \right), \qquad \underset{\sim}{\mathbf{s}} = -\underset{\sim}{\lambda}^{\chi}\,, \qquad \underset{\approx}{\underline{\mathbf{M}}} = \underset{\approx}{\lambda}^{K}\,.
\tag{2.132}
$$

Furthermore, Eq. (2.129) can be evaluated for a rigid translation and a rigid rotation yielding $\underline{\lambda}^U = 0$ and $\operatorname{skw}\left(\underset{\sim}{\lambda}^{\nabla U} + \underset{\sim}{\lambda}^{\chi\mathrm{T}}\right) = 0$ as conditions of total equilibrium of the volume element ΔV. Consequently, the last two terms in Eq. (2.131) being related to macroscopic rigid body motions $\dot{\underline{\mathbf{U}}}$ and $\underset{\sim}{\mathbf{W}} = \operatorname{skw} \underline{\nabla}_{\mathbf{X}} \dot{\underline{\mathbf{U}}}$ vanish identically.

With these results, the strong form to Eq. (2.129) can be written as

$$\underline{\nabla}_{\mathbf{x}} \cdot \underset{\sim}{\sigma} = \underset{\sim}{\mathbf{s}} \cdot \underset{\sim}{\mathbf{G}}^{-1} \cdot \underset{\sim}{\xi} + \left(\underset{\approx}{\mathbf{I}}_{\mathrm{T}} : \underset{\approx}{\mathbf{M}} \right) : \underset{\sim}{\mathbf{G}}^{-1} \qquad \forall \underset{\sim}{\xi} \in \Delta V \tag{2.133}$$

$$\underline{\mathbf{n}} \cdot \underset{\sim}{\sigma} = \underline{\mathbf{n}} \cdot \left(\bar{\underset{\sim}{\sigma}} + \underset{\sim}{\mathbf{s}}^{\mathrm{T}} \right) + \underline{\mathbf{n}} \cdot \underset{\approx}{\mathbf{M}} \cdot \underset{\sim}{\mathbf{G}}^{-1} \cdot \underset{\sim}{\xi} \qquad \forall \underset{\sim}{\xi} \in \partial \Delta V \tag{2.134}$$

Obviously, in absence of non-classical stresses $\underset{\sim}{\mathbf{s}} = 0$ and $\underset{\approx}{\mathbf{M}} = 0$, the boundary-value problem reduces to the classical homogenisation with static boundary conditions (2.43). Thus, the concept of minimal loading conditions may be interpreted as extension of static boundary conditions towards micromorphic homogenisation. However, in classical homogenisation a micro-macro relation (2.40) is imposed for the stress as well which has to be satisfied by static boundary conditions. To the author's knowledge, no such relations were proposed yet for the micromorphic homogenisation.

For the classical homogenisation, the macroscopic stress can be defined as volume average (2.35) or via a surface integral according to Eq. (2.40). Both definitions coincide since $\underline{\nabla}_{\mathbf{x}} \cdot \underset{\sim}{\sigma} = 0$ is imposed $\forall \underset{\sim}{\xi} \in \Delta V$ in Eq. (2.38). In contrast, by means of the minimal loading conditions concept, in their role as Lagrange multipliers certain macroscopic stresses act like volume forces in Eq. (2.133). In particular, the volume terms are associated with those deformation measures whose kinematic micro-macro relations cannot be converted to surface integrals. In view of Eq. (2.118), Forest and Sab [77] interpreted the microdeformation tensor $\underset{\sim}{\chi}$ as "relaxed" gradient of displacements. In this sense, the appearance of the difference stress $\underset{\sim}{\mathbf{s}}$ as distributed volume force in Eq. (2.133) can be interpreted as a penalty for the difference between $\underset{\sim}{\chi}$ and the actual gradient of displacements.

Evaluating the volume and surface definitions Eqs. (2.35) and (2.40) under consideration of Eq. (2.120) as

$$\frac{1}{\Delta V} \oint_{\partial \Delta V} \underset{\sim}{\xi} \otimes \underline{\mathbf{n}} \cdot \underset{\sim}{\sigma} \, \mathrm{d}S = \bar{\underset{\sim}{\sigma}} + \underset{\sim}{\mathbf{s}}^{\mathrm{T}} \tag{2.135}$$

$$\left\langle \underset{\sim}{\sigma} \right\rangle_V = \frac{1}{\Delta V} \oint_{\partial \Delta V} \underset{\sim}{\xi} \otimes \underline{\mathbf{n}} \cdot \underset{\sim}{\sigma} \, \mathrm{d}S - \left\langle \underset{\sim}{\xi} \otimes \left(\underline{\nabla}_{\mathbf{x}} \cdot \underset{\sim}{\sigma} \right) \right\rangle_V = \bar{\underset{\sim}{\sigma}} \tag{2.136}$$

shows that the surface integral yields the external stress $\underset{\sim}{\mathbf{\Sigma}} = \bar{\underset{\sim}{\sigma}} + \underset{\sim}{\mathbf{s}}^{\mathrm{T}}$ whereas the volume average yields the internal stress $\bar{\underset{\sim}{\sigma}}$.

According to Mindlin, the second gradient theory is a special case of the micromorphic theory. Thus, it is appealing to insert the stress field related to Eq. (2.133) with static boundary condition (2.134) to the micro-macro relation (2.87) of Kouznetsova, Gologanu et al. The latter was written either as a volume integral or a surface integral. For Eqs. (2.133)–(2.134), both integrals evaluate to

$$\frac{1}{2\Delta V} \oint_{\partial \Delta V} \xi_i n_m \sigma_{mj} \xi_k \, \mathrm{d}S = \frac{1}{2} \left(M_{ijk} + M_{kji} + M_{mjp} {G_{mp}}^{-1} G_{ik} \right) \tag{2.137}$$

$$\frac{1}{2} \left\langle \xi_i \sigma_{jk} + \sigma_{ij} \xi_k \right\rangle_V = \frac{1}{2\Delta V} \oint_{\partial \Delta V} \xi_i n_m \sigma_{mj} \xi_k \, \mathrm{d}S - \left\langle \xi_i \sigma_{mj,m} \xi_k \right\rangle_V = \frac{1}{2} \left(M_{ijk} + M_{kji} \right) . \tag{2.138}$$

It turns out that both integrals are related only to the part of the double stress $\underset{\approx}{\mathbf{M}}$ which is symmetric with respect to its first and third index. The skew-symmetric part does not contribute to either of the integrals. This observation is related to the fact that within the second-gradient theory, the second displacement gradient $\underset{\sim}{\mathbf{K}}^{\nabla\nabla U}$ or, equivalently, the strain gradient $\underset{\sim}{\mathbf{K}}^{\nabla E}$ as additional deformation measures exhibits a symmetry and so do their work-conjugate stress measures $\underset{\approx}{\mathbf{M}}^{\nabla\nabla U}$ and $\underset{\approx}{\mathbf{M}}^{\nabla E}$, respectively. For the micromorphic theory, the stress $\underset{\approx}{\mathbf{M}}$ defined to be work-conjugate to the gradient of the microdeformation $\underset{\approx}{\mathbf{K}}$ does not exhibit necessarily such a symmetry. For the same reason, a quadratic polynomial (2.65) cannot be used as kinematic boundary condition to satisfy the kinematic micro-macro relation (2.125) for $\underset{\approx}{\mathbf{K}}$ ad hoc.

Anyway, for a hyperelastic material, the Hill-Mandel condition (2.131) with Eq. (2.132) can be integrated towards a macroscopic strain energy density

$$\overline{W}(\underset{\sim}{\mathbf{E}}, \underset{\sim}{\mathbf{e}}, \underset{\approx}{\mathbf{K}}) = \langle W \rangle_V \tag{2.139}$$

as average of its microscopic counterpart. It forms indeed a potential for the macroscopic stresses $\bar{\underset{\sim}{\sigma}}$, $\underset{\sim}{\mathbf{s}}$ and $\underset{\approx}{\mathbf{M}}$ as in Mindlin's theory, Eq. (2.29) (and assumed e. g. in [4, 47]). By means of Ritz' method, approximate solutions to the variational problem (2.128) can be constructed. In particular, a polynomial ansatz like Eq. (2.126) may be chosen for $\underset{\sim}{\xi} \in \Delta V(\underline{\mathbf{X}})$. By means of interpretation as Ritz approach to the problem of minimal loading conditions, it is immediately clear how the spurious coefficients of cubic, quartic or even higher terms are to be determined. Vice versa, a polynomial ansatz (2.126) with arbitrarily fixed coefficients which satisfy the kinematic micro-macro relations provides a rigorous upper bound — however, in general not the best one among cubic polynomials.

Remarks

The kinematic micro-macro relations of the average field theory can be implemented using the minimal loading conditions concept. In this way, a boundary-value is formulated at the microscale whose solution allows to derive macroscopic constitutive laws for any material behavior at the microscale. The surface and volume integrals from classical theory of homogenisation constitute suitable kinetic micro-macro relations for the internal and the external stress, respectively. However, no such relation could be found for the double stress $\underset{\approx}{\mathbf{M}}$ and no kinematic boundary condition could be identified. The minimal loading conditions concept can be seen as extension of static boundary conditions in classical theory of homogenisation. However, static boundary conditions are seldom chosen in classical homogenisation as they yield generally a response which underestimates the effective stiffness.

2.3. Scope of the present thesis

Comparing the discussed approaches, it can be found that Mindlin, Kouznetsova and Gologanu, Forest et al. incorporate kinematic relations at the microscale. However, the macroscopic balance equations are postulated via the method of virtual power. In contrast, Eringen derived the balance equations from an averaging procedure. However, kinematic micro-macro relations are missing in his theory as well as a rigorous definition of the utilized "surface operator".

A micromorphic theory should contain the strain-gradient theory as a special case. A comparison of the (modified) strain-gradient framework of Gologanu, Kouznetsova et al. with the micromorphic theory shows indeed several similarities. The (modified) kinematic micro-macro relation (2.94) for the second gradient contains several components of the corresponding relation (2.125) in the micromorphic theory. The kinetic micro-macro relation for the double stress from the strain-gradient theory yields at least the symmetric part of the micromorphic double stress, Eq. (2.138). The surface and volume definitions of the macroscopic stress from the classical theory of homogenisation allow to distinguish internal and external stress in Forest's approach to micromorphic theory. And both types of stresses are present in Eringen's approach as well.

Regarding the minimal loading conditions concept, it was found that the Lagrange multipliers which enforce those kinematic micro-macro relations which cannot be transformed to pure surface integrals, act like volume forces at the microscale in Eq. (2.133). Size effects are often observed for porous media like foams. However, the pores cannot carry such volume forces. The problem arises from the fact that the respective kinematic micro-macro relations require to have a displacement field defined everywhere at the microscale. Though, this is not uniquely possible within a pore.

The scope of the present thesis is modify the aforementioned approaches in a complete and consistent theory of micromorphic homogenisation, including the most relevant special cases of strain-gradient theory, micropolar theory and micropolar theory. Selected example applications, in particular for porous media, shall serve to demonstrate the method and to discuss its possibilities and limitations.

3. Homogenisation towards a micromorphic continuum

3.1. Thermodynamic considerations and generalized Hill-Mandel lemma

Let us assume, that the continuum at the microlevel does not only obey balance equations (2.103)–(2.106), but that it is furthermore a Coleman-Noll continuum [78] so that the specific internal energy $\Phi(\eta, \underset{\sim}{\mathbf{F}}, h)$ forms a potential for temperature θ and (Piola-Kirchhoff) stress $\underset{\sim}{\sigma}^{\mathrm{PK}}$:

$$\theta = \frac{\partial \Phi}{\partial \eta}, \qquad \underset{\sim}{\sigma}^{\mathrm{PK}} = \rho_0 \frac{\partial \Phi}{\partial \underset{\sim}{\mathbf{F}}} \tag{3.1}$$

Consequently, the microscopic energy balance (2.103) reduces to

$$\rho D - \rho\theta\dot{\eta} = \underline{\nabla}_{\underline{\mathbf{x}}} \cdot \underline{\mathbf{q}}\,, \tag{3.2}$$

wherein

$$D = -\frac{\partial \Phi}{\partial h}\dot{h} \tag{3.3}$$

denotes the specific dissipation due to a change of internal variables h. Equation (3.2) is again of balance type. Consequently, average lemma (2.101) leads to a macroscopic relation

$$\underbrace{\langle \rho D\rangle_V}_{=:\overline{\rho}\overline{D}} - \underbrace{\langle \rho\theta\dot{\eta}\rangle_V}_{=:\overline{\rho}\Theta\dot{S}} = \underline{\nabla}_{\underline{\mathbf{X}}} \cdot \underline{\mathbf{Q}}\,, \tag{3.4}$$

which implies the given definition of macroscopic values Θ and $\overline{D}$ of temperature and dissipation, respectively. For a material model at the microscale with $D \geq 0$, this definition implies $\overline{D} \geq 0$ at the macroscale. Equation (3.4) can be used to eliminate the heatflux $\underline{\mathbf{Q}}$ from the macroscopic balance of internal energy (2.115):

$$\overline{\rho}\dot{\overline{\Phi}} = \underset{\sim}{\mathbf{\Sigma}} : \underline{\nabla}_{\underline{\mathbf{X}}}\underline{\mathbf{V}} + \left(\underset{\sim}{\overline{\sigma}}^{\mathrm{T}} - \underset{\sim}{\mathbf{\Sigma}}^{\mathrm{T}}\right) : \underset{\sim}{\mathbf{L}}^{\chi} + \underset{\approx}{\underline{\mathbf{M}}} \vdots \underline{\underset{\sim}{\mathbf{L}}}^{K} + \overline{\rho}\Theta\dot{S} - \overline{\rho}\overline{D} \tag{3.5}$$

Furthermore, (3.1) has the consequence that the left-hand side of (3.5) can be written as

$$\overline{\rho}\dot{\overline{\Phi}} = \left\langle \rho\dot{\Phi}\right\rangle_V = \langle \rho\theta\dot{\eta}\rangle_V + \left\langle \underset{\sim}{\sigma} : \underset{\sim}{\mathbf{d}}\right\rangle_V - \langle \rho D\rangle_V\;. \tag{3.6}$$

Equating this relation to (3.5) and eliminating identical terms on both sides using (3.8) and the definitions in (3.4) leads to a generalized Hill-Mandel lemma

$$\begin{aligned}\left\langle \underset{\sim}{\sigma} : \underset{\sim}{\mathbf{d}}\right\rangle_V =& \underset{\sim}{\mathbf{\Sigma}} : \underline{\nabla}_{\underline{\mathbf{X}}}\underline{\mathbf{V}} + \left(\underset{\sim}{\overline{\sigma}}^{\mathrm{T}} - \underset{\sim}{\mathbf{\Sigma}}^{\mathrm{T}}\right) : \underset{\sim}{\mathbf{L}}^{\chi} + \underset{\approx}{\underline{\mathbf{M}}} \vdots \underline{\underset{\sim}{\mathbf{L}}}^{K} \\ =& \underset{\sim}{\overline{\sigma}} : \underset{\sim}{\mathbf{D}} + \underset{\sim}{\mathbf{s}} : \underset{\sim}{\mathbf{L}}^{e} + \underset{\approx}{\underline{\mathbf{M}}} \vdots \underline{\underset{\sim}{\mathbf{L}}}^{K}\end{aligned} \tag{3.7}$$

However, in contrast to classical homogenisation it is no ad-hoc requirement but a *consequence* of the employed definitions of macroscopic quantities and the fact that the continuum at the microscale is of Coleman-Noll type.

If the macroscopic specific internal energy can be identified as a function $\overline{\Phi}(\underset{\sim}{\mathbf{E}}, \underset{\sim}{\mathbf{e}}, \underset{\approx}{\mathbf{K}}, S, H)$ of macroscopic entropy S and intrinsic variables H as well as (Lagrangian) deformation measures $\underset{\sim}{\mathbf{E}}$, $\underset{\sim}{\mathbf{e}}$ and $\underset{\approx}{\mathbf{K}}$ then Eq. (3.5) can be fulfilled for all kinematically admissible fields $\underline{\mathbf{V}}(\underline{\mathbf{X}})$, $\underset{\sim}{\mathbf{L}}^{\chi}(\underline{\mathbf{X}})$ and $S(\underline{\mathbf{X}})$ (and thus also arbitrary values of their gradients) if and only if

$$\bar{\underset{\sim}{\sigma}}^{\mathrm{PK}} = \overline{\rho}\frac{\partial \overline{\Phi}}{\partial \underset{\sim}{\mathbf{E}}}, \qquad \underset{\sim}{\mathbf{s}}^{\mathrm{PK}} = \overline{\rho}\frac{\partial \overline{\Phi}}{\partial \underset{\sim}{\mathbf{e}}}, \qquad \underset{\approx}{\mathbf{M}}^{\mathrm{PK}} = \overline{\rho}\frac{\partial \overline{\Phi}}{\partial \underset{\approx}{\mathbf{K}}}, \qquad \Theta = \frac{\partial \overline{\Phi}}{\partial S}\,. \tag{3.8}$$

Thus, a homogenisation can equivalently be performed with respect to $\overline{\Phi}$ and $\overline{D}$ (and fluxes $\underline{\mathbf{Q}}$ and $\underline{\mathbf{H}}$ of heat and entropy in thermomechanical problems) as done e. g. in [4, 47].

Equations (3.8) would be a common finding of a Coleman-Noll procedure. However, in contrast to the latter no a priori constitutive law on the flux of entropy $\underline{\mathbf{H}}$ is necessary.

3.2. Surface operator and kinetic micro-macro relations

In the micromorphic theory of Eringen as outlined in Section 2.2.3, flux-like macroscopic quantities like the external stress $\underset{\sim}{\boldsymbol{\Sigma}}$, the double stress $\underset{\approx}{\mathbf{M}}$ or the fluxes $\underline{\mathbf{Q}}$ and $\underline{\mathbf{H}}$ of heat and entropy, respectively, are defined by application of the *surface operator* $\langle(\circ)\rangle_{\Delta}$ to the respective microscopic quantities. Unfortunately, Eringen did not provide an exact definition of the surface operator. However, the envisaged theory of homogenisation towards a micromorphic continuum shall contain the special case of classical homogenisation as presented in Section 2.2.1. In this section was shown that the macroscopic stress can be computed from a *surface integral* in Eq. (2.40) (as done also by Berglund [67]). A comparison of Eq. (2.40) with Eringen's definition of the macroscopic external stress $\underset{\sim}{\boldsymbol{\Sigma}}$ in (2.108) shows that both definitions coincide if the surface operator is defined as

$$\langle(\circ)\rangle_{\Delta} := \frac{1}{\Delta V}\oint\limits_{\partial\Delta V} \underline{\xi}\otimes\underline{\mathbf{n}}\cdot(\circ)\,\mathrm{d}S\,. \tag{3.9}$$

Consequently, the kinetic micro-macro relations for $\underset{\sim}{\boldsymbol{\Sigma}}$ and double stress $\underset{\approx}{\mathbf{M}}$ read

$$\underset{\sim}{\boldsymbol{\Sigma}} = \langle\underset{\sim}{\sigma}\rangle_{\Delta} = \frac{1}{\Delta V}\oint\limits_{\partial\Delta V} \underline{\xi}\otimes\underline{\mathbf{n}}\cdot\underset{\sim}{\sigma}\,\mathrm{d}S\,, \tag{3.10}$$

$$\underset{\approx}{\mathbf{M}} = \langle\underset{\sim}{\sigma}\underline{\xi}\rangle_{\Delta} = \frac{1}{\Delta V}\oint\limits_{\partial\Delta V} \underline{\xi}\otimes\underline{\mathbf{n}}\cdot\underset{\sim}{\sigma}\otimes\underline{\xi}\,\mathrm{d}S\,. \tag{3.11}$$

The internal stress as volume average

$$\bar{\underset{\sim}{\sigma}} = \langle\underset{\sim}{\sigma}\rangle_{V} \tag{3.12}$$

was already introduced by Eringen in Eq. (2.110). It has to be remarked that according to (3.11), the double stress $\underset{\approx}{\mathbf{M}}$ is symmetric with respect to its first and last index — a symmetry which is not required per se in Mindlin's theory as outlined in Section 2.1.3. Due to this symmetry, only the part $L^{K\mathrm{s}}_{ijk} = (L^{K}_{ijk} + L^{K}_{kji})/2$ of the gradient of rate of microdeformation $\underset{\approx}{\mathbf{L}}^{K}$ contributes to the internal energy which has the same symmetry. Consequently, the generalized Hill-Mandel lemma (3.7) becomes

$$\left\langle\underset{\sim}{\sigma}:\underset{\sim}{\mathbf{d}}\right\rangle_{V} = \underset{\sim}{\boldsymbol{\Sigma}}:\underline{\nabla}_{\underline{\mathbf{X}}}\underline{\mathbf{V}} + \left(\bar{\underset{\sim}{\sigma}}^{\mathrm{T}} - \underset{\sim}{\boldsymbol{\Sigma}}^{\mathrm{T}}\right):\underset{\sim}{\mathbf{L}}^{\chi} + \underset{\approx}{\mathbf{M}}\,\vdots\,\underset{\approx}{\mathbf{L}}^{K\mathrm{s}}\,. \tag{3.13}$$

Note that Eq. (3.11) is identical to the respective definition (2.87) in the second-gradient theory, up to a factor of 1/2. However, in Section 2.2.4 it was demonstrated that definition (3.11) of $\underset{\approx}{\mathbf{M}}$ is not compatible with the kinematic micro-macro relations of Forest et al. within the concept of minimal loading conditions.

3.3. Kinematic micro-macro relations

The question is thus, how the kinematic micro-macro relations need to be formulated such that they are compatible with the kinetic micro-macro relations (3.10)–(3.12) in the sense that they satisfy the generalized Hill-Mandel lemma (3.7). In Section 2.2.4 it was shown that a generalized Hill-Mandel condition can be satisfied by means of the concept of minimal loading conditions where the macroscopic stresses appear as Lagrange multipliers to enforce the kinematic micro-macro relations. This approach lead to a boundary value problem (2.133)–(2.134) at the microscale.

In order to reconstruct the kinematic micro-macro relations which are compatible with (3.10)–(3.12), it is advantageous to construct the minimal loading conditions in inverse direction, starting with the boundary value problem at the microscale.

In the Hill-Mandel lemma (3.7), the difference $\underset{\sim}{\mathbf{\Sigma}} - \underset{\sim}{\bar{\sigma}}$ between external and internal stress appears as work-conjugate term to the rate of microdeformation $\underset{\sim}{\mathbf{L}}^{\chi}$. Inserting Eqs. (3.10)–(3.12) and applying the Gauss theorem

$$\underset{\sim}{\mathbf{\Sigma}} - \underset{\sim}{\bar{\sigma}} = \left\langle \underline{\xi} \otimes \left(\underline{\nabla}_{\underline{\mathbf{x}}} \cdot \underset{\sim}{\sigma} \right) \right\rangle_V . \tag{3.14}$$

shows that the stress difference is related to $\underline{\nabla}_{\underline{\mathbf{x}}} \cdot \underset{\sim}{\sigma}$ at the microscale as was already found in Section 2.2.4. Therein, a linear dependency of $\underline{\nabla}_{\underline{\mathbf{x}}} \cdot \underset{\sim}{\sigma}$ on $\underline{\xi}$ was found as well as a linear dependency of the tractions $\underset{\sim}{\sigma} \cdot \underline{\mathbf{n}}$ at the boundary.

For this reason, such linear ansatzes are adopted here as well for the boundary-value problem at the microscale:

$$\underline{\nabla}_{\underline{\mathbf{x}}} \cdot \underset{\sim}{\sigma} = \underset{\sim}{\mathbf{A}} \cdot \underline{\xi} + \underline{\mathbf{B}} - \underline{\lambda}^V \qquad \text{in } \Delta V(\underline{\mathbf{X}}) \tag{3.15}$$

$$\underline{\mathbf{n}} \cdot \underset{\sim}{\sigma} = \underline{\mathbf{n}} \cdot \underset{\sim}{\mathbf{D}} + \underline{\mathbf{n}} \cdot \underset{\approx}{\mathbf{C}} \cdot \underline{\xi} \qquad \text{on } \partial\Delta V(\underline{\mathbf{X}}) . \tag{3.16}$$

Note that the Lagrange multiplier $\underline{\lambda}^V$ was inserted in Eq. (3.15) to enforce

$$\underline{\mathbf{V}} = \langle \underline{\mathbf{v}} \rangle_V , \tag{3.17}$$

compare Eqs. (2.91) and (2.121). However, $\underline{\lambda}^V = 0$ needs to hold since no work shall be associated with a rigid translation $\underline{\mathbf{V}}$. Thus, the kinetic micro-macro relations (3.10)–(3.12) together with the total balance equations for ΔV provide exactly as many linear equations as there are coefficients[1] in Eqs. (3.15)–(3.16). For simplicity only the case $\langle \underline{\xi} \rangle_V = 0$ shall be considered, i. e. that the geometric center coincides with the bary center of the volume element ΔV. In this case certain equations decouple. Firstly, it is found by inserting Eq. (3.16) to Eq. (3.10) that the coefficient $\underset{\sim}{\mathbf{D}}$ has to be identified with the external stress $\underset{\sim}{\mathbf{\Sigma}}$. Furthermore, inserting the ansatz to (3.11) and (3.14) allows to express the coefficients in terms of the additional stress measures:

$$\underset{\sim}{\mathbf{A}} = \left(\underset{\sim}{\mathbf{\Sigma}}^{\mathrm{T}} - \underset{\sim}{\bar{\sigma}}^{\mathrm{T}} \right) \cdot \underset{\sim}{\mathbf{G}}^{-1} \tag{3.18}$$

$$C_{ijk} = \frac{1}{2} M_{ijm} G^{-1}_{mk} - \frac{1}{2\,(2+n)} \delta_{ik} M_{mjn} G^{-1}_{mn} \tag{3.19}$$

Therein, $\underset{\sim}{\mathbf{G}}$ refers to the second geometric moment of ΔV according to Eq. (2.82). Note, that the linear boundary term (3.19) is in general not self-equilibrating in Eq. (3.16). Consequently,

[1] Due to the symmetry of the hyperstress $\underset{\approx}{\mathbf{M}}$, not all components of $\underset{\approx}{\mathbf{C}}$ contribute to $\underset{\approx}{\mathbf{M}}$. Vice versa, (3.11) does not determine $\underset{\approx}{\mathbf{C}}$ uniquely. Eq. (3.19) incorporates only those components of $\underset{\approx}{\mathbf{C}}$ which have the respective symmetry and which are thus uniquely defined.

for the boundary value problem (3.15)–(3.16) at the microscale to have a solution, the non-equilibrating part needs to be compensated by the volume term

$$
\begin{aligned}
\underline{\mathbf{B}} &= \left(\underset{\approx}{\mathbf{I}}_{\mathrm{T}} : \underline{\underset{\sim}{\mathbf{C}}}\right) : \underset{\sim}{\mathbf{I}} = \frac{1}{2+n}\left[\underset{\approx}{\mathbf{I}}_{\mathrm{T}} : \left(\underline{\underset{\sim}{\mathbf{M}}} \cdot \underset{\sim}{\mathbf{G}}^{-1}\right)\right] : \underset{\sim}{\mathbf{I}}, \\
B_j &= C_{iji} = \frac{1}{2+n} M_{mjn} G^{-1}_{mn} \,.
\end{aligned}
\tag{3.20}
$$

Finally, the balance equation and natural boundary conditions at the microscale become

$$
\underline{\nabla}_{\underline{\mathbf{x}}} \cdot \underset{\sim}{\sigma} = \left(\underset{\sim}{\mathbf{\Sigma}}^{\mathrm{T}} - \underset{\sim}{\bar{\sigma}}^{\mathrm{T}}\right) \cdot \underset{\sim}{\mathbf{G}}^{-1} \cdot \underline{\xi} + \frac{1}{2+n}\left(\underset{\approx}{\mathbf{I}}_{\mathrm{T}} : \underline{\underset{\sim}{\mathbf{M}}}\right) : \underset{\sim}{\mathbf{G}}^{-1} - \underline{\lambda}^{V}, \quad \underset{\sim}{\sigma}^{\mathrm{T}} = \underset{\sim}{\sigma} \quad \text{in } \Delta V(\underline{\mathbf{X}}) \tag{3.21}
$$

$$
\sigma_{ij,i} = \left(\Sigma_{kj} - \bar{\sigma}_{kj}\right) G^{-1}_{km} \xi_m + \frac{1}{2+n} M_{kjm} G^{-1}_{km} - \lambda^V_j
$$

$$
\underline{\mathbf{n}} \cdot \underset{\sim}{\sigma} = \underline{\mathbf{n}} \cdot \underset{\sim}{\mathbf{\Sigma}} + \frac{1}{2}\underline{\mathbf{n}} \cdot \underline{\underset{\sim}{\mathbf{M}}} \cdot \underset{\sim}{\mathbf{G}}^{-1} \cdot \underline{\xi} - \frac{1}{2\,(2+n)}\underline{\mathbf{n}} \cdot \underline{\xi}\left(\underset{\approx}{\mathbf{I}}_{\mathrm{T}} : \underline{\underset{\sim}{\mathbf{M}}}\right) : \underset{\sim}{\mathbf{G}}^{-1} \qquad \text{on } \partial\Delta V(\underline{\mathbf{X}}) \tag{3.22}
$$

$$
n_i \sigma_{ij} = n_i \Sigma_{ij} + \frac{1}{2} n_i M_{ijp} G^{-1}_{pm} \xi_m - \frac{1}{2(2+n)} n_i \xi_i M_{njp} G^{-1}_{np}
$$

Equations (3.21) and (3.22) are the Euler-Lagrange equations of the stationarity condition

$$
\begin{aligned}
0 = {}&\left\langle \underset{\sim}{\sigma} : \delta\underset{\sim}{\varepsilon}\right\rangle_V - \underset{\sim}{\mathbf{\Sigma}} : \left\langle \underline{\nabla}_{\underline{\mathbf{x}}} \delta\underline{\mathbf{u}}\right\rangle_V - \underline{\lambda}^V \cdot \left\langle \delta\underline{\mathbf{u}}\right\rangle_V + \left(\underset{\sim}{\mathbf{\Sigma}}^{\mathrm{T}} - \underset{\sim}{\bar{\sigma}}^{\mathrm{T}}\right) : \left(\left\langle \delta\underline{\mathbf{u}} \otimes \underline{\xi}\right\rangle_V \cdot \underset{\sim}{\mathbf{G}}^{-1}\right) \\
&- \underline{\underset{\sim}{\mathbf{M}}} \vdots \frac{1}{2}\left[\underset{\approx}{\mathbf{I}}_{\mathrm{S}} : \left(\underset{\sim}{\mathbf{G}}^{-1} \cdot \left\langle \underline{\xi} \otimes \underline{\nabla}_{\underline{\mathbf{x}}} \delta\underline{\mathbf{u}}\right\rangle_V - \frac{1}{2+n}\underset{\sim}{\mathbf{G}}^{-1}\left\langle \underline{\xi} \cdot \underline{\nabla}_{\underline{\mathbf{x}}} \delta\underline{\mathbf{u}}\right\rangle_V\right) : \underset{\approx}{\mathbf{I}}_{\mathrm{T}}\right] .
\end{aligned}
\tag{3.23}
$$

In the last term in Eq. (3.23), the symmetry of $\underline{\underset{\sim}{\mathbf{M}}}$ was taken into account which is why only the part of its co-factor contributes which has the same symmetry. The actual microscopic velocity field $\underline{\mathbf{v}}(\underline{\xi})$ is among the admissible test fields $\delta\underline{\mathbf{u}}(\underline{\xi})$ so that (3.23) holds also if $\delta\underline{\mathbf{u}}(\underline{\xi})$ is replaced by $\underline{\mathbf{v}}(\underline{\xi})$. Then, a comparison with the Hill-Mandel lemma (3.13) shows that the macroscopic rates of deformation have to be identified as

$$
\begin{aligned}
\underline{\nabla}_{\underline{\mathbf{X}}} \underline{\mathbf{V}} &= \left\langle \underline{\nabla}_{\underline{\mathbf{x}}} \underline{\mathbf{v}}\right\rangle_V \\
\underset{\sim}{\mathbf{L}}^{\chi} &= \left\langle \underline{\mathbf{v}} \otimes \underline{\xi}\right\rangle_V \cdot \underset{\sim}{\mathbf{G}}^{-1} \\
\underline{\underset{\sim}{\mathbf{L}}}^{K\mathrm{s}} &= \frac{1}{2}\underset{\approx}{\mathbf{I}}_{\mathrm{S}} : \left(\underset{\sim}{\mathbf{G}}^{-1} \cdot \left\langle \underline{\xi} \otimes \underline{\nabla}_{\underline{\mathbf{x}}} \underline{\mathbf{v}}\right\rangle_V - \frac{1}{2+n}\underset{\sim}{\mathbf{G}}^{-1}\left\langle \underline{\xi} \cdot \underline{\nabla}_{\underline{\mathbf{x}}} \underline{\mathbf{v}}\right\rangle_V\right) : \underset{\approx}{\mathbf{I}}_{\mathrm{T}}
\end{aligned}
\tag{3.24}
$$

$$
L^{K\mathrm{s}}_{ijk} = \frac{1}{2}\left[\frac{1}{2}\left\langle v_{j,i}\xi_m\right\rangle_V G^{-1}_{mk} + \frac{1}{2}\left\langle v_{j,k}\xi_m\right\rangle_V G^{-1}_{mi} - \frac{1}{2+n}\left\langle v_{j,m}\xi_m\right\rangle_V G^{-1}_{ik}\right] . \tag{3.25}
$$

Equation (3.17) for the macroscopic velocity remains valid together with $\underline{\lambda}^V = 0$. If the stresses $\underset{\sim}{\sigma}$ have a variational potential $\delta W = \underset{\sim}{\sigma} : \delta\underset{\sim}{\varepsilon}$ and only small deformations are considered, then the variational problem to (3.23) and (3.24) reads

$$
\begin{aligned}
\mathcal{L} = {}&\langle W\rangle_V + \underset{\sim}{\mathbf{\Sigma}} : \left(\underline{\nabla}_{\underline{\mathbf{X}}} \underline{\mathbf{U}} - \left\langle \underline{\nabla}_{\underline{\mathbf{x}}} \underline{\mathbf{u}}\right\rangle_V\right) + \underline{\lambda}^V \cdot \left(\underline{\mathbf{U}} - \langle \underline{\mathbf{u}}\rangle_V\right) + \left(\underset{\sim}{\bar{\sigma}}^{\mathrm{T}} - \underset{\sim}{\mathbf{\Sigma}}^{\mathrm{T}}\right) : \left(\underset{\sim}{\chi} - \left\langle \underline{\mathbf{u}} \otimes \underline{\xi}\right\rangle_V \cdot \underset{\sim}{\mathbf{G}}^{-1}\right) \\
&+ \underline{\underset{\sim}{\mathbf{M}}} \vdots \left[\underline{\underset{\sim}{\mathbf{K}}}^{\mathrm{s}} - \frac{1}{2}\underset{\approx}{\mathbf{I}}_{\mathrm{S}} : \left(\underset{\sim}{\mathbf{G}}^{-1} \cdot \left\langle \underline{\xi} \otimes \underline{\nabla}_{\underline{\mathbf{x}}} \underline{\mathbf{u}}\right\rangle_V - \frac{1}{2+n}\underset{\sim}{\mathbf{G}}^{-1}\left\langle \underline{\xi} \cdot \underline{\nabla}_{\underline{\mathbf{x}}} \underline{\mathbf{u}}\right\rangle_V\right) : \underset{\approx}{\mathbf{I}}_{\mathrm{T}}\right] \to \text{Min.}
\end{aligned}
\tag{3.26}
$$

Therein, the macroscopic stresses $\underset{\sim}{\mathbf{\Sigma}}$, $\underset{\sim}{\mathbf{s}} = \underset{\sim}{\mathbf{\Sigma}}^{\mathrm{T}} - \underset{\sim}{\bar{\sigma}}^{\mathrm{T}}$ and $\underline{\underset{\sim}{\mathbf{M}}}$ have the role of Lagrange multipliers to enforce the kinematic micro-macro relations (3.24).

In Eq. (3.24), all deformation measures are insensitive to rigid translations. A pure rotation $\underline{\mathbf{v}} = \underset{\sim}{\mathbf{W}} \cdot \underline{\xi}$ with $\underset{\sim}{\mathbf{W}}^{\mathrm{T}} = \underset{\sim}{\mathbf{W}}^{-1}$ does not affect $\underline{\underset{\sim}{\mathbf{L}}}^{K\mathrm{s}}$ but leads to identical values $\underline{\mathbf{V}} \otimes \underline{\nabla}_{\underline{\mathbf{X}}} = \underset{\sim}{\mathbf{L}}^{\chi} = \underset{\sim}{\mathbf{W}}$. Consequently, the measures of rate of deformation $\underset{\sim}{\mathbf{D}} = \operatorname{sym}(\underline{\nabla}_{\underline{\mathbf{X}}} \underline{\mathbf{V}})$, $\operatorname{sym}(\underset{\sim}{\mathbf{L}}^{\chi})$,

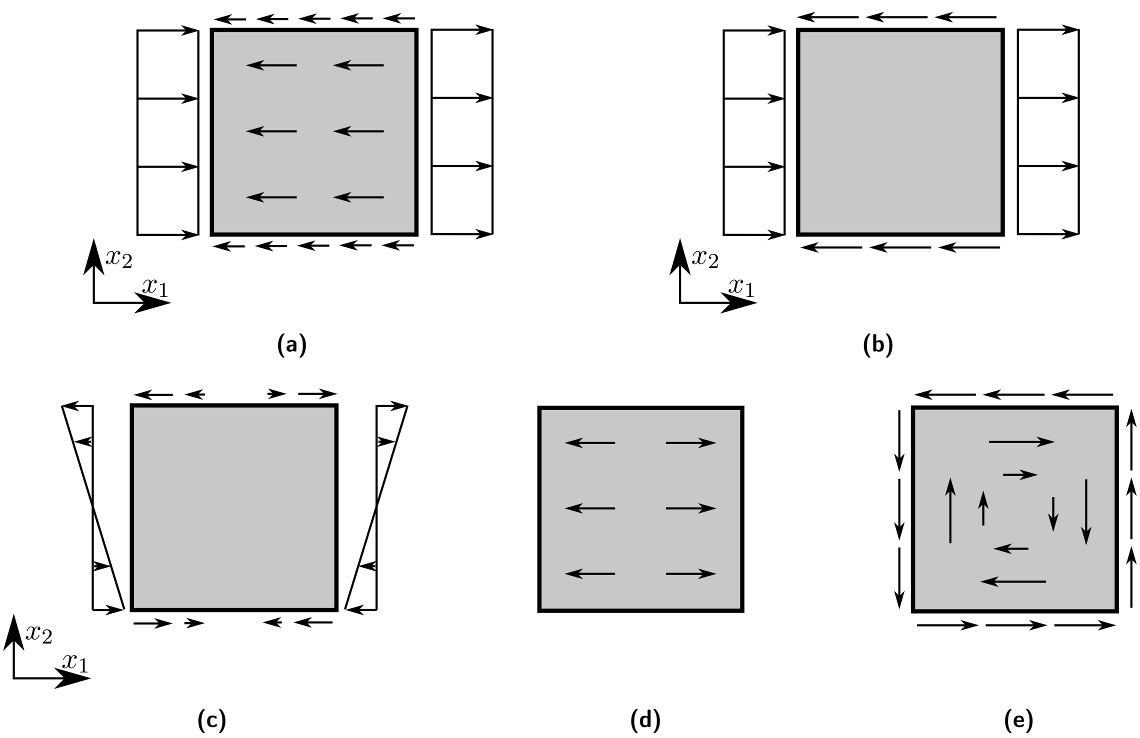

Fig. 3.1.: Loading of the volume element $\Delta V(\underline{\mathbf{X}})$ by non-classical stresses: (a) $\underset{\approx}{\mathbf{M}} = \underline{\mathbf{b}}_1\underline{\mathbf{b}}_1\underline{\mathbf{b}}_1$, (b) $\underset{\approx}{\mathbf{M}} = \underline{\mathbf{b}}_1\underline{\mathbf{b}}_1\underline{\mathbf{b}}_1 - \underline{\mathbf{b}}_1\underline{\mathbf{b}}_2\underline{\mathbf{b}}_1$, (c) $\underset{\approx}{\mathbf{M}} = \underline{\mathbf{b}}_1\underline{\mathbf{b}}_1\underline{\mathbf{b}}_2 + \underline{\mathbf{b}}_2\underline{\mathbf{b}}_1\underline{\mathbf{b}}_1$, (d) $\bar{\underset{\sim}{\sigma}} - \underset{\sim}{\boldsymbol{\Sigma}} = \underline{\mathbf{b}}_1\underline{\mathbf{b}}_1$, (e) $\underset{\sim}{\boldsymbol{\Sigma}} = \underline{\mathbf{b}}_1\underline{\mathbf{b}}_2 - \underline{\mathbf{b}}_2\underline{\mathbf{b}}_1$

$\underset{\sim}{\mathbf{L}}^e = \underline{\nabla}_{\underline{\mathbf{X}}}\underline{\mathbf{V}} - \underset{\sim}{\mathbf{L}}^{\chi\mathrm{T}}$ and $\underset{\sim}{\mathbf{L}}^{K\mathrm{s}}$ defined in Eqs. (2.115)–(2.116) are also invariant to a superimposed rotation and are thus objective and so are their work-conjugate stresses $\bar{\underset{\sim}{\sigma}}$, $\underset{\sim}{\mathbf{s}}$ $\underset{\sim}{\boldsymbol{\Sigma}}$ and $\underset{\approx}{\mathbf{M}}$, respectively.

Note that the micro-macro relations for the deformation measures $\underline{\nabla}_{\underline{\mathbf{X}}}\underline{\mathbf{V}}$ and $\underset{\sim}{\mathbf{L}}^{\chi}$ in (3.24) are identical to the definitions (2.121)–(2.122) of Forest et al. In particular, definitions (3.17) and (3.24) for the macroscopic values of $\underline{\mathbf{V}}$ and $\underset{\sim}{\mathbf{L}}^{\chi}$ (together with (2.120) for the macroscopic location $\underline{\mathbf{X}}$) are equivalent to a minimum average error

$$\left\langle (\tilde{\underline{\mathbf{v}}} - \underline{\mathbf{v}})^2 \right\rangle_V \xrightarrow{\underline{\mathbf{V}},\underset{\sim}{\mathbf{L}}^{\chi}} \min \tag{3.27}$$

between the microscopic velocity field $\underline{\mathbf{v}}$ and its macroscopic approximation $\tilde{\underline{\mathbf{v}}}$ according to Eq. (2.107). Thus, the kinematic micro-macro relations (3.24) are kinematically consistent in a sense that $\tilde{\underline{\mathbf{v}}}$ from (2.107) leads to identities for $\underline{\mathbf{V}}$ and $\underset{\sim}{\mathbf{L}}^{\chi}$. However, expression $(3.24)_3$ for $\underset{\sim}{\mathbf{K}}^{\mathrm{s}}$ differs to Eq. (2.125) of Forest et al. Furthermore, it can be remarked that, in contrast to the derivation of the deformation measures by Forest et al. as outlined in Section 2.2.4, the present approach does not require that the macroscopic gradients of the geometry entities $\Delta V(\underline{\mathbf{X}})$ and $\underset{\sim}{\mathbf{G}}(\underline{\mathbf{X}})$ vanish.

The loading of the volume element according to (3.23) for natural boundary conditions is sketched in Fig. 3.1 for several non-classical cases for a rectangular ΔV. Thereby, the $\underline{\mathbf{b}}_i$ denote to the base vectors of the coordinate system. Fig. 3.1a shows the effect of hyperstress M_{111} for which volume loads occur due to a non-vanishing "spherical" part of $\underset{\approx}{\mathbf{M}}$ according to (3.20). In contrast, for a "deviatoric" hyperstress $M_{111} = -M_{121}$ in Fig. 3.1b the macroscopic stress results only in tractions at the microscopic boundary. In both cases, the tractions at opposite faces are identical, i. e. in the terminology of classical homogenisation they are periodic. In contrast, the bending-type mode in Fig. 3.1c leads to anti-periodic tractions. The effect of an internal stress difference is sketched in Fig. 3.1d. Fig. 3.1e shows the loading of

ΔV for a skew-symmetric extrinsic stress $\Sigma_{12} = -\Sigma_{21}$. In this case the torque of the tractions is compensated by volume contributions of opposite direction which twist the volume element ΔV internally.

3.4. Porous material

Size-effects as deviations from the predictions of the Cauchy-Boltzmann theory were observed in particular for foams and motivated phenomenological modeling by generalized continuum theories, e. g. [18, 21, 23, 27, 30, 79–81]. Also ductile failure is caused by growth of voids and the associated localization of deformations requires a continuum model with an intrinsic length scale, e. g. [81–90].

It is desirable to obtain the macroscopic constitutive behavior for a porous material by homogenisation by solving the respective boundary value problem at the microscale. For the boundary value problem (3.21) and (3.22) formulated in the previous section, and analogously Eqs. (2.133)–(2.134) in Section 2.2.4, some non-classical stresses act like volume forces, compare also Fig. 3.1.

A porous medium can thus be not homogenized by this procedure since pores cannot carry volume forces. Note that the non-classical stresses appear as volume terms in their role as Lagrange multipliers to enforce those non-classical kinematic micro-macro which cannot be transformed to surface integrals. This finding is related to the fact that the microscopic displacement field $\underline{\mathbf{u}}(\underline{\mathbf{x}})$ needs to be uniquely-defined in the complete volume element $\underline{\mathbf{x}} \in \Delta V(\underline{\mathbf{X}})$ in order to evaluate the non-classical kinematic micro-macro relations (2.121) and (2.125) or (3.24) and (3.25), respectively.

In contrast, in classical homogenisation $\underline{\mathbf{u}}(\underline{\mathbf{x}})$ needs to be defined uniquely only at the boundary $\underline{\mathbf{x}} \in \partial\Delta V$. For that reason it is no problem to apply classical homogenisation to porous materials, although no unique displacement field can be defined in the pores. When transforming the classical micro-macro relation (2.35) for the strain to a surface integral (2.41) by Gauss theorem, it suffices to assume that a displacement field $\underline{\mathbf{u}}(\underline{\mathbf{x}})$ of sufficient regularity could be defined arbitrarily in the void.

To sum up, the non-classical kinematic micro-macro relations given so far require a uniquely defined displacement field in the pores and their enforcement by Lagrange multipliers generates volume forces in the void which cannot be carried by the "empty material" there. Thus, in order to homogenize a porous material to a micromorphic continuum, the non-classical kinematic micro-macro relations (2.125), (3.24) and (3.25) need to be modified in such a way that only the displacement field of the matrix, outside the pores, is required. Then, no volume forces will appear in the voids and no arbitrary displacement field needs to be defined in the pores.

However, note that the averaging procedure of Eringen as outlined in Section 2.2.3 requires that the material at the microscale is of Cauchy-Boltzmann type, i. e. that the local balance equations (2.103)–(2.106) hold *everywhere* at the microscale $\underline{\mathbf{x}} \in \Delta V(\underline{\mathbf{X}})$. For this purpose, vanishing fields of stress $\underset{\sim}{\sigma}(\underline{\mathbf{x}}) = 0$ and density $\rho = 0$ can be defined for the pores without any problem. This definition ensures sufficient regularity of tractions at the surface of the pores and the local balance equations (2.103)–(2.106) are satisfied identically in the pores.

In order to derive the kinematic micro-macro in an inverse manner as in the previous section, the right-hand side of the local equilibrium condition (3.21) is multiplied by a weighting function $\mathrm{H}_V\left(\underline{\xi}\right)$:

$$\underline{\nabla}_{\underline{\mathbf{x}}} \cdot \underset{\sim}{\sigma} = \mathrm{H}_V\left(\underline{\xi}\right) \left[\underset{\sim}{\underline{\mathbf{A}}} \cdot \underline{\xi} + \underline{\mathbf{B}} - \underline{\lambda}^V\right] \qquad \text{in } \Delta V(\underline{\mathbf{X}}) \tag{3.28}$$

Firstly, let us assume that this weighting function is 1 in the matrix material and 0 in the pores. Thus, the equilibrium conditions are satisfied identically in the pores. The static boundary

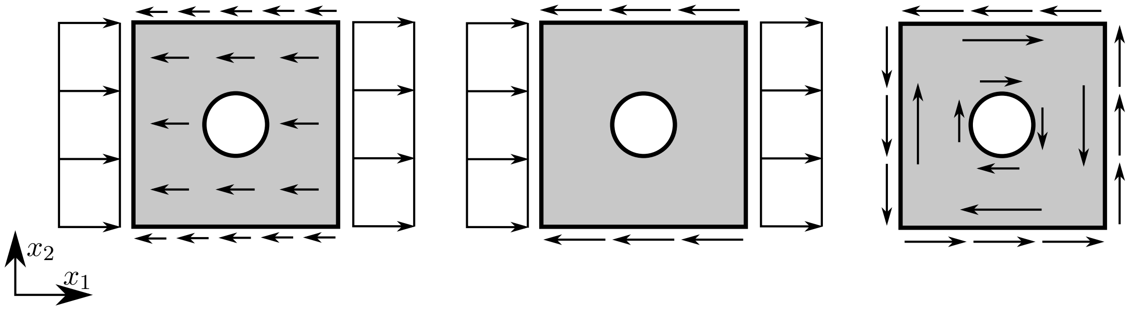

(a) (b) (c)

Fig. 3.2.: Loading of the volume element $\Delta V(\underline{\mathbf{X}})$ with void for several non-classical stresses: (a) $\underset{\approx}{\mathbf{M}} = \underline{\mathbf{b}}_1\underline{\mathbf{b}}_1\underline{\mathbf{b}}_1$, (b) $\underset{\approx}{\mathbf{M}} = \underline{\mathbf{b}}_1\underline{\mathbf{b}}_1\underline{\mathbf{b}}_1 - \underline{\mathbf{b}}_1\underline{\mathbf{b}}_2\underline{\mathbf{b}}_1$, (c) $\underset{\sim}{\boldsymbol{\Sigma}} = \underline{\mathbf{b}}_1\underline{\mathbf{b}}_2 - \underline{\mathbf{b}}_2\underline{\mathbf{b}}_1$

conditions (3.16) are retained which requires that no pores intersect with the boundary $\partial\Delta V$ of the volume element . Otherwise "empty" material of the pores would have to carry the finite boundary tractions. This restriction applies already to classical homogenisation with static boundary conditions (2.43) and shall not be addressed here. Note only that if this restriction shall be overcome, Eq. (3.16) just needs to be weighted by $\mathrm{H}_V\left(\underline{\xi}\right)$ as well.

Anyway, the ansatz (3.16) and (3.28) is inserted again to the kinetic micro-macro relation (3.14) and the condition of total equilibrium of ΔV in order to identify the coefficients as

$$A_{ij} = \frac{1}{\left\langle \mathrm{H}_V\left(\underline{\xi}\right)\right\rangle_V} \left(\Sigma_{jk} - \bar{\sigma}_{jk}\right) G^{\mathrm{M}-1}_{jk}\,, \tag{3.29}$$

$$B_j = \frac{1}{\left\langle \mathrm{H}_V\left(\underline{\xi}\right)\right\rangle_V} \frac{1}{2+n} M_{mjn} G^{-1}_{mn}\,. \tag{3.30}$$

Therein, it was assumed geometric centers of cell and matrix coincide $\left\langle \underline{\xi}\mathrm{H}_V\left(\underline{\xi}\right)\right\rangle_V = 0$. Furthermore, the second geometric moment of the matrix were defined as

$$\underset{\sim}{\mathbf{G}}^{\mathrm{M}} = \left\langle \underline{\xi}\underline{\xi}\right\rangle_{\mathrm{M}}\,, \tag{3.31}$$

whereby the operator

$$\langle(\circ)\rangle_{\mathrm{M}} = \frac{1}{\left\langle \mathrm{H}_V\left(\underline{\xi}\right)\right\rangle_V \Delta V} \int\limits_{\Delta V(\underline{\mathbf{X}})} \mathrm{H}_V\left(\underline{\xi}\right)(\circ)\,\mathrm{d}V \tag{3.32}$$

computes the average over the matrix. By Eqs. (3.29) and (3.30), Eq. (3.28) becomes

$$\underline{\nabla}_{\underline{\mathbf{x}}} \cdot \underset{\sim}{\sigma} = \frac{\mathrm{H}_V\left(\underline{\xi}\right)}{\left\langle \mathrm{H}_V\left(\underline{\xi}\right)\right\rangle_V} \left[\left(\underset{\sim}{\boldsymbol{\Sigma}}^{\mathrm{T}} - \bar{\underset{\sim}{\sigma}}^{\mathrm{T}}\right) \cdot \left(\underset{\sim}{\mathbf{G}}^{\mathrm{M}}\right)^{-1} \cdot \underline{\xi} + \frac{1}{2+n}\left(\underset{\approx}{\mathbf{I}}_{\mathrm{T}} : \underset{\approx}{\mathbf{M}}\right) : \underset{\sim}{\mathbf{G}}^{-1} - \underline{\lambda}^V\right]\,, \tag{3.33}$$

$$\sigma_{ij,i} = \frac{\mathrm{H}_V\left(\underline{\xi}\right)}{\left\langle \mathrm{H}_V\left(\underline{\xi}\right)\right\rangle_V} \left[\left(\Sigma_{kj} - \bar{\sigma}_{kj}\right) G^{\mathrm{M}-1}_{km}\xi_m + \frac{1}{2+n} M_{kjm} G^{-1}_{km} - \lambda^V_j\right]\,.$$

The loading resulting from (3.33) together with the natural boundary condition (3.22) is visualized in Fig. 3.2 for some non-classical loading cases. Equation (3.33) together with the natural boundary condition (3.22) allow to compute $\langle \underset{\sim}{\sigma} : \underset{\sim}{\mathbf{d}} \rangle_V$. From the generalized Hill-Mandel lemma (3.13), the kinematic micro-macro relations can thus be identified as

$$\underline{\mathbf{V}} = \langle \underline{\mathbf{v}} \rangle_{\mathrm{M}} \tag{3.34}$$

$$\underset{\sim}{\mathbf{L}}^{\chi} = \langle \underline{\mathbf{v}} \otimes \underline{\xi} \rangle_{\mathrm{M}} \cdot \left(\underset{\sim}{\mathbf{G}}^{\mathrm{M}}\right)^{-1} \tag{3.35}$$

$$\underline{\nabla_{\underline{\mathbf{X}}} \underline{\mathbf{V}}} = \frac{1}{\Delta V} \oint\limits_{\partial \Delta V} \underline{\mathbf{n}} \otimes \underline{\mathbf{v}} \, \mathrm{d}S \tag{3.36}$$

$$\begin{aligned} \underset{\approx}{\mathbf{L}}^{K\mathrm{s}} = & \frac{1}{4\Delta V} \left[\oint\limits_{\partial \Delta V} \underline{\mathbf{n}} \underline{\mathbf{v}} \underline{\xi} \, \mathrm{d}S \cdot \underset{\sim}{\mathbf{G}}^{-1} + \underset{\sim}{\mathbf{G}}^{-1} \cdot \oint\limits_{\partial \Delta V} \underline{\xi} \underline{\mathbf{v}} \underline{\mathbf{n}} \, \mathrm{d}S - \underset{\approx}{\mathbf{I}}_{\mathrm{T}} : \left(\frac{2}{2+n} \oint\limits_{\partial \Delta V} \underline{\mathbf{v}} \underline{\mathbf{n}} \cdot \underline{\xi} \, \mathrm{d}S \underset{\sim}{\mathbf{G}}^{-1} \right) \right] \\ & - \underset{\approx}{\mathbf{I}}_{\mathrm{T}} : \left(\frac{1}{2+n} \langle \underline{\mathbf{v}} \rangle_{\mathrm{M}} \underset{\sim}{\mathbf{G}}^{-1} \right) \end{aligned} \tag{3.37}$$

$$\begin{aligned} L_{ijk}^{K\mathrm{s}} = & \frac{1}{4\Delta V} \left[\oint\limits_{\partial \Delta V} v_j n_i \xi_m \, \mathrm{d}S G_{mk}^{-1} + G_{im}^{-1} \oint\limits_{\partial \Delta V} \xi_m v_j n_k \, \mathrm{d}S - \frac{2}{2+n} \oint\limits_{\partial \Delta V} v_j n_m \xi_m \, \mathrm{d}S G_{ik}^{-1} \right] \\ & - \frac{1}{2+n} \langle v_j \rangle_{\mathrm{M}} G_{ik}^{-1} \,. \end{aligned}$$

Compared to Eqs. (3.17) and (3.24) for the compact material, in Eqs. (3.34)–(3.37) all volume averages which cannot be transformed to surface integrals appear only as average $\langle (\circ) \rangle_{\mathrm{M}}$ over the matrix material. Vice versa, Eqs. (3.17) and (3.24) for the compact material are a special of Eqs. (3.34)–(3.37) when the matrix material $\langle (\circ) \rangle_{\mathrm{M}}$ encompasses the complete volume element ΔV. The micro-macro relations (3.34) and (3.35) for $\underline{\mathbf{V}}$ and $\underset{\sim}{\mathbf{L}}^{\chi}$ are equivalent to

$$\left\langle \left(\underline{\tilde{\mathbf{v}}} - \underline{\mathbf{v}}\right)^2 \right\rangle_{\mathrm{M}} \xrightarrow{\underline{\mathbf{V}}, \underset{\sim}{\mathbf{L}}^{\chi}} \min \tag{3.38}$$

This means that Eqs. (3.17) and (3.24) minimize the discrepancy between the actual velocity field $\underline{\mathbf{v}}(\underline{\mathbf{x}})$ and its approximation (2.107) *in the matrix* only, not in the complete volume element ΔV as in Eqs. (2.119) and (3.27).

Furthermore, note that Eqs. (3.34)–(3.37) were derived without any assumption with respect to the absolute value of the weighting function $\mathrm{H}_V\left(\underline{\xi}\right)$ or its differentiability. This means that it does not necessarily need to be identified with the indicator function. Also other choices like the e. g. the mass density $\mathrm{H}_V\left(\underline{\xi}\right) = \rho$ would be possible. Recently, Biswas and Poh [91] proposed a homogenisation theory which defines the kinematic micro-macro relation for microdeformation $\underset{\sim}{\chi}$ as a surface integral over intrinsic interfaces of the material. The approach of Forest [36] to prescribe a "relative rotation of the microstructure with respect to the material lines" to determine the "resistance to inner rotation" for a Cosserat theory may be interpreted in the same sense. The definition of $\underset{\sim}{\chi}$ over an interface can be covered by Eq. (3.35) by choosing $\mathrm{H}_V\left(\underline{\xi}\right)$ as Dirac-Function at the interface.

3.5. Kinematic and periodic boundary conditions

Kinematic boundary conditions

In classical homogenisation, kinematic boundary conditions (2.45) are constructed by a polynomial to satisfy the kinematic micro-macro relation (2.36) which can be converted to a surface integral (2.41). For the homogenisation towards a micromorphic continuum, the respective kinematic micro-macro relations (3.34)–(3.37) cannot be transformed completely to surface integrals and can thus not be satisfied completely by kinematic boundary conditions.

However, kinematic boundary conditions can be constructed in such a way to satisfy at least those kinematic micro-macro relations which can be written as surface integrals. This is the classical velocity gradient $\underline{\nabla_{\underline{\mathbf{X}}}\mathbf{V}}$ in Eq. (3.36).

Equation (3.37) for symmetric part of the gradient of the rate of microdeformation $\underset{\sim}{\underline{\underline{\mathbf{L}}}}^{K\mathrm{s}}$ contains both surface integrals and a volume average which need to be split. The spherical[2] part

$$L^{K\mathrm{s}}_{ijk}G_{ik} = \frac{1}{2+n}\left[\frac{1}{\Delta V}\oint\limits_{\partial\Delta V} v_j n_m \xi_m \,\mathrm{d}S - n\left\langle v_j\right\rangle_{\mathrm{M}}\right] \tag{3.39}$$

of $\underset{\sim}{\underline{\underline{\mathbf{L}}}}^{K\mathrm{s}}$ contains the macroscopic velocity $\underline{\mathbf{V}} = \langle\underline{\mathbf{v}}\rangle_{\mathrm{M}}$ as volume average and can thus not be prescribed as kinematic boundary condition. This is consistent with the fact that the corresponding part of the double stress appears as volume term in the microscopic equilibrium condition (3.33). However, the deviatoric part of $\underset{\sim}{\underline{\underline{\mathbf{L}}}}^{K\mathrm{s}}$

$$\begin{aligned} L^{K\mathrm{sd}}_{ijk} :=& L^{K\mathrm{s}}_{ijk} - \frac{1}{n}L^{K\mathrm{s}}_{ljm}G_{lm}G^{-1}_{ik} \\ =& \frac{1}{4\Delta V}\left[\oint\limits_{\partial\Delta V} v_j n_i \xi_m \,\mathrm{d}S G^{-1}_{mk} + \oint\limits_{\partial\Delta V} v_j n_k \xi_m \,\mathrm{d}S G^{-1}_{mi} - \frac{2}{n}\oint\limits_{\partial\Delta V} v_j n_m \xi_m \,\mathrm{d}S G^{-1}_{ik}\right] \end{aligned} \tag{3.40}$$

can be expressed in terms of surface integrals and thus be prescribed by kinematic boundary conditions. In particular, the quadratic ansatz (2.65) of Gologanu et al. [44] is adopted

$$\underline{\mathbf{v}} = \underline{\mathbf{V}}^0 + \underline{\xi}\cdot\underline{\nabla_{\underline{\mathbf{X}}}\mathbf{V}} + \underline{\xi}\cdot\underset{\sim}{\underline{\mathbf{D}}}\cdot\underline{\xi} \qquad \text{on } \partial\Delta V(\underline{\mathbf{X}}) \tag{3.41}$$

here wherein the linear term satisfies Eq. (3.36) for the velocity gradient as usual. Inserting (3.41) to (3.39) and (3.40) leads to a linear system of equations

$$L^{K\mathrm{s}}_{ijk}G_{ik} = D_{ljm}G_{lm} - \frac{n}{2+n}\left(V_j - V^0_j\right) \tag{3.42}$$

$$L^{K\mathrm{sd}}_{ijk} = D_{ijk} - \frac{1}{n}D_{ljm}G_{lm}G^{-1}_{ik} \tag{3.43}$$

for the components D_{ijk} of the quadratic term (actually only those which are symmetric with respect to i and k and thus contribute to (3.41)) whereby definition (3.34) of the macroscopic velocity was inserted. The solution to this system of equations for D_{ijk} is

$$D_{ijk} = L^{K\mathrm{s}}_{ijk} + \frac{1}{2+n}\left(V_j - V^0_j\right)G^{-1}_{ik} \tag{3.44}$$

Thus, the kinematic boundary condition (3.41) becomes

$$\underline{\mathbf{v}} = \underline{\mathbf{V}}^0 + \underline{\xi}\cdot\underline{\nabla_{\underline{\mathbf{X}}}\mathbf{V}} + \underline{\xi}\cdot\underset{\sim}{\underline{\underline{\mathbf{L}}}}^{K\mathrm{s}}\cdot\underline{\xi} + \frac{1}{2+n}\left(\underline{\mathbf{V}} - \underline{\mathbf{V}}^0\right)\underline{\xi}\cdot\underset{\sim}{\mathbf{G}}^{-1}\cdot\underline{\xi} \tag{3.45}$$

The microscopic equilibrium condition (3.33) remains valid where those stresses act, in their role of Lagrange multipliers, as volume forces whose kinematic micro-macro relation could not be converted to surface integrals.

[2]For the practically most relevant shapes of the volume element ΔV of a cube or sphere (square and circle in 2D), the geometric moment $\underset{\sim}{\mathbf{G}}$ is a spherical tensor.

The kinematic boundary condition (3.45) satisfies the kinematic micro-macro relations (3.36) and (3.40) for arbitrary $\underline{\mathbf{V}}^0$. It has to verified in addition, that the generalized Hill-Mandel condition (3.13) is not violated. For that purpose, the average power is written as

$$\langle \underset{\sim}{\sigma} : \underset{\sim}{\mathbf{d}} \rangle_V = \frac{1}{\Delta V} \oint_{\partial \Delta V} \underline{\mathbf{n}} \cdot \underset{\sim}{\sigma} \cdot \underline{\mathbf{v}} \, \mathrm{d}S - \left\langle \underline{\mathbf{v}} \cdot \left(\underline{\nabla}_{\underline{\mathbf{x}}} \cdot \underset{\sim}{\sigma} \right) \right\rangle_V . \tag{3.46}$$

Inserting the kinematic boundary condition (3.45) to the surface integral and the microscopic equilibrium condition (3.33) to the volume average on the right-hand side yields

$$\begin{aligned} \langle \underset{\sim}{\sigma} : \underset{\sim}{\mathbf{d}} \rangle_V = & \left(\frac{1}{\Delta V} \oint_{\partial \Delta V} \underline{\xi} \otimes \underline{\mathbf{n}} \cdot \underset{\sim}{\sigma} \, \mathrm{d}S \right) : \underline{\nabla}_{\underline{\mathbf{X}}} \underline{\mathbf{V}} + \left(\frac{1}{\Delta V} \oint_{\partial \Delta V} \underline{\xi} \otimes \underline{\mathbf{n}} \cdot \underset{\sim}{\sigma} \otimes \underline{\xi} \, \mathrm{d}S \right) \vdots \underset{\approx}{\underline{\mathbf{L}}}^{Ks} \\ & - \left(\left\langle \underline{\mathbf{v}} \otimes \underline{\xi} \right\rangle_{\mathrm{M}} \cdot \left(\underset{\sim}{\mathbf{G}}^{\mathrm{M}} \right)^{-1} \right) : \left(\underset{\sim}{\mathbf{\Sigma}}^{\mathrm{T}} - \underset{\sim}{\bar{\sigma}}^{\mathrm{T}} \right) \end{aligned} \tag{3.47}$$

under condition

$$\underline{\mathbf{V}}^0 = \underline{\mathbf{V}} = \langle \underline{\mathbf{v}} \rangle_{\mathrm{M}} . \tag{3.48}$$

Obviously, the Hill-Mandel lemma (3.7) is satisfied by Eq. (3.47) together with the kinetic micro-macro relations (3.10) and (3.11) for $\underset{\sim}{\mathbf{\Sigma}}$ and $\underset{\approx}{\underline{\mathbf{M}}}$, respectively, and Eq. (3.35) for the rate of microdeformation. Due to Eq. (3.48), the kinematic boundary condition finally reads

$$\underline{\mathbf{v}} = \underline{\mathbf{V}} + \underline{\xi} \cdot \underline{\nabla}_{\underline{\mathbf{X}}} \underline{\mathbf{V}} + \underline{\xi} \cdot \underset{\approx}{\underline{\mathbf{L}}}^{K} \cdot \underline{\xi} \qquad \text{on } \partial \Delta V(\underline{\mathbf{X}}) \tag{3.49}$$

Therein, $\underset{\approx}{\underline{\mathbf{L}}}^{Ks}$ was replaced equivalently by $\underset{\approx}{\underline{\mathbf{L}}}^{K}$ as, due to double contraction with $\underline{\xi}$, only those part enters which are symmetric with respect to its first and third indices (as the double stress $\underset{\approx}{\underline{\mathbf{M}}}$).

In the case that the material is hyperelastic and small deformations are considered, the boundary-value problem at the microscale can be specified in variational form by the Lagrangian (3.26) together with the kinematic boundary condition (3.49). However, since the boundary condition (3.49) already fulfills the kinematic constraints for $\underline{\nabla}_{\underline{\mathbf{X}}} \underline{\mathbf{V}}$ and $\underset{\approx}{\underline{\mathbf{L}}}^{K}$, the Lagrangian (3.26) can be reduced to

$$\mathcal{L} = \langle W \rangle_V + \tilde{\underline{\lambda}}_V : (\underline{\mathbf{U}} - \langle \underline{\mathbf{u}} \rangle_{\mathrm{M}}) + \left(\underset{\sim}{\bar{\sigma}}^{\mathrm{T}} - \underset{\sim}{\mathbf{\Sigma}}^{\mathrm{T}} \right) : \left(\underset{\sim}{\chi} - \left\langle \underline{\mathbf{u}} \otimes \underline{\xi} \right\rangle_{\mathrm{M}} \cdot \left(\underset{\sim}{\mathbf{G}}^{\mathrm{M}} \right)^{-1} \right) \to \mathrm{Min.} \tag{3.50}$$

whereby it has to be remarked that the Lagrange multiplier

$$\tilde{\underline{\lambda}}_V = \underline{\lambda}^V - \frac{1}{2+n} \left[\underset{\approx}{\mathbf{I}}_{\mathrm{T}} : \left(\underset{\approx}{\underline{\mathbf{M}}} \cdot \underset{\sim}{\mathbf{G}}^{-1} \right) \right] : \underset{\sim}{\mathbf{I}}$$

needs to be distinguished from $\underline{\lambda}^V$ for the Euler-Lagrange equations of (3.50) to be consistent with the microscopic equilibrium conditions (3.33). The difference between $\tilde{\underline{\lambda}}_V$ and $\underline{\lambda}^V$ arises from having inserted the kinematic micro-macro relation (3.34) for the velocity $\underline{\mathbf{V}}$ to Eq. (3.39) for eliminating the volume integral. Thus, $\tilde{\underline{\lambda}}_V$ is in general non-zero and corresponds to the spherical part of $\underset{\approx}{\underline{\mathbf{M}}}$. For this reason, the kinematic micro-macro relation (3.34) needs to be enforced even when imposing the kinematic boundary condition (3.49).

Periodic boundary conditions

For extending the concept of periodic boundary conditions to the micromorphic theory, a fluctuation field $\Delta \underline{\mathbf{v}}(\underline{\xi})$ is amended to the kinematic boundary condition (3.49)

$$\underline{\mathbf{v}} = \underline{\mathbf{V}} + \underline{\xi} \cdot \underline{\nabla}_{\underline{\mathbf{X}}} \underline{\mathbf{V}} + \underline{\xi} \cdot \underset{\approx}{\underline{\mathbf{L}}}^{Ks} \cdot \underline{\xi} + \Delta \underline{\mathbf{v}}(\underline{\xi}) \qquad \text{on } \partial \Delta V(\underline{\mathbf{X}}) \tag{3.51}$$

Assuming the fluctuations to be periodic according to Eq. (2.78) ensures that the classical micro-macro relation (3.36) is satisfied. However, this periodicity does not satisfy per se relation (3.37) for the gradient of the microdeformation but additional requirements are necessary. The search for adequate additional requirements leads to the question on the scope of periodic boundary conditions. To the authors opinion, periodic boundary conditions shall ensure that for a periodic microstructure, the response of a large sample with *uniform* far-field loading is recovered by the homogenised theory. For the homogenised micromorphic theory, a uniform far-field loading implies vanishing non-classical stresses and respective deformations. As these terms do not appear in the scenario aimed at by periodic boundary conditions, no further attempts are necessary to characterize the symmetry properties of the local fields in presence of non-classical fields.

Lacking an explicit micro-macro relation for the second gradient, Kouznetsova et al. imposed integral constraint (2.79) to the fluctuation field. This integral constraint forms an implicit kinematic micro-macro relation as outlined in Section 2.2.2. In contrast, for the micromorphic theory, explicit micro-macro relations (3.34), (3.35) and (3.37) are available for velocity, microdeformation and its gradient. For a comparison with the approach of Kouznetsova et al., Eq. (3.37) is applied to (3.51) yielding

$$0 = \oint\limits_{\partial\Delta V} n_i \Delta v_j \xi_m \, \mathrm{d}S G^{-1}_{mk} + \oint\limits_{\partial\Delta V} n_k \Delta v_j \xi_m \, \mathrm{d}S G^{-1}_{mi} - \frac{2}{2+n} \oint\limits_{\partial\Delta V} n_m \Delta v_j \xi_m \, \mathrm{d}S G^{-1}_{ik} \,. \tag{3.52}$$

Equation (3.52) is similar to proposal (2.79) of Kouznetsova et al. and for a rectangular volume element $\partial\Delta V$ (as actually envisaged by Kouznetsova et al.), both definitions coincide in Eq. (2.80).

Anyway, for formulating a boundary-value problem with respect to the local displacements and velocities, the fluctuation field $\Delta\underline{\mathbf{v}}(\underline{\xi})$ is favorably eliminated from the periodicity condition (2.78) by Eq. (3.51) yielding

$$\underline{\mathbf{v}}(\underline{\xi}^+) - \underline{\mathbf{v}}(\underline{\xi}^-) = \left(\underline{\xi}^+ - \underline{\xi}^-\right) \cdot \underline{\nabla_{\mathbf{X}}} \underline{\mathbf{V}} + \underline{\xi}^+ \cdot \underset{\sim}{\underline{\mathbf{L}}}^{K\mathrm{s}} \cdot \underline{\xi}^+ - \underline{\xi}^- \cdot \underset{\sim}{\underline{\mathbf{L}}}^{K\mathrm{s}} \cdot \underline{\xi}^- \qquad \text{on } \partial\Delta V(\underline{\mathbf{X}}) \,. \tag{3.53}$$

As mentioned already, Eq. (3.51) satisfies the classical micro-macro relation (3.36) ad hoc. The remaining micro-macro relations (3.34), (3.35) and (3.37) are imposed in integral form. For a hyperelastic material, the corresponding Lagrangian (2.51) thus needs to be extended towards

$$\begin{aligned} \mathcal{L} = \langle W \rangle_V &- \frac{1}{\Delta V} \int\limits_{\partial\Delta V^+} \underline{\lambda}(\underline{\xi}^+) \cdot \left[\underline{\mathbf{u}}(\underline{\xi}^+) - \underline{\mathbf{u}}(\underline{\xi}^-) - \left(\underline{\xi}^+ - \underline{\xi}^-\right) \cdot \underline{\nabla_{\mathbf{X}}} \underline{\mathbf{U}} + \underline{\xi}^+ \cdot \underset{\sim}{\underline{\mathbf{K}}}^{\mathrm{s}} \cdot \underline{\xi}^+ - \underline{\xi}^- \cdot \underset{\sim}{\underline{\mathbf{K}}}^{\mathrm{s}} \cdot \underline{\xi}^- \right] \mathrm{d}S \\ &+ \underset{\sim}{\underline{\lambda}} \vdots \left\{ \underset{\sim}{\underline{\mathbf{K}}}^{\mathrm{s}} - \frac{1}{4\Delta V} \left[\oint\limits_{\partial\Delta V} \underline{\mathbf{n}} \underline{\mathbf{u}} \underline{\xi} \, \mathrm{d}S \cdot \underset{\sim}{\mathbf{G}}^{-1} + \underset{\sim}{\mathbf{G}}^{-1} \cdot \oint\limits_{\partial\Delta V} \underline{\xi} \underline{\mathbf{u}} \underline{\mathbf{n}} \, \mathrm{d}S - \underset{\approx}{\mathbf{I}}_{\mathrm{T}} : \left(\frac{2}{2+n} \oint\limits_{\partial\Delta V} \underline{\mathbf{u}} \underline{\mathbf{n}} \cdot \underline{\xi} \, \mathrm{d}S \underset{\sim}{\mathbf{G}}^{-1} \right) \right] \right. \\ &\left. + \underset{\approx}{\mathbf{I}}_{\mathrm{T}} : \left(\frac{1}{2+n} \langle \underline{\mathbf{u}} \rangle_{\mathrm{M}} \underset{\sim}{\mathbf{G}}^{-1} \right) \right\} + \underline{\lambda}^V \cdot \left(\underline{\mathbf{U}} - \langle \underline{\mathbf{u}} \rangle_{\mathrm{M}} \right) - \underset{\sim}{\mathbf{s}} : \left(\underset{\sim}{\chi} - \left\langle \underline{\mathbf{u}} \otimes \underline{\xi} \right\rangle_{\mathrm{M}} \cdot \left(\underset{\sim}{\mathbf{G}}^{\mathrm{M}} \right)^{-1} \right) \end{aligned} \tag{3.54}$$

which has to be minimized with respect to the functions $\underline{\mathbf{u}}(\underline{\xi})$ and $\underline{\lambda}(\underline{\xi}^+)$ and with respect to the Lagrange multipliers $\underset{\sim}{\underline{\lambda}}$, $\underline{\lambda}^V$ and $\underset{\sim}{\mathbf{s}} = \underset{\sim}{\mathbf{\Sigma}}^{\mathrm{T}} - \underset{\sim}{\bar{\sigma}}^{\mathrm{T}}$. The stationarity condition to this variational problem are the local equilibrium condition (3.33) in the domain and

$$n_i \sigma_{ij} = \pm \lambda_j(\underline{\xi}) + \frac{1}{2} n_i \lambda_{ijp} G^{-1}_{pm} \xi_m - \frac{1}{2(2+n)} n_i \xi_i \lambda_{njp} G^{-1}_{np} \tag{3.55}$$

at the boundary with $\underline{\lambda}(\underline{\xi})$ to enforce Eq. (3.51). Thereby, the plus sign in the first term refers to $\underline{\xi} \in \partial\Omega^+$ and the minus to $\underline{\xi} \in \partial\Omega^-$. Thus, the tractions resulting from $\underline{\lambda}(\underline{\xi})$ are anti-periodic. However, Eq. (3.55) comprises additional contributions of double stress-type which are linear both in normal $\underline{\mathbf{n}}$ and in relative location $\underline{\xi}$. From these double stress loadings, there are both periodic and anti-periodic contributions, compare Fig. 3.1a–Fig. 3.1c. This finding complies with the requirement of Forest and Trinh [68] that the "anti-periodicity condition must be abandoned in the presence of overall stress and strain gradients."[3]

The work associated with Eqs. (3.33) and (3.55) is

$$\begin{aligned}\langle \underset{\sim}{\sigma} : \underset{\sim}{\mathbf{d}} \rangle_V = &\left[\frac{1}{\Delta V} \int\limits_{\partial \Delta V^+} (\underline{\xi}^+ - \underline{\xi}^-) \otimes \underline{\lambda} \, \mathrm{d}S \right] : \nabla_{\underline{\mathbf{X}}} \underline{\mathbf{V}} + \left[\underset{\sim}{\lambda} + \frac{1}{\Delta V} \int\limits_{\partial \Delta V^+} \underline{\xi}^+ \underline{\lambda} \underline{\xi}^+ - \underline{\xi}^- \underline{\lambda} \underline{\xi}^- \, \mathrm{d}S \right] \vdots \underset{\sim}{\underline{\mathbf{L}}}^{K\mathrm{s}} \\ &- \left[\langle \underline{\mathbf{v}} \otimes \underline{\xi} \rangle_{\mathrm{M}} \cdot \left(\underset{\sim}{\mathbf{G}}^{\mathrm{M}}\right)^{-1} \right] : \left(\underset{\sim}{\mathbf{\Sigma}}^{\mathrm{T}} - \underset{\sim}{\bar{\sigma}}^{\mathrm{T}} \right)\end{aligned} \tag{3.56}$$

The co-factors of $\nabla_{\underline{\mathbf{X}}} \underline{\mathbf{V}}$ and $\underset{\sim}{\underline{\mathbf{L}}}^{K\mathrm{s}}$ coincide with the external stress $\underset{\sim}{\mathbf{\Sigma}}$ and double stress $\underset{\approx}{\mathbf{M}}$ computed from Eqs. (3.10) and (3.11). Together with the kinematic micro-macro relation (3.35) for the last term in Eq. (3.56), the Hill-Mandel condition (3.7) is thus satisfied.

For a centro-symmetric problem $\underline{\xi}^- = -\underline{\xi}^+$, the double stress $\underset{\approx}{\mathbf{M}}$ coincides with the Lagrange multiplier $\underset{\sim}{\lambda}$ and Eq. (3.55) can be interpreted as superposition between classical, anti-periodic tractions , Eq. (2.52), and a linear term with double stress $\underset{\approx}{\mathbf{M}}$ as in static boundary conditions (3.22).

If the implicit description (2.49) of periodic boundary conditions from classical theory of homogenisation were adapted instead of (3.53), the term with $\underset{\sim}{\mathbf{K}}^{\mathrm{s}}$ would drop from the square bracket in the first line of Eq. (3.54). Consequently, the term with $\underline{\lambda}$ would not appear in the co-factor of $\underset{\sim}{\underline{\mathbf{L}}}^{K\mathrm{s}}$. However, the stationarity condition for the boundary would still be Eq. (3.55) (though with another value of λ_j) and consequently the value of $\underset{\approx}{\mathbf{M}}$ computed by the kinetic micro-macro relation (3.11) would still comprise $\underline{\lambda}$, so that the generalized Hill-Mandel condition would be violated in general.

3.6. Special cases

3.6.1. Strain-gradient theory / Second gradient theory

Macroscopic theory

Mindlin [10] argued that a second gradient theory is obtained as special case of a micromorphic theory if the rate of microdeformation is identified ad-hoc with the macroscopic velocity gradient according to (2.33)

$$\underset{\sim}{\mathbf{L}}^{\chi} := \underline{\mathbf{V}} \otimes \nabla_{\underline{\mathbf{X}}} \tag{3.57}$$

so that the approximation (2.107) of velocity field $\underline{\mathbf{v}}(\underline{\mathbf{x}})$ becomes

$$\tilde{\underline{\mathbf{v}}} = \underline{\mathbf{V}}(\underline{\mathbf{X}}) + \left(\underline{\mathbf{V}} \otimes \nabla_{\underline{\mathbf{X}}} \right) \cdot (\underline{\mathbf{x}} - \underline{\mathbf{X}}) \,. \tag{3.58}$$

Under the kinematic constraint (3.57), the extrinsic stress $\underset{\sim}{\mathbf{\Sigma}}$ drops out from the balances of total and internal energy, so that Eq. (2.115) becomes

$$\bar{\rho} \dot{\bar{\Phi}} = \underset{\sim}{\bar{\sigma}} : \underset{\sim}{\mathbf{D}} + \underset{\approx}{\mathbf{M}} \vdots \underset{\sim}{\underline{\mathbf{L}}}^{K} - \nabla_{\underline{\mathbf{X}}} \cdot \underline{\mathbf{Q}} \tag{3.59}$$

with the macroscopic rates of deformation being

$$\underset{\sim}{\mathbf{D}} = \frac{1}{2} \left(\nabla_{\underline{\mathbf{X}}} \underline{\mathbf{V}} + \underline{\mathbf{V}} \otimes \nabla_{\underline{\mathbf{X}}} \right) \qquad\qquad \underset{\sim}{\underline{\mathbf{L}}}^{K} = \nabla_{\underline{\mathbf{X}}} \underline{\mathbf{V}} \otimes \nabla_{\underline{\mathbf{X}}} \,. \tag{3.60}$$

[3] Actually, Forest and Trinh [68] criticized the works of Kouznetsova et al. and "the condition of anti-periodic traction vector, tacitly used in these works". However, requirement Eq. (2.79) imposed by Kouznetsova et al. leads to boundary terms similar to Eq. (3.55) which is not inevitable anti-periodic.

Consequently, $\underset{\sim}{\mathbf{\Sigma}}$ can be eliminated from the balances of momenta by inserting (2.110) as

$$\underset{\sim}{\mathbf{\Sigma}} = \bar{\underset{\sim}{\sigma}} - \underset{\approx}{\mathbf{M}}^{\mathrm{T}} \cdot \underline{\nabla}_{\mathbf{X}} - \bar{\rho}\underset{\sim}{\mathbf{m}}^{\mathrm{T}} + \underset{\sim}{\mathbf{G}}_{\rho} \cdot \left(\underline{\nabla}_{\mathbf{X}}\dot{\underline{\mathbf{V}}}\right) \tag{3.61}$$

into (2.108) yielding

$$0 = \underline{\nabla}_{\mathbf{X}} \cdot \left[\bar{\underset{\sim}{\sigma}} - \underset{\approx}{\mathbf{M}}^{\mathrm{T}} \cdot \underline{\nabla}_{\mathbf{X}} - \bar{\rho}\underset{\sim}{\mathbf{m}}^{\mathrm{T}} + \underset{\sim}{\mathbf{G}}_{\rho} \cdot \left(\underline{\nabla}_{\mathbf{X}}\dot{\underline{\mathbf{V}}}\right)\right] + \bar{\rho}\bar{\underline{\mathbf{f}}} - \bar{\rho}\dot{\underline{\mathbf{V}}}\,. \tag{3.62}$$

The balance of angular momentum $\bar{\underset{\sim}{\sigma}}^{\mathrm{T}} = \bar{\underset{\sim}{\sigma}}$ (eq. (2.111)) remains valid.

Micro-macro transition

With constraint (3.57), the Hill-Mandel lemma (3.13) becomes

$$\left\langle \underset{\sim}{\sigma} : \underset{\sim}{\mathbf{d}} \right\rangle_V = \bar{\underset{\sim}{\sigma}} : \underset{\sim}{\mathbf{D}} + \underset{\approx}{\mathbf{M}} \vdots \underset{\approx}{\mathbf{L}}^{K\mathrm{s}}\,. \tag{3.63}$$

A comparison with the original form (3.13) shows that there are two opportunities to obtain Eq. (3.63):

1. $\underset{\sim}{\mathbf{e}} = 0$ or
2. $\underset{\sim}{\mathbf{s}} = 0$.

Opportunity 1) means that constraint (3.57) is enforced on the microscale by inserting the kinematic micro-macro relations (3.35)–(3.36) to Eq. (3.57):

$$\frac{1}{\Delta V} \oint_{\partial \Delta V} \underline{\mathbf{n}} \otimes \underline{\mathbf{v}} \,\mathrm{d}S = \left\langle \underline{\mathbf{v}} \otimes \underline{\xi} \right\rangle_{\mathrm{M}} \cdot \left(\underset{\sim}{\mathbf{G}}^{\mathrm{M}}\right)^{-1} \tag{3.64}$$

Consequently, the difference stress $\underset{\sim}{\mathbf{s}} = \underset{\sim}{\mathbf{\Sigma}}^{\mathrm{T}} - \bar{\underset{\sim}{\sigma}}$ still appears in the microscopic equilibrium condition (3.33) as Lagrange multiplier to enforce Eq. (3.64). Consequently, the kinetic micro-macro relations (3.10) and (3.12) for internal and external stress $\underset{\sim}{\mathbf{\Sigma}}$ and $\bar{\underset{\sim}{\sigma}}$ remain valid.

For opportunity 2, the kinematical constraint (3.64) is *relaxed* at the microscale. Thus, the equilibrium condition (3.33) at the microscale retains only a constant term

$$\underline{\nabla}_{\mathbf{x}} \cdot \underset{\sim}{\sigma} = \frac{\mathrm{H}_V\left(\underline{\xi}\right)}{\left\langle \mathrm{H}_V\left(\underline{\xi}\right)\right\rangle_V} \left[\frac{1}{2+n}\left[\underset{\approx}{\mathbf{I}}_{\mathrm{T}} : \left(\underset{\approx}{\mathbf{M}} \cdot \underset{\sim}{\mathbf{G}}^{-1}\right)\right] : \underset{\sim}{\mathbf{I}} - \underline{\lambda}^V\right] \tag{3.65}$$

which enforces the kinematic micro-macro relation (3.34) for the pure translation. Consequently, the kinetic micro-macro relations (3.10) and (3.12) with surface integral or volume integral yield the same value $\bar{\underset{\sim}{\sigma}}$. That is why, Eq. (3.10) for the external stress $\underset{\sim}{\mathbf{\Sigma}}$ must be abandoned at the microscale but $\underset{\sim}{\mathbf{\Sigma}}$ gets defined only by the macroscopic equilibrium condition (2.20), comparable the the lateral forces in Euler beam theory or Kirchhoff-Love theory of plates.

Comparison with theory of Gologanu, Kouznetsova et al.

For both opportunities, the kinematic micro-macro relation (3.37) for the second gradient $\underset{\approx}{\mathbf{L}}^{K\mathrm{s}} = \underset{\approx}{\mathbf{L}}^{\nabla\nabla U}$ remains valid as well as the corresponding kinetic relation (3.11) for the double stress $\underset{\approx}{\mathbf{M}} = \underset{\approx}{\mathbf{M}}^{\nabla\nabla U}$. A comparison of the kinematically-relaxed approach 2 with the theory of Gologanu, Kouznetsova et al. outlined in Section 2.2.2 exhibits two main differences:

Firstly, even for the kinematically relaxed case, a constant term appears in the microscopic equilibrium condition (3.65) compared to $\underline{\nabla}_{\mathbf{x}} \cdot \underset{\sim}{\sigma} = 0$ in the theory of Gologanu, Kouznetsova et al. In Section 3.3, the contribution of the double stress $\underset{\sim}{\underline{\mathbf{M}}}$ to the volume term $\underline{\nabla}_{\mathbf{X}} \cdot \underset{\sim}{\sigma}$ was introduced to allow arbitrary values of $\underset{\sim}{\underline{\mathbf{M}}}$ in the static boundary condition (3.22). If this volume term was taken into account, the "spherical part" $M_{ijk}G^{-1}_{ik}$ would need to vanish as noted by Gologanu et al. [44]. When constructing the work-conjugate deformation measure $\underset{\sim}{\underline{\mathbf{L}}}^{Ks}$ to $\underset{\sim}{\underline{\mathbf{M}}}$ by means of the Hill-Mandel lemma (3.7), this volume contribution of the spherical part is associated with the appearance of the macroscopic velocity, defined as volume integral (3.34), in the kinematic micro-macro relation (3.37). The kinematic micro-macro relation (2.81) of Kouznetsova et al. [45] does not feature such a term but is, for exactly this reason, not objective as discussed in Section 2.2.2. The proposed modification (2.88) towards an objective micro-macro relation (2.94) requires to impose the volume constraint (2.91) for the macroscopic translations as well. The kinematic micro-macro relation (2.125) for $\underset{\sim}{\underline{\mathbf{K}}}$ by Forest is objective but leads to volume terms as well in Eq. (2.133).

Secondly, the derived kinematic boundary condition (3.49) is almost identical to Eq. (2.76) by Gologanu et al. [44] except a missing factor of 1/2 in front of the quadratic term. Vice versa, the kinetic micro-macro relation (2.87) contains a factor of 1/2 which is not present in definition (3.11) of the double stress $\underset{\sim}{\underline{\mathbf{M}}}$. Both definitions are consistent in the sense that they satisfy the respective generalized Hill-Mandel lemma. The different appearance of this factor 1/2 requires an explanation. In the theory of Gologanu, Kouznetsova et al., the factor 1/2 arises from the interpretation of the quadratic kinematic boundary condition Eqs. (2.65) and (2.77), respectively, as a Taylor expansion. Subsequently, a Hill-Mandel condition (2.83) is postulated. The macroscopic equilibrium conditions were derived by Gologanu et al. [44] and Kouznetsova et al. [45] via the method of virtual power, i. e. actually they were postulated as discussed in Section 2.1.4. In the present approach, the macroscopic equilibrium conditions were derived by Eringen's method of averaging the balance equations which lead, under an approximation, to definition (3.11) without a factor 1/2. Currently, the author does not see an advantage of disadvantage of one approach over the other which could justify a discrepancy of 100%.

Linearly constrained theory

It is often argued that a second gradient theory is obtained by enforcing the microdeformation and macrodeformation to be *equal*, Eq. (3.57). This is true without any doubt. However, this is not the only opportunity to derive a second gradient theory from a micromorphic theory. Rather, it suffices that microdeformation and macrodeformation are *linearly linked*[4]:

$$\underset{\sim}{\mathbf{L}}^{\chi} := \alpha \underline{\mathbf{V}} \otimes \underline{\nabla}_{\mathbf{X}} \,. \tag{3.66}$$

Under the kinematic constraint (3.66), the balances of internal energy (2.115) becomes

$$\overline{\rho}\dot{\overline{\Phi}} = \left[(1-\alpha)\,\underset{\sim}{\mathbf{\Sigma}} + \alpha\overline{\underset{\sim}{\sigma}}\right] : \underline{\nabla}_{\mathbf{X}}\underline{\mathbf{V}} + \alpha\underset{\sim}{\underline{\mathbf{M}}} \vdots \underline{\nabla}_{\mathbf{X}}\underline{\mathbf{V}} \otimes \underline{\nabla}_{\mathbf{X}} - \underline{\nabla}_{\mathbf{X}} \cdot \underline{\mathbf{Q}} \,. \tag{3.67}$$

Thus, as work-conjugate quantity to the second gradient $\underline{\nabla}_{\mathbf{X}}\underline{\mathbf{V}} \otimes \underline{\nabla}_{\mathbf{X}}$ has to be identified the quantity

$$\underset{\sim}{\underline{\mathbf{M}}}^{\nabla\nabla U} = \alpha\underset{\sim}{\underline{\mathbf{M}}} = \frac{\alpha}{\Delta V} \oint\limits_{\partial\Delta V} \underline{\xi} \otimes \underline{\mathbf{n}} \cdot \underset{\sim}{\sigma} \otimes \underline{\xi}\, \mathrm{d}S \,. \tag{3.68}$$

Furthermore, with Eq. (3.66) the kinematic boundary condition (3.49) reads

$$\underline{\mathbf{v}} = \underline{\mathbf{V}} + \underline{\xi} \cdot \underline{\nabla}_{\mathbf{X}}\underline{\mathbf{V}} + \alpha\underline{\xi} \cdot \underline{\nabla}_{\mathbf{X}}\underline{\mathbf{V}} \otimes \underline{\nabla}_{\mathbf{X}} \cdot \underline{\xi} \qquad \text{on } \partial\Delta V(\underline{\mathbf{X}}) \,. \tag{3.69}$$

[4] In general, α in Eq. (3.66) could even be a forth order tensor. For simplicity, only a scalar is considered here.

A comparison of Eqs. (3.68)–(3.69) with Eqs. (2.76) and (2.87) shows that the theory of Gologanu, Kouznetsova et al. is recovered if the constraint factor is set to $\alpha = 1/2$. The finding that a second gradient theory is obtained for arbitrary values of $\alpha > 0$ and with or without relaxation of the constraint on the microscale implies the question on the optimal choice of these parameters.

3.6.2. Micropolar theory (Cosserat theory)

Macroscopic theory

The continuum theory of the Cosserat brothers extends the Cauchy-Boltzmann theory towards moment-type stresses together with independent rotational degrees of freedom, cf. [92]. In the context of micromorphic theories, theories of this type are denoted as micropolar theories and are obtained by assuming the rate of microdeformation $\underset{\sim}{\mathbf{L}}^\chi$ to be skew-symmetric. Thus, $\underset{\sim}{\mathbf{L}}^\chi$ can be written in terms of an axial vector of microrotation $\underline{\mathbf{\Omega}}^\chi$ as

$$\underset{\sim}{\mathbf{L}}^\chi = -\,\underline{\mathbf{\Omega}}^\chi \cdot \underset{\sim}{\underline{\epsilon}}\,. \tag{3.70}$$

Therein, $\underset{\sim}{\underline{\epsilon}}$ is the permutation tensor. Consequently, the velocity approximation (2.107) reads

$$\underline{\tilde{\mathbf{v}}} = \underline{\mathbf{V}}(\underline{\mathbf{X}}) - \underline{\mathbf{\Omega}}^\chi(\underline{\mathbf{X}}) \cdot \underset{\sim}{\underline{\epsilon}} \cdot (\underline{\mathbf{x}} - \underline{\mathbf{X}}) = \underline{\mathbf{V}}(\underline{\mathbf{X}}) + \underline{\mathbf{\Omega}}^\chi(\underline{\mathbf{X}}) \times (\underline{\mathbf{x}} - \underline{\mathbf{X}})\,. \tag{3.71}$$

By Eq. (3.71), the averaged energy balance (2.113) becomes

$$\begin{aligned} &\underbrace{\left\langle \rho\dot{\Phi} \right\rangle_V}_{=\overline{\rho}\dot{\overline{\Phi}}} + \frac{1}{2} \underbrace{\langle\rho\rangle_V}_{=:\overline{\rho}} \left(\underline{\mathbf{V}} \cdot \underline{\mathbf{V}}\right)^{\boldsymbol{\cdot}} + \frac{1}{2}\Big[\underline{\mathbf{\Omega}}^\chi \cdot \underbrace{\left\langle \rho \left(\underset{\sim}{\mathbf{I}}\underline{\xi} \cdot \underline{\xi} - \underline{\xi}\underline{\xi}\right) \right\rangle_V}_{=:\underset{\sim}{\mathbf{G}}^{\mathrm{r}}} \cdot \underline{\mathbf{\Omega}}^\chi\Big]^{\boldsymbol{\cdot}} \\ &= \underline{\nabla}_{\underline{\mathbf{X}}} \cdot \Big[\underbrace{\langle \underset{\sim}{\sigma} \rangle_\Delta}_{=\underset{\sim}{\mathbf{\Sigma}}} \cdot \underline{\mathbf{V}} + \underbrace{\left\langle \underset{\sim}{\sigma} \cdot \underset{\sim}{\underline{\epsilon}} \cdot \underline{\xi} \right\rangle_\Delta}_{=:\underset{\sim}{\underline{\mathbf{M}}}^{\mathrm{r}}} \cdot \underline{\mathbf{\Omega}}^\chi\Big] - \underline{\nabla}_{\underline{\mathbf{X}}} \cdot \underbrace{\langle \underline{\mathbf{q}} \rangle_\Delta}_{=\underline{\mathbf{Q}}} + \underbrace{\langle \rho\underline{\mathbf{f}} \rangle_V}_{=\overline{\rho}\underline{\overline{\mathbf{f}}}} \cdot \underline{\mathbf{V}} + \underbrace{\left\langle \rho\underline{\mathbf{f}} \times \underline{\xi} \right\rangle_V}_{=:\underline{\overline{\mathbf{f}}}^{\mathrm{r}}} \cdot \underline{\mathbf{\Omega}}^\chi \end{aligned} \tag{3.72}$$

and allows to define the polar double stress $\underset{\sim}{\underline{\mathbf{M}}}^{\mathrm{r}}$, polar micro-inertia $\underset{\sim}{\mathbf{G}}^{\mathrm{r}}$ and a volumetric moment $\underline{\overline{\mathbf{f}}}^{\mathrm{r}}$, in addition to quantities which were already defined. A comparison with Eq. (3.11) shows, that $\underset{\sim}{\underline{\mathbf{M}}}^{\mathrm{r}}$ is related to the double stress of the general micromorphic theory as

$$\begin{aligned} M^{\mathrm{r}}_{ij} &= \frac{1}{\Delta V} \oint\limits_{\partial \Delta V} \xi_i n_k \sigma_{km} \epsilon_{mjp} \xi_p \,\mathrm{d}S = M_{imp}\epsilon_{mjp} \\ \underset{\sim}{\underline{\mathbf{M}}}^{\mathrm{r}} &= \frac{1}{\Delta V} \oint\limits_{\partial \Delta V} \underline{\xi} \otimes \underline{\mathbf{n}} \cdot \underset{\sim}{\sigma} \cdot \underset{\sim}{\underline{\epsilon}} \cdot \underline{\xi} \,\mathrm{d}S = -\underset{\approx}{\underline{\mathbf{M}}} : \underset{\sim}{\underline{\epsilon}}\,. \end{aligned} \tag{3.73}$$

Equation (3.73) shows directly, that the sub-symmetry of the double stress due to definition (3.11) results in a vanishing trace

$$\underset{\sim}{\underline{\mathbf{M}}}^{\mathrm{r}} : \underset{\sim}{\mathbf{I}} = -\underset{\approx}{\underline{\mathbf{M}}} \vdots \underset{\sim}{\underline{\epsilon}} = 0 \tag{3.74}$$

of the polar double stress $\underset{\sim}{\underline{\mathbf{M}}}^{\mathrm{r}}$.

For obtaining the balance of internal energy, balance equations for $\underline{\nabla}_{\underline{\mathbf{X}}} \cdot \underset{\sim}{\mathbf{\Sigma}}$ and $\underline{\nabla}_{\underline{\mathbf{X}}} \cdot \underset{\sim}{\underline{\mathbf{M}}}^{\mathrm{r}}$ are necessary to replace the first term on the right-hand side of Eq. (3.72) by local quantities. Firstly, this is the macroscopic balance of linear momentum (2.108). Secondly, by means of Eq. (3.73) and definitions in Eq. (3.72), the macroscopic balance of angular momentum (2.112) can be written as

$$0 = \underline{\nabla}_{\underline{\mathbf{X}}} \cdot \underset{\sim}{\underline{\mathbf{M}}}^{\mathrm{r}} + \underset{\sim}{\mathbf{\Sigma}} : \underset{\sim}{\underline{\epsilon}} + \underline{\overline{\mathbf{f}}}^{\mathrm{r}} - \underline{\dot{\mathbf{\Omega}}}^\chi \cdot \underset{\sim}{\mathbf{G}}^{\mathrm{r}}\,. \tag{3.75}$$

Finally, the balance of internal energy becomes

$$\overline{\rho}\dot{\Phi} = \underset{\sim}{\mathbf{\Sigma}} : \underbrace{\left(\nabla_{\underline{\mathbf{X}}}\underline{\mathbf{V}} - \underset{\sim}{\underline{\epsilon}} \cdot \underline{\mathbf{\Omega}}^{\chi}\right)}_{:=\underset{\sim}{\mathbf{D}}^{\mathrm{r}}} + \underset{\sim}{\mathbf{M}}^{\mathrm{r}} : \underbrace{\left(\nabla_{\underline{\mathbf{X}}}\underline{\mathbf{\Omega}}^{\chi}\right)}_{:=\underset{\sim}{\mathbf{L}}^{\mathrm{r}}} - \nabla_{\underline{\mathbf{X}}} \cdot \underline{\mathbf{Q}} \tag{3.76}$$

which implies the definitions of the rates of deformation $\underset{\sim}{\mathbf{D}}^{\mathrm{r}}$ and $\underset{\sim}{\mathbf{L}}^{\mathrm{r}}$ which are work conjugate to the stresses $\underset{\sim}{\mathbf{\Sigma}}$ and $\underset{\sim}{\mathbf{M}}^{\mathrm{r}}$, respectively. Alternatively, the first term on the right-hand side of Eq. (3.76) may be split into symmetric and skew-symmetric parts

$$\underset{\sim}{\mathbf{\Sigma}} : \left(\nabla_{\underline{\mathbf{X}}}\underline{\mathbf{V}} - \underset{\sim}{\underline{\epsilon}} \cdot \underline{\mathbf{\Omega}}^{\chi}\right) = \operatorname{sym}\underset{\sim}{\mathbf{\Sigma}} : \underset{\sim}{\mathbf{D}} + \left(\underset{\sim}{\underline{\epsilon}} : \underset{\sim}{\mathbf{\Sigma}}\right) \cdot \left(\frac{1}{2}\underset{\sim}{\underline{\epsilon}} : \nabla_{\underline{\mathbf{X}}}\underline{\mathbf{V}} - \underline{\mathbf{\Omega}}^{\chi}\right) . \tag{3.77}$$

This shows that the symmetric part of $\underset{\sim}{\mathbf{\Sigma}}$ is work-conjugate to the classical rate of deformation $\underset{\sim}{\mathbf{D}}$ whereas its skew-symmetric part is work-conjugate to the difference between macroscopic and micro-scopic rotation.

Regarding the second term in Eq. (3.76) it has to be mentioned that the double stress $\underset{\sim}{\mathbf{M}}^{\mathrm{r}}$ is deviatoric, Eq. (3.74), which is why only the deviatoric part $\underset{\sim}{\mathbf{L}}^{\mathrm{rd}} = \underset{\sim}{\mathbf{L}}^{\mathrm{r}} - \frac{1}{n}\underset{\sim}{\mathbf{I}}\underset{\sim}{\mathbf{I}} : \underset{\sim}{\mathbf{L}}^{\mathrm{r}}$ of $\underset{\sim}{\mathbf{L}}^{\mathrm{r}}$ of the gradient of the rotation contributes to the internal power with $\underset{\sim}{\mathbf{M}}^{\mathrm{r}} : \underset{\sim}{\mathbf{L}}^{\mathrm{r}} = \underset{\sim}{\mathbf{M}}^{\mathrm{r}} : \underset{\sim}{\mathbf{L}}^{\mathrm{rd}}$.

Micro-macro transition

Under the condition outlined in Section 3.1, the generalized Hill-Mandel lemma for the micropolar theory takes the form

$$\left\langle \underset{\sim}{\sigma} : \underset{\sim}{\mathbf{d}} \right\rangle_V = \underset{\sim}{\mathbf{\Sigma}} : \left(\nabla_{\underline{\mathbf{X}}}\underline{\mathbf{V}} - \underset{\sim}{\underline{\epsilon}} \cdot \underline{\mathbf{\Omega}}^{\chi}\right) + \underset{\sim}{\mathbf{M}}^{\mathrm{r}} : \underset{\sim}{\mathbf{L}}^{\mathrm{rd}} . \tag{3.78}$$

Regarding the transition from the general micromorphic theory to the special case of a micropolar theory, the question arises, how constraint (3.70) on the rate of microdeformation is transferred to the microscale. The question is in particular how to deal with those quantities which do not appear anymore in the micropolar theory, i. e. with the symmetric part of the microdeformation and its gradient. In order to satisfy the Hill-Mandel lemma (3.78) there are two opportunities: either the respective kinematic quantities are set to zero or their work-conjugate stresses are relaxed. For a micropolar theory, it would surely not be reasonable to constrain the symmetric part of the microdeformation to vanish. Rather, only the non-vanishing part of Eq. (3.70) is enforced. Inserting the kinematic micro-macro relation (3.35), the kinematic micro-macro relation for the rotation thus reads

$$\underline{\mathbf{\Omega}}^{\chi} = -\frac{1}{2}\underset{\sim}{\underline{\epsilon}} : \left(\left\langle \underline{\mathbf{v}} \otimes \underline{\xi} \right\rangle_{\mathrm{M}} \cdot \left(\underset{\sim}{\mathbf{G}}^{\mathrm{M}}\right)^{-1}\right) = \frac{1}{2}\left\langle \left(\underline{\xi} \cdot \left(\underset{\sim}{\mathbf{G}}^{\mathrm{M}}\right)^{-1}\right) \times \underline{\mathbf{v}} \right\rangle_{\mathrm{M}} . \tag{3.79}$$

More difficult is the question how the double stress $\underset{\approx}{\underline{\mathbf{M}}}$ and the gradient of microdeformation $\underset{\approx}{\underline{\mathbf{L}}}^{K}$ are to be handled, both quantities which are defined over surface integrals in Eqs. (3.11) and (3.37) (up to the rigid translation which is, however, present anyway). In this context, the question should be addressed how the presented theory for general micromorphic media needs to be “disarmed” to the classical theory of homogenisation. This consideration leads to the finding that it depends on the type of boundary conditions to be applied at the microscale: if kinematic boundary conditions (3.49) are applied, the gradient of microdeformation $\underset{\approx}{\underline{\mathbf{L}}}^{K}$ needs to vanish in order to recover the classical theory in Eq. (2.45). In contrast, if static boundary conditions (3.22) are applied, the double stress $\underset{\approx}{\underline{\mathbf{M}}}$ needs to be set to zero to recover the classical case in Eq. (2.43).

For constructing static boundary conditions for the micropolar theory, it has firstly be noted that Eq. (3.73) cannot just be solved for $\underset{\approx}{\underline{\mathbf{M}}}$. Rather, the kinematic relation (3.70) needs to be incorporated. In the full micromorphic theory, the double stress $\underset{\approx}{\underline{\mathbf{M}}}$ is work-conjugate to $\underset{\sim}{\underline{\mathbf{L}}}^{K\mathrm{s}}$, the symmetric part of the gradient of rate of microdeformation. For the micropolar theory (3.73), this quantity has the value

$$L^{K\mathrm{s}}_{ijk} = \frac{1}{2}\left(\epsilon_{jmk} L^{\mathrm{r}}_{m,i} + \epsilon_{jmi} L^{\mathrm{r}}_{m,k}\right) \tag{3.80}$$

For $L^{K\mathrm{s}}_{ijk}$, the kinematic micro-macro relation (3.37) is available for the full micromorphic theory which could be inserted to the left-hand side of Eq. (3.80). Such an equation contains also vanishing components on its right-hand side. If only the non-vanishing components shall be considered, then Eq. (3.80) is projected to the permutation tensor

$$\underset{\sim}{\underline{\mathbf{L}}}^{K\mathrm{s}} : \underset{\sim}{\underline{\epsilon}} = -\frac{3}{2}\underset{\sim}{\mathbf{L}}^{\mathrm{rd}} . \tag{3.81}$$

Now the kinematic micro-macro relation (3.37) can be inserted yielding the kinematic micro-macro relation of the micropolar theory as

$$\begin{aligned}
\underset{\sim}{\mathbf{L}}^{\mathrm{rd}} &= \frac{1}{6\Delta V}\left[\left(\oint\limits_{\partial\Delta V} \underline{\mathbf{n}}\underline{\mathbf{v}}\underline{\xi}\ \mathrm{d}S\right)\cdot \underset{\sim}{\mathbf{G}}^{-1} + \underset{\sim}{\mathbf{G}}^{-1}\cdot\left(\oint\limits_{\partial\Delta V} \underline{\xi}\underline{\mathbf{n}}\underline{\mathbf{v}}\ \mathrm{d}S\right)\right.\\
&\quad\left. -\frac{2}{2+n}\underset{\sim}{\mathbf{G}}^{-1}\left(\oint\limits_{\partial\Delta V} \underline{\mathbf{v}}\,\underline{\mathbf{n}}\cdot\underline{\xi}\ \mathrm{d}S\right)\right] : \underset{\sim}{\underline{\epsilon}} - \frac{2}{3(2+n)}\left(\underset{\sim}{\mathbf{G}}^{-1}\left\langle\underline{\mathbf{v}}\right\rangle_{\mathrm{M}}\right) : \underset{\sim}{\underline{\epsilon}}, \qquad (3.82)\\
L^{\mathrm{rd}}_{ip} &= \frac{1}{6\Delta V}\left[\left(\oint\limits_{\partial\Delta V} n_i v_j \xi_m\ \mathrm{d}S\right) G^{-1}_{mk} + G^{-1}_{im}\left(\oint\limits_{\partial\Delta V} \xi_m n_k v_j\ \mathrm{d}S\right)\right.\\
&\quad\left. -\frac{2}{2+n}G^{-1}_{ik}\left(\oint\limits_{\partial\Delta V} v_j n_m \xi_m\ \mathrm{d}S\right)\right]\epsilon_{kjp} - \frac{2}{3(2+n)}G^{-1}_{ik}\left\langle v_j\right\rangle_{\mathrm{M}}\epsilon_{kjp} .
\end{aligned}$$

The boundary-value problem at the micro-scale can be obtained again via concept of minimal loading conditions. Enforcing the kinematic micro-macro relations (3.79) and (3.37) in addition to the classical ones leads to an equilibrium condition

$$\begin{aligned}
\underline{\nabla}_{\underline{\mathbf{x}}}\cdot\underset{\sim}{\sigma} &= \frac{\mathrm{H}_V\left(\underline{\xi}\right)}{\left\langle\mathrm{H}_V\left(\underline{\xi}\right)\right\rangle_V}\left[\frac{1}{2}\left(\underset{\sim}{\mathbf{\Sigma}}^{\mathrm{T}} - \underset{\sim}{\mathbf{\Sigma}}\right)\cdot\left(\underset{\sim}{\mathbf{G}}^{\mathrm{M}}\right)^{-1}\cdot\underline{\xi} - \frac{2}{3(2+n)}\underset{\sim}{\underline{\epsilon}} : \left(\underset{\sim}{\mathbf{G}}^{-1}\cdot\underset{\sim}{\underline{\mathbf{M}}}^{\mathrm{r}}\right) - \underline{\lambda}^V\right],\\
\sigma_{ij,i} &= \frac{\mathrm{H}_V\left(\xi\right)}{\left\langle\mathrm{H}_V\left(\xi\right)\right\rangle_V}\left[\frac{1}{2}\left(\Sigma_{kj} - \Sigma_{jk}\right)G^{\mathrm{M}-1}_{km}\xi_m - \frac{2}{3(2+n)}\epsilon_{jkm}G^{-1}_{kl}M^{\mathrm{r}}_{lm} - \lambda^V_j\right],
\end{aligned} \tag{3.83}$$

and the *static boundary conditions* on $\partial\Delta V(\underline{\mathbf{X}})$ read

$$\begin{aligned}
\underline{\mathbf{n}}\cdot\underset{\sim}{\sigma} &= \underline{\mathbf{n}}\cdot\underset{\sim}{\mathbf{\Sigma}} - \frac{1}{6}\left[\underline{\mathbf{n}}\cdot\underset{\sim}{\underline{\mathbf{M}}}^{\mathrm{r}}\cdot\underset{\sim}{\underline{\epsilon}}\cdot\underset{\sim}{\mathbf{G}}^{-1}\cdot\underline{\xi} + \underline{\xi}\cdot\underset{\sim}{\mathbf{G}}^{-1}\cdot\underset{\sim}{\underline{\mathbf{M}}}^{\mathrm{r}}\cdot\underset{\sim}{\underline{\epsilon}}\cdot\underline{\mathbf{n}} - \frac{2}{2+n}\underline{\mathbf{n}}\cdot\underline{\xi}\left(\underset{\sim}{\mathbf{G}}^{-1}\cdot\underset{\sim}{\underline{\mathbf{M}}}^{\mathrm{r}}\right) : \underset{\sim}{\underline{\epsilon}}\right]\\
n_i\sigma_{ij} &= n_i\Sigma_{ij} - \frac{1}{6}\left[n_i M^{\mathrm{r}}_{ip}\epsilon_{pjk}G^{-1}_{km}\xi_m + \xi_m G^{-1}_{mi}M^{\mathrm{r}}_{ip}\epsilon_{pjk}n_k - \frac{2}{2+n}n_m\xi_m G^{-1}_{ki}M^{\mathrm{r}}_{ip}\epsilon_{kpj}\right].
\end{aligned} \tag{3.84}$$

Of course, in Eq. (3.84), the prescribed polar double stress $\underset{\sim}{\underline{\mathbf{M}}}^{\mathrm{r}}$ needs to be deviatoric $\underset{\sim}{\underline{\mathbf{M}}}^{\mathrm{r}} : \underset{\sim}{\mathbf{I}} = 0$, in consistency with Eq. (3.74). Equations (3.83)–(3.84) satisfy the Hill-Mandel condition (3.78). With static boundary conditions (3.84), only those parts of the general double stress tensor $\underset{\sim}{\underline{\mathbf{M}}}$ are non-zero which are associated with its micro-polar counter-part $\underset{\sim}{\underline{\mathbf{M}}}^{\mathrm{r}}$, Eq. (3.73).

In contrast, *kinematic boundary conditions* are found by inserting Eq. (3.70) to the kinematic boundary condition (3.49) of the general micromorphic theory

$$\underline{\mathbf{v}} = \underline{\mathbf{V}} + \underline{\xi} \cdot \nabla_{\underline{\mathbf{X}}} \underline{\mathbf{V}} + \left(\underline{\xi} \cdot \underset{\sim}{\mathbf{L}}^{\mathrm{r}}\right) \times \underline{\xi} \qquad \text{on } \partial \Delta V \,. \tag{3.85}$$

so that only those parts of the gradient $\underset{\approx}{\mathbf{L}}^{K\mathrm{s}}$ of the rate of microdeformation are non-zero which are associated with the micro-polar curvature $\underset{\sim}{\mathbf{L}}^{\mathrm{r}}$. Note, that the spherical part of $\underset{\sim}{\mathbf{L}}^{\mathrm{r}}$ does not contribute to (3.85), in consistency with Eq. (3.74).

The non-classical deformation modes of the micropolar theory are sketched in Fig. 3.3 for both types of boundary conditions. Figures 3.3a and 3.3b show that the off-diagonal

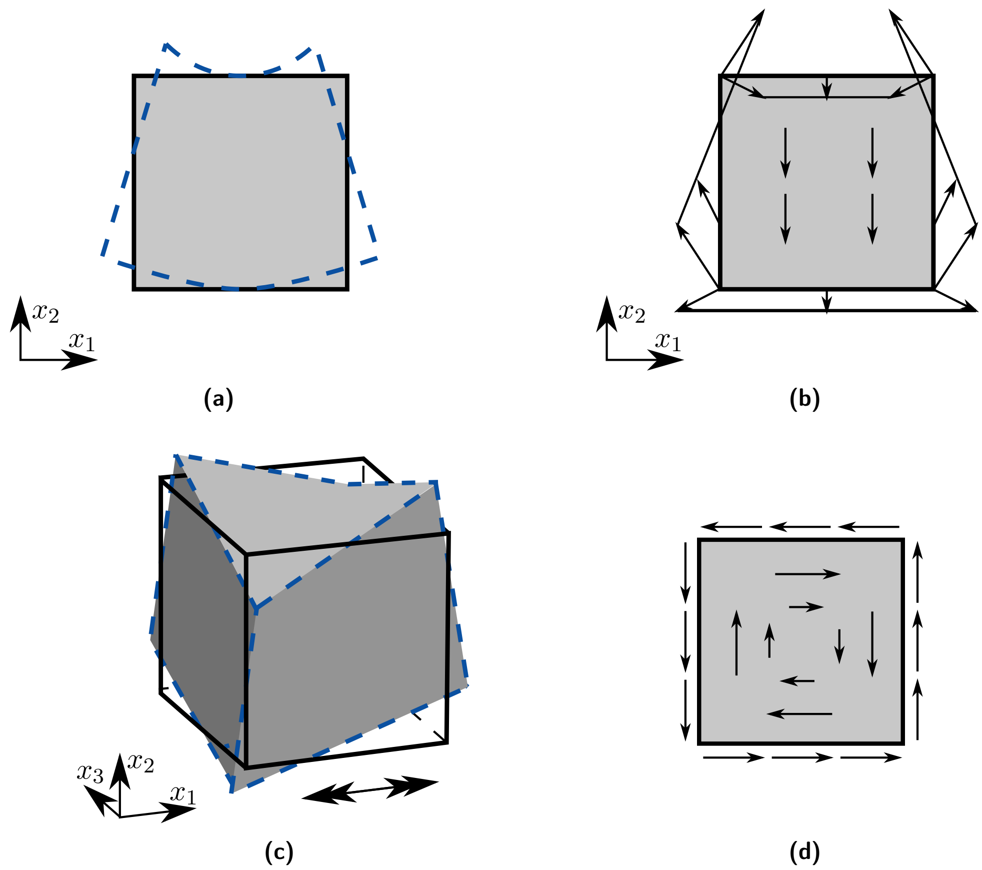

Fig. 3.3.: Non-classical micropolar deformation modes of the volume element ΔV: (a) kinematic boundary condition (3.85) with $\underset{\sim}{\mathbf{L}}^{\mathrm{r}} = \underline{\mathbf{b}}_1 \underline{\mathbf{b}}_3$, (b) static boundary condition (3.84) with $\underset{\sim}{\mathbf{M}}^{\mathrm{r}} = \underline{\mathbf{b}}_1 \underline{\mathbf{b}}_3$, (c) kinematic boundary condition (3.85) with $\underset{\sim}{\mathbf{L}}^{\mathrm{r}} = \underline{\mathbf{b}}_1 \underline{\mathbf{b}}_1$, (d) static boundary condition (3.84) $\underset{\sim}{\mathbf{\Sigma}} = \underline{\mathbf{b}}_1 \underline{\mathbf{b}}_2 - \underline{\mathbf{b}}_2 \underline{\mathbf{b}}_1$

components of $\underset{\sim}{\mathbf{L}}^{\mathrm{r}}$ and $\underset{\sim}{\mathbf{M}}^{\mathrm{r}}$ induce bending-type deformation modes of the volume element. Figures 3.3c illustrates the effect of a diagonal component of $\underset{\sim}{\mathbf{L}}^{\mathrm{r}}$ which twists the opposite surfaces of the volume element against each other. The antimetric part of $\underset{\sim}{\mathbf{\Sigma}}$ drives an internal twisting of the volume element as can be seen in Fig. 3.3d.

Periodic boundary conditions can be implemented as discussed in Section 3.5 for the general micromorphic theory by amending a periodic fluctuation field $\Delta \underline{\mathbf{v}}(\underline{\xi})$ to the right-hand side of Eq. (3.85) under global enforcement of the kinematic micro-macro relations (3.34), (3.79) and (3.82), respectively.

Plane case

If a body is considered which deforms only in the x_1-x_2-plane, the vector of micro-rotation is directed in x_3 direction $\underline{\boldsymbol{\Omega}}^\chi = \Omega^\chi\,\underline{\mathbf{b}}_3$. Consequently, the remaining components of the rate of curvature $\underset{\sim}{\mathbf{L}}^{\mathrm{r}}$ and polar double stress can be collected in vectors

$$\underline{\mathbf{L}}^{\mathrm{r}} = \underset{\sim}{\mathbf{L}}^{\mathrm{r}} \cdot \underline{\mathbf{b}}_3\,, \qquad\qquad \underline{\mathbf{M}}^{\mathrm{r}} = \underset{\sim}{\mathbf{M}}^{\mathrm{r}} \cdot \underline{\mathbf{b}}_3\,. \tag{3.86}$$

On the microscale, these vectors drive the bending type deformation types, Figs. 3.3a and 3.3b.

In terms of these planar vectors, Eqs. (3.83)–(3.85) become

$$\underline{\nabla}_{\mathbf{x}} \cdot \underset{\sim}{\sigma} = \frac{\mathrm{H}_V(\underline{\xi})}{\langle \mathrm{H}_V(\underline{\xi})\rangle_V}\left[\frac{1}{2}\left(\underset{\sim}{\boldsymbol{\Sigma}}^{\mathrm{T}} - \underset{\sim}{\boldsymbol{\Sigma}}\right)\cdot\left(\underset{\sim}{\mathbf{G}}^{\mathrm{M}}\right)^{-1}\cdot\underline{\xi} - \frac{1}{6}\underset{\sim}{\epsilon}\cdot\underset{\sim}{\mathbf{G}}^{-1}\cdot\underline{\mathbf{M}}^{\mathrm{r}} - \underline{\lambda}^V\right], \tag{3.87}$$

$$\underline{\mathbf{n}}\cdot\underset{\sim}{\sigma} = \underline{\mathbf{n}}\cdot\underset{\sim}{\boldsymbol{\Sigma}} - \frac{1}{6}\underset{\sim}{\epsilon}\cdot\left[\underset{\sim}{\mathbf{G}}^{-1}\cdot\underline{\xi}\,\underline{\mathbf{n}}\cdot\underline{\mathbf{M}}^{\mathrm{r}} + \underline{\mathbf{n}}\,\underline{\xi}\cdot\underset{\sim}{\mathbf{G}}^{-1}\cdot\underline{\mathbf{M}}^{\mathrm{r}} - \frac{1}{2}\underset{\sim}{\mathbf{G}}^{-1}\cdot\underline{\mathbf{M}}^{\mathrm{r}}\,\underline{\mathbf{n}}\cdot\underline{\xi}\right] \text{ on } \partial\Delta V\,, \tag{3.88}$$

$$\underline{\mathbf{v}} = \underline{\mathbf{V}} + \underline{\xi}\cdot\underline{\nabla}_{\mathbf{X}}\underline{\mathbf{V}} + \underset{\sim}{\epsilon}\cdot\underline{\xi}\,\underline{\mathbf{L}}^{\mathrm{r}}\cdot\underline{\xi} \text{ on } \partial\Delta V\,. \tag{3.89}$$

Therein, the symbol $\underset{\sim}{\epsilon} = \underset{\approx}{\epsilon}\cdot\underline{\mathbf{b}}_3$ was introduced for the projection of the permutation tensor to the x_3-direction.

Constrained micropolar theory (Couple Stress theory)

The couple stress theory is a micropolar theory with linear constraint between micro-rotation $\underline{\boldsymbol{\Omega}}^\chi$ and macro-rotation skw $\underline{\nabla}_{\mathbf{X}}\underline{\mathbf{V}}$.

$$\underline{\boldsymbol{\Omega}}^\chi = \frac{1}{2}\underset{\approx}{\epsilon} : \left(\underline{\nabla}_{\mathbf{X}}\underline{\mathbf{V}}\right) \tag{3.90}$$

Consequently, the rate of torsion-curvature becomes

$$\underset{\sim}{\mathbf{L}}^{\mathrm{r}} = \underset{\sim}{\mathbf{L}}^{\mathrm{rd}} = \underline{\nabla}_{\mathbf{X}}\underline{\boldsymbol{\Omega}}^\chi = \frac{1}{2}\underline{\nabla}_{\mathbf{X}}\underline{\nabla}_{\mathbf{X}}\underline{\mathbf{V}} : \underset{\approx}{\epsilon} \tag{3.91}$$

The Hill-Mandel condition (3.78) thus reads

$$\left\langle \underset{\sim}{\sigma} : \dot{\underset{\sim}{\varepsilon}}\right\rangle_V = \underset{\sim}{\boldsymbol{\Sigma}} : \frac{1}{2}\left[\underline{\nabla}_{\mathbf{X}}\underline{\mathbf{V}} + \underline{\mathbf{V}}\otimes\underline{\nabla}_{\mathbf{X}}\right] + \underset{\sim}{\mathbf{M}}^{\mathrm{r}} : \underset{\sim}{\mathbf{L}}^{\mathrm{r}}\,. \tag{3.92}$$

Obviously, only the symmetric parts of $\underset{\sim}{\boldsymbol{\Sigma}}$ and $\underline{\nabla}_{\mathbf{X}}\underline{\mathbf{V}}$ contribute to the work. Again, a microscopic counterpart to the constraint (3.90) can be constructed by means of kinematic micro-macro relations (3.36) and(3.79) of the general micropolar theory. If this constraint is enforced at the microscale, the microscopic equilibrium condition (3.83) and definition (3.10) of the external stress $\underset{\sim}{\boldsymbol{\Sigma}}$ remain valid. Otherwise, $\underset{\sim}{\boldsymbol{\Sigma}}$ drops from Eq. (3.83) and the skew-symmetric part of $\underset{\sim}{\boldsymbol{\Sigma}}$ is defined only at the macroscale by the global balance of angular momentum (3.75). The static boundary condition (3.84) remains valid and with Eq. (3.90), the kinematic boundary condition (3.85) can be written as

$$\underline{\mathbf{v}} = \underline{\mathbf{V}} + \underline{\xi}\cdot\underline{\nabla}_{\mathbf{X}}\underline{\mathbf{V}} + \frac{1}{2}\underline{\xi}\cdot\left(\underline{\nabla}_{\mathbf{X}}\underline{\nabla}_{\mathbf{X}}\underline{\mathbf{V}} - \underline{\nabla}_{\mathbf{X}}\underline{\mathbf{V}}\otimes\underline{\nabla}_{\mathbf{X}}\right)\cdot\underline{\xi} \qquad \text{on } \partial\Delta V\,. \tag{3.93}$$

It is identical with the boundary condition given by Forest [36] for the plane case. Bouyge et al. [37] employed a slightly different quadratic term for the kinematic boundary conditions and also the linear term in their static boundary conditions differs from Eq. (3.88). Both types of boundary conditions were adapted from the problem of bending of a beam. Bouyge et al. did neither provide micro-macro relations for the double stress $\underset{\sim}{\mathbf{M}}^{\mathrm{r}}$ nor for the curvature

$\underset{\sim}{\mathbf{L}}^{\mathrm{r}}$. Branke et al. [70] have an additional prefactor 2/3 in front of the quadratic term. They employed the polynomial approach, Section 2.2.4. They faced the problem, that the coefficients of the quadratic term are not uniquely defined by the respective kinematic micro-macro relation without a kinetic micro-macro relation for the polar double stress $\underset{\approx}{\mathbf{M}}^{\mathrm{r}}$.

As discussed in section 3.6.1, an additional constraint factor α may be incorporated in Eqs. (3.90)–(3.93).

3.6.3. Microstrain theory

Macroscopic theory

In a microstrain theory [11], the tensor of microdeformation is assumed to be symmetric

$$\underset{\sim}{\mathbf{L}}^{\chi} = \underset{\sim}{\mathbf{L}}^{\chi\mathrm{T}} =: \underset{\sim}{\mathbf{L}}^{\chi\mathrm{s}} . \tag{3.94}$$

Thus, with Eq. (2.107) the macroscopic energy balance (2.113) becomes

$$\begin{aligned} \bar{\rho}\dot{\bar{\Phi}} + \frac{1}{2}\bar{\rho}\left(\underline{\mathbf{V}}\cdot\underline{\mathbf{V}}\right)^{\bullet} + \frac{1}{2}\underset{\sim}{\mathbf{G}}_{\rho} : \left(\underset{\sim}{\mathbf{L}}^{\chi\mathrm{s}}\cdot\underset{\sim}{\mathbf{L}}^{\chi\mathrm{s}}\right)^{\bullet} \\ = \underline{\nabla}_{\underline{\mathbf{X}}}\cdot\left(\underset{\sim}{\mathbf{\Sigma}}\cdot\underline{\mathbf{V}} + \underset{\approx}{\mathbf{M}}^{\mathrm{s}} : \underset{\sim}{\mathbf{L}}^{\chi\mathrm{s}}\right) - \underline{\nabla}_{\underline{\mathbf{X}}}\cdot\underline{\mathbf{Q}} + \bar{\rho}\underline{\bar{\mathbf{f}}}\cdot\underline{\mathbf{V}} + \bar{\rho}\underset{\sim}{\mathbf{m}}^{\mathrm{s}} : \underset{\sim}{\mathbf{L}}^{\chi\mathrm{s}} \end{aligned} \tag{3.95}$$

Therein, the symmetric parts of the higher order volumetric force $\underset{\sim}{\mathbf{m}}^{\mathrm{s}} = \operatorname{sym}\underset{\sim}{\mathbf{m}}$ and the right-subsymmetric part

$$M^{\mathrm{s}}_{ijk} = \frac{1}{2}\left(M_{ijk} + M_{ikj}\right) = \frac{1}{2\Delta V}\oint\limits_{\partial\Delta V} \xi_i n_m \left(\sigma_{mj}\xi_k + \sigma_{mk}\xi_j\right)\,\mathrm{d}S \tag{3.96}$$

of the micromorphic double stress $\underset{\approx}{\mathbf{M}}$ were defined. Remarkably, due to the symmetry of $\underset{\approx}{\mathbf{M}}$, Eq. (3.11), all components of $\underset{\approx}{\mathbf{M}}$ are uniquely determined by Eq. (3.96) and can be determined by a cyclic permutation as

$$M_{ijk} = M^{\mathrm{s}}_{ijk} + M^{\mathrm{s}}_{kji} - M^{\mathrm{s}}_{jik} . \tag{3.97}$$

The required expression for $\underline{\nabla}_{\underline{\mathbf{X}}}\cdot\underset{\approx}{\mathbf{M}}^{\mathrm{s}}$ is obtained as the right-subsymmetric part of the higher-order balance (2.110) as

$$0 = \underline{\nabla}_{\underline{\mathbf{X}}}\cdot\underset{\approx}{\mathbf{M}}^{\mathrm{s}} + \underset{\sim}{\mathbf{\Sigma}} - \underset{\sim}{\bar{\sigma}} + \bar{\rho}\underset{\sim}{\mathbf{m}}^{\mathrm{s}} - \frac{1}{2}\left(\dot{\underset{\sim}{\mathbf{L}}}^{\chi\mathrm{s}}\cdot\underset{\sim}{\mathbf{G}}_{\rho} + \underset{\sim}{\mathbf{G}}_{\rho}\cdot\dot{\underset{\sim}{\mathbf{L}}}^{\chi\mathrm{s}}\right) . \tag{3.98}$$

Therein, it was used that the internal stress $\underset{\sim}{\bar{\sigma}}$ is symmetric, Eq. (2.111), and that the balance of angular momentum of a microstrain continuum reduces to the classical relation

$$\underset{\sim}{\mathbf{\Sigma}}^{\mathrm{T}} = \underset{\sim}{\mathbf{\Sigma}} . \tag{3.99}$$

Consequently, the balance of internal energy reads

$$\begin{aligned} \bar{\rho}\dot{\bar{\Phi}} &= \underset{\sim}{\mathbf{\Sigma}} : \underset{\sim}{\mathbf{D}} + \left(\underset{\sim}{\bar{\sigma}} - \underset{\sim}{\mathbf{\Sigma}}\right) : \underset{\sim}{\mathbf{L}}^{\chi\mathrm{s}} + \underset{\approx}{\mathbf{M}}^{\mathrm{s}} \vdots \underline{\nabla}_{\underline{\mathbf{X}}}\underset{\sim}{\mathbf{L}}^{\chi\mathrm{s}} - \underline{\nabla}_{\underline{\mathbf{X}}}\cdot\underline{\mathbf{Q}} \\ &= \underset{\sim}{\bar{\sigma}} : \underset{\sim}{\mathbf{D}} + \left(\underset{\sim}{\mathbf{\Sigma}} - \underset{\sim}{\bar{\sigma}}\right) : \left(\underset{\sim}{\mathbf{D}} - \underset{\sim}{\mathbf{L}}^{\chi\mathrm{s}}\right) + \underset{\approx}{\mathbf{M}}^{\mathrm{s}} \vdots \underline{\nabla}_{\underline{\mathbf{X}}}\underset{\sim}{\mathbf{L}}^{\chi\mathrm{s}} - \underline{\nabla}_{\underline{\mathbf{X}}}\cdot\underline{\mathbf{Q}} . \end{aligned} \tag{3.100}$$

In the microstrain theory, the rate of microdeformation $\underset{\sim}{\mathbf{L}}^{\chi\mathrm{s}}$ is objective itself, in contrast to the general micromorphic theory. Thus, two equivalent sets of possible work conjugate measures of stress and deformation can be identified for the microstrain theory: $\underset{\sim}{\bar{\sigma}}$ and $\underset{\sim}{\mathbf{s}} = \underset{\sim}{\mathbf{\Sigma}} - \underset{\sim}{\bar{\sigma}}$ conjugate to $\underset{\sim}{\mathbf{D}}$ and $\underset{\sim}{\mathbf{L}}^{es} := \underset{\sim}{\mathbf{D}} - \underset{\sim}{\mathbf{L}}^{\chi\mathrm{s}}$, respectively (as in Mindlin's theory, Section 2.1.3), or $\underset{\sim}{\mathbf{\Sigma}}$ and $\underset{\sim}{\bar{\mathbf{s}}} := -\underset{\sim}{\mathbf{s}}$ conjugate to $\underset{\sim}{\mathbf{D}}$ and $\underset{\sim}{\mathbf{L}}^{\chi\mathrm{s}}$, in both cases accompanied by $\underset{\approx}{\mathbf{M}}^{\mathrm{s}}$ conjugate to $\underline{\nabla}_{\underline{\mathbf{X}}}\underset{\sim}{\mathbf{L}}^{\chi\mathrm{s}}$.

Micro-macro transition

For the microstrain theory, the generalized Hill-Mandel lemma (3.7) thus reads

$$\left\langle \underset{\sim}{\sigma} : \underset{\sim}{\mathbf{d}} \right\rangle_V = \underset{\sim}{\mathbf{\Sigma}} : \underset{\sim}{\mathbf{D}} + \left(\underset{\sim}{\bar{\sigma}} - \underset{\sim}{\mathbf{\Sigma}}\right) : \underset{\sim}{\mathbf{L}}^{\chi \mathrm{s}} + \underset{\approx}{\underline{\mathbf{M}}}^{\mathrm{s}} \vdots \underline{\nabla}_{\underline{\mathbf{X}}} \underset{\sim}{\mathbf{L}}^{\chi \mathrm{s}} \,. \tag{3.101}$$

According to Eq. (3.94), the kinematic micro-macro relation for the rate of microstrain is the symmetric part of the respective relation (3.35) of the general micromorphic theory:

$$\underset{\sim}{\mathbf{L}}^{\chi \mathrm{s}} = \operatorname{sym} \underset{\sim}{\mathbf{L}}^{\chi} = \frac{1}{2} \left(\left\langle \underline{\mathbf{v}} \otimes \underline{\xi} \right\rangle_{\mathrm{M}} \cdot \left(\underset{\sim}{\mathbf{G}}^{\mathrm{M}}\right)^{-1} + \left(\underset{\sim}{\mathbf{G}}^{\mathrm{M}}\right)^{-1} \cdot \left\langle \underline{\xi} \otimes \underline{\mathbf{v}} \right\rangle_{\mathrm{M}} \right) . \tag{3.102}$$

Furthermore, the symmetric part of the gradient of the rate of microdeformation $\underset{\approx}{\underline{\mathbf{L}}}^{K\mathrm{s}}$ has the value

$$\underset{\approx}{\underline{\mathbf{L}}}^{K\mathrm{s}} = \frac{1}{2} \left(\underline{\nabla}_{\underline{\mathbf{X}}} \underset{\sim}{\mathbf{L}}^{\chi \mathrm{s}} + \underset{\sim}{\mathbf{L}}^{\chi \mathrm{s}} \otimes \underline{\nabla}_{\underline{\mathbf{X}}} \right) . \tag{3.103}$$

By cyclic permutation, this equation can be solved for the components of $\underline{\nabla}_{\underline{\mathbf{X}}} \underset{\sim}{\mathbf{L}}^{\chi \mathrm{s}}$, analogously to Eq. (3.97), as

$$L^{\chi \mathrm{s}}_{jk,i} = L^{K\mathrm{s}}_{ijk} + L^{K\mathrm{s}}_{ikj} - L^{K\mathrm{s}}_{jik} \,. \tag{3.104}$$

Now the kinematic micro-macro relation (3.37) can be inserted to the right-hand side of Eq. (3.104). This yields

$$\begin{aligned} L^{\chi \mathrm{s}}_{jk,i} = \frac{1}{4\Delta V} \oint_{\partial \Delta V} & v_j n_i \xi_m G^{-1}_{mk} + v_j n_k \xi_m G^{-1}_{mi} + v_k n_i \xi_m G^{-1}_{mj} + v_k n_j \xi_m G^{-1}_{mi} - v_i n_j \xi_m G^{-1}_{mk} \\ & - v_i n_k \xi_m G^{-1}_{mj} - \frac{2}{2+n} \left(v_k n_m \xi_m G^{-1}_{ij} + v_j n_m \xi_m G^{-1}_{ik} - v_i n_m \xi_m G^{-1}_{jk} \right) \mathrm{d}S \\ & - \frac{1}{2+n} \left(\langle v_j \rangle_{\mathrm{M}} G^{-1}_{ik} + \langle v_k \rangle_{\mathrm{M}} G^{-1}_{ij} - \langle v_i \rangle_{\mathrm{M}} G^{-1}_{jk} \right) \end{aligned} \tag{3.105}$$

By Eq. (3.97), the local equilibrium condition (3.33) and the static boundary condition (3.22) become

$$\underline{\nabla}_{\underline{\mathbf{x}}} \cdot \underset{\sim}{\sigma} = \frac{\mathrm{H}_V(\underline{\xi})}{\left\langle \mathrm{H}_V(\underline{\xi}) \right\rangle_V} \left[\left(\underset{\sim}{\mathbf{\Sigma}} - \underset{\sim}{\bar{\sigma}}\right) \cdot \left(\underset{\sim}{\mathbf{G}}^{\mathrm{M}}\right)^{-1} \cdot \underline{\xi} + \frac{1}{2+n} \left(2 \underset{\approx}{\mathbf{I}}_{\mathrm{T}} : \underset{\approx}{\underline{\mathbf{M}}}^{\mathrm{s}} - \underset{\approx}{\underline{\mathbf{M}}}^{\mathrm{s}} \right) : \underset{\sim}{\mathbf{G}}^{-1} - \underline{\lambda}^V \right] , \tag{3.106}$$

$$\sigma_{ij,i} = \frac{\mathrm{H}_V(\underline{\xi})}{\left\langle \mathrm{H}_V(\underline{\xi}) \right\rangle_V} \left[\left(\Sigma_{jk} - \bar{\sigma}_{jk} \right) G^{\mathrm{M}-1}_{km} \xi_m + \frac{1}{2+n} \left(2 M^{\mathrm{s}}_{kjm} - M^{\mathrm{s}}_{jkm} \right) G^{-1}_{km} - \lambda^V_j \right]$$

$$\begin{aligned} \underline{\mathbf{n}} \cdot \underset{\sim}{\sigma} = & \underline{\mathbf{n}} \cdot \underset{\sim}{\mathbf{\Sigma}} + \frac{1}{2} \left[\underline{\mathbf{n}} \cdot \underset{\approx}{\underline{\mathbf{M}}}^{\mathrm{s}} \cdot \underset{\sim}{\mathbf{G}}^{-1} \cdot \underline{\xi} + \underline{\xi} \cdot \underset{\sim}{\mathbf{G}}^{-1} \cdot \underset{\approx}{\underline{\mathbf{M}}}^{\mathrm{s}} \cdot \underline{\mathbf{n}} - \underset{\approx}{\underline{\mathbf{M}}}^{\mathrm{s}} : \left(\underline{\mathbf{n}} \otimes \underset{\sim}{\mathbf{G}}^{-1} \cdot \underline{\xi} \right) \right] \\ & - \frac{1}{2\,(2+n)} \underline{\mathbf{n}} \cdot \underline{\xi} \left(2 \underset{\approx}{\mathbf{I}}_{\mathrm{T}} : \underset{\approx}{\underline{\mathbf{M}}}^{\mathrm{s}} - \underset{\approx}{\underline{\mathbf{M}}}^{\mathrm{s}} \right) : \underset{\sim}{\mathbf{G}}^{-1} \qquad \text{on } \partial \Delta V(\underline{\mathbf{X}}) \end{aligned} \tag{3.107}$$

$$n_i \sigma_{ij} = n_i \Sigma_{ij} + \frac{1}{2} n_i \left(M^{\mathrm{s}}_{ijp} + M^{\mathrm{s}}_{pji} - M^{\mathrm{s}}_{jip} \right) G^{-1}_{pm} \xi_m - \frac{1}{2(2+n)} n_i \xi_i \left(2 M^{\mathrm{s}}_{kjm} - M^{\mathrm{s}}_{jkm} \right) G^{-1}_{km}$$

The respective kinematic boundary condition (3.49) becomes with Eq. (3.104)

$$\underline{\mathbf{v}} = \underline{\mathbf{V}} + \underline{\xi} \cdot \underline{\nabla}_{\underline{\mathbf{X}}} \underline{\mathbf{V}} + \underline{\xi} \cdot \left(\underline{\nabla}_{\underline{\mathbf{X}}} \underset{\sim}{\mathbf{L}}^{\chi \mathrm{s}} \right) \cdot \underline{\xi} \qquad \text{on } \partial \Delta V(\underline{\mathbf{X}}) \,. \tag{3.108}$$

Due to the unique relations (3.97) and (3.104) between the micromorphic double stress $\underset{\approx}{\underline{\mathbf{M}}}$ and the microstrain double stress $\underset{\approx}{\underline{\mathbf{M}}}^{\mathrm{s}}$ as well as its work-conjugate quantities, the boundary-value problems at the micro-scale for the micromorphic theory and the microstrain theory are almost identical. The only difference is that the difference stress $\underset{\sim}{\mathbf{\Sigma}} - \underset{\sim}{\bar{\sigma}}$ in (3.106) of the microstrain theory is symmetric whereas it is not per se symmetric in Eq. (3.33) of the micromorphic theory. On the macroscale, the weighted balance (2.110) of the micromorphic theory provides nine independent equations whereas the corresponding Eq. (3.98) of the microstrain theory has six independent components (in 3D).

Due to the unique relation of the non-classical loading at the microscale, the respective deformation modes shall not be repeated here. By Eq. (3.97), Figs. 3.1a, 3.1b and 3.1c corresponds to $\underset{\sim}{\underline{\mathbf{M}}}^{\mathrm{s}} = \underline{\mathbf{b}}_1\underline{\mathbf{b}}_1\underline{\mathbf{b}}_1$, $\underset{\sim}{\underline{\mathbf{M}}}^{\mathrm{s}} = \underline{\mathbf{b}}_1\underline{\mathbf{b}}_1\underline{\mathbf{b}}_1 - 1/2\underline{\mathbf{b}}_1(\underline{\mathbf{b}}_2\underline{\mathbf{b}}_1 + \underline{\mathbf{b}}_1\underline{\mathbf{b}}_2)$ and $\underset{\sim}{\underline{\mathbf{M}}}^{\mathrm{s}} = \underline{\mathbf{b}}_1 1/2(\underline{\mathbf{b}}_1\underline{\mathbf{b}}_2 + \underline{\mathbf{b}}_2\underline{\mathbf{b}}_1) + \underline{\mathbf{b}}_2\underline{\mathbf{b}}_1\underline{\mathbf{b}}_1$, respectively.

3.6.4. Microdilatational theory

Macroscopic theory

The microstrain theory contains the special case of the microdilatational theory, where the rate of microdeformation is identified as a spherical tensor

$$\underset{\sim}{\mathbf{L}}^{\chi} = \frac{1}{n}\dot{\chi}^{\mathrm{v}}\underset{\sim}{\mathbf{I}} \tag{3.109}$$

with the rate of microdilatation $\dot{\chi}^{\mathrm{v}}(\underline{\mathbf{X}})$ as amplitude.

Thus, with Eq. (2.107) the macroscopic energy balance (2.113) becomes

$$\begin{aligned}
&\overline{\rho}\dot{\overline{\Phi}} + \overline{\rho}\frac{1}{2}\left(\underline{\mathbf{V}}\cdot\underline{\mathbf{V}}\right)^{\bullet} + \underbrace{\left\langle \frac{1}{n^2}\rho\underline{\xi}\cdot\underline{\xi}\right\rangle_V}_{=:\overline{\rho}I_r}\left[\frac{1}{2}\left(\dot{\chi}^{\mathrm{v}}\right)^2\right]^{\bullet} \\
&\qquad = \underline{\nabla}_{\underline{\mathbf{X}}}\cdot\big[\underset{\sim}{\mathbf{\Sigma}}\cdot\underline{\mathbf{V}} + \underbrace{\left\langle\frac{1}{n}\underset{\sim}{\sigma}\cdot\underline{\xi}\right\rangle_{\Delta}}_{=:\underline{\mathbf{M}}^{\mathrm{v}}}\dot{\chi}^{\mathrm{v}}\big] - \underline{\nabla}_{\underline{\mathbf{X}}}\cdot\underline{\mathbf{Q}} + \overline{\rho}\overline{\underline{\mathbf{f}}}\cdot\underline{\mathbf{V}} + \underbrace{\left\langle\frac{1}{n}\rho\underline{\mathbf{f}}\cdot\underline{\xi}\right\rangle_V}_{=:\overline{\rho}\overline{f}_{\mathrm{h}}}\dot{\chi}^{\mathrm{v}}\,.
\end{aligned} \tag{3.110}$$

Therein, the dilatational microinertia I_r, volume forces $\overline{f}_{\mathrm{h}}$ and the dilatational double stress $\underline{\mathbf{M}}^{\mathrm{v}}$ are defined. The latter corresponds to the right spherical part of the general micromorphic double stress $\underset{\sim}{\underline{\mathbf{M}}}$:

$$\underline{\mathbf{M}}^{\mathrm{v}} = \frac{1}{n}\frac{1}{\Delta V(\underline{\mathbf{X}})}\oint_{\partial\Delta V}\underline{\xi}\otimes\underline{\mathbf{n}}\cdot\underset{\sim}{\sigma}\cdot\underline{\xi}\;\mathrm{d}S = \frac{1}{n}\underset{\sim}{\underline{\mathbf{M}}}:\underset{\sim}{\mathbf{I}} \tag{3.111}$$

Consequently, the weighted balance for the microdilatational theory is obtained as right spherical part of the general micromorphic balance (2.110) as

$$0 = \underline{\nabla}_{\underline{\mathbf{X}}}\cdot\underline{\mathbf{M}}^{\mathrm{v}} + s_{\mathrm{h}} + \overline{\rho}\overline{f}_{\mathrm{h}} - \overline{\rho}I_r\ddot{\chi}^{\mathrm{v}}\,. \tag{3.112}$$

The macroscopic balance of angular momentum remains that the external stress $\underset{\sim}{\mathbf{\Sigma}}$ is symmetric, Eq. (3.99).

In Eq. (3.112), the microdilatational difference stress $\tilde{s}_{\mathrm{h}}$ was defined as

$$s_{\mathrm{h}} = \frac{1}{n}\left[\underset{\sim}{\mathbf{\Sigma}} - \underset{\sim}{\bar{\sigma}}\right]:\underset{\sim}{\mathbf{I}} = \frac{1}{n}\underset{\sim}{\mathbf{s}}:\underset{\sim}{\mathbf{I}}\,. \tag{3.113}$$

Consequently, the balance of internal energy is obtained from (3.110) as

$$\begin{aligned}
\overline{\rho}\dot{\overline{\Phi}} &= \underset{\sim}{\bar{\sigma}}:\underset{\sim}{\mathbf{D}} + s_{\mathrm{h}}(\underset{\sim}{\mathbf{D}}:\underset{\sim}{\mathbf{I}} - \dot{\chi}^{\mathrm{v}}) + \underline{\mathbf{M}}^{\mathrm{v}}\cdot\underline{\mathbf{L}}^{K\mathrm{v}} - \underline{\nabla}_{\underline{\mathbf{X}}}\cdot\underline{\mathbf{Q}} \\
&= \underset{\sim}{\mathbf{\Sigma}}:\underset{\sim}{\mathbf{D}} + \tilde{s}_{\mathrm{h}}\dot{\chi}^{\mathrm{v}} + \underline{\mathbf{M}}^{\mathrm{v}}\cdot\underline{\mathbf{L}}^{K\mathrm{v}} - \underline{\nabla}_{\underline{\mathbf{X}}}\cdot\underline{\mathbf{Q}}
\end{aligned} \tag{3.114}$$

whereby $\underline{\mathbf{L}}^{K\mathrm{v}} = \underline{\nabla}_{\underline{\mathbf{X}}}\dot{\chi}^{\mathrm{v}}$ refers to the gradient of the rate of microdilatation. Furthermore, $\tilde{s}_{\mathrm{h}} = -s_{\mathrm{h}}$ was introduced as work-conjugate quantity to the microdilatation as discussed in Section 3.6.3. For the microdilatational theory, it seems more convenient to work with $\underset{\sim}{\mathbf{\Sigma}}$ and $\tilde{s}_{\mathrm{h}}$ since the external stress appears in the balance of linear momentum and $\dot{\chi}^{\mathrm{v}}$ is objective. Otherwise, the external stress has to be replaced by $\underset{\sim}{\mathbf{\Sigma}} = \underset{\sim}{\bar{\sigma}} + s_{\mathrm{h}}\underset{\sim}{\mathbf{I}}$.

Micro-macro transition

For a microdilatational theory, the generalized Hill-Mandel lemma (3.7) thus takes the form

$$\left\langle \underset{\sim}{\boldsymbol{\sigma}} : \underset{\sim}{\mathbf{d}} \right\rangle_V = \underset{\sim}{\boldsymbol{\Sigma}} : \underset{\sim}{\mathbf{D}} + \tilde{s}_{\mathrm{h}} \dot{\chi}^{\mathrm{v}} + \underline{\mathbf{M}}^{\mathrm{v}} \cdot \underline{\mathbf{L}}^{K\mathrm{v}} \,. \tag{3.115}$$

According to Eq. (3.109), the rate of microdilatation $\dot{\chi}^{\mathrm{v}}$ corresponds to the trace of the rate of microdeformation. By the kinematic micro-macro relation (3.35) of the general micromorphic theory, $\dot{\chi}^{\mathrm{v}}$ can be related to the microscopic velocity field $\underline{\mathbf{v}}(\underline{\mathbf{x}})$ by

$$\dot{\chi}^{\mathrm{v}} = \underset{\sim}{\mathbf{L}}^{\chi} : \underset{\sim}{\mathbf{I}} = \left\langle \underline{\mathbf{v}} \otimes \underline{\xi} \right\rangle_{\mathrm{M}} : \left(\underset{\sim}{\mathbf{G}}^{\mathrm{M}} \right)^{-1} . \tag{3.116}$$

The gradient of the rate of microdilatation $\underline{\mathbf{L}}^{K\mathrm{v}}$ is computed as spherical part of the gradient of the rate of microstrain[5] in Eq. (3.105)

$$\begin{aligned} \underline{\mathbf{L}}^{K\mathrm{v}} = \frac{1}{2\Delta V} \oint_{\partial \Delta V} & \Big(\underline{\mathbf{n}}\underline{\xi} \cdot \underset{\sim}{\mathbf{G}}^{-1} + \underset{\sim}{\mathbf{G}}^{-1} \cdot \underline{\xi}\underline{\mathbf{n}} \Big) \cdot \underline{\mathbf{v}} - \underline{\mathbf{v}}\underline{\xi} \cdot \underset{\sim}{\mathbf{G}}^{-1} \cdot \underline{\mathbf{n}} - \frac{1}{2+n} \Big(2\underset{\sim}{\mathbf{G}}^{-1} \cdot \underline{\mathbf{v}}\underline{\mathbf{n}} \cdot \underline{\xi} - \underline{\mathbf{v}}\underline{\mathbf{n}} \cdot \underline{\xi}\underset{\sim}{\mathbf{G}}^{-1} : \underset{\sim}{\mathbf{I}} \Big) \,\mathrm{d}S \\ & - \frac{1}{2+n} \Big(2\underset{\sim}{\mathbf{G}}^{-1} \cdot \langle \underline{\mathbf{v}} \rangle_{\mathrm{M}} - \langle \underline{\mathbf{v}} \rangle_{\mathrm{M}} \underset{\sim}{\mathbf{G}}^{-1} : \underset{\sim}{\mathbf{I}} \Big) \end{aligned} \tag{3.117}$$

$$\begin{aligned} L_i^{K\mathrm{v}} = \frac{1}{2\Delta V} \oint_{\partial \Delta V} & \Big(n_i \xi_m G^{-1}_{mk} + G^{-1}_{mi} \xi_m n_k \Big) v_k - v_i \xi_m G^{-1}_{mk} n_k - \frac{1}{2+n} \Big(2G^{-1}_{ik} v_k n_m \xi_m - v_i n_m \xi_m G^{-1}_{kk} \Big) \,\mathrm{d}S \\ & - \frac{1}{2+n} \Big(2G^{-1}_{ik} \langle v_k \rangle_{\mathrm{M}} - \langle v_i \rangle_{\mathrm{M}} G^{-1}_{kk} \Big) \end{aligned}$$

Enforcing the microdilatational kinematic micro-macro relations (3.116) and (3.117) in addition to the classical ones implies a local equilibrium condition

$$\underline{\nabla}_{\underline{\mathbf{x}}} \cdot \underset{\sim}{\boldsymbol{\sigma}} = \frac{\mathrm{H}_V\left(\underline{\xi}\right)}{\left\langle \mathrm{H}_V\left(\underline{\xi}\right) \right\rangle_V} \left[\frac{1}{2+n} \left(2\underline{\mathbf{M}}^{\mathrm{v}} \cdot \underset{\sim}{\mathbf{G}}^{-1} - \underline{\mathbf{M}}^{\mathrm{v}} \underset{\sim}{\mathbf{G}}^{-1} : \underset{\sim}{\mathbf{I}} \right) - \tilde{s}_{\mathrm{h}} \underline{\xi} \cdot \underset{\sim}{\mathbf{G}}^{\mathrm{M}-1} - \underline{\lambda}^V \right] , \tag{3.118}$$

and static boundary conditions

$$\begin{aligned} \underset{\sim}{\boldsymbol{\sigma}} \cdot \underline{\mathbf{n}} = \underset{\sim}{\boldsymbol{\Sigma}} \cdot \underline{\mathbf{n}} + \frac{1}{2} \underline{\mathbf{n}} \cdot \Big[& \underline{\mathbf{M}}^{\mathrm{v}} \underline{\xi} \cdot \underset{\sim}{\mathbf{G}}^{-1} + \underset{\sim}{\mathbf{I}} \underline{\xi} \cdot \underset{\sim}{\mathbf{G}}^{-1} \cdot \underline{\mathbf{M}}^{\mathrm{v}} \\ & - \underset{\sim}{\mathbf{G}}^{-1} \cdot \underline{\xi}\, \underline{\mathbf{M}}^{\mathrm{v}} - \frac{1}{2+n} \left(2\underline{\xi}\, \underset{\sim}{\mathbf{G}}^{-1} \cdot \underline{\mathbf{M}}^{\mathrm{v}} - \underline{\xi} \underset{\sim}{\mathbf{G}}^{-1} : \underset{\sim}{\mathbf{I}}\, \underline{\mathbf{M}}^{\mathrm{v}} \right) \Big] . \end{aligned} \tag{3.119}$$

Conditions of total equilibrium of ΔV require $\underset{\sim}{\boldsymbol{\Sigma}}$ to be symmetric and $\underline{\lambda}^V = 0$ so that the Hill-Mandel condition (3.115) is satisfied.

Alternatively to (3.119), kinematic boundary conditions can be described. They are found by inserting Eq. (3.109) to Eq. (3.108) as

$$\underline{\mathbf{v}} = \underline{\mathbf{V}} + \underline{\xi} \cdot \underline{\nabla}_{\underline{\mathbf{X}}} \underline{\mathbf{V}} + \frac{1}{n} \underline{\xi}\underline{\mathbf{L}}^{K\mathrm{v}} \cdot \underline{\xi} \qquad \text{on } \partial \Delta V(\underline{\mathbf{X}}) \,. \tag{3.120}$$

The respective non-classical deformation modes are sketched in Fig. 3.4. Figures 3.4a and 3.4b show the effect of a gradient of microdeformation $\underline{\mathbf{L}}^{K\mathrm{v}}$ and of its work-conjugate double stress $\underline{\mathbf{M}}^{\mathrm{v}}$, respectively. In Fig. 3.4c it can be seen that the microdilatational difference stress $\tilde{s}_{\mathrm{h}}$ drives a distributed dilatation.

[5] Equation (3.117) differs slightly from an expression which was given by the author previously in [3]. The previous expression was specified without the intermediate step over the microstrain theory. However, without this step, the mapping from the fully micromorphic $\underset{\sim}{\underline{\mathbf{L}}}^{K\mathrm{s}}$ to $\underline{\mathbf{L}}^{K\mathrm{v}}$ is not unique.

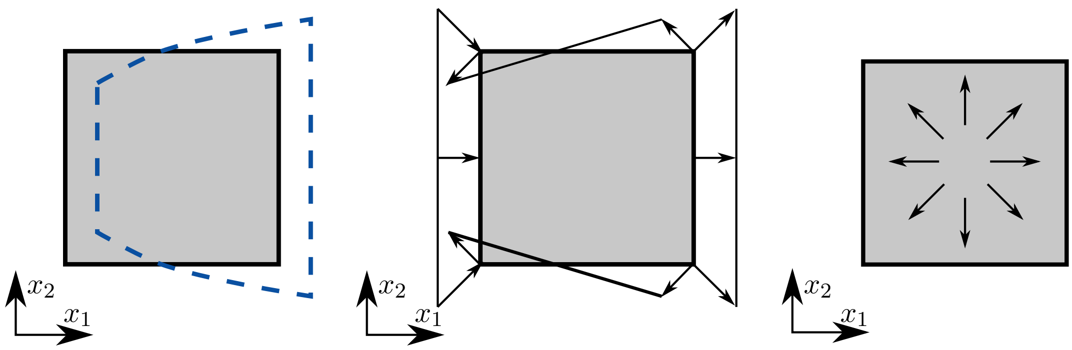

(a) **(b)** **(c)**

Fig. 3.4.: Non-classical microdilatational deformation modes of the volume element ΔV: (a) essential boundary condition (3.120) with $\underline{\mathbf{L}}^{K\mathrm{v}} = \underline{\mathbf{b}}_1$, (b) static boundary condition (3.119) with $\underline{\mathbf{M}}^{\mathrm{v}} = \underline{\mathbf{b}}_1$, (c) loading (3.118) of $\tilde{s}_{\mathrm{h}}$

4. Elastic Behaviour

4.1. Uniaxial case

The developed homogenisation procedure shall be demonstrated for the one-dimensional case with periodic microstructure as shown in Fig. 4.1. In particular, for a volume element $\Delta V = \{\xi \in [-L/2, L/2]\}$ of length L, the geometric moment is computed as $G = L^2/12$ so that equilibrium conditions (3.21) for the volume element become

$$\sigma'(\xi) = \frac{12}{L^2}(\Sigma - \bar{\sigma})\xi + \frac{4}{L^2}M \text{ for } \xi \in [-L/2, L/2] \tag{4.1}$$

For the 1D case, equilibrium condition (4.1) allows to determine the microscopic stress field $\sigma(\xi)$ directly up to a constant of integration. Either static boundary conditions (3.22)

$$\sigma(\pm L/2) = \Sigma \pm \frac{2}{L}M \tag{4.2}$$

or kinematic boundary conditions (3.49)

$$u(\pm L/2) = \pm\frac{L}{2}\frac{\mathrm{d}U}{\mathrm{d}X} + \frac{L^2}{4}K + U \tag{4.3}$$

complete the boundary value problem at the microscale. In the former case, the constant of integration is computed from (4.2) whereas for kinematic boundary conditions (4.3), the constant can be determined from definition (3.9) $\Sigma = [\underset{\sim}{\sigma}(L/2) + \underset{\sim}{\sigma}(-L/2)]/2$. For both types of boundary conditions, the relation (3.11) for the dilatational double stress M is fulfilled identically and the microscopic stress field becomes

$$\sigma(\xi) = \Sigma + \frac{3}{2}(\bar{\sigma} - \Sigma)\left[1 - \frac{\xi^2}{L^2/4}\right] + \frac{4}{L^2}M\xi \tag{4.4}$$

Let us now consider the macroscopic problem sketched in Fig. 4.1a of a volume loading f under static conditions so that the macroscopic balance equations (2.111) and (2.110) read

$$0 = \frac{\mathrm{d}\Sigma}{\mathrm{d}X} + \overline{\rho f} \tag{4.5}$$

$$0 = \frac{\mathrm{d}M}{\mathrm{d}X} + \Sigma - \bar{\sigma} + \overline{\rho}m \tag{4.6}$$

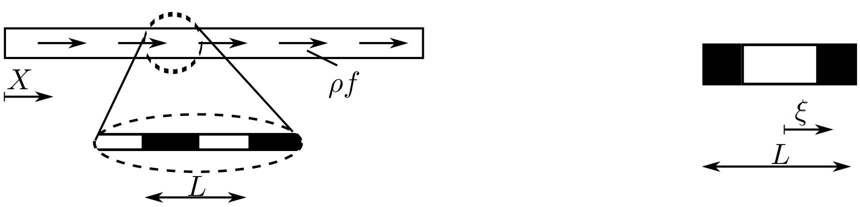

(a) Macroscopic problem

(b) Microscopic volume element

Fig. 4.1.: Homogenisation for uniaxial two-phase laminate

In the special case $f = 0$, i. e. uniform macroscopic deformations, it is obvious that, if only trivial natural boundary conditions for the higher order terms are specified, the macroscopic stresses $M = 0$ and $\Sigma - \bar{\sigma} = 0$ fulfill the higher order balance of momentum (4.6) identically. What remains is (4.5) together with the boundary value problem (4.1) at the microscale $\sigma'(\xi) = 0$, $\sigma(\pm L/2) = \Sigma$. This corresponds to the classical homogenisation (which is in the 1D case furthermore the exact solution of the problem with resolved microstructure everywhere) whatever the material law $\sigma(\varepsilon)$ is at the microscale and which volume element is chosen (The situation changes when dynamic effect are considered since then non-vanishing double stresses M and a difference $\Sigma - \bar{\sigma}$ are in this case necessary in general to compensate the higher order inertia which will lead, realistically, to dispersion of waves, cf. [10]).

Elastic behavior For non-vanishing $f \neq 0$, the higher order balance of momentum (4.6) is statically indeterminate so that the solution depends on the particular micromorphic constitutive law. The latter shall be derived for linear-elastic behavior $\sigma = E^{(\mathrm{m})} u'$ of all constituents whereby $E^{(\mathrm{m})}$ denotes Young's modulus. By use of the stress field (4.4), the microscopic material law can be solved for $u'(\xi)$. Inserting it to the definitions (3.24) of the macroscopic deformation measures yields for (a centro-symmetric unit cell $E^{(\mathrm{m})}(-\xi) = E^{(\mathrm{m})}(\xi)$) the macroscopic constitutive law

$$
\begin{aligned}
\frac{\mathrm{d}U}{\mathrm{d}X} &= \langle u' \rangle_V = \Sigma \left\langle \frac{1}{E^{(\mathrm{m})}} \right\rangle_V + (\bar{\sigma} - \Sigma) \left\langle \frac{1}{E^{(\mathrm{m})}} \frac{3}{2} \left[1 - \frac{4\xi^2}{L^2} \right] \right\rangle_V , \\
\chi &= \frac{1}{G} \langle u\xi \rangle_V = \Sigma \left\langle \frac{1}{E^{(\mathrm{m})}} \frac{3}{2} \left[1 - \frac{4\xi^2}{L^2} \right] \right\rangle_V + \frac{9}{4} (\bar{\sigma} - \Sigma) \left\langle \frac{1}{E^{(\mathrm{m})}} \left[1 - \frac{4\xi^2}{L^2} \right]^2 \right\rangle_V , \\
K &= \frac{4}{L^2} \langle u'\xi \rangle_V = M \frac{4}{L^2} \left\langle \frac{1}{E^{(\mathrm{m})}} \frac{4\xi^2}{L^2} . \right\rangle_V
\end{aligned}
\tag{4.7}
$$

The simplest case which contains gradient effects is a constant volumetric loading $\rho f =$ const. In this case, the macroscopic volume loads become $\overline{\rho f} = \rho f$ and $m = 0$ according to (2.111) and (2.110). Thus, for the constitutive law (4.7) a particular solution of the macroscopic boundary value problem is $\underset{\sim}{\mathbf{M}} =$ const and $\Sigma = \bar{\sigma}$ together with the statically determined and classical solution of (4.5). Consequently, the *microscopic stress field* (4.4) depends linearly on the location as in the exact solution with discretely resolved microstructure everywhere, a prediction which lies beyond the possibilities of classical homogenisation. If macroscopic boundary conditions with respect to M or χ are specified which do not coincide with this particular solution, then additional exponentially decaying terms of $\underset{\sim}{\mathbf{M}}$ and $\bar{\sigma} - \Sigma$ occur at the macroscopic boundaries. According to $(4.7)_1$, such terms have an effect on the macroscopic displacements $U(X)$, i. e. on the macroscopic stiffness. This is reasonable as for non-homogeneous loading ρf the distribution of the microscopic stiffness has indeed an effect on the macroscopic stiffness. Of course, this effect becomes negligible as the ratio of macroscopic length and intrinsic length L increases.

As a second case, one might consider a constant force per mass $f =$ const (e. g. gravity) which acts on a material with inhomogeneous but periodic distribution of mass density ρ at the microscale. Such a loading will again induce a constant volumetric force at the macroscale $\overline{\rho f} =$ const. But additionally, the volumetric moment will be present $m \neq 0$. According to the macroscopic balance (4.6), such loading will induce again a constant double stress $M =$ const (under suitable boundary conditions) and additionally a stress difference $\Sigma - \bar{\sigma} = -\bar{\rho} m$. Equation (4.4) shows that the local stresses at the microscale will thus be redistributed and higher stress gradients appear in parts with a higher local mass density ρ as it is the case for the exact solution of the non-homogenized problem.

For further discussion, the macroscopic constitutive law (4.7) shall be provided for homogeneous elastic properties i. e. $E^{(\mathrm{m})} = \text{const.}$:

$$\bar{\sigma} = E^{(\mathrm{m})}\frac{\mathrm{d}U}{\mathrm{d}X}\,, \qquad \Sigma - \bar{\sigma} = 5E^{(\mathrm{m})}\left[\frac{\mathrm{d}U}{\mathrm{d}X} - \chi\right]\,, \qquad M = \frac{3E^{(\mathrm{m})}L^2}{4}K\,. \tag{4.8}$$

Second gradient theory For the transition of the micromorphic theory towards a second gradient theory, several opportunities were discussed in Section 3.6.1. The effects of the different opportunities shall be illustrated by the simple, uniaxial case. The strictest assumption is to impose the constraint $\chi = \mathrm{d}U/\mathrm{d}X$ at the macroscale and the respective counterpart $\langle u\xi\rangle_V / G = \langle u'\rangle_V$ at the microscale. In this case, the microscopic boundary value problem (4.1)–(4.3) remains the same as in the unconstrained micromorphic theory. On the macrolevel, the higher order deformation measure in $(4.7)_3$ is identified as $K = \mathrm{d}^2U/\mathrm{d}X^2$ and the external stress Σ can be eliminated from the macroscopic balances. Thus, in the case of homogeneous linear-elastic material at the microscale, the macroscopic relations (4.5), (4.6) and (4.8) become

$$0 = \frac{\mathrm{d}}{\mathrm{d}X}\left[\bar{\sigma} - \frac{\mathrm{d}M}{\mathrm{d}X}\right]\,, \qquad \bar{\sigma} = E^{(\mathrm{m})}\frac{\mathrm{d}U}{\mathrm{d}X}\,, \qquad M = \frac{3E^{(\mathrm{m})}L^2}{4}\frac{\mathrm{d}^2U}{\mathrm{d}X^2}\,. \tag{4.9}$$

If the constraint between microdeformation and macrodeformation is relaxed at the microscale, the difference stress $\Sigma - \bar{\sigma}$ drops from the local equilibrium condition (4.1) and the right-hand side of microscopic equilibrium condition (4.1) retains only its constant term

$$\sigma'(\xi) = \frac{4}{\alpha L^2}M\,. \tag{4.10}$$

Therein, the constraint factor α was incorporated defined through the macroscopic constraint $K = \alpha\mathrm{d}^2U/\mathrm{d}X^2$, see Section 3.6.1. For homogeneous linear-elastic material, the governing macroscopic equations become

$$0 = \frac{\mathrm{d}}{\mathrm{d}X}\left[\bar{\sigma} - \frac{\mathrm{d}M^{\nabla\nabla U}}{\mathrm{d}X}\right]\,, \qquad \bar{\sigma} = E^{(\mathrm{m})}\frac{\mathrm{d}U}{\mathrm{d}X}\,, \qquad M^{\nabla\nabla U} = \alpha^2\frac{3E^{(\mathrm{m})}L^2}{4}\frac{\mathrm{d}^2U}{\mathrm{d}X^2}\,. \tag{4.11}$$

For $\alpha = 1$, Eq. (4.9) is recovered. However, also $\alpha = 1/2$ was used in literature, see Section 3.6.1. Note, that the square of α enters in the constitutive law $(4.11)_3$.

In the theory of Gologanu, Kouznetsova et al., the volumetric micro-macro relation for the displacements is *not* enforced, compare Sections 2.2.2 and 3.6.1. Consequently, also the constant term on the right-hand side of Eq. (4.10) drops and the double stress vanishes $M^{\nabla\nabla U} = 0$ in the uniaxial case. This result is related to the fact that the quadratic term with K in the kinematic boundary condition (4.3) reflects a pure rigid translation as was discussed already by Gologanu et al. [44].

4.2. Upper bound estimates by Ritz' method

For an elastic material, the boundary-value problem at the microscale can be specified as a variational problem (3.26). Approximate solutions $\underline{\tilde{\mathbf{u}}}(\underline{\xi})$ can be constructed by Ritz' method which provide upper bounds for the macroscopic strain energy $\overline{W}$. If kinematic boundary conditions (3.49) are specified, they have to be satisfied a priori by $\underline{\tilde{\mathbf{u}}}(\underline{\xi})$. Finding such an ansatz for the quadratic terms is not trivial. For the Voigt approach to classical homogenisation, the linear polynomial of the boundary condition is extended to the complete domain. In the same way, one could take the quadratic polynomial from the boundary conditions (3.49) as ansatz for $\underline{\tilde{\mathbf{u}}}(\underline{\xi})$. However, the microdeformation and the difference stress are defined via volume terms which is why such a quadratic polynomial is insufficient for an unconstrained micromorphic theory. For this reason, the cubic ansatz

$$\underline{\tilde{\mathbf{u}}}(\underline{\xi}) = \underline{\mathbf{A}} + \underset{\sim}{\underline{\mathbf{B}}} \cdot \underline{\xi} + \underset{\sim}{\underline{\mathbf{C}}} : \underline{\xi\xi} + \underset{\approx}{\underline{\mathbf{D}}} \vdots \underline{\xi\xi\xi} \tag{4.12}$$

is necessary as often used in the context of micromorphic continua, compare Section 2.2.4. However, it is not trivial to satisfy the kinematic boundary conditions (3.49) ad hoc by Eq. (4.12). This problem does not appear if static boundary conditions (3.22) are prescribed. In this case, Ritz's method yields a conventional optimization problem

$$\begin{aligned}\mathcal{L} = \langle W(\underline{\tilde{\mathbf{u}}})\rangle_V - \Sigma_{ij}\left(\frac{1}{\Delta V}\oint\limits_{\partial\Delta V} n_i\tilde{u}_j\right) - s_{jk}\left\langle\tilde{u}_j\xi_m\right\rangle_{\mathrm{M}} G^{\mathrm{M}-1}_{km} + \frac{1}{2+n}M_{kjm}G^{-1}_{km}\left\langle\tilde{u}_j\right\rangle_{\mathrm{M}} \\ - \frac{1}{2\Delta V}M_{ijp}G^{-1}_{pm}\oint\limits_{\partial\Delta V}\tilde{u}_j n_i\tilde{u}_j\xi_m - \frac{1}{2+n}\delta_{im}n_k\xi_k\tilde{u}_j\,\mathrm{d}S \xrightarrow{\underline{\mathbf{A}},\underset{\sim}{\underline{\mathbf{B}}},\underset{\sim}{\underline{\mathbf{C}}},\underset{\approx}{\underline{\mathbf{D}}}} \mathrm{Min.}\end{aligned} \tag{4.13}$$

for the coefficients of the polynomial (4.12). Of course, out of these coefficients only those are uniquely defined which contribute to Eq. (4.13). So, $\underline{\mathbf{A}}$ and the skew-symmetric part of $\underset{\sim}{\underline{\mathbf{B}}}$ represent rigid body motions and are not uniquely determined under purely static boundary conditions. From the quadratic and cubic coefficients $\underset{\sim}{\underline{\mathbf{C}}}$ and $\underset{\approx}{\underline{\mathbf{D}}}$, respectively, only the right sub-symmetric parts contribute to the polynomial (4.12).

For homogeneous linear elastic material $W = 1/2\underset{\sim}{\varepsilon} : \underset{\approx}{\underline{\mathbf{S}}} : \underset{\sim}{\varepsilon}$, Eq. (4.13) implies the optimality conditions

$$0 = \frac{\partial\mathcal{L}}{\partial B_{ji}} = s_{ji} - \Sigma_{ij} + \left\langle \mathrm{H}_V\left(\underline{\xi}\right)\right\rangle_V S_{ijkl}\left(B_{kl} + 3D_{k((lmn))}G^{\mathrm{M}}_{mn}\right) \tag{4.14}$$

$$0 = \frac{\partial\mathcal{L}}{\partial C_{jim}} = -M_{ijm} + \frac{1}{2+n}M_{kjl}{G_{kl}}^{-1}G^{\mathrm{M}}_{im} + 2\left\langle \mathrm{H}_V\left(\underline{\xi}\right)\right\rangle_V\left(S_{ijkl}G^{\mathrm{M}}_{qm} + S_{mjkl}G^{\mathrm{M}}_{qi}\right)C_{k(lq)} \tag{4.15}$$

$$\begin{aligned}0 = \frac{\partial\mathcal{L}}{\partial D_{jimn}} = &-\Sigma_{ij}G_{mn} - \Sigma_{mj}G_{in} - \Sigma_{nj}G_{mi} + s_{jk}G^{\mathrm{M}-1}_{kp}G^{\mathrm{M}}_{pimn} \\ &+ 3\left\langle \mathrm{H}_V\left(\underline{\xi}\right)\right\rangle_V\left(S_{ijkl}G^{\mathrm{M}}_{mnqp} + S_{njkl}G^{\mathrm{M}}_{imqp} + S_{mjkl}G^{\mathrm{M}}_{niqp}\right)D_{k((lpq))} \\ &+ \left\langle \mathrm{H}_V\left(\underline{\xi}\right)\right\rangle_V\left(S_{ijkl}G^{\mathrm{M}}_{mn} + S_{mjkl}G^{\mathrm{M}}_{in} + S_{njkl}G^{\mathrm{M}}_{im}\right)B_{kl}\end{aligned} \tag{4.16}$$

Therein, a central symmetry was assumed so that third moments vanish and $G^{\mathrm{M}}_{mnqp} = \left\langle\xi_m\xi_n\xi_q\xi_p\right\rangle_{\mathrm{M}}$ refers to the forth geometric moment. Furthermore, $D_{k((lmn))}$ denotes the part of D_{klmn} which is completely symmetric with respect to the indices l, m and n. As mentioned already, only this subsymmetric part of D_{klmn} contributes to the displacement field $\underline{\tilde{\mathbf{u}}}(\underline{\xi})$.

Inserting the polynomial ansatz (4.12) to the kinematic micro-macro relations (3.34)–(3.37) yields:

$$U_{i,j} = B_{ij} + 3D_{i((jkl))}G_{kl} \tag{4.17}$$

$$\chi_{ij} = B_{ij} + D_{iklm}G^{\mathrm{M}}_{klmn}G^{\mathrm{M}-1}_{nj} \tag{4.18}$$

$$K^{\mathrm{s}}_{ijk} = C_{j(ik)} - C_{jmp}G^{\mathrm{M}}_{mp}G^{-1}_{ik} \tag{4.19}$$

Equation (4.19) shows that the quadratic coefficients $\underset{\sim}{\underline{\mathbf{C}}}$ are directly related to the symmetric gradient of microdeformation $\underset{\sim}{\underline{\mathbf{K}}}^{\mathrm{s}}$. Furthermore, Eqs. (4.18) and (4.19) contain a rigid rotation within the skew-symmetric part of B_{ij}. Objective deformation measures are (Section 2.1.3)

$$E_{ij} = U_{(i,j)} = B_{(ij)} + \frac{3}{2}\left(D_{i((jkl))} + D_{j((ikl))}\right)G_{kl} \tag{4.20}$$

$$e_{ij} = U_{i,j} - \chi_{ij} = 3D_{i((jkl))}G_{kl} - D_{iklm}G^{\mathrm{M}}_{klmn}G^{\mathrm{M}-1}_{nj} \tag{4.21}$$

respectively. Equation (4.21) shows that the cubic coefficients $D_{i((jkl))}$ are directly related to the relative deformation $D_{i((jkl))}$. However, the tensor $\underset{\approx}{\mathbf{D}}$ has more independent components than $\underset{\sim}{\mathbf{e}}$, compare e. g. [93, 94].

The linear system of equations (4.14)–(4.16) can be solved for all relevant components of $\underset{\sim}{\mathbf{B}}$, $\underset{\sim}{\underset{\sim}{\mathbf{C}}}$ and $\underset{\approx}{\mathbf{D}}$ as functions of the stresses $\underset{\sim}{\mathbf{\Sigma}}$, $\underset{\sim}{\mathbf{s}}$ and $\underset{\sim}{\underset{\sim}{\mathbf{M}}}$. The macroscopic constitutive relations are obtained (in compliance form) by inserting these coefficients to Eqs. (4.19)–(4.21).

Equation (4.15) for the quadratic coefficients $\underset{\sim}{\underset{\sim}{\mathbf{C}}}$ can be solved as follows: By means of a cyclic permutation with respect to i, j and m, Eq. (4.15) is solved for $S_{ijkl}C_{k(lq)}G^{\mathrm{M}}_{qm}$. The resulting equation can be multiplied with the inverses of S_{ijkl} and G^{M}_{qm} which yields an equation for the symmetric part $C_{k(lq)} + C_{l(kq)}$ with respect to k and l. A further cyclic permutation allows to solve for $C_{k(lq)}$ which can be inserted to Eq. (4.19). This gives the constitutive law

$$
\begin{aligned}
K^{\mathrm{s}}_{ijk} =& \frac{1}{4(1-f)}\left[2M_{lmn} - M_{lnm} - \frac{1}{2+n}\left(2M_{pmq}G^{\mathrm{M}}_{ln} - M_{pnq}G^{\mathrm{M}}_{lm}\right)G^{-1}_{pq}\right]\cdot \\
&\cdot\left[G^{\mathrm{M}-1}_{kn}S^{-1}_{ijlm} + G^{\mathrm{M}-1}_{in}S^{-1}_{jklm} - G^{\mathrm{M}-1}_{jn}S^{-1}_{iklm} - \frac{1}{2+n}\left(2S^{-1}_{jnlm} - S^{-1}_{lmrs}G^{\mathrm{M}}_{rs}G^{\mathrm{M}-1}_{jn}\right)G^{\mathrm{M}}{}^{-1}_{ik}\right]
\end{aligned}
\tag{4.22}
$$

in compliance form. The respective stiffness form can be obtained as follows: Firstly, Eq. (4.15) is multiplied by G^{-1}_{im}. The resulting equation can be solved for $M_{ijm}G^{-1}_{im}$. Reinserting the result into Eq. (4.15) allows to express the double stress M_{ijm} solely in terms of the cubic coefficients $C_{k(lq)}$. The latter can be obtained by solving (4.19) in the same way for $C_{k(lq)}$. Finally, the macroscopic constitutive law for the double stress for arbitrary geometries and microscopic elastic laws $\underset{\approx}{\mathbf{S}}$ reads

$$
\begin{aligned}
M_{ijk} = 2\left\langle \mathrm{H}_V\left(\underset{\sim}{\xi}\right)\right\rangle_V &\left(K^{\mathrm{s}}_{lmn} + \frac{1}{2+n-G^{\mathrm{M}}_{rs}G^{-1}_{rs}}K^{\mathrm{s}}_{pmq}G^{\mathrm{M}}_{pq}G^{-1}_{ln}\right)\cdot \\
&\cdot\left(\frac{2}{2+n-G^{\mathrm{M}}_{rs}G^{-1}_{rs}}S_{jpml}G^{\mathrm{M}}_{nt}G^{-1}_{tp}G^{\mathrm{M}}_{ik} + S_{ijml}G^{\mathrm{M}}_{kn} + S_{kjml}G^{\mathrm{M}}_{in}\right).
\end{aligned}
\tag{4.23}
$$

In the remaining equations, the linear coefficients B_{kl} can be eliminated by inserting Eq. (4.14) into Eq. (4.16)

$$
\begin{aligned}
0 =& -\Sigma_{ij}G_{mn} - \Sigma_{mj}G_{in} - \Sigma_{nj}G_{mi} + s_{jk}G^{\mathrm{M}-1}_{kp}G^{\mathrm{M}}_{pimn} \\
&+ \left(\Sigma_{ij} - s_{ji}\right)G^{\mathrm{M}}_{mn} + \left(\Sigma_{mj} - s_{jm}\right)G^{\mathrm{M}}_{in} + \left(\Sigma_{nj} - s_{jn}\right)G^{\mathrm{M}}_{im} \\
&+ 3\left\langle \mathrm{H}_V\left(\underset{\sim}{\xi}\right)\right\rangle_V\left(S_{ijkl}G^{\mathrm{M}}_{mnqp} + S_{njkl}G^{\mathrm{M}}_{imqp} + S_{mjkl}G^{\mathrm{M}}_{niqp}\right)D_{k((lpq))} \\
&- 3\left\langle \mathrm{H}_V\left(\underset{\sim}{\xi}\right)\right\rangle_V\left(S_{ijkl}G^{\mathrm{M}}_{mn} + S_{mjkl}G^{\mathrm{M}}_{in} + S_{njkl}G^{\mathrm{M}}_{im}\right)D_{k((lpq))}G^{\mathrm{M}}_{pq}
\end{aligned}
\tag{4.24}
$$

resulting in an equation for the cubic coefficients D_{jimn} as functions of the stresses $\underset{\sim}{\mathbf{\Sigma}}$ and $\underset{\sim}{\mathbf{s}}$. Equation (4.24) shows already that for a compact material $\underset{\sim}{\mathbf{G}}^{\mathrm{M}} = \underset{\sim}{\mathbf{G}}$, the external macroscopic stress $\underset{\sim}{\mathbf{\Sigma}}$ drops out and $\underset{\approx}{\mathbf{D}}$ and thus the relative deformation $\underset{\sim}{\mathbf{e}}$ depend only on the difference stress $\underset{\sim}{\mathbf{s}}$.

However, the author could not find a general solution for Eq. (4.24) which would be necessary in Eqs. (4.20)–(4.21) for extracting the macroscopic constitutive relations between $\underset{\sim}{\mathbf{E}}$, $\underset{\sim}{\mathbf{e}}$ and $\underset{\sim}{\mathbf{\Sigma}}$ and $\underset{\sim}{\mathbf{s}}$, respectively. For this reason we continua with a particular case.

4.3. Isotropic porous material

A spherical pore of radius R_{void} in a spherical volume element ΔV of radius R is considered, see Fig. 4.2. It may be interpreted as the approximation to the polyhedral cells around

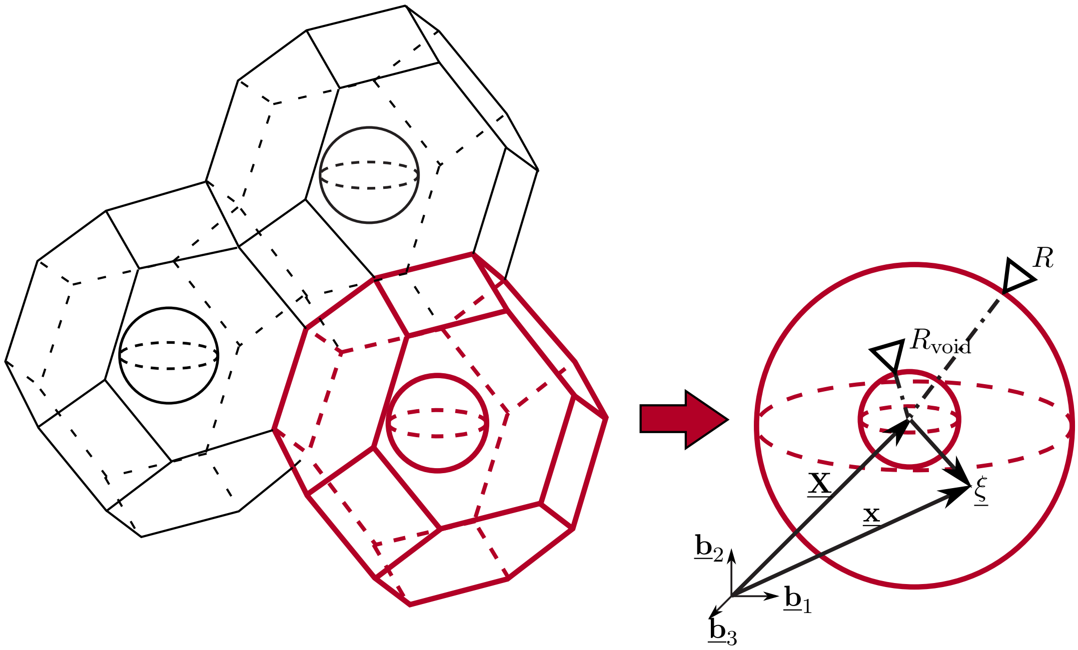

Fig. 4.2.: Unit cell of a porous material

spherical pores as obtained e. g. by Voronoi tesselation. A spherical volume element has the advantage that it has an isotropic geometry. If the matrix material behaves isotropically as well, elastically or inelastically, the macroscopic behavior will thus be isotropic, too. In addition to the three-dimensional case of a sphere, the corresponding plane case of a circle shall be covered, too. In a unified sense, a circle corresponds to sphere of dimension $n = 2$ and will be covered by the term "sphere" in the following. In this sense, the porosity of the spherical volume element with pore amounts to $f = (R_{\text{void}}/R)^n$.

For a sphere, the volume average operator (2.23) can favorably be written as [95]

$$\langle(\circ)\rangle_V = \frac{n}{R^n} \int\limits_0^R r^{n-1} \langle(\circ)\rangle_{S(r)} \,\mathrm{d}r \tag{4.25}$$

wherein $\langle(\circ)\rangle_{S(r)}$ denotes the arithmetic average over a spherical surface of radius $r = |\underline{\xi}|$.

The expression for the average $\langle(\circ)\rangle_{\mathrm{M}}$ over the matrix material corresponds to Eq. (4.25) with the lower limit of the integral replaced by R_{void} and the R^n in the prefactor replaced by $R^n - R^n_{\text{void}} = (1-f)R^n$. Consequently, the average over the weight function is $\left\langle \mathrm{H}_V\left(\underline{\xi}\right)\right\rangle_V = 1 - f$. Furthermore, the required geometric moments of the complete ΔV and of the matrix are obtained as

$$\underset{\sim}{\mathbf{G}} = \frac{R^2}{n+2}\underset{\sim}{\mathbf{I}}, \quad \underset{\sim}{\mathbf{G}}^{\mathrm{M}} = \frac{R^2}{n+2}\,\frac{1-f^{\frac{n+2}{n}}}{1-f}\underset{\sim}{\mathbf{I}}, \quad \underset{\approx}{\mathbf{G}}^{\mathrm{M}} = \frac{R^4}{(n+2)(n+4)}\,\frac{1-f^{\frac{n+4}{n}}}{1-f}\left(2\underset{\approx}{\mathbf{I}}_{\mathrm{S}} + \underset{\sim}{\mathbf{I}}\underset{\sim}{\mathbf{I}}\right), \tag{4.26}$$

respectively.

Thus, firstly the constitutive relation (4.23) for the double stress reads

$$M_{ijk} = \frac{2R^2}{n+2}\left(1 - f^{\frac{n+2}{n}}\right)\left(K^{\mathrm{s}}_{lmn} + \frac{\frac{1-f^{\frac{n+2}{n}}}{1-f}}{2 - nf\frac{1-f^{\frac{2}{n}}}{1-f}} K^{\mathrm{s}}_{qmq}\delta_{ln}\right) \cdot$$
$$\cdot \left(\frac{2\frac{1-f^{\frac{n+2}{n}}}{1-f}}{2 - nf\frac{1-f^{\frac{2}{n}}}{1-f}} S_{jnml}\delta_{ik} + S_{ijml}\delta_{kn} + S_{kjml}\delta_{in}\right) . \quad (4.27)$$

Secondly, relation (4.21) between the cubic coefficients and the relative deformation becomes

$$e_{ij} = \frac{3R^2}{n+2}\left(1 - \frac{n+2}{n+4}\frac{1-f^{\frac{n+4}{n}}}{1-f^{\frac{n+2}{n}}}\right) D_{i((jkk))} \, . \quad (4.28)$$

In Eqs. (4.14) and (4.20), only this (right) trace $D_{i((jkk))}$ of the cubic coefficients appears. Elimination of this trace and of the linear coefficients $B_{(ij)}$ from Eqs. (4.14), (4.20) and (4.28) yields the constitutive relation

$$\bar{\sigma}_{ij} = (1-f)S_{ijkl}E_{kl} + f\frac{1-f^{2/n}}{1 - \frac{n+2}{n+4}\frac{1-f^{\frac{n+4}{n}}}{1-f^{\frac{n+2}{n}}}} S_{ijkl}e_{kl} \quad (4.29)$$

for the internal stress $\bar{\sigma}_{ij} = \Sigma_{ij} - s_{ji}$. As expected, the $\bar{\sigma}_{ij}$ is symmetric and depends only on the symmetric part of the relative deformation e_{kl}. Furthermore, note that the coupling between $\bar{\sigma}_{ij}$ and e_{kl} vanishes for homogeneous, compact material $f = 0$.

With the geometric moments (4.26) of the spherical volume element, Eq. (4.24) for the cubic coefficients becomes

$$\begin{aligned} 0 =& f\frac{1-f^{\frac{2}{n}}}{1-f}\left(\bar{\sigma}_{ij}\delta_{mn}+\bar{\sigma}_{mj}\delta_{in}+\bar{\sigma}_{nj}\delta_{mi}\right) + \left(\frac{1}{3}\frac{n+2}{n+4}\frac{1-f^{\frac{n+4}{n}}}{1-f^{\frac{n+2}{n}}} - 1\right)\left(s_{ji}\delta_{mn}+s_{jm}\delta_{in}+s_{jn}\delta_{im}\right) \\ &+ \frac{1}{1 - \frac{n+2}{n+4}\frac{1-f^{\frac{n+4}{n}}}{1-f^{\frac{n+2}{n}}}}\left[\frac{n+2}{n+4}\left(1-f^{\frac{n+4}{n}}\right) - \frac{\left(1-f^{\frac{n+2}{n}}\right)^2}{1-f}\right]\left(S_{ijkl}\delta_{mn}+S_{njkl}\delta_{im}+S_{mjkl}\delta_{in}\right)e_{kl} \\ &+ \frac{6R^2}{n+4}\left(1-f^{\frac{n+4}{n}}\right)\left(S_{ijkl}D_{k((lmn))} + S_{njkl}D_{k((ilm))} + S_{mjkl}D_{k((iln))}\right) =: R_{jimn} \, . \quad (4.30) \end{aligned}$$

Finally, this equation does not need to be solved for all components of $\underset{\approx}{\mathbf{D}}$. Rather, a macroscopic constitutive law $\underset{\sim}{\mathbf{e}}$ as function of $\underset{\sim}{\bar{\sigma}}$ and $\underset{\sim}{\mathbf{s}}$ shall be extracted. That is why, Eq. (4.28) was used, where possible, to replace the right spherical part of $\underset{\approx}{\mathbf{D}}$ by $\underset{\sim}{\mathbf{e}}$. However, in the last square bracket of Eq. (4.30) there are terms which cannot be replaced immediately. Note that the symbol R_{jimn} was assigned to the right-hand side of Eq. (4.30).

For obtaining an expression for $\underset{\sim}{\mathbf{e}}$ it is worth to have a look on the left and right spherical parts R_{jimm} and R_{mmij}. It turns out that within both parts, almost all appearances of $\underset{\approx}{\mathbf{D}}$ can be replaced by $\underset{\sim}{\mathbf{e}}$ for isotropic matrix material $S_{ijkl} = \mu(\delta_{ik}\delta_{jl} + \delta_{il}\delta_{jk}) + \lambda\delta_{ij}\delta_{kl}$, except terms $D_{k((kij))}$. These terms can be eliminated by computing $2(\mu+\lambda)R_{mmij} - (4\mu+\lambda(2+n))R_{jimm}$ resulting in an equation which contains solely $\underset{\sim}{\mathbf{e}}$, $\underset{\sim}{\bar{\sigma}}$ and $\underset{\sim}{\mathbf{s}}$. A split into the spherical, skew-symmetric and symmetric-deviatoric parts (with respect to i and j) gives the macroscopic constitutive relations

$$s_{ji}-s_{ij} = \frac{4\mu}{n+4}\frac{1-f^{\frac{n+4}{n}}}{\left(1-\frac{n+2}{n+4}\frac{1-f^{\frac{n+4}{n}}}{1-f^{\frac{n+2}{n}}}\right)^2}(e_{ji}-e_{ij}) \tag{4.31}$$

$$\begin{aligned} s_{kk}-f\frac{\frac{1-f^{\frac{2}{n}}}{1-f}}{1-\frac{n+2}{n+4}\frac{1-f^{\frac{n+4}{n}}}{1-f^{\frac{n+2}{n}}}}\bar{\sigma}_{kk} \\ =\frac{(2\mu+n\lambda)}{\left(1-\frac{n+2}{n+4}\frac{1-f^{\frac{n+4}{n}}}{1-f^{\frac{n+2}{n}}}\right)^2}\left[\frac{n+2}{n+4}\left(1-f^{\frac{n+4}{n}}\right)\left(1+2\frac{6\mu+(n+2)\lambda}{(n+2)(2\mu+n\lambda)}\right)-\frac{\left(1-f^{\frac{n+2}{n}}\right)^2}{1-f}\right]e_{kk} \end{aligned} \tag{4.32}$$

$$\begin{aligned} s^{\mathrm{ds}}_{(ij)}-f\frac{\frac{1-f^{\frac{2}{n}}}{1-f}}{1-\frac{n+2}{n+4}\frac{1-f^{\frac{n+4}{n}}}{1-f^{\frac{n+2}{n}}}}\bar{\sigma}^{\mathrm{ds}}_{(ij)} \\ =\frac{2\mu}{\left(1-\frac{n+2}{n+4}\frac{1-f^{\frac{n+4}{n}}}{1-f^{\frac{n+2}{n}}}\right)^2}\left[\frac{n+2}{n+4}\left(1-f^{\frac{n+4}{n}}\right)\left(1+4\frac{3\mu+(n+1)\lambda}{4(n+1)\mu+n(n+4)\lambda}\right)-\frac{\left(1-f^{\frac{n+2}{n}}\right)^2}{1-f}\right]e^{\mathrm{ds}}_{(ij)}\,. \end{aligned} \tag{4.33}$$

Finally, the constitutive equation (4.29) needs to be used to eliminate the internal stress $\bar{\underset{\sim}{\sigma}}$ from Eqs. (4.32) and (4.33). This yields the constitutive relations for the symmetric parts of the difference stress $\underset{\sim}{\mathbf{s}}$ in stiffness form

$$\begin{aligned} s_{kk} =&\frac{(2\mu+n\lambda)\,e_{kk}}{\left(1-\frac{n+2}{n+4}\frac{1-f^{\frac{n+4}{n}}}{1-f^{\frac{n+2}{n}}}\right)^2}\left[\frac{n+2}{n+4}\left(1-f^{\frac{n+4}{n}}\right)\left(1+2\frac{6\mu+(n+2)\lambda}{(n+2)(2\mu+n\lambda)}\right)-\left(1+f-2f^{\frac{n+2}{n}}\right)\right] \\ &+(2\mu+n\lambda)\,f\frac{1-f^{\frac{2}{n}}}{1-\frac{n+2}{n+4}\frac{1-f^{\frac{n+4}{n}}}{1-f^{\frac{n+2}{n}}}}E_{kk} \end{aligned} \tag{4.34}$$

$$\begin{aligned} s^{\mathrm{ds}}_{(ij)} =&\frac{2\mu e^{\mathrm{ds}}_{(ij)}}{\left(1-\frac{n+2}{n+4}\frac{1-f^{\frac{n+4}{n}}}{1-f^{\frac{n+2}{n}}}\right)^2}\left[\frac{n+2}{n+4}\left(1-f^{\frac{n+4}{n}}\right)\left(1+4\frac{3\mu+(n+1)\lambda}{4(n+1)\mu+n(n+4)\lambda}\right)-\left(1+f-2f^{\frac{n+2}{n}}\right)\right] \\ &+2\mu f\frac{1-f^{\frac{2}{n}}}{1-\frac{n+2}{n+4}\frac{1-f^{\frac{n+4}{n}}}{1-f^{\frac{n+2}{n}}}}E^{\mathrm{d}}_{ij}\,. \end{aligned} \tag{4.35}$$

As expected from the existence of a strain energy as potential, the coefficients of the coupled term between $\underset{\sim}{\mathbf{s}}$ and $\underset{\sim}{\mathbf{E}}$ are identical to those between $\bar{\underset{\sim}{\sigma}}$ and $\underset{\sim}{\mathbf{e}}$ in Eq. (4.29).

Furthermore, it shall be mentioned that the coefficients of the classical strain $\underset{\sim}{\mathbf{E}}$ in Eqs. (4.34)–(4.35) do *not* correspond to the effective macroscopic moduli. Rather, the micromorphic balance, Eq. (2.31) or Eq. (2.110), respectively, requires that the difference stress $\underset{\sim}{\mathbf{s}}$ vanishes for macroscopically uniform states of loading. Thus, in such a uniform state the relative rotation vanishes, Eq. (4.31), and Eqs. (4.34) and (4.35) imply linear relations between $\underset{\sim}{\mathbf{E}}$ and the relative deformation $\underset{\sim}{\mathbf{e}}$. These relations can be reinserted to Eq. (4.14)

$$\bar{\sigma}_{kk} = \underbrace{(2\mu + n\lambda)\frac{1-f}{1+\frac{f^2\left(1-f^{2/n}\right)^2}{\frac{n+2}{n+4}(1-f)\left(1-f^{\frac{n+4}{n}}\right)\left(1+2\frac{6\mu+(n+2)\lambda}{(n+2)(2\mu+n\lambda)}\right)-\left(1-f^{\frac{n+2}{n}}\right)^2}}}_{=nK^{(\mathrm{eff})}} E_{kk} \tag{4.36}$$

$$\bar{\sigma}^{\mathrm{d}}_{ij} = \underbrace{2\mu\frac{1-f}{1+\frac{f^2\left(1-f^{2/n}\right)^2}{\frac{n+2}{n+4}(1-f)\left(1-f^{\frac{n+4}{n}}\right)\left(1+4\frac{3\mu+(n+1)\lambda}{4(n+1)\mu+n(n+4)\lambda}\right)-\left(1-f^{\frac{n+2}{n}}\right)^2}}}_{=2\mu^{(\mathrm{eff})}} E^{\mathrm{d}}_{ij} \tag{4.37}$$

and allow to extract the effective macroscopic values $K^{(\mathrm{eff})}$ and $\mu^{(\mathrm{eff})}$ of bulk modulus and shear modulus, respectively.

Verification The quality of these Ritz estimates of $K^{(\mathrm{eff})}$ and $\mu^{(\mathrm{eff})}$ can be verified by certain exact solution to the boundary value problem. Firstly, the effective bulk modulus relates hydrostatic stress Σ^{h} and volumetric strain $\underset{\sim}{\mathbf{E}} : \underset{\sim}{\mathbf{I}}$. For pure loading by a hydrostatic stress $\underset{\sim}{\mathbf{\Sigma}} = \Sigma^{\mathrm{h}}\underset{\sim}{\mathbf{I}}$ of the spherical or circular volume element, Fig. 4.2, the problem becomes spherosymmetric or axisymmetric, respectively, and can be solved exactly by elementary methods. The details will be given below in Section 4.5 in the context of the microdilatational theory. Furthermore, the effective shear modulus $\mu^{(\mathrm{eff})}$ can be determined exactly for the plane case $n = 2$. In this case, the stress state at the microscale can be characterized by an Airy stress function $F(\underset{\sim}{\xi})$. For symmetry reasons, the Airy function has to have the structure

$$F = g(r)\underset{\sim}{\mathbf{\Sigma}}^{\mathrm{d}} : \underline{\xi\xi}\,. \tag{4.38}$$

corresponding to a stress field

$$\underset{\sim}{\sigma} = \Delta F\underset{\sim}{\mathbf{I}} - \underline{\nabla\nabla} F = \left[\frac{(g'r^4)'}{r^4}\underset{\sim}{\mathbf{I}} - \frac{1}{r}\left(\frac{g'}{r}\right)'\underline{\xi\xi}\right]\underset{\sim}{\mathbf{\Sigma}}^{\mathrm{d}} : \underline{\xi\xi} - 2g\underset{\sim}{\mathbf{\Sigma}}^{\mathrm{d}} - 2\frac{g'}{r}\left[\left(\underset{\sim}{\mathbf{\Sigma}}^{\mathrm{d}}\cdot\underline{\xi}\right)\underline{\xi} + \underline{\xi}\left(\underset{\sim}{\mathbf{\Sigma}}^{\mathrm{d}}\cdot\underline{\xi}\right)\right] \tag{4.39}$$

The compatibility condition

$$0 = \Delta\Delta F = \frac{1}{r^5}\left[\left(\frac{(g'r^5)'}{r^5}\right)' r^5\right]'\underset{\sim}{\mathbf{\Sigma}}^{\mathrm{d}} : \underline{\xi\xi} \tag{4.40}$$

provides an ODE for the open radial function $g(r)$. This homogeneous ODE has the well-known Mitchell solutions to the bi-potential equation

$$g(r) = C_1 r^2 + \frac{C_2}{r^2} + \frac{C_3}{r^4} + C_4\,. \tag{4.41}$$

The static boundary condition (2.43) and a traction free void surface imply

$$g(R) = -\frac{1}{2}, \qquad g'(R) = 0, \qquad g(R_{\mathrm{void}}) = 0, \qquad g'(R_{\mathrm{void}}) = 0, \tag{4.42}$$

respectively, and determine the coefficients C_1 to C_4. The strain field to Eq. (4.78) is computed as $\underset{\sim}{\varepsilon} = (\underset{\sim}{\sigma} - \nu\underset{\sim}{\sigma} : \underline{\mathbf{II}})/(2\mu)$. The corresponding displacement field could be constructed by means of the Cesaro integrals [96]. Subsequently, the macroscopic strain $\underset{\sim}{\mathbf{E}}$ could be calculated from

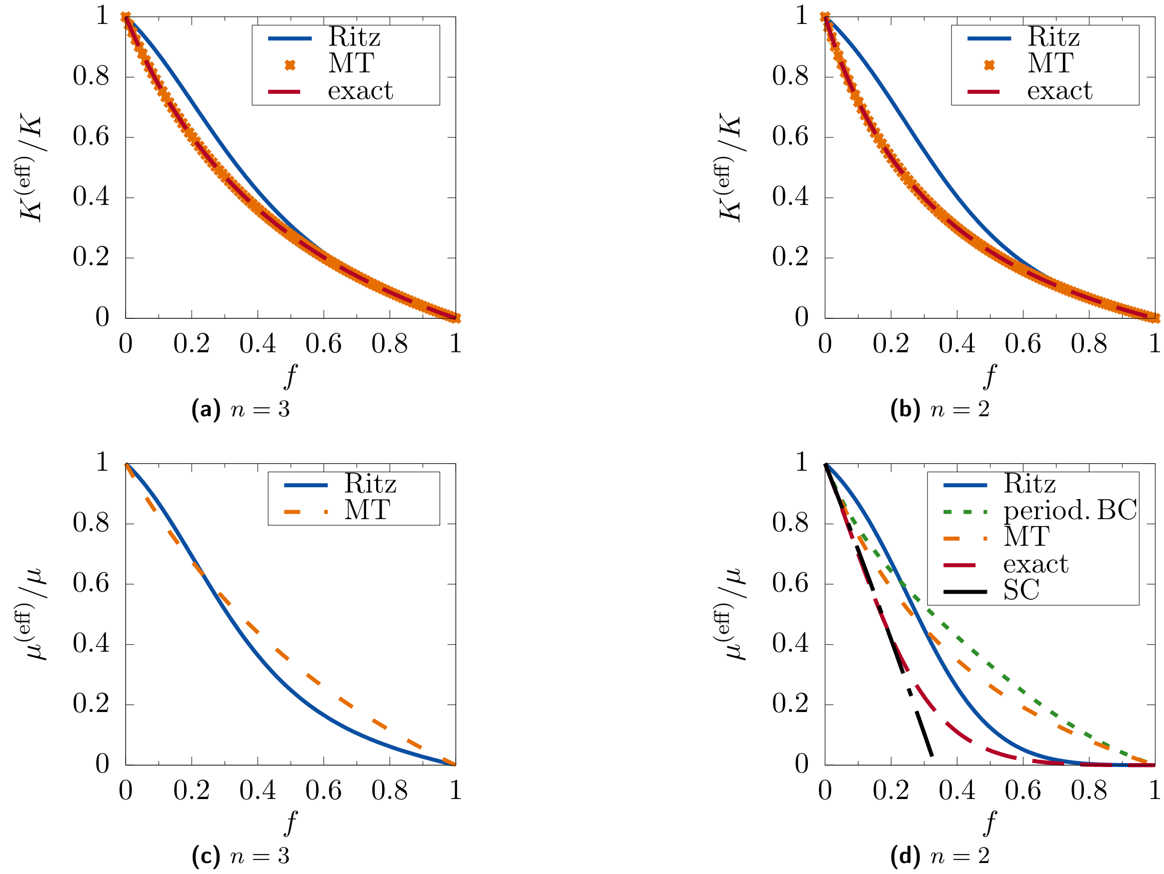

Fig. 4.3.: Comparison of effective moduli ($\nu = 0.3$)

the kinematic micro-macro relation (2.41). Instead of this lengthy procedure, $\underset{\sim}{\mathbf{E}}$ shall be computed here via Castigliano's method as $\underset{\sim}{\mathbf{E}} = \partial \overline{W} / \partial \underset{\sim}{\mathbf{\Sigma}}$. For this purpose, the macroscopic complementary strain energy needs to be computed which is equal the strain energy $\overline{W} = 1/2 \left\langle \underset{\sim}{\sigma} : \underset{\sim}{\varepsilon} \right\rangle_V$ for the linear problem under consideration. In particular for the stress field (4.40), a strain energy

$$\overline{W} = \frac{1}{4\mu} \frac{1 + f + 7f^2 + 3f^3 - 4\nu f(1 + f + f^2)}{(1-f)^3} \underset{\sim}{\mathbf{\Sigma}}^{\mathrm{d}} : \underset{\sim}{\mathbf{\Sigma}}^{\mathrm{d}} \tag{4.43}$$

is obtained[1]. The effective shear modulus $\mu^{(\mathrm{eff})}$ corresponds to four times the inverse of the cofactor of $\underset{\sim}{\mathbf{\Sigma}}^{\mathrm{d}} : \underset{\sim}{\mathbf{\Sigma}}^{\mathrm{d}}$ in Eq. (4.43). Analogously, $\mu^{(\mathrm{eff})}$ can be found for kinematic and periodic boundary conditions as shown in detail in Appendix A.1. Remarkably, kinematic and periodic boundary conditions yield identical values of $\mu^{(\mathrm{eff})}$ for the circular volume element with concentric void under consideration.

Figure 4.3 compares the mentioned exact solutions for $K^{(\mathrm{eff})}$ and $\mu^{(\mathrm{eff})}$ with the Ritz estimates (4.36)–(4.37). Furthermore, the figures incorporate estimates by the Mori-Tanaka method ("MT") and by the Self-consistent method ("SC") [97], respectively. Firstly, the comparison shows that the Ritz method with cubic ansatz provides indeed upper bounds to all considered exact solutions. The exact solutions for the bulk moduli coincide with the Mori-Tanaka estimates, Figs. 4.3a and 4.3a. Figure 4.3c shows that the predicted values of the effective shear modulus $\mu^{(\mathrm{eff})}$ for Ritz method and Mori-Tanaka method compare quite well for spherical voids $n = 3$. In contrast, Fig. 4.3d indicates even a qualitative disagreement for

[1] The commitment of the undergraduate student Vincent von Oertzen for the detailed elaboration of Eqs. (4.39)–(4.43) is gratefully acknowledged.

the plane case $n = 2$. The present model of a circular volume element with static boundary conditions predicts a *perculation* behavior, both for exact solution and Ritz estimate: beyond $f \gtrsim 0.6$, the effective shear modulus $\mu^{(\text{eff})}$ vanishes virtually. In contrast, the Mori-Tanaka method predicts a steady decrease of $\mu^{(\text{eff})}$ until $f = 1$. However, perculation is predicted by the Self-consistency method, though at a lower value of the porosity f. Percolation behavior is known to appear in systems with stochastic arrangement of pores [98, 99]. However, for regular arrangements as the one under consideration, periodic boundary conditions are known to provide the best results. Figure 4.3d shows that the exact solution for periodic boundary conditions does not exhibit percolation but lies close to the Mori-Tanaka estimate.

4.4. Micropolar theory

The micropolar and microdilatational theories are special cases of the micromorphic theory, compare Sections 3.6.2 and 3.6.4. Consequently, the preceding results for the elastic micromorphic properties of an isotropic porous medium include the micropolar and microdilatational properties.

For the micropolar theory, the micromorphic static boundary condition (3.22) is replaced by the micropolar one (3.84). For the latter, the micromorphic double stress $\underset{\approx}{\mathbf{M}}$ according to Eq. (3.11) amounts to

$$M_{ijk} = -\frac{1}{3}\left(M^{\mathrm{r}}_{ip}\epsilon_{pjk} + M^{\mathrm{r}}_{kp}\epsilon_{pji}\right) . \tag{4.44}$$

The polar double stress $\underset{\sim}{\mathbf{M}}^{\mathrm{r}}$ constitutes some components of $\underset{\approx}{\mathbf{M}}$ whereas certain "non-polar" components of M_{ijk} vanish under static boundary conditions. However, this does not inevitably mean that the respective components in the symmetric gradient of microdeformation K^{s}_{ijk} need to vanish as well. Rather, Eq. (4.44) has to be inserted to the compliance form constitutive equation (4.22). Subsequently, in a micropolar theory those components out of all micromorphic components of K^{s}_{ijk} have to be selected which are transferred to the macroscale. According to Eq. (3.81), this yields a constitutive relation between the gradient of rotation and the polar double stress in compliance form of

$$K^{\mathrm{rd}}_{im} = \frac{5}{18\mu R^2}\cdot\frac{1}{1-f^{\frac{5}{3}}}\left[6M^{\mathrm{r}}_{im} - (M^{\mathrm{r}}_{im} - M^{\mathrm{r}}_{mi})\left(\frac{4\nu}{1+\nu} + \frac{8+4\nu}{5(1+\nu)}\,\frac{1-f^{\frac{5}{3}}}{1-f} - \frac{7+6\nu}{25(1+\nu)}\,\frac{\left(1-f^{\frac{5}{3}}\right)^2}{(1-f)^2}\right)\right] . \tag{4.45}$$

for spherical pores $n = 3$ or

$$\underline{\mathbf{K}}^{\mathrm{r}} = \frac{17 - 16\nu - f(6-f)}{18(1-f^2)\mu R^2}\underline{\mathbf{M}}^{\mathrm{r}} \tag{4.46}$$

for the plane (strain) case $n = 2$, respectively.

In addition, for the transition of the micromorphic theory to a micropolar one, the difference stress involves only the skew-symmetric part of the external stress $s_{ij} = 1/2(\Sigma_{ji} - \Sigma_{ij})$. Consequently, Eq. (4.31) for the skew-symmetric part of the relative deformation and Eqs. (4.36) and (4.37) for the effective bulk modulus and shear modulus, respectively, are relevant for the micropolar theory.

In the theory of linear elasticity of micropolar continua, an isotropic constitutive relation

$$\underset{\sim}{\mathbf{\Sigma}} = \lambda^{(\text{eff})}\underset{\sim}{\mathbf{E}}^{\mathrm{r}} : \underset{\approx}{\mathbf{II}} + (\mu^{\mathrm{r}} + \kappa^{\mathrm{r}})\underset{\sim}{\mathbf{E}}^{\mathrm{r}} + \mu^{\mathrm{r}}(\underset{\sim}{\mathbf{E}}^{\mathrm{r}})^{\mathrm{T}} \tag{4.47}$$

$$\underset{\sim}{\mathbf{M}}^{\mathrm{r}} = \alpha^{\mathrm{r}}\underset{\sim}{\mathbf{K}}^{\mathrm{r}} : \underset{\approx}{\mathbf{II}} + \beta^{\mathrm{r}}(\underset{\sim}{\mathbf{K}}^{\mathrm{r}})^{\mathrm{T}} + \gamma^{\mathrm{r}}\underset{\sim}{\mathbf{K}}^{\mathrm{r}} \tag{4.48}$$

is specified typically [e. g. 17, 100] in terms of the six Lamé-type constants $\lambda^{(\mathrm{eff})}$, μ^{r}, κ^{r}, α^{r}, β^{r}, γ^{r} under definition of the the micropolar strain

$$\underset{\sim}{\mathbf{E}}^{\mathrm{r}} = \underline{\nabla_{\mathbf{X}}\mathbf{U}} - \underset{\approx}{\epsilon} \cdot \underline{\boldsymbol{\Phi}}^{\mathrm{r}} \,, \tag{4.49}$$

compare Eq. (3.76). Therein, the Lamé parameters μ^{r} and λ are known from the classical theory of elasticity. However, note that μ^{r} does *not* correspond to the shear modulus. Rather, the effective modulus as ratio between shear stress and shearing amounts to $\mu^{(\mathrm{eff})} = \mu^{\mathrm{r}} + \kappa^{\mathrm{r}}/2$ and involves additionally the so-called *coupling modulus* κ^{r} associated with skew-symmetric parts. These parameters can be identified by comparing Eqs. (4.47)–(4.48) with the results of the present estimates. In particular, the coupling modulus is identified from Eq. (4.31) as

$$\kappa^{\mathrm{r}} = \frac{4\mu}{n+4} \frac{1 - f^{\frac{n+4}{n}}}{\left(1 - \frac{n+2}{n+4}\frac{1-f^{\frac{n+4}{n}}}{1-f^{\frac{n+2}{n}}}\right)^2} \,. \tag{4.50}$$

Subsequently, the Lame constants are obtained from the macroscopic bulk and shear moduli $K^{(\mathrm{eff})}$ and $\mu^{(\mathrm{eff})}$, respectively, from Eqs. (4.36) and (4.37) as

$$\mu^{\mathrm{r}} = \mu^{(\mathrm{eff})} - \frac{\kappa^{\mathrm{r}}}{2} \,, \qquad \lambda^{(\mathrm{eff})} = K^{(\mathrm{eff})} - \frac{2\mu^{\mathrm{r}}}{n} \,. \tag{4.51}$$

The coefficients α^{r}, β^{r}, γ^{r}, which are related to the polar double stress $\underset{\sim}{\mathbf{M}}^{\mathrm{r}}$ in Eq. (4.48), apply to the three-dimensional case $n = 3$ only. In the plane case $n = 2$, a single parameter γ^{r} is sufficient for isotropic material, compare Eq. (4.46). For $n = 3$, Eq. (4.45) can be split into symmetric and skew-symmetric parts which can be compared with the respective parts of Eq. (4.48). In this context it has to be recalled that $\underset{\sim}{\mathbf{M}}^{\mathrm{r}}$ is deviatoric in the present theory, compare Eq. (3.74). Consequently, the remaining parameters are identified as

$$\begin{aligned}
\alpha^{\mathrm{r}} &= -\frac{\mu}{10R^2}\left(1 - f^{5/3}\right) \\
\beta^{\mathrm{r}} &= \frac{3\mu}{20R^2}\left(1 - f^{5/3}\right)\left[1 - \frac{6(1+\nu)}{3 - \nu - \frac{8+4\nu}{5}\frac{1-f^{5/3}}{1-f} + \frac{7+6\nu}{25}\frac{\left(1-f^{5/3}\right)^2}{(1-f)^2}}\right] \\
\gamma^{\mathrm{r}} &= \frac{3\mu}{20R^2}\left(1 - f^{5/3}\right)\left[1 + \frac{6(1+\nu)}{3 - \nu - \frac{8+4\nu}{5}\frac{1-f^{5/3}}{1-f} + \frac{7+6\nu}{25}\frac{\left(1-f^{5/3}\right)^2}{(1-f)^2}}\right]
\end{aligned} \tag{4.52}$$

Alternatively to the Lamé-type constants, a linear-elastic isotropic micropolar medium can be characterized by engineering constants [17, 22]. These engineering constants appear in solutions for simple loading cases and can thus be related to respective experiments. In addition to Young's modulus and Poisson ratio, these are the coupling number N^{r}, polar ratio Ψ^{r} and the characteristic lengths $l^{\mathrm{r}}_{\mathrm{b}}$ and $l^{\mathrm{r}}_{\mathrm{t}}$ under bending and torsion, respectively:

$$\Psi^{\mathrm{r}} = \frac{\beta^{\mathrm{r}} + \gamma^{\mathrm{r}}}{\alpha^{\mathrm{r}} + \beta^{\mathrm{r}} + \gamma^{\mathrm{r}}} \,, \qquad N^{\mathrm{r}} = \sqrt{\frac{\kappa^{\mathrm{r}}}{2\mu^{(\mathrm{eff})} + \kappa^{\mathrm{r}}}} \,, \tag{4.53}$$

$$l^{\mathrm{r}}_{\mathrm{t}} = \sqrt{\frac{\beta^{\mathrm{r}} + \gamma^{\mathrm{r}}}{2\mu^{(\mathrm{eff})}}} \,, \qquad l^{\mathrm{r}}_{\mathrm{b}} = \sqrt{\frac{\gamma^{\mathrm{r}}}{4\mu^{(\mathrm{eff})}}} \,. \tag{4.54}$$

Due to the deviatoric double stress $\underset{\sim}{\mathbf{M}}^{\mathrm{r}}$, the polar ratio evaluates to $\Psi^{\mathrm{r}} = 3/2$ independent of the particular values of β^{r} and γ^{r}. This value of Ψ^{r} leads to a bounded stiffness of torsion specimens of arbitrarily small size as discussed by Neff [101]. The predicted coupling number

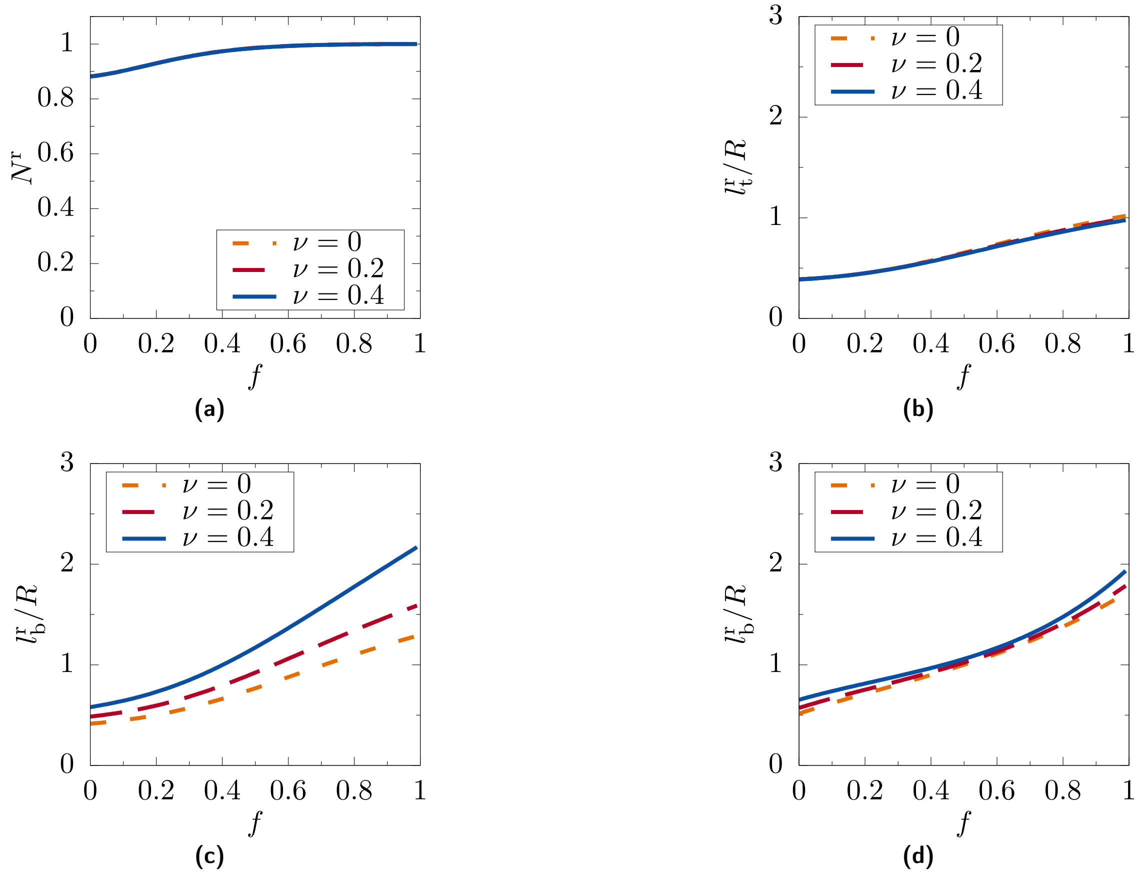

Fig. 4.4.: Non-classical Cosserat parameters: (a) coupling number, (b) characteristic length under torsion, (c) characteristic length under bending for spherical pores $n = 3$ and (d) for circular pores $n = 2$

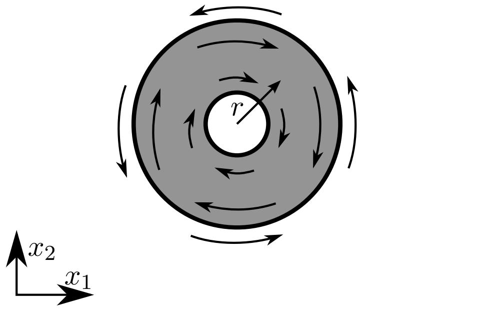

Fig. 4.5.: Plane circular cell under skew-symmetric external stress

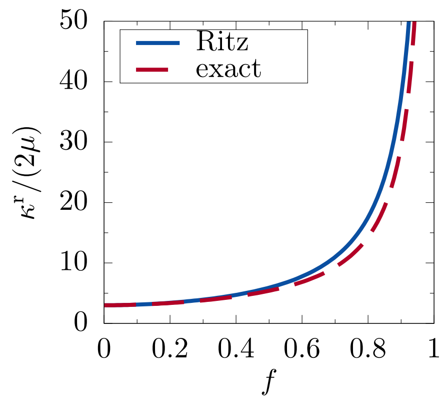

Fig. 4.6.: Cosserat coupling modulus from exact solution and Ritz' solution

N^{r} from Eqs. (4.37) and (4.50) is plotted in Fig. 4.4a versus the porosity f. It lies between 0.9 and 1 and increases with increasing porosity f. The influence of the Poisson ratio ν of the matrix material on N^{r} can be neglected. Figures 4.4b and 4.4c show the influence on the characteristic length scales $l_{\mathrm{t}}^{\mathrm{r}}$ and $l_{\mathrm{b}}^{\mathrm{r}}$, respectively, for spherical pores $n = 3$. Both characteristic lengths increase with increasing porosity f for a given value of R. Even for $f \to 1$, both $l_{\mathrm{t}}^{\mathrm{r}}$ and $l_{\mathrm{b}}^{\mathrm{r}}$ remain finite although the effective shear modulus $\mu^{(\mathrm{eff})}$ tends to zero and appears in the denominator in Eq. (4.54). In particular, for highly porous materials $f \gtrsim 0.7$, the internal length scales attain values $l_{\mathrm{t}}^{\mathrm{r}} \approx R$ and $l_{\mathrm{b}}^{\mathrm{r}} \approx 2R$ for $\nu \geq 0.2$, respectively. In this context it is recalled that for real porous materials, R might be interpreted as half average distance between pores. The Poisson ratio has hardly any influence on $l_{\mathrm{t}}^{\mathrm{r}}$ and a moderate influence on $l_{\mathrm{b}}^{\mathrm{r}}$. Figure 4.4d shows the length scale for bending $l_{\mathrm{b}}^{\mathrm{r}}$ for the plane case, i. e. with circular pores. Qualitatively and quantitatively, the results are comparable with those for the spherical pores in Fig. 4.4c. However, note that $l_{\mathrm{b}}^{\mathrm{r}}$ in Fig. 4.4d was computed with the effective shear modulus $\mu^{(\mathrm{eff})}$ from periodic boundary conditions. If the values for $\mu^{(\mathrm{eff})}$ from static boundary conditions, either solved exactly or by Ritz' method, were taken, the questionable percolation behavior would lead to unbounded values of $l_{\mathrm{b}}^{\mathrm{r}}$ as f reaches the percolation limit $f \gtrsim 0.6$, compare Fig. 4.3d.

Lakes and co-workers [19, 21, 24, 26] performed a number of bending and torsion experiments with specimens from different foam-like materials. They identified the Cosserat parameters by a regression of the stiffnesses which were measured with specimens of different cross section. They found indeed that a polar ratio $\Psi^{\mathrm{r}} = 3/2$ matches quite well. For commercial foams, they obtained a coupling number N^{r} well below unity [21] but also a value $N^{\mathrm{r}} = 0.99$ [24]. Recently, they employed artificially printed foams for which they obtained again values of N^{r} close to unity and concluded that lower values were attributed to surface layers which were damaged during the manufacturing of the specimens. Regarding the intrinsic length scales $l_{\mathrm{t}}^{\mathrm{r}}$ and $l_{\mathrm{b}}^{\mathrm{r}}$, they stated in their recent review [26] that they were much smaller than the cell size in “stretch dominated” foams and “greater than the cell size ... in bend dominated lattices”. Figure 4.4 shows that the predictions of the proposed homogenisation procedure matches quite well with these experimental findings.

Verification For estimating the quality of the approximate solution by means of Ritz' method with cubic ansatz, it needs to be verified. In particular, in the plane case the problem for the coupling modulus κ^{r} is axisymmetric, Fig. 4.5, and can be solved exactly. The respective Lamé equation [see e. g. 102] to Eq. (3.83) for the circumferencial displacement $u_\varphi(r)$ reads

$$\frac{1}{r^2}\left[r^3\left(\frac{u_\varphi}{r}\right)'\right]' = -\frac{2}{(1-f^2)R^2}\,\frac{\Sigma^{\mathrm{skw}}}{\mu}\,r\,. \tag{4.55}$$

Therein, the geometric moments from Eq. (4.26) were used and the prime $()'$ refers to the derivative with respect to r. Furthermore, $\Sigma^{\mathrm{skw}} = \underset{\sim}{\epsilon} : \underset{\sim}{\mathbf{\Sigma}}$ refers to the skew-symmetric part of the macroscopic stress $\underset{\sim}{\mathbf{\Sigma}}$. This skew-symmetric part acts like a circumferencial volume force which goes linear with r and drives the relative rotation, compare Eq. (3.83). Equation (4.55) can be integrated twice yielding

$$u_{\varphi}(r) = -\frac{1}{1-f^2}\frac{\Sigma^{\mathrm{skw}}}{4\mu}\frac{r^3}{R^2} + \frac{c_1}{r} + c_2 r \tag{4.56}$$

with two constants of integration c_1 and c_2. Constant c_1 is determined from the condition of a traction free surface of the pore $(u_{\varphi}/r)'|_{r=R_{\mathrm{void}}} = 0$. The term with c_2 corresponds to an irrelevant rigid rotation. The kinematic micro-macro relations (3.36) and (3.79) for the macroscopic and the microscopic rotation, respectively, become

$$\Phi^{\nabla U} = \frac{1}{2}\underset{\sim}{\epsilon} : \underline{\nabla_{\mathbf{X}}}\underline{\mathbf{U}} = \frac{u_{\varphi}(R)}{R}, \qquad \Phi^{\mathrm{r}} = \frac{4}{R^4}\frac{1}{1-f^2}\int\limits_{R_{\mathrm{void}}}^{R} r^2 u_{\varphi}(r)\mathrm{d}r\,. \tag{4.57}$$

Finally, the coupling modulus κ^{r} can be extracted from the resulting relation between the relative rotation $\Phi^{\nabla U} - \Phi^{\mathrm{r}}$ and the skew-symmetric part Σ^{skw} of the macroscopic stress as

$$\kappa^{\mathrm{r}} = 6\mu\frac{(1+f)^2}{(1-f)(1+3f)}\,. \tag{4.58}$$

Figure 4.6 compares the exact value of κ^{r} from Eq. (4.58) with the cubic Ritz' estimate (4.50). As expected, Ritz' method provides an upper bound. For a compact material $f = 0$, it even yields the exact result $\kappa^{\mathrm{r}} = 6\mu$ since the exact solution (4.56) is cubic in this case. For other values of porosity f, the discrepancy between exact solution and Ritz estimate remains moderate. For $f \to 1$, the coupling modulus κ^{r} diverges, compare Eqs. (4.50) and (4.58), which is why the coupling number N^{r} tends to unity, Fig. 4.4a.

For verification of the coefficients β^{r} and γ^{r}, which relate the double stress and gradient of rotation, the most simple case is considered: the compact material $f = 0$ for the plane case $n = 2$. In this case, the stress field

$$\underset{\sim}{\sigma} = \frac{7}{3R^2}\underset{\sim}{\mathbf{I}}\underline{\xi}\cdot\underset{\sim}{\epsilon}\cdot\underline{\mathbf{M}}^{\mathrm{r}} - \frac{1}{R^2}\left(\underline{\xi}\otimes\underset{\sim}{\epsilon}\cdot\underline{\mathbf{M}}^{\mathrm{r}} + \underset{\sim}{\epsilon}\cdot\underline{\mathbf{M}}^{\mathrm{r}}\otimes\underline{\xi}\right) \tag{4.59}$$

can be identified as solution to the static boundary conditions (3.88) and equilibrium condition (3.87), respectively, for loading by the polar double stress vector $\underline{\mathbf{M}}^{\mathrm{r}}$. This stress field is linear in $\underline{\xi}$ and thus satisfies the compatibility condition for any homogeneous, linear elastic material. Again, $\underline{\mathbf{K}}^{\mathrm{r}}$ is computed here via Castigliano's method as $\underline{\mathbf{K}}^{\mathrm{r}} = \partial\overline{W}/\partial\underline{\mathbf{M}}^{\mathrm{r}}$. For this purpose, the macroscopic complementary strain energy is computed as $\overline{W} = \left\langle\underset{\sim}{\sigma} : \underset{\sim}{\sigma} - \nu(\underset{\sim}{\sigma} : \underset{\sim}{\mathbf{I}})^2\right\rangle_V/(2\mu)$ for the linear problem under consideration. In particular for the stress field (4.59), a complementary strain energy

$$\overline{W} = \frac{1}{2}\frac{17-16\nu}{18}\underline{\mathbf{M}}^{\mathrm{r}}\cdot\underline{\mathbf{M}}^{\mathrm{r}} \tag{4.60}$$

is obtained. The double stress modulus γ^{r} corresponds to half of the inverse of the cofactor of $\underline{\mathbf{M}}^{\mathrm{r}}\cdot\underline{\mathbf{M}}^{\mathrm{r}}$

$$\gamma^{\mathrm{r}} = \mu R^2\frac{18}{17-16\nu}\,. \tag{4.61}$$

Equation (4.61) indicates an non-negligible influence of the Poisson ratio ν of the matrix material (for a plane stress case, ν has to be replaced by $\nu/(1+\nu)$).

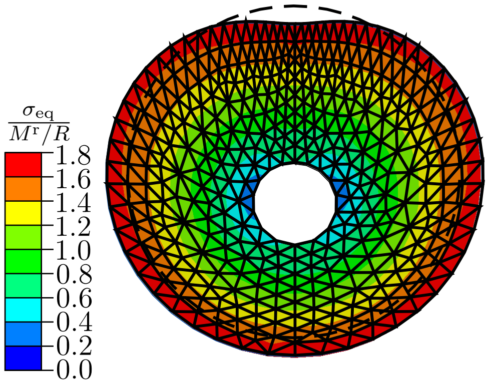

Fig. 4.7.: Microscopic deformation and stresses from a micropolar double stress $\underline{\mathbf{M}}^{\mathrm{r}} = \underline{\mathbf{b}}_1$ ($f = 0.0625$, $\nu = 0.3$)

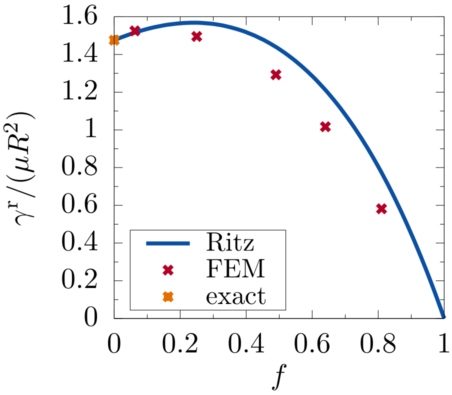

Fig. 4.8.: Micropolar double stress modulus from exact solution, Ritz' solution and FEM ($\nu = 0.3$)

Corresponding FEM computations have been performed for the verification with finite porosities f. Triangular elements with linear shape functions are used. The static boundary conditions (3.88) were implemented into the commercial FEM code Abaqus by means of the UTRACLOAD interface. The results of such a computation are shown in Fig. 4.7. The double stress modulus γ^{r} was extracted from the strain energy, too.

Figure 4.8 compares the resulting values of γ^{r} between the exact solution (4.52), Ritz approximation (4.52) and FEM computations. It turns out again that the Ritz approximation provides a reasonable accuracy for all values of porosity f. For $f = 0$, even the exact solution is obtained since the microscopic displacement field is a quadratic polynomial in this case.

The good agreement of the Ritz estimates with the given exact and numerical solutions for the plane case $n = 2$ raises the hope that the Ritz estimates (4.50), (4.46) and (4.52) are sufficiently accurate for the spatial case $n = 3$ as well.

4.5. Microdilatational theory

The microdilatational theory is obtained from the general micromorphic theory by allowing only hydrostatic parts of the difference stress $\underset{\sim}{\mathbf{s}} = s_{\mathrm{h}}\underset{\sim}{\mathbf{I}}$ and by replacing the micromorphic static boundary condition (3.22) by Eq. (3.119). Thus, from the Ritz' solution for the general micromorphic model, Eqs. (4.34) and (4.37) do remain. With the microdilatational static boundary condition (3.119), the micromorphic double stress $\underset{\approx}{\mathbf{M}}$ according to Eq. (3.11) amounts to

$$M_{ijk} = -\frac{1}{3}\left(M^{\mathrm{r}}_{ip}\epsilon_{pjk} + M^{\mathrm{r}}_{kp}\epsilon_{pji}\right) . \tag{4.62}$$

This value can be inserted to Eq. (4.22) to obtain the symmetrized gradient of microdeformation $\underset{\approx}{\mathbf{K}}^{\mathrm{s}}$. From this tensor, only the gradient of microdilatation $\underline{\mathbf{K}}^{\mathrm{v}}$ is transferred to the macroscale. According to Eq. (3.104), the gradient of microdilatation comprises the components $K^{\mathrm{v}}_i = 2K^{\mathrm{s}}_{ijj} - K^{\mathrm{s}}_{jij}$ of $\underset{\approx}{\mathbf{K}}^{\mathrm{s}}$. Thus, the the cubic ansatz results in a constitutive relation

$$\underline{\mathbf{M}}^{\mathrm{v}} = \mu R^2 \frac{8(1+\nu)(1-f^{5/3})}{5(23-26\nu) - 2\,(9+4\nu)\,\frac{1-f^{\frac{5}{3}}}{1-f} + \frac{7+6\nu}{5}\left(\frac{1-f^{\frac{5}{3}}}{1-f}\right)^2}\underline{\mathbf{K}}^{\mathrm{v}} \tag{4.63}$$

for the double stress for spherical voids $n = 3$ and

$$\underline{\mathbf{M}}^{\mathrm{v}} = \mu R^2 \frac{1-f^2}{6-8\nu}\underline{\mathbf{K}}^{\mathrm{v}} \tag{4.64}$$

for the plane case $n = 2$, respectively.

The linear elastic microdilatational theory was proposed by Cowin and Nunziato [103] as "linear theory of elastic materials with voids"[2]. In this theory, an isotropic linear elastic material is described by the constitutive relations

$$\begin{aligned} \underset{\approx}{\mathbf{\Sigma}} &= 2\mu^{(\mathrm{eff})}\underset{\approx}{\mathbf{E}} + \lambda^{(\mathrm{eff})}\underset{\approx}{\mathbf{E}} : \underset{\approx}{\mathbf{II}} + \beta^{\mathrm{v}}\chi^{\mathrm{v}}\underset{\approx}{\mathbf{I}}, \\ \tilde{s}_{\mathrm{h}} &= \xi^{\mathrm{v}}\chi^{\mathrm{v}} + \beta^{\mathrm{v}}\underset{\approx}{\mathbf{E}} : \underset{\approx}{\mathbf{I}}, \\ \underline{\mathbf{M}}^{\mathrm{v}} &= \alpha^{\mathrm{v}}\underline{\mathbf{K}}^{\mathrm{v}} \end{aligned} \tag{4.65}$$

with parameters β^{v}, ξ^{v} and α^{v} in addition to classical Lamé parameters $\mu^{(\mathrm{eff})}$ and $\lambda^{(\mathrm{eff})}$. Thereby, the symbols for the measures of stress and deformation were adapted to the present notation[3]. In contrast to the micropolar theory, several definitions of a coupling nomber for the microdilatational theory were used in the literature[4]. For an overview the reader is referred to Lakes [20]. Consensus seems to apply only to the definition of a characteristic length

$$l^{\mathrm{v}} = \sqrt{\frac{\alpha^{\mathrm{v}}}{\xi^{\mathrm{v}} - \frac{(\beta^{\mathrm{v}})^2}{2\mu^{(\mathrm{eff})}+\lambda^{(\mathrm{eff})}}}}\,. \tag{4.66}$$

which appears in closed-form solutions for the bending problem [103, 104].

A comparison of Eq. (4.65) with Eq. (4.34) allows to identify

$$\xi^{\mathrm{v}} = \frac{K}{\left(1 - \frac{n+2}{n+4}\frac{1-f^{\frac{n+4}{n}}}{1-f^{\frac{n+2}{n}}}\right)^2}\left[\frac{n+2}{n+4}\left(1 - f^{\frac{n+4}{n}}\right)\left(1 + 2\frac{6\mu + (n+2)\lambda}{(n+2)(2\mu + n\lambda)}\right) - \left(1 + f - 2f^{\frac{n+2}{n}}\right)\right] \tag{4.67}$$

$$\beta^{\mathrm{v}} = -Kf\frac{1 - f^{\frac{2}{n}}}{1 - \frac{n+2}{n+4}\frac{1-f^{\frac{n+4}{n}}}{1-f^{\frac{n+2}{n}}}} - \xi^{\mathrm{v}}\,. \tag{4.68}$$

from the Ritz approximation. Therein, $K = 2\mu/n + \lambda$ is the bulk modulus of the matrix. The effective macroscale bulk modulus corresponds to the case $\tilde{s}_{\mathrm{h}} = 0$ as discussed already. Thus, it is related to the parameters in Eq. (4.65) by $K^{(\mathrm{eff})} = 2\mu^{(\mathrm{eff})}/n + \lambda^{(\mathrm{eff})} - (\beta^{\mathrm{v}})^2/\xi^{\mathrm{v}}$. This relation allows to compute $\lambda^{(\mathrm{eff})}$ from the effective moduli $\mu^{(\mathrm{eff})}$ and $K^{(\mathrm{eff})}$ in Eqs. (4.36) and (4.37), respectively. The coefficient α^{v} of the double stress can directly be anticipated from Eqs. (4.63)–(4.64) and does not need to be repeated here. The related characteristic length l^{v} is plotted in Fig. 4.9. The plot shows that l^{v} depends strongly on the Poisson ratio ν of the matrix material and on the porosity f. This strong dependency was not observed for the characteristic length scales of the micropolar theory, compare Fig. 4.4. The comparison with Fig. 4.4 shows furthermore that for a given microstructure size R, the obtained microdilatational length l^{v} is considerably smaller than the respective micropolar values $l^{\mathrm{r}}_{\mathrm{t}}$ and $l^{\mathrm{r}}_{\mathrm{b}}$. Furthermore, in contrast to the latter, l^{v} decreases towards zero for high porosities $f \to 1$. This fact complies with the finding of Lakes [20] that the contribution of the micropolar terms to the size effect for foams under bending is stronger than the contribution of the microdilatational terms.

[2] Materials with voids can be modeled by means of all continuum theories which are considered within the present thesis, including the classical Cauchy-Boltzmann theory. That is why the author prefers the term "microdilatational theory".

[3] In the theory of Cowin and Nunziato [103], χ^{v} is interpreted as "change in volume fraction" and denoted by φ. The double stress $\underline{\mathbf{M}}^{\mathrm{v}}$ corresponds to the "equilibrated stress vector" $\underline{\mathbf{h}}$ and $s_{\mathrm{h}} = -\tilde{s}_{\mathrm{h}}$ to the "intrinsic equilibrated body force" g, respectively.

[4] This problem is related to the fact that a single coupling number and an intrinsic length l^{v} due not suffice to characterize the three non-classical parameters ξ^{v}, β^{v} and α^{v}.

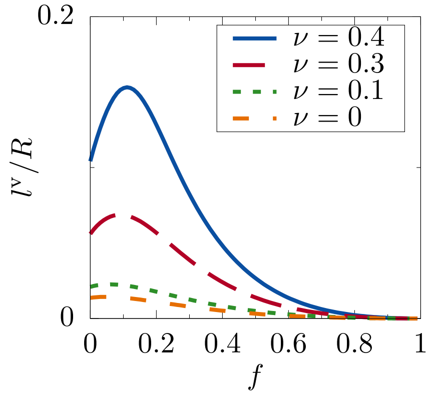

Fig. 4.9.: Characteristic length of microdilatational theory ($n = 3$)

Verification Also for the homogenization towards a microdilatational theory, some exact solutions can be found. In particular, for the considered spherical volume element with spherical pore, a microdilatational difference stress $\tilde{s}_{\mathrm{h}}$ and a hydrostatic external stress $\underset{\sim}{\boldsymbol{\Sigma}} = \Sigma^{\mathrm{h}}\underset{\sim}{\mathbf{I}}$ impose an axisymmetric problem in the plane case $n = 2$ or a spherical symmetrical problem for $n = 3$. The respective Lamé equation [102] to Eq. (3.118) read

$$\left(\frac{1}{r^{n-1}}(r^{n-1}u)'\right)' = -\frac{n+2}{(1-f^{\frac{n+2}{n}})R^2}\frac{\tilde{s}_{\mathrm{h}}}{2\mu+\lambda}r \tag{4.69}$$

with displacements $\underline{\mathbf{u}} = u(r)\underline{\mathbf{b}}_r$ in radial direction. This ODE can be integrated

$$u(r) = -\frac{1}{2}\frac{1}{1-f^{\frac{n+2}{n}}}\frac{\tilde{s}_{\mathrm{h}}}{2\mu+\lambda}\frac{r^3}{R^2} + c_1 r + c_2\frac{R^n}{r^{n-1}} \tag{4.70}$$

yielding two constants of integration c_1 and c_2. The corresponding radial stresses are

$$\sigma_{rr} = -\frac{1}{2}\frac{1}{1-f^{\frac{n+2}{n}}}\frac{6\mu+(n+2)\lambda}{2\mu+\lambda}\frac{r^2}{R^2}\tilde{s}_{\mathrm{h}} + (2\mu+n\lambda)\,c_1 - 2(n-1)\mu c_2\frac{R^n}{r^n} \tag{4.71}$$

For the hollow sphere under spherical-symmetrical loading, the kinematic and kinetic micro-macro relations (3.36), (5.8) and (3.110), respectively, become

$$E^{\mathrm{v}} := \underset{\sim}{\mathbf{E}} : \underset{\sim}{\mathbf{I}} = \frac{n}{R}u(R), \quad \chi^{\mathrm{v}} = \frac{n(n+1)}{R^{n+2}}\frac{1}{1-f^{\frac{n+2}{n}}}\int\limits_{R_{\mathrm{void}}}^{R} r^n u(r)\mathrm{d}r, \quad \Sigma^{\mathrm{h}} = \frac{1}{n}\underset{\sim}{\boldsymbol{\Sigma}} : \underset{\sim}{\mathbf{I}} = \sigma_{rr}(r=R) \tag{4.72}$$

For the ODE (4.69), it makes no difference whether $(4.72)_1$ or $(4.72)_3$ is applied as kinematic or static boundary condition (3.120) or (3.22), respectively. For simplicity, the constants of integration c_1 and c_2 are determined firstly by $(4.72)_3$ together with the natural boundary

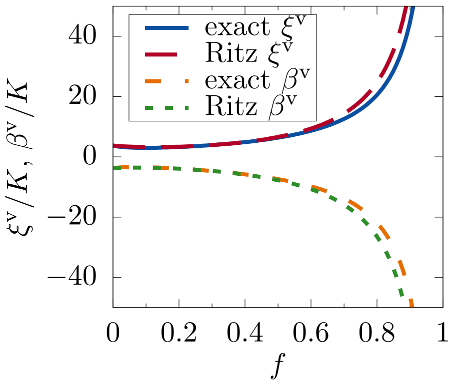

Fig. 4.10.: Non-classical microdilatational moduli ξ^{v} and β^{v} from exact solution and Ritz' solution ($n = 3$, $\nu = 0.3$)

condition $\sigma_{rr}(r = R_{\mathrm{void}}) = 0$ at the void surface. With these values, the kinematic relations $(4.72)_1$ or $(4.72)_2$ become

$$E^{\mathrm{v}} = \frac{1}{K}\frac{1}{1-f}\left[1 + \frac{f}{n-1}\frac{2\mu+n\lambda}{2\mu}\right]\Sigma^{\mathrm{h}} + \frac{1}{K}\frac{1}{1-f}\left[1 + \frac{f}{2}\frac{2\mu+n\lambda}{2\mu}\frac{n+2}{n-1}\frac{1-f^{2/n}}{1-f^{\frac{n+2}{n}}}\right]\tilde{s}_{\mathrm{h}} \tag{4.73}$$

$$\chi^{\mathrm{v}} = \frac{1}{K}\frac{1}{1-f}\left[1 + \frac{f}{2}\frac{2\mu+n\lambda}{2\mu}\frac{n+2}{n-1}\frac{1-f^{2/n}}{1-f^{\frac{n+2}{n}}}\right]\Sigma^{\mathrm{h}} + \frac{1}{K}\frac{1}{1-f}\frac{6\mu+(n+2)\lambda}{2(2\mu+\lambda)}\left[1+ \frac{n+2}{n-1}\frac{2\mu+n\lambda}{2\mu}\frac{f}{2}\left(\frac{1-f^{\frac{2}{n}}}{1-f^{\frac{n+2}{n}}}\right)^2 - \frac{n+2}{n+4}\frac{2\mu+n\lambda}{6\mu+(n+2)\lambda}\frac{(1-f)\left(1-f^{\frac{n+4}{n}}\right)}{\left(1-f^{\frac{n+2}{n}}\right)^2}\right]\tilde{s}_{\mathrm{h}}\,. \tag{4.74}$$

Due to the existence of a strain energy, the crossed coefficients are equal, $\partial E^{\mathrm{v}}/\partial\tilde{s}_{\mathrm{h}} = \partial\chi^{\mathrm{v}}/\partial\Sigma^{\mathrm{h}}$. These two equations can easily be inverted for Σ^{h} and $\tilde{s}_{\mathrm{h}}$ yielding the parameters β^{v}, ξ^{v} and, together with $\mu^{(\mathrm{eff})}$, the Lamé parameter $\lambda^{(\mathrm{eff})}$. The effective bulk modulus $K^{(\mathrm{eff})}$ can be extracted for the case $\tilde{s}_{\mathrm{h}} = 0$ as discussed already in section 4.3. Thus, $K^{(\mathrm{eff})}$ corresponds to the inverse of the first term on the right-hand side of Eq. (4.73).

The exact values for the effective bulk modulus $K^{(\mathrm{eff})}$ have been compared with corresponding Ritz estimates already in Figs. 4.3a–4.3b in Section 4.3. The comparison between the exact values of the non-classical microdilatational properties ξ^{v} and β^{v}, respectively, and their approximations by cubic polynomials is shown in Fig. 4.10. It shows that Ritz' method recovers the exact values $f = 0$. Note that in this case, ξ^{v} and β^{v} have the same amount but opposite sign. This means that the coupling between internal stress $\overline{\sigma}_{\mathrm{h}} = \Sigma^{\mathrm{h}} + \tilde{s}_{\mathrm{h}}$ and relative deformation $e^{\mathrm{v}} = E^{\mathrm{v}} - \chi^{\mathrm{v}}$ vanishes. For increasing values of porosity f, the discrepancy between exact and approximate values of ξ^{v} and β^{v}, respectively, increases but remains at an acceptable level. For $f \to 1$, both quantities diverge as found already for the Cosserat coupling modulus in the previous section (compare Fig. 4.6).

In addition, the modulus α^{v} for the dilatational double stress $\underline{\mathbf{M}}^{\mathrm{v}}$, Eq. $(4.65)_3$, can be determined exactly for isotropic porous material in the plane case $n = 2$. In this case, there are no volume forces related to $\underline{\mathbf{M}}^{\mathrm{v}}$ in Eq. (4.65) but $\underline{\mathbf{M}}^{\mathrm{v}}$ appears only in the static boundary condition (3.119). Consequently, the resulting stress state at the microscale can be characterized by an Airy stress function $F(\underline{\xi})$. For symmetry reasons, the Airy function has to have the structure

$$F = g(r)\underline{\mathbf{M}}^{\mathrm{v}} \cdot \underline{\xi}\,. \tag{4.75}$$

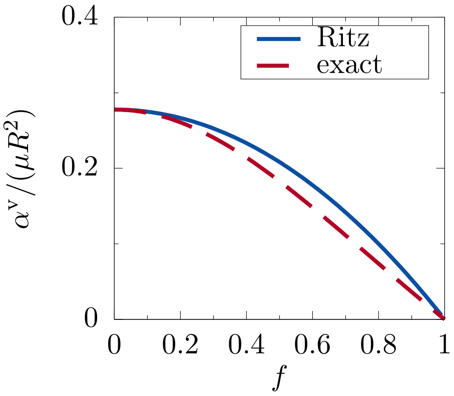

Fig. 4.11.: Microdilatational double stress modulus from exact solution and Ritz' solution ($\nu = 0.3$)

The compatibility condition

$$0 = \Delta\Delta F = \frac{1}{r^3}\left[\left(\frac{(g' r^3)'}{r^3}\right)' r^3\right]' \underline{\mathbf{M}}^{\mathrm{v}} \cdot \underline{\xi} \tag{4.76}$$

provides an ODE for the radial function $g(r)$ (for non-vanishing $\underline{\mathbf{M}}^{\mathrm{v}}$) whose solution

$$g(r) = C_1 r^2 + \frac{C_2}{r^2} + C_3 \ln(r) + C_4 \tag{4.77}$$

are respective terms of the well-known Mitchell series. The coefficient C_4 does not contribute to the stresses. Furthermore, it is required that C_3 vanishes since the term $C_3 \ln(r)$ is related to a displacement field which is not periodic in tangential direction, compare §31 in Timoshenko and Goodier [105]. The resulting stress field is

$$\underset{\sim}{\sigma} = \Delta F \underset{\sim}{\mathbf{I}} - \underline{\nabla\nabla} F = 2\left[\left(3C_1 + \frac{C_2}{r^4}\right)\underset{\sim}{\mathbf{I}} - \frac{4C_2}{r^6}\underline{\xi\xi}\right]\underline{\mathbf{M}}^{\mathrm{v}} \cdot \underline{\xi} - 2\left(C_1 - \frac{C_2}{r^4}\right)\left[\underline{\mathbf{M}}^{\mathrm{v}}\underline{\xi} + \underline{\xi}\underline{\mathbf{M}}^{\mathrm{v}}\right] \tag{4.78}$$

The static boundary condition (3.119) and a traction free void surface require

$$g'(R) = \frac{2}{R}, \qquad g'(R_{\mathrm{void}}) = 0, \tag{4.79}$$

respectively, and allow to compute the remaining coefficients C_1 and C_2. Again, the macroscopic constitutive law is computed via Castigliano's method as $\underline{\mathbf{K}}^{\mathrm{v}} = \partial\overline{W}/\partial\underline{\mathbf{M}}^{\mathrm{v}}$. In particular for the stress field (4.78), a strain energy

$$\overline{W} = \frac{1}{2}\frac{2}{\mu R^2}\frac{3 - 4\nu + f^2}{1 - f^2}\underline{\mathbf{M}}^{\mathrm{v}} \cdot \underline{\mathbf{M}}^{\mathrm{v}} \tag{4.80}$$

is obtained[5]. The double stress modulus α^{v} corresponds to the half the inverse of the cofactor of $\underline{\mathbf{M}}^{\mathrm{v}} \cdot \underline{\mathbf{M}}^{\mathrm{v}}$ in Eq. (4.80).

Figure 4.11 shows a comparison between the exact solution (4.80) and Ritz approximation (4.63). Ritz' method provides an upper bound of reasonable accuracy. For compact material $f = 0$, it even provides the exact solution as the displacement field is a quadratic polynomial.

[5]The commitment of the undergraduate student Vincent von Oertzen for the detailed elaboration of Eqs. (4.76)–(4.80) is gratefully acknowledged.

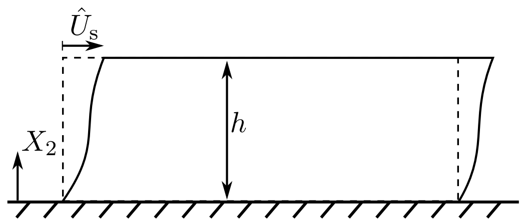

Fig. 4.12.: Simple shearing of an infinitely wide layer

Remarks

The comparison of the Ritz estimates with selected exact solutions and FEM solutions exhibited an accuracy of the estimates for the micropolar and microdilatational terms which should be sufficient for most engineering purposes. It might be expected that the Ritz estimates with a cubic polynomial provide a reasonable accuracy for the microdeviatoric terms as well.

4.6. Size effect in simple shear

In order to investigate the predictions of the presented model, the simple shearing of an infinitely wide layer of height h of the homogenized micromorphic material is considered as sketched in Fig. 4.12. This one-dimensional problem can be solved analytically which is why it is often used as a benchmark to study size effects predicted by generalized continuum theories, e. g. in [27, 30, 69, 106–111].

For an analytical solution to this problem for a micropolar continuum, the ansatz

$$\underline{\mathbf{U}} = U\left(X_2\right)\underline{\mathbf{b}}_1, \qquad \underline{\mathbf{\Phi}}^{\mathrm{r}} = \Phi^{\mathrm{r}}\left(X_2\right)\underline{\mathbf{b}}_3 \tag{4.81}$$

is adopted that the horizontal displacement as well as the rotation depend solely on the vertical coordinate X_2. Therein, $\underline{\mathbf{b}}_1$, $\underline{\mathbf{b}}_2$ and $\underline{\mathbf{b}}_3$ denote the unit base vectors. Based on these field, the deformations are obtained as

$$\underset{\sim}{\mathbf{E}}^{\mathrm{r}} = \left(U' + \Phi^{\mathrm{r}}\right)\underline{\mathbf{b}}_2\underline{\mathbf{b}}_1 - \Phi^{\mathrm{r}}\underline{\mathbf{b}}_1\underline{\mathbf{b}}_2, \qquad \underset{\sim}{\mathbf{K}}^{\mathrm{r}} = \left(\Phi^{\mathrm{r}}\right)'\underline{\mathbf{b}}_2\underline{\mathbf{b}}_3 \tag{4.82}$$

whereby the prime $()'$ refers to the derivative with respect to X_2. Firstly, these deformations are inserted into the constitutive relations (4.47) and (4.48) to get the stress fields $\underset{\sim}{\mathbf{\Sigma}}$ and $\underset{\approx}{\mathbf{M}}^{\mathrm{r}}$

$$\begin{aligned}\underset{\sim}{\mathbf{\Sigma}} &= \left[(\mu^{\mathrm{r}} + \kappa^{\mathrm{r}})U' + \kappa^{\mathrm{r}}\Phi^{\mathrm{r}}\right]\underline{\mathbf{b}}_2\underline{\mathbf{b}}_1 + \left[\mu^{\mathrm{r}}U' - \kappa^{\mathrm{r}}\Phi^{\mathrm{r}}\right]\underline{\mathbf{b}}_1\underline{\mathbf{b}}_2\,,\\ \underset{\approx}{\mathbf{M}}^{\mathrm{r}} &= \left(\Phi^{\mathrm{r}}\right)'\left(\beta^{\mathrm{r}}\underline{\mathbf{b}}_3\underline{\mathbf{b}}_2 + \gamma^{\mathrm{r}}\underline{\mathbf{b}}_2\underline{\mathbf{b}}_3\right)\end{aligned}$$

respectively. Subsequently, the equilibrium conditions (2.108) and (3.75) yield two second order ODEs for the two functions $U\left(X_2\right)$ and $\Phi^{\mathrm{r}}\left(X_2\right)$, respectively. These ODEs can be solved e. g. by elimination of $U\left(X_2\right)$. In addition to the classical displacement boundary conditions $U\left(0\right) = 0$ and $U\left(h\right) = \hat{U}_{\mathrm{s}}$, boundary conditions for the microrotations Φ^{r} have to be specified. Here, so-called micro-clamped boundary conditions $\Phi^{\mathrm{r}}\left(0\right) = \Phi^{\mathrm{r}}\left(h\right) = 0$ are prescribed in order to address size effects. Finally, the stress

$$\Sigma_{21} = \frac{\hat{U}_{\mathrm{s}}}{h}\frac{\mu^{(\mathrm{eff})}}{1 - (N^{\mathrm{r}})^2\frac{2l_{\mathrm{s}}^{\mathrm{r}}}{h}\tanh(\frac{h}{2l_{\mathrm{s}}^{\mathrm{r}}})} \text{ with } l_{\mathrm{s}}^{\mathrm{r}} = \frac{\sqrt{2}l_{\mathrm{b}}^{\mathrm{r}}}{N^{\mathrm{r}}} \tag{4.83}$$

is obtained which corresponds the resistance to the displacement $\hat{U}_{\mathrm{s}}$. Obviously, the tanh() term reflects the size effect with $l_{\mathrm{s}}^{\mathrm{r}}$ as characteristic intrinsic length. Equation (4.83) shows

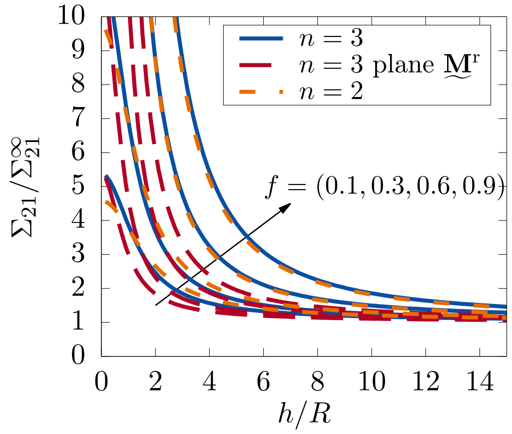

Fig. 4.13.: Size effect in simple shearing: comparison between spherical ("3D") and circular pores ("2D") ($\nu = 0.3$)

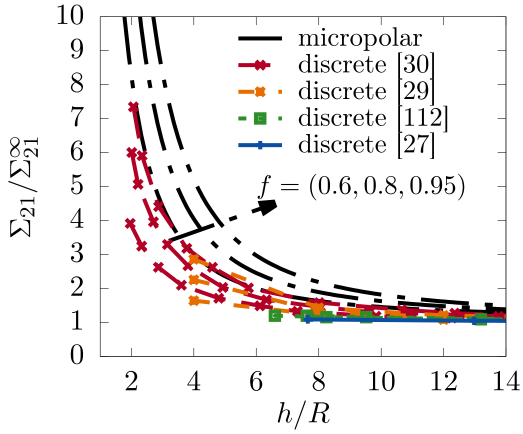

Fig. 4.14.: Size effect in simple shearing: comparison with simulations with discrete microstructure from literature

that the size effect would vanish if the coupling number N^{r} would be zero. However, the present theory predicts values of N^{r} close to one as discussed above.

Figure 4.13 visualizes the size effect. For this purpose, the reaction shear stress Σ_{21} is related to its limit $\Sigma_{21}^{\infty} = \mu^{(\mathrm{eff})}\hat{U}_{\mathrm{s}}/h$ for thick layers $h/l_{\mathrm{s}}^{\mathrm{r}} \to \infty$ and plotted versus height h normalized by the intrinsic length R. In this representation, classical Cauchy-Boltzmann theory predicts a horizontal line $\Sigma_{21}^{\infty} = \Sigma_{21}$. In contrast, the micropolar theory predicts a size effect as deviation from this horizontal line. The figure shows that the size effect increases considerably with increasing f, whereas the difference between spherical pores $n = 3$ and circular pores $n = 2$ is not significant (again under the premise that $\mu^{(\mathrm{eff})}$ in $l_{\mathrm{b}}^{\mathrm{r}}$ is computed via periodic boundary conditions).

In the context of the spatial case $n = 3$ it has to be mentioned that it was assumed in Eq. (4.81) that the microrotation $\underline{\boldsymbol{\Phi}}^{\mathrm{r}}$ remains normal to the plane which is why $\underset{\sim}{\mathbf{K}}^{\mathrm{r}}$ has only a $\underline{\mathbf{b}}_2\underline{\mathbf{b}}_3$ component but the double stress has an out-of-plane component M_{32}^{r}, Eq. $(4.83)_2$. Vice versa, it can be assume that M_{32}^{r} vanishes and $\underset{\sim}{\mathbf{K}}^{\mathrm{r}}$ has an out of plane component $\underline{\mathbf{b}}_3\underline{\mathbf{b}}_2$. Though, in the latter case the field $\underset{\sim}{\mathbf{K}}^{\mathrm{r}}$ will in general not be compatible. These considerations are analogous to the models of plane stress and plain strain in classical theory of elasticity. Anyway, Figure 4.13 shows that the predicted size effect decreases considerable in the case of plane double stress. Furthermore, it may be remarked that the derived micropolar model allows to compute a response for all values of the height h of the strip, though, based on the fact that the employed volume element has a size of $2R$, no reasonable prediction are expected for $h \lesssim 2R$.

Figure 4.14 compares the *predictions* of the present micropolar approach to respective FEM simulations of foam-like materials with discretely resolved microstructure (sometimes termed "direct numerical simulation", DNS). In particular, Jänicke [93] and Liebenstein et al. [27] investigated honeycomb microstructures whereas Tekoğlu et al. [29, 30] simulated random Voronoi microstructures. For the simulations with discrete microstructure an equivalent intrinsic length R was defined as radius of a circle of equal area of the (average of the) discrete cells. Only the simulations of Tekoğlu et al. activate a strong size effect. Jänicke and Liebenstein et al. performed simulations in the regime $h \gtrsim 7R$ where the deviation from the classical theory amounts to less than 30%. All mentioned research groups employed plane microstructures which is why their results are compared with the micropolar results for circular pores $n = 2$. Furthermore, Tekoğlu et al. as well as Liebenstein et al. used beam models which is why $\nu = 0$ is chosen for the micropolar model (the effect of ν is weak anyway). Figure 4.14 shows that the predictions of the present micropolar model comply quite well with the discrete simulations. The discrete simulations were performed for porosities $f \gtrsim 0.9$. For such values of f, the present model overestimates the size effect moderately. It is to be expected that the predicted size effect increases further if fully micromorphic model would be used, i. e. additional microdeviatoric effects were incorporated. In this context it has to be remarked that in [4] the author made an attempt to model the size effect of foams in simple shear (based on Forest's theory of micromorphic homogenisation, Section 2.2.4) *without* the adoptions to porous material proposed in Section 3.4. Actually, this means that a displacement field had to be assigned arbitrarily to the pore. For that reason the theory in [4] overestimated the size effect in shearing severely, by orders of magnitude, for larger porosities $f \gtrsim 0.5$. In this sense, the present theory constitutes a large progress.

The fact that the present theory still overestimates the size effect moderately might be related to the choice of the volume element, compare Fig. 4.2 at page 66. In this volume element, the stress-carrying material is located only far away from the center. Thus, it exhibits a large stiffness under bending type loadings. Equivalently, one could choose a realization of the same microstructure where the material is located mostly near the center. Such a realization would yield lower stiffnesses for the double stress terms, i. e. lower values of β^{r} and γ^{r}. Finally, one could compute the ensemble average over all possible realizations as done e. g. in [27, 113].

5. Damage Models

In this chapter, the proposed homogenisation procedure is applied to derive nonlinear micromorphic models for the mechanism of quasi-brittle failure and for ductile failure.

5.1. Quasi-brittle damage

Quasi-brittle materials like ceramics or concrete soften due to initiation and propagation of microcracks. Typically, these microcracks initiate at pores or inclusions. Mühlich et al. [114] formulated a corresponding damage model by assuming that the damaged spherical layer of thickness Δa can be considered as *effective growth of pores* as sketched in Fig. 5.1. Thus, an effective porosity can be introduced as

$$f^* = \left(\frac{R_{\text{void}} + \Delta a}{R}\right)^n . \tag{5.1}$$

after some amount of crack growth Δa as internal variable. This approach is adopted here to derive a micromorphic damage mechanics model based on the presented homogenisation. In particular, all constitutive parameters of elasticity were determined as functions of the porosity f which is why the macroscopic internal energy $\overline{\rho}\overline{\Phi} = \langle \rho\Phi \rangle_V$ is a function of the macroscopic measures of deformation as well as of f.

For the model of quasi-brittle damage, it is assumed that no residual strains appear during quasi-brittle failure so that the damaged zone stores no recoverable strain energy anymore. That is why f in the macroscopic internal energy density is replaced by f^*:

$$\overline{\Phi} = \overline{\Phi}(\underset{\sim}{\mathbf{E}}, \underset{\sim}{\mathbf{e}}, \underset{\sim}{\underline{\mathbf{K}}}^{\text{s}}, f^*) \tag{5.2}$$

It is recalled here that it was shown in Section 3.1 that the internal energy $\overline{\Phi}$ constitutes a potential for the stresses even for irreversible behavior, compare Eq. (3.8).

Furthermore, an evolution equation for f^* needs to be formulated. For this purpose the dissipation $\mathcal{D}$ associated with microcrack growth is investigated. Firstly, consider the spatial

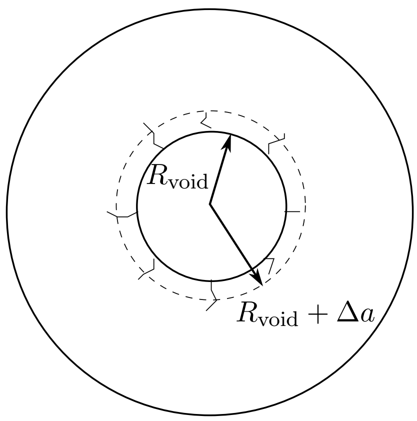

Fig. 5.1.: Increase of effective porosity due to propagation of microcracks (after Mühlich et al. [114])

case $n = 3$. It is assumed that a number m of microcracks propagate whose crack fronts remain circular. Thus, for a fracture toughness of the matrix material $\mathit{\Gamma}_0$ (which may depend on Δa), the dissipation during ongoing microcrack growth is

$$\mathcal{D} = m\mathit{\Gamma}_0 2\pi(R_{\text{void}} + \Delta a)\Delta\dot{a} \,. \tag{5.3}$$

By means of Eq. (5.1), this expression can be rearranged to

$$\mathcal{D} = \frac{2\pi m R^2 \mathit{\Gamma}_0}{3\sqrt[3]{f^*}}\dot{f}^* \,. \tag{5.4}$$

The corresponding macroscopic dissipation is obtained after Eq. (3.4) as $\overline{\rho}\overline{D} = \mathcal{D}/\Delta V(\underline{\mathbf{X}})$. Furthermore, for the particular internal (5.2) the reduced balance of energy (3.5) yields $\overline{D} = Z\dot{f}^*$ with $Z = -\overline{\rho}\overline{\Phi}_{,f^*}$ being the driving force (or energy release rate) of $\dot{f}^*$. Thus, for ongoing microcrack growth $\dot{f}^* \geq 0$, Eq. (5.4) has to be equal to $Z\dot{f}^*V$. Otherwise, there is no growth of microcracks, i. e. $\dot{f}^* = 0$. This behavior can be expressed in terms of a damage function

$$\mathit{\Phi} = Z - \gamma(f^*) \tag{5.5}$$

with material resistance

$$\gamma(f^*) = \frac{m\mathit{\Gamma}_0}{2R\sqrt[3]{f^*}} \tag{5.6}$$

and the corresponding loading-unloading conditions

$$\mathit{\Phi} \leq 0, \qquad \dot{f}^* \geq 0, \qquad \mathit{\Phi}\dot{f}^* = 0 \,. \tag{5.7}$$

For the plane model $n = 2$, analogous considerations lead to $\gamma(f^*) = m\mathit{\Gamma}_0/\left(\pi R\sqrt{f^*}\right)$.

If the internal energy potential (5.2) is obtained by Ritz' method, Section 4.2, then $(1 - f^*)$ appears in the constitutive equation (4.29) for the internal stress $\underset{\sim}{\bar{\sigma}}$ as prefactor of $\underset{\approx}{\mathbf{S}} : \underset{\sim}{\mathbf{E}}$. The latter term would be the stress in the compact matrix material in absence of non-classical deformations. Such a stiffness reduction is employed also in Kachanov effective stress type isotropic damage models, see e. g. [115]. In the context of such models the internal variable f^* is denominated just as damage variable. Some heuristic extensions of effective stress damage models to nonlocal or implicit gradient enriched theories have been proposed in the literature [e.g. 15, 116–119]. According to Forest [14], the gradient formulations fit in the framework of generalized micromorphic media. Therein, higher order terms that contain the intrinsic length are included typically linearly and reversibly (corresponding to $\underset{\sim}{\underline{\mathbf{M}}} = c\,\underset{\sim}{\underline{\mathbf{K}}}$ in present notation with a constant c). In contrast, within the present micromorphic homogenisation approach also the constitutive relations for the nonclassical stresses exhibit irreversible behavior and are obtained as a straight-forward result of the homogenisation procedure. However, in an FEM implementation, the heuristically gradient-enriched models require only a single additional nodal degree of freedom and not the complete tensor of microdeformation $\underset{\sim}{\chi}$ as with the micromorphic model. Anyway, the regularisation capabilities of such a micromorphic model of quasi-brittle damage was demonstrated by an FEM implementation by the graduate student Rostyslav Skrypnyk [120, 121].

5.2. Microdilatational extension of Gurson's model of ductile damage

The ductile mechanism consists of the nucleation, growth and coalescence of microscopic voids during plastic deformations. The constitutive model of Gurson [122, 123] and its numerous modifications are established to simulate the ductile damage and failure of components. For recent reviews, the reader is referred to [95, 124–126].

Heuristic nonlocal [82–84] and gradient extensions of Gurson's model [85, 86] were proposed to overcome its spurious mesh dependency. In contrast, Gologanu et al. [44] extended Gurson's homogenisation approach to the strain-gradient theory. Thus, the additional gradient terms, and consequently the distance of voids as intrinsic length, enter the yield function and do have indeed a highly non-linear contribution. Numerical results [127, 128] show that this model overcomes the spurious mesh dependency in principle. The problem with the model of [44] (GLPD model) is its cumbersome FE implementation. A strain gradient theory imposes stronger restrictions to the continuity which cannot be fulfill by standard polynomial shape functions. Even if this problem is circumvented by hybrid or penalty formulations, the computational effort raises dramatically since the complete strain tensor becomes a nodal variable[1].

To sum up the current state of ductile damage models which can handle localization, it can be said that one has to chose between computationally efficient but purely heuristic implicit-gradient enriched Gurson models [85, 86] or the micromechanically sound but computationally expensive strain-gradient GLPD model [44]. Comparing these approaches shows that both types are subclasses of generalized micromorphic continua in the sense of Forest [14]. The implicit-gradient enriched models postulate an additional PDE of balance type on the porosity, which drives the softening in Gurson's model, or the directly related dilatational strain, which is why they can be classified as microdilatational continua.

In order to combine the computational efficiency of implicit-gradient enriched models with the micromechanically sound basis of the GLPD model, Gurson's model shall be extended to the theory of unconstrained microdilatational media by homogenisation. As in Gurson's original model and in GLPD model, a spherical void of radius R_{void} in a spherical volume element $n = 3$ of radius R is considered, see Fig. 4.2 and Section 4.3. For this geometry, the kinematic micro-macro relations (3.116) and (3.117) simplify to

$$\dot{\chi}^{\text{v}} = \frac{5(1-f)}{(1-f^{5/3})R^2} \left\langle \underline{\mathbf{v}} \cdot \underline{\xi} \right\rangle_{\text{M}} \tag{5.8}$$

$$\underline{\mathbf{L}}^{K\text{v}} = \frac{1}{R^2} \left[3 \left\langle 5 \underline{\mathbf{b}}_r \, \underline{\mathbf{v}} \cdot \underline{\mathbf{b}}_r - 2 \underline{\mathbf{v}} \right\rangle_{S(R)} + \underline{\mathbf{V}} \right] \tag{5.9}$$

whereby it was used that for the boundary of the spherical cell, the normal $\underline{\mathbf{n}}$ coincides with the radial unit vector $\underline{\mathbf{b}}_r = \underline{\xi}/R = \underline{\mathbf{n}}$.

5.2.1. Limit load analysis for rigid ideal-plastic material

For an ideal rigid-plastic material the microscopic specific dissipation is $\pi := \rho D = \underset{\sim}{\sigma} : \underset{\sim}{\mathbf{d}}$. According to Eq. (3.4), the macroscopic dissipation corresponds to the average of its microscopic counterpart. For an ideal rigid-plastic material, the dissipation is equal to the internal work. Thus, for a microdilatational theory, Eq. (3.115), a limit-load analysis yields

$$\underset{\sim}{\mathbf{\Sigma}} : \underset{\sim}{\mathbf{D}} + \tilde{s}_{\text{h}} \dot{\chi}^{\text{v}} + \underline{\mathbf{M}}^{\text{v}} \cdot \underline{\mathbf{L}}^{K\text{v}} \leq \Pi \left(\underset{\sim}{\mathbf{D}}, \dot{\chi}^{\text{v}}, \underset{\sim}{\mathbf{D}} \right) := \inf \left\langle \pi \right\rangle_V \tag{5.10}$$

whereby the infinimum is taken over all kinematically admissible fields [95]. For a Mises material, the microscopic plastic dissipation is

$$\pi = \sigma_0 d_{\text{eq}} \qquad \text{with } d_{\text{eq}} = \sqrt{\frac{2}{3} \underset{\sim}{\mathbf{d}} : \underset{\sim}{\mathbf{d}}} \qquad \underset{\sim}{\mathbf{d}} = \operatorname{sym}\left(\nabla_{\underline{\mathbf{x}}} \underline{\mathbf{v}} \right) \tag{5.11}$$

Kinematically admissible are all incompressible fields

$$\underset{\sim}{\mathbf{d}} : \underset{\sim}{\mathbf{I}} = \nabla_{\underline{\mathbf{x}}} \cdot \underline{\mathbf{v}} = 0 \tag{5.12}$$

[1] The recently proposed technique by Bergheau et al. [128] requires fundamental modifications of the compilation of the global system of equations and is thus hardly suitable for standard multi-purpose FE codes.

which fulfill the kinematic micro-macro relations (3.36), (3.116) and (3.117) of the microdilatational theory for prescribed values of the macroscopic deformation rates $\underset{\sim}{\mathbf{D}}$, $\dot{\chi}^{\mathrm{v}}$ and $\underline{\mathbf{L}}^{K\mathrm{v}}$. A subclass of this definition would incorporate only those fields which are additionally compatible with the kinematic boundary condition (3.120).

The yield surface is given in parametric form as

$$\underset{\sim}{\mathbf{\Sigma}} = \frac{\partial \Pi}{\partial \underset{\sim}{\mathbf{D}}}, \qquad \tilde{s}_{\mathrm{h}} = \frac{\partial \Pi}{\partial \dot{\chi}^{\mathrm{v}}}, \qquad \underline{\mathbf{M}}^{\mathrm{v}} = \frac{\partial \Pi}{\partial \underline{\mathbf{L}}^{K\mathrm{v}}} \,. \tag{5.13}$$

A common result (see e. g. [95]) for this type of models is that the yield surface $\Phi(\underset{\sim}{\mathbf{\Sigma}}, \tilde{s}_{\mathrm{h}}, \underline{\mathbf{M}}^{\mathrm{v}}) = 0$ is convex and the direction of plastic flow

$$\underset{\sim}{\mathbf{D}} = \lambda \frac{\partial \Phi}{\partial \underset{\sim}{\mathbf{\Sigma}}}, \qquad \dot{\chi}^{\mathrm{v}} = \lambda \frac{\partial \Phi}{\partial \tilde{s}_{\mathrm{h}}}, \qquad \underline{\mathbf{L}}^{K\mathrm{v}} = \lambda \frac{\partial \Phi}{\partial \underline{\mathbf{M}}^{\mathrm{v}}} \tag{5.14}$$

is orthogonal to it, whereby λ is the plastic multiplier.

Trial fields

With symmetric tensor $\underset{\sim}{\mathbf{D}}$, vector $\underline{\mathbf{L}}^{K\mathrm{v}}$ and scalar $\dot{\chi}^{\mathrm{v}}$, we have ten independent kinematic components which would require at least ten incompressible trial fields to cover them independently, i. e. at least four more than in Gurson's classical model. For the hollow sphere under consideration (Fig. 4.2), the kinematic micro-macro relations for micro and macro dilatation, $\dot{\chi}^{\mathrm{v}}$ and $\underset{\sim}{\mathbf{D}} : \underset{\sim}{\mathbf{I}}$, respectively, exhibit a spherical symmetry which is why this symmetry applies also to the respective trial fields. However, there is only a single incompressible field with spherical symmetry, namely that of Rice and Tracey [129] which is already among Gurson's classical trial fields. Thus, for an incompressible matrix there will be a kinematic constraint between the plastic parts of $\dot{\chi}^{\mathrm{v}}$ and $\underset{\sim}{\mathbf{D}} : \underset{\sim}{\mathbf{I}}$. This means, in addition to Gurson's trial velocity field, only an additional term $\underline{\mathbf{v}}_K(\underline{\xi})$ is required to account for the gradient $\underline{\mathbf{L}}^{K\mathrm{v}}$ of the microdilatation:

$$\underline{\mathbf{v}}(\underline{\xi}) = A \frac{R^3}{r^3} \underline{\xi} + \underset{\sim}{\beta} \cdot \underline{\xi} + \underline{\mathbf{v}}_K(\underline{\xi}) \tag{5.15}$$

The incompressible matrix (5.12) requires $\underset{\sim}{\beta} : \underset{\sim}{\mathbf{I}} = 0$ for the field to be kinematically admissible. Due to the point symmetry/antisymmetry of the respective operators, the parameters A and $\underset{\sim}{\beta}$ can be determined independently of a specific choice of $\underline{\mathbf{v}}_K(\underline{\xi})$ if $\underline{\mathbf{v}}_K(-\underline{\xi}) = \underline{\mathbf{v}}_K(\underline{\xi})$. In particular, inserting (5.15) into the kinematic relations (3.36) and (5.8) yields

$$\dot{\chi}^{\mathrm{v}} = \frac{15}{2} \frac{1 - f^{2/3}}{1 - f^{5/3}} A \qquad \underset{\sim}{\mathbf{D}} = \underset{\sim}{\beta} + A \underset{\sim}{\mathbf{I}} \tag{5.16}$$

As in the classical Gurson model, the coefficients can thus be linked to the deviatoric $\underset{\sim}{\beta} = \underset{\sim}{\mathbf{D}}^{\mathrm{d}}$ and dilatational part $A = 1/3 \underset{\sim}{\mathbf{D}} : \underset{\sim}{\mathbf{I}}$ of the macroscopic rate of deformation $\underset{\sim}{\mathbf{D}}$. Furthermore, (5.16) yields the kinematic constraint

$$\dot{\chi}^{\mathrm{v}} = \frac{5}{2} \frac{1 - f^{2/3}}{1 - f^{5/3}} D^{\mathrm{v}} \tag{5.17}$$

between the rates of microdilatation and macrodilatation, $\dot{\chi}^{\mathrm{v}}$ and $D^{\mathrm{v}} = \underset{\sim}{\mathbf{D}} : \underset{\sim}{\mathbf{I}}$, respectively. The test field $\underline{\mathbf{v}}_K(\underline{\xi})$ of the gradient $\underline{\mathbf{L}}^{K\mathrm{v}}$ of microdilatation needs to be linear and axially symmetric with respect to the vector $\underline{\mathbf{L}}^{K\mathrm{v}}$ and incompressible. Thus, the approach of Gologanu et al. [44] is adopted and $\underline{\mathbf{v}}_K(\underline{\xi})$ is derived in terms of a Helmholtz decomposition. The condition of incompressibility (5.12) requires that $\underline{\mathbf{v}}_K(\underline{\xi})$ derives from a vector potential $\underline{\mathbf{\Psi}}(\underline{\xi})$:

$$\underline{\mathbf{v}}_K(\underline{\xi}) = \nabla \times \underline{\mathbf{\Psi}}(\underline{\xi}) \,. \tag{5.18}$$

The axial symmetry with respect to $\underline{\mathbf{L}}^{K\mathrm{v}}$ is ensured by choosing

$$\underline{\boldsymbol{\Psi}}(\underline{\xi}) = \underline{\mathbf{L}}^{K\mathrm{v}} \times \underline{\xi}\, g_K(r) \tag{5.19}$$

According to Eq. (5.18), this corresponds to a velocity field

$$\underline{\mathbf{v}}_K(\underline{\xi}) = \left(2g_K + r g_K'\right) \underline{\mathbf{L}}^{K\mathrm{v}} - \frac{g_K'}{r} \underline{\xi}\,\underline{\xi} \cdot \underline{\mathbf{L}}^{K\mathrm{v}} . \tag{5.20}$$

Obviously, a constant value of the yet undetermined function $g_K(r)$ corresponds to a pure rigid body translation in direction of $\underline{\mathbf{L}}^{K\mathrm{v}}$. The macroscopic velocity (3.34) associated with the field (5.20) amounts to

$$\underline{\mathbf{V}}(\underline{\mathbf{X}}) = \frac{2}{1-f} \underline{\mathbf{L}}^{K\mathrm{v}} \left[g_K(R) - f g_K(R_{\mathrm{void}})\right] . \tag{5.21}$$

Inserting the field (5.20) into to the kinematic micro-macro relation (3.117) leads to[2]

$$\underline{\mathbf{L}}^{K\mathrm{v}} = \frac{2}{R^2} \underline{\mathbf{L}}^{K\mathrm{v}} \left[\frac{f}{1-f}\left(g_K(R) - g_K(R_{\mathrm{void}})\right) - 2R g_K'(R)\right] \tag{5.22}$$

Thus, it is required that the square bracket in Eq. (5.22) equals $R^2/2$.

The macroscopic plastic dissipation (5.10) is bounded from above as in most Gurson-type models by

$$\Pi = \sigma_0 \frac{3}{R^3} \int\limits_{R_{\mathrm{void}}}^{R} r^2 \sqrt{\frac{2}{3} \left\langle \underset{\sim}{\mathbf{d}} : \underset{\sim}{\mathbf{d}} \right\rangle_{S(r)}} \mathrm{d}r \, . \tag{5.23}$$

For the velocity field (5.20), the local rate of deformation amounts to

$$\underset{\sim}{\mathbf{d}}_K = \frac{1}{2r}\left(r^2 g_K'\right)' \left[\underline{\mathbf{L}}^{K\mathrm{v}} \underline{\mathbf{b}}_r + \underline{\mathbf{b}}_r \underline{\mathbf{L}}^{K\mathrm{v}}\right] - r^2 \left(\frac{g_K'}{r}\right)' \underline{\mathbf{b}}_r \underline{\mathbf{b}}_r\, \underline{\mathbf{L}}^{K\mathrm{v}} \cdot \underline{\mathbf{b}}_r - g_K' \underset{\sim}{\mathbf{I}}\, \underline{\mathbf{L}}^{K\mathrm{v}} \cdot \underline{\mathbf{b}}_r \tag{5.24}$$

with a magnitude of

$$\underset{\sim}{\mathbf{d}}_K : \underset{\sim}{\mathbf{d}}_K = \frac{1}{2r}\left[\left(r^2 g_K'\right)'\right] \underline{\mathbf{L}}^{K\mathrm{v}} \cdot \underline{\mathbf{L}}^{K\mathrm{v}} + \left(\underline{\mathbf{L}}^{K\mathrm{v}} \cdot \underline{\mathbf{b}}_r\right)^2 \left[4(g_K')^2 - 2r g_K'' g_K' - \frac{r^2}{2}\left(g_K''\right)^2\right] . \tag{5.25}$$

Thus, the upper bound (5.23) becomes

$$\Pi = \sigma_0 \frac{3}{R^3} \int\limits_{R_{\mathrm{void}}}^{R} r^2 \sqrt{4A^2 \frac{R^6}{r^6} + \frac{2}{3} \underset{\sim}{\beta} : \underset{\sim}{\beta} + \frac{2}{9} \underline{\mathbf{L}}^{K\mathrm{v}} \cdot \underline{\mathbf{L}}^{K\mathrm{v}} \left[10(g_K')^2 + (r g_K'')^2 + 4r g_K' g_K''\right]} \, \mathrm{d}r \, . \tag{5.26}$$

The first derivative $g_K'(r)$ dominates the term with the gradient $\underline{\mathbf{L}}^{K\mathrm{v}}$ of microdilatation until the porosity is not too small. Consequently, a linear ansatz is chosen for $g_K(r)$. Thus, (5.22) leads to

$$g_K(r) = \frac{R^2}{2} \frac{1-f}{2 - 3f + f^{4/3}} \left(\frac{1 - f^{4/3}}{1-f} - \frac{r}{R}\right) \tag{5.27}$$

whereby the offset value was chosen arbitrarily such that the macroscopic velocity $\underline{\mathbf{V}}$ according to (5.21) vanishes. The trial field $\underline{\mathbf{v}}_K(\underline{\xi})$ with linear ansatz (5.27) is visualized in Fig. 5.2.

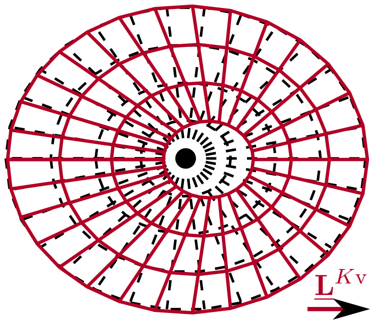

Fig. 5.2.: Trial field $\underline{\mathbf{v}}_K(\underline{\xi})$ (vector $\underline{\mathbf{K}}^{\mathrm{v}}$ in horizontal direction)

The linear ansatz (5.27) has the advantage that the contribution of the $\underline{\mathbf{L}}^{K\mathrm{v}}$ term to the radicand in (5.26) is a constant so that the integral in (5.26) can be solved exactly preserving the rigorous upper-bound character of the solution. The integral yields

$$\Pi(\eta, B_{\mathrm{eq}}) = \eta\sigma_0 B_{\mathrm{eq}} \int_{\eta}^{\eta/f} \frac{\sqrt{1+w^2}}{w^2}\mathrm{d}w \qquad = \eta\sigma_0 B_{\mathrm{eq}} \left[\operatorname{arcsinh}(w) - \frac{\sqrt{1+w^2}}{w}\right]_{w=\eta}^{\eta/f} \tag{5.28}$$

whereby the abbreviations

$$w = \eta\,(R/r)^3 \quad \text{with} \quad \eta = 2A/B_{\mathrm{eq}} \tag{5.29}$$

$$B_{\mathrm{eq}}^2 = \frac{2}{3}\underset{\sim}{\mathbf{D}}^{\mathrm{d}} : \underset{\sim}{\mathbf{D}}^{\mathrm{d}} + \frac{R^2}{q_M}\underline{\mathbf{L}}^{K\mathrm{v}} \cdot \underline{\mathbf{L}}^{K\mathrm{v}} \quad \text{with} \quad q_M = \frac{9}{5}\left(\frac{2-3f+f^{4/3}}{1-f}\right)^2 \tag{5.30}$$

were introduced.

Yield function

For obtaining the yield locus, the macroscopic plastic dissipation Π in (5.13) needs to be amended by the kinematic constraint (5.17) which is enforced by a Lagrange multiplier λ^{v}:

$$\widetilde{\Pi} = \Pi + \lambda^{\mathrm{v}}\left[\dot{\chi}^{\mathrm{v}} - \frac{5}{2}\frac{1-f^{2/3}}{1-f^{5/3}}D^{\mathrm{v}}\right] \tag{5.31}$$

The parametric form of the macroscopic yield surface is obtained according to (5.13) from $\widetilde{\Pi}$. Firstly, inserting (5.31) to the corresponding relation for the microdilatation

$$\tilde{s}_{\mathrm{h}} = \frac{\partial\widetilde{\Pi}}{\partial\dot{\chi}^{\mathrm{v}}} = \lambda^{\mathrm{v}} \tag{5.32}$$

shows that the Lagrange multiplier corresponds to the microdilatational stress difference. With this finding, the remaining relations from (5.13) read

$$\underset{\sim}{\mathbf{\Sigma}} = \frac{\partial\widetilde{\Pi}}{\partial\underset{\sim}{\mathbf{D}}} = \underbrace{\left(\frac{\partial\Pi}{\partial B_{\mathrm{eq}}} - \frac{\eta}{B_{\mathrm{eq}}}\frac{\partial\Pi}{\partial\eta}\right)}_{=:Q}\frac{\frac{2}{3}\underset{\sim}{\mathbf{D}}^{\mathrm{d}}}{B_{\mathrm{eq}}} + \underbrace{\frac{2}{3}\frac{1}{B_{\mathrm{eq}}}\frac{\partial\Pi}{\partial\eta}}_{=:P}\underset{\sim}{\mathbf{I}} - \tilde{s}_{\mathrm{h}}\frac{5}{2}\frac{1-f^{2/3}}{1-f^{5/3}}\underset{\sim}{\mathbf{I}}, \tag{5.33}$$

$$\underline{\mathbf{M}}^{\mathrm{v}} = \frac{\partial\widetilde{\Pi}}{\partial\underline{\mathbf{L}}^{K\mathrm{v}}} = \left(\frac{\partial\Pi}{\partial B_{\mathrm{eq}}} + \frac{\partial\Pi}{\partial\eta}\frac{\partial\eta}{\partial B_{\mathrm{eq}}}\right)\frac{\partial B_{\mathrm{eq}}}{\partial\underline{\mathbf{L}}^{K\mathrm{v}}} = Q\frac{R^2}{q_M}\frac{\underline{\mathbf{L}}^{K\mathrm{v}}}{B_{\mathrm{eq}}}\,. \tag{5.34}$$

[2] As in [130] solely the kinematic micro-macro relation (3.117) is imposed and not the stricter kinematic boundary condition (3.120). The latter would imply the additional requirement $g'_K(R) = -R/3$.

In order to get an implicit expression, the quantities Q and P (which correspond to Mises stress Σ^{eq} and hydrostatic stress $\Sigma^{\mathrm{h}} = \frac{1}{3}\underset{\sim}{\boldsymbol{\Sigma}} : \underset{\sim}{\mathbf{I}}$ in Gurson's original model, respectively) need to be expressed in terms of the stresses $\underset{\sim}{\boldsymbol{\Sigma}}$, $\tilde{s}_{\mathrm{h}}$ and $\underline{\mathbf{M}}^{\mathrm{v}}$. For the hydrostatic part of (5.33) this is

$$P = \Sigma^{\mathrm{h}} + \frac{5}{2}\frac{1 - f^{2/3}}{1 - f^{5/3}}\tilde{s}_{\mathrm{h}} \tag{5.35}$$

whereas a close look on the deviatoric part of (5.33) and (5.34) in the light of (5.30) reveals that

$$Q^2 = (\Sigma^{\mathrm{eq}})^2 + \frac{q_M}{R^2}\,(M^{\mathrm{v}})^2 \tag{5.36}$$

where $(M^{\mathrm{v}})^2 = \underline{\mathbf{M}}^{\mathrm{v}} \cdot \underline{\mathbf{M}}^{\mathrm{v}}$. The parameters η and B_{eq} of the implicit description $Q(\eta, B_{\mathrm{eq}})$ and $P(\eta, B_{\mathrm{eq}})$ can now be eliminated as in Gurson's original model. Finally, the yield function becomes

$$\Phi = \frac{Q^2}{\sigma_0^2} + 2f\cosh\left(\frac{3}{2}\frac{P}{\sigma_0}\right) - (1 + f^2) \tag{5.37}$$

It can easily verified that an associated flow rule (5.14) and Φ with P in form of Eq. (5.35) satisfy the kinematic constraint (5.17).

5.2.2. Phenomenological extensions

In a strict sense, Gurson's yield function applies to rigid ideal-plastic material only. It is thus of little practical use until several phenomenological extensions are introduced. Of course, this is the case for its microdilatational extension as well which is why several established extensions shall be discussed and adapted to the present microdilatational model. Most significant are presumably the extensions to work-hardening, to the evolution of the porosity f and to elastic-plastic behavior.

The extensions to work hardening and the evolution of f were proposed by Gurson [122] himself. Isotropic hardening is incorporated by replacing the matrix yield stress σ_0 in yield function (5.37) by some effective value $\tilde{\Sigma} = \tilde{\Sigma}(E_{\mathrm{eq}})$ which is postulated to be a function of the equivalent accumulated plastic strain E_{eq} [122]. The evolution of E_{eq} is driven by the macroscopic plastic dissipation. For the microdilatational model with flow rule (5.14) and a yield function Φ in the form of (5.37), the evolution equation becomes

$$\dot{E}_{\mathrm{eq}} = \frac{1}{(1-f)\tilde{\Sigma}}\left(\underset{\sim}{\boldsymbol{\Sigma}} : \underset{\sim}{\mathbf{D}} + \tilde{s}_{\mathrm{h}}\dot{\chi}^{\mathrm{v}} + \underline{\mathbf{M}}^{\mathrm{v}} \cdot \underline{\mathbf{L}}^{K\mathrm{v}}\right) = \lambda\frac{\frac{\partial\Phi}{\partial Q}Q + \frac{\partial\Phi}{\partial P}P}{(1-f)\tilde{\Sigma}}\,. \tag{5.38}$$

The evolution equation of f

$$\dot{f} = (1-f)D^{\mathrm{v}} + \dot{f}_{\mathrm{N}} \tag{5.39}$$

can be adapted one-by-one from Gurson. The growth term $\dot{f}_{\mathrm{G}} = (1-f)D^{\mathrm{v}}$ was derived from the condition of plastic incompressibility of the matrix. Note that the rate of microdilatation $\dot{\chi}^{\mathrm{v}}_{\mathrm{pl}}$ is linked to the macroscopic plastic dilatation D^{v} by the kinematic constraint (5.17), which could be inserted equivalently to (5.39). The incompressibility of the matrix implies also the evolution equation

$$\dot{R} = \frac{R}{3}D^{\mathrm{v}} \tag{5.40}$$

of the intrinsic length R which is to be interpreted as mean half-distance of voids.

Without any problem, the models of continuous strain-controlled void nucleation by Chu and Needleman [131] or by Zhang [132] can be used for $\dot{f}_{\mathrm{N}}$. In this case the intrinsic length

R is to be interpreted as the mean of the half distance of potential nuclei. The adaption of stress-controlled nucleation would require to specify the roles of the additional stress measures $\tilde{s}_{\mathrm{h}}$ and $\underline{\mathbf{M}}^{\mathrm{v}}$ on this process, in the simplest case they are neglected.

Needleman and Rice [133] proposed a hypoelastic-plastic extension of Gurson's model. Also hyperelastic-plastic models were proposed in literature. In the context of ductile failure of engineering alloys, typically the elastic deformations are much smaller than the plastic ones and a hypoelastic-plastic formulation provides sufficient accuracy which is why it shall be employed in the following. In such a formulation, all macroscopic rates of deformation are split into elastic and plastic parts

$$\underset{\sim}{\mathbf{D}} = \underset{\sim}{\mathbf{D}}_{\mathrm{el}} + \underset{\sim}{\mathbf{D}}_{\mathrm{pl}}, \qquad \dot{\chi}^{\mathrm{v}} = \dot{\chi}^{\mathrm{v}}_{\mathrm{el}} + \dot{\chi}^{\mathrm{v}}_{\mathrm{pl}}, \qquad \underline{\mathbf{L}}^{K\mathrm{v}} = \underline{\mathbf{L}}^{K\mathrm{v}}_{\mathrm{el}} + \underline{\mathbf{L}}^{K\mathrm{v}}_{\mathrm{pl}}\,. \tag{5.41}$$

Consistently, the total rates of deformation in flow rule (5.14) as well as in evolution equations (5.38)–(5.40) are replaced by the plastic parts $\underset{\sim}{\mathbf{D}}_{\mathrm{pl}}$, $\dot{\chi}^{\mathrm{v}}_{\mathrm{pl}}$, $\underline{\mathbf{L}}^{K\mathrm{v}}_{\mathrm{pl}}$, respectively. The elastic constitutive equations (4.65) are converted to rate form

$$\begin{aligned}
\overset{\triangledown}{\underset{\sim}{\mathbf{\Sigma}}} &= 2\mu^{(\mathrm{eff})}\underset{\sim}{\mathbf{D}}_{\mathrm{el}} + \lambda^{(\mathrm{eff})}\underset{\sim}{\mathbf{D}}_{\mathrm{el}} : \underset{\approx}{\mathbf{II}} + \beta^{\mathrm{v}}\dot{\chi}^{\mathrm{v}}_{\mathrm{el}}\underset{\sim}{\mathbf{I}}, \\
\overset{\triangledown}{\tilde{s}}_{\mathrm{h}} &= \xi^{\mathrm{v}}\dot{\chi}^{\mathrm{v}}_{\mathrm{el}} + \beta^{\mathrm{v}}\underset{\sim}{\mathbf{D}}_{\mathrm{el}} : \underset{\sim}{\mathbf{I}}, \\
\overset{\triangledown}{\underline{\mathbf{M}}}{}^{\mathrm{v}} &= \alpha^{\mathrm{v}}\underline{\mathbf{L}}^{K\mathrm{v}}_{\mathrm{el}}\,.
\end{aligned} \tag{5.42}$$

For objectivity reasons, the Jaumann rate $(\overset{\triangledown}{\circ})$ (or another objective rate) of the stresses needs to be used on the left-hand side. For the scalar $\tilde{s}_{\mathrm{h}}$, the Jaumann rate coincides with the material rate. The elastic parameters $\mu^{(\mathrm{eff})}$, $\lambda^{(\mathrm{eff})}$, β^{v}, ξ^{v} and α^{v} can be taken from Section 4.5. For infinitesimal elastic deformations, the hypoelastic formulation (5.42) reduces to the hyperelastic relation (4.65) only if the elastic parameters are constants. This means that they must not be computed for the current porosity f but for the initial value f_0. This simplification is usual for the application of Gurson-type models.

Although the derivation of the yield function (5.37) ensures that it is a rigorous bound for rigid ideal-plastic matrix material, for practical applications it is more relevant to improve the predictive quality of the model for elastic-plastic material with hardening. For this purpose, Tvergaard [134] introduced the parameters q_1 and q_2 and replaced in the Gurson yield function f by $q_1 f$ and P by $q_2 P$, respectively. Extensive parameter studies with cell models were performed in literature, see e. g. [135]. Although such cell models did not incorporate the non-classical macroscopic deformation measures of the present theory, the classical theory and thus the performed cell model simulations are a special case of the microdilatational framework and should therefore be captured adequately as well. For this reason it seems reasonable to introduce q_1 and q_2 and their particular values also in the microdilatational yield function (5.37). In this context, it suggests itself to calibrate the coefficient q_M of the double stress term to respective cell model simulations with non-vanishing gradient $\underline{\mathbf{K}}^{\mathrm{v}}$ of microdilatation. Gologanu et al. [44] performed cell model simulations for their extension of Gurson's model to the strain gradient theory. If only the gradient of the mean rate of deformation $D^{\mathrm{m}} = 1/3\underset{\sim}{\mathbf{D}} : \underset{\sim}{\mathbf{I}}$ is considered, their kinematic boundary conditions (2.65) becomes

$$\underline{\mathbf{v}} = \underline{\mathbf{V}}_0(\underline{\mathbf{X}}) + \underline{\xi} \cdot \left(\underline{\nabla}_{\underline{\mathbf{X}}}\underline{\mathbf{V}}\right) + \frac{1}{2}\left(2\underset{\approx}{\mathbf{I}}\underline{\nabla}_{\underline{\mathbf{X}}}D^{\mathrm{m}} - \underline{\nabla}_{\underline{\mathbf{X}}}D^{\mathrm{m}}\underset{\sim}{\mathbf{I}}\right) : \underline{\xi}\underline{\xi} \qquad \text{on } \partial\Delta V\,. \tag{5.43}$$

For the considered spherical volume element, $\underline{\nabla}_{\underline{\mathbf{X}}}D^{\mathrm{v}}\underset{\sim}{\mathbf{I}} : \underline{\xi}\underline{\xi} = \underline{\nabla}_{\underline{\mathbf{X}}}D^{\mathrm{v}}R^2$ represents a rigid translation. Thus, up to this irrelevant translation, the dilatational part of the kinematic boundary conditions (5.43) of Gologanu et al. is identical to the corresponding term in Eq. (3.120) of the present contribution (and a factor 1/3 which is related to the choice of dilatational part and

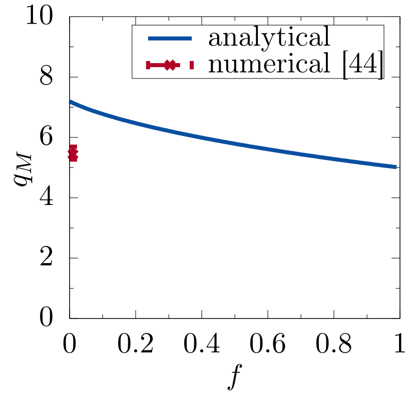

Fig. 5.3.: Comparison of values for coefficient q_M

mean value of the rate of deformation, respectively). Thus, the results of the cell model computations by Gologanu et al. [44] can be compared directly to q_M. In particular, a comparison of the respective generalized Hill-Mandel lemmas in context of the mentioned quadratic part of the microscopic boundary condition shows that the calibration parameter Δ_{CC} of [44] can be related to the present model as $q_M = 9/\Delta_{CC}$. Gologanu et al. [44] determined this parameter numerically as $1.58 \lesssim \Delta_{CC} \lesssim 1.71$ for small porosities $f \leq 0.01$. In Fig. 5.3, these results are plotted together with the analytical estimates Eq. $(5.30)_2$ of the present study. It shows that the values are comparable. In this context it has to be remarked that Gologanu et al. imposed only boundary condition (5.43). In contrast, it is recalled that in the present study the weaker kinematic micro-macro relation (3.117) is imposed for the gradient of microdilatation. However, in contrast to Gologanu et al., the present study involves the kinematic micro-macro relation (3.34) as additional integral constraint.

The last class of heuristic extensions encompasses the modeling of void coalescence. The most prominent representative thereof is surely the model of Tvergaard and Needleman [136] wherein the f in the yield function is replaced by the effective porosity f^*. The effective porosity

$$f^* = \begin{cases} f & f \leq f_\mathrm{c} \\ f_\mathrm{c} + (f - f_\mathrm{c})\,\kappa & f_\mathrm{c} < f \leq f_\mathrm{f} \\ f_\mathrm{u} & f_\mathrm{f} < f \end{cases} \quad \text{with } \kappa = \frac{f_\mathrm{u} - f_\mathrm{c}}{f_\mathrm{f} - f_\mathrm{c}},\ f_\mathrm{u} = \frac{1}{q_1}\,. \tag{5.44}$$

coincides with the actual one f until f reaches f_c and coalescence is assumed to initiate. In the coalescence stage, f^* increases faster then f does according to (5.39). The Tvergaard-Needleman coalescence model can be adapted to the present extension of Gurson's model since it ensures that the macroscopic softening is driven only by dilatational deformations which are regularized by the microdilatational theory[3]

$$\Phi = \frac{Q^2}{\tilde{\Sigma}^2} + 2q_1 f^* \cosh\left(\frac{3q_2}{2}\frac{P}{\tilde{\Sigma}}\right) - 1 - (q_1 f^*)^2\,. \tag{5.45}$$

Recently, coalescence models of Thomason-type attracted research activities (for a recent review the reader is referred to Benzerga et al. [125]). If they are implemented as a second yield condition they are not suitable for the present microdilatational framework since softening can then be driven also by deviatoric deformations. For the same reason the shear modification of Nahshon and Hutchinson [137] is inadequate. However, well-suited for the microdilatational model is the approach of Zhang [132] to implement the approach of Tvergaard and Needleman

[3]Strictly speaking, the nucleation term in (5.39) may violate this condition. However, this is of no practical relevance if the nucleation parameters are chosen such that the nucleation occurs mainly before reaching f_c.

[136] with f_c determined from Thomason's criterion (or one of its recent enhancements) in in dependence of the current stress state.

The role of the difference stress

The yield function (5.45) has such a structure, that the yield surface Φ shrinks to a point at the origin in the P-Q space for completely failed material $q_1 f^* \to 1$. The equivalent stress Q is defined in Eq. (5.36) by a quadratic relation in terms of $\underset{\sim}{\boldsymbol{\Sigma}}^\mathrm{d}$ and $\underline{\mathbf{M}}^\mathrm{v}$. Consequently, not only does complete failure imply $\underset{\sim}{\boldsymbol{\Sigma}}^\mathrm{d} = 0$ but also the double stress vanishes $\underline{\mathbf{M}}^\mathrm{v} = 0$. The latter consequence is favorable insofar as it satisfies directly a free-surface condition $\underline{\mathbf{M}}^\mathrm{v} \cdot \underline{\mathbf{n}} = 0$. That means that the double stress does not require separate treatment when new surfaces are formed in regions of completely failed material (in contrast to heuristically gradient-enriched models with linear relations for the double stress, cmp. [31]).

However, the situation with the hydrostatic-type stresses Σ^h and $\tilde{s}_\mathrm{h}$ is different since Eq. (5.35) constitutes a linear relation between P, Σ^h and $\tilde{s}_\mathrm{h}$. This means that $P = 0$ does not necessarily imply $\Sigma^\mathrm{h} = \tilde{s}_\mathrm{h} = 0$. In this context it is instructive to reconsider purely hydrostatic cases of purely loading by Σ^h and $\tilde{s}_\mathrm{h}$. In particular, the Navier solution (4.70) from Section 4.5 allows to identify the $\Sigma^\mathrm{h} - \tilde{s}_\mathrm{h}$ surface of initial microscopic plastification. Without going into the detail it shall be mentioned, that even for compact material $f = 0$, a plastification by a hydrostatic difference stress of amount $|\tilde{s}_\mathrm{h}| = (1-2\nu)/(1-\nu)\sigma_0$ is possible. However, the yield condition (5.45) does not incorporate a plastification in this case. The reason is that loadings in the $\Sigma^\mathrm{h} - \tilde{s}_\mathrm{h}$ space normal to lines $P = \mathrm{const}$ do not posses a limit load, although they may in general initiate local plastic deformations. Rather, such loadings lead to an unbounded hardening behavior, even for ideal plastic behavior at the microscale. This means that the macroscopic load has to be increased and increased to propagate the local front of the zone of plastification at the microscale. Though, Fig. 4.10 shows that certain non-classic elastic moduli diverge as well as the (effective) porosity tends to unity.

Thus, the derived yield condition (5.37) is an correct upper bound for the limit loads. However, it is an open issue for future work how those elastic-plastic modes of deformation, which do not posses a limit load, can be incorporated in a heuristic way. Favorably, such a heuristic extension would be constructed in such a way that complete failure implies $\Sigma^\mathrm{h} = \tilde{s}_\mathrm{h} = 0$. Due to the diverging non-classical elastic moduli, this problem might be relevant also for the model of quasi-brittle damage from Section 5.1.

5.2.3. FEM implementation

Weak form

A finite element implementation requires weak forms of the governing balance equations. For the microdilatational theory, these are balances of linear and angular momentum, Eqs. (2.108) and (3.99), and the weighted balance (3.112), respectively. Multiplication by test functions $\delta\underline{\mathbf{U}}(\underline{\mathbf{X}})$ and $\delta\chi^\mathrm{v}$, respectively, and application of the divergence theorem yields

$$0 = \int\limits_{\Omega_{\underline{\mathbf{X}}}} \underset{\sim}{\boldsymbol{\Sigma}} : \delta\underset{\sim}{\mathbf{E}}\,\mathrm{d}V - \int\limits_{\Omega_{\underline{\mathbf{X}}}} \overline{\rho}\underline{\overline{\mathbf{f}}} \cdot \delta\underline{\mathbf{U}}\,\mathrm{d}V - \int\limits_{\partial\Omega_{\underline{\mathbf{X}}}} \underline{\mathbf{n}} \cdot \underset{\sim}{\boldsymbol{\Sigma}} \cdot \delta\underline{\mathbf{U}}\,\mathrm{d}S + \int\limits_{\Omega_{\underline{\mathbf{X}}}} \overline{\rho}\underline{\dot{\mathbf{V}}} \cdot \delta\underline{\mathbf{U}}\,\mathrm{d}V \tag{5.46}$$

$$0 = \int\limits_{\Omega_{\underline{\mathbf{X}}}} \underline{\mathbf{M}}^\mathrm{v} \cdot \delta\underline{\mathbf{K}}^\mathrm{v} + \tilde{s}_\mathrm{h}\delta\chi^\mathrm{v}\,\mathrm{d}V - \int\limits_{\Omega_{\underline{\mathbf{X}}}} \overline{\rho}\overline{f}_\mathrm{h}\delta\chi^\mathrm{v}\,\mathrm{d}V - \int\limits_{\partial\Omega_{\underline{\mathbf{X}}}} \underline{\mathbf{n}} \cdot \underline{\mathbf{M}}^\mathrm{v}\delta\chi^\mathrm{v}\,\mathrm{d}S + \int\limits_{\Omega_{\underline{\mathbf{X}}}} \overline{\rho}I_r\ddot{\chi}^\mathrm{v}\delta\chi^\mathrm{v}\,\mathrm{d}V\,. \tag{5.47}$$

Both equations might be combined to the principle of virtual power

$$
\begin{aligned}
0 = \delta W = \int\limits_{\Omega_{\underline{\mathbf{X}}}} \underset{\sim}{\boldsymbol{\Sigma}} : \delta \underset{\sim}{\mathbf{E}} + \underline{\mathbf{M}}^{\mathrm{v}} \cdot \delta \underline{\mathbf{K}}^{\mathrm{v}} + \tilde{s}_{\mathrm{h}} \delta \chi^{\mathrm{v}} \; \mathrm{d}V + \int\limits_{\Omega_{\underline{\mathbf{X}}}} \overline{\rho} \dot{\underline{\mathbf{V}}} \cdot \delta \underline{\mathbf{U}} + \overline{\rho} I_r \ddot{\chi}^{\mathrm{v}} \delta \chi^{\mathrm{v}} \; \mathrm{d}V \\
- \int\limits_{\Omega_{\underline{\mathbf{X}}}} \overline{\rho} \underline{\overline{\mathbf{f}}} \cdot \delta \underline{\mathbf{U}} + \overline{\rho} \overline{f}_{\mathrm{h}} \delta \chi^{\mathrm{v}} \; \mathrm{d}V - \int\limits_{\partial \Omega_{\underline{\mathbf{X}}}} \underline{\mathbf{n}} \cdot \underset{\sim}{\boldsymbol{\Sigma}} \cdot \delta \underline{\mathbf{U}} + \underline{\mathbf{n}} \cdot \underline{\mathbf{M}}^{\mathrm{v}} \delta \chi^{\mathrm{v}} \; \mathrm{d}S \, .
\end{aligned}
\tag{5.48}
$$

However, Eqs. (5.46) and (5.47) are sufficient.

For the spatial discretization, a Galerkin approach is adopted. In a Voigt notation, the relevant components of the essential field quantities thus read

$$
[\underline{\mathbf{U}}] = [\mathbf{N}]_U \cdot \widehat{[\underline{\mathbf{U}}]} \qquad \chi^{\mathrm{v}} = [\mathbf{N}]_\chi \cdot \widehat{[\chi^{\mathrm{v}}]} \tag{5.49}
$$

$$
\delta\, [\underline{\mathbf{U}}] = [\mathbf{N}]_U \cdot \delta \widehat{[\underline{\mathbf{U}}]} \qquad \delta\chi^{\mathrm{v}} = [\mathbf{N}]_\chi \cdot \delta \widehat{[\chi^{\mathrm{v}}]} \, . \tag{5.50}
$$

with $[\mathbf{N}]_U$ and $[\mathbf{N}]_\chi$ being the shape functions for displacements and microdilatation, respectively. Furthermore, the notation $\widehat{[(\circ)]}$ refers to nodal values of a quantity and $[(\circ)]$ denotes the column vector of the independent components of a quantity in Voigt notation with respect to a given cartesian frame. The B-matrices

$$
\delta\, [\underset{\sim}{\mathbf{E}}] = [\mathbf{B}]_U \cdot \delta \widehat{[\underline{\mathbf{U}}]} \qquad \delta\, [\underline{\mathbf{K}}^{\mathrm{v}}] = [\mathbf{B}]_\chi \cdot \delta \widehat{[\chi^{\mathrm{v}}]} \tag{5.51}
$$

provide the mapping between nodal quantities and the required gradients of the essential field variables.

Inserting Eqs. (5.49)–(5.51) to Eqs. (5.46)–(5.47) yields the discretized weak form

$$
0 = \widehat{[R]}_U = \underbrace{\left(\int\limits_{\Omega} \overline{\rho} [\mathbf{N}]_U{}^{\mathrm{T}} \cdot [\mathbf{N}]_U \; \mathrm{d}V \right)}_{:=[\mathbf{M}]_U} \cdot \widehat{[\ddot{\underline{\mathbf{U}}}]} + \underbrace{\int\limits_{\Omega} [\mathbf{B}]_U{}^{\mathrm{T}} \cdot [\underset{\sim}{\boldsymbol{\Sigma}}] \; \mathrm{d}V}_{:=\widehat{[F]}_U^{\mathrm{int}}} - \widehat{[F]}_U^{\mathrm{ext}} \tag{5.52}
$$

$$
0 = \widehat{[R]}_\chi = \underbrace{\left(\int\limits_{\Omega} \overline{\rho} I_r [\mathbf{N}]_\chi{}^{\mathrm{T}} \cdot [\mathbf{N}]_\chi \; \mathrm{d}V \right)}_{:=[\mathbf{M}]_\chi} \cdot \widehat{[\ddot{\chi}^{\mathrm{v}}]} + \underbrace{\int\limits_{\Omega} [\mathbf{B}]_\chi{}^{\mathrm{T}} \cdot [\underline{\mathbf{M}}^{\mathrm{v}}] + [\mathbf{N}]_\chi{}^{\mathrm{T}} \tilde{s}_{\mathrm{h}} \; \mathrm{d}V}_{:=\widehat{[F]}_\chi^{\mathrm{int}}} - \widehat{[F]}_\chi^{\mathrm{ext}} \tag{5.53}
$$

which allows to define internal nodal "forces" $\widehat{[F]}_U^{\mathrm{int}}$ and $\widehat{[F]}_\chi^{\mathrm{int}}$, respectively, as well as mass matrices $[\mathbf{M}]_U$ and $[\mathbf{M}]_\chi$. The external nodal forces $\widehat{[F]}_U^{\mathrm{ext}}$ and $\widehat{[F]}_\chi^{\mathrm{ext}}$ comprise contributions from non-trivial natural boundary conditions or volume loads and will not be needed for the following investigations. The discretized weak form (5.52)–(5.53) is complemented by essential boundary conditions.

The discretized weak form is solved by the Newton-Raphson method. Consequently, the internal nodal forces need to be linearized as

$$\Delta\widehat{[F]}_U^{\text{int}} \approx \left[\int_\Omega [\mathbf{B}]_U{}^{\mathrm{T}} \cdot \frac{\mathrm{d}\,[\underset{\sim}{\boldsymbol{\Sigma}}]}{\mathrm{d}\Delta[\underset{\sim}{\mathbf{E}}]} \cdot [\mathbf{B}]_U \;\mathrm{d}V\right] \cdot \Delta\widehat{[\underline{\mathbf{U}}]}$$
$$+ \left[\int_\Omega [\mathbf{B}]_U{}^{\mathrm{T}} \cdot \left(\frac{\mathrm{d}\,[\underset{\sim}{\boldsymbol{\Sigma}}]}{\mathrm{d}\Delta\chi^{\mathrm{v}}} \cdot [\mathbf{N}]_\chi + \frac{\mathrm{d}\,[\underset{\sim}{\boldsymbol{\Sigma}}]}{\mathrm{d}\Delta[\underline{\mathbf{K}}^{\mathrm{v}}]} \cdot [\mathbf{B}]_\chi\right) \mathrm{d}V\right] \cdot \Delta\widehat{[\chi^{\mathrm{v}}]} \tag{5.54}$$

$$\Delta\widehat{[F]}_\chi^{\text{int}} \approx \left[\int_\Omega \left([\mathbf{B}]_\chi{}^{\mathrm{T}} \cdot \frac{\mathrm{d}\,[\underline{\mathbf{M}}^{\mathrm{v}}]}{\mathrm{d}\Delta[\underset{\sim}{\mathbf{E}}]} + [\mathbf{N}]_\chi{}^{\mathrm{T}} \frac{\mathrm{d}\tilde{s}_{\mathrm{h}}}{\mathrm{d}\Delta[\underset{\sim}{\mathbf{E}}]}\right) \cdot [\mathbf{B}]_U \;\mathrm{d}V\right] \cdot \Delta\widehat{[\underline{\mathbf{U}}]}$$
$$+ \left[\int_\Omega [\mathbf{B}]_\chi{}^{\mathrm{T}} \cdot \left(\frac{\mathrm{d}\,[\underline{\mathbf{M}}^{\mathrm{v}}]}{\mathrm{d}\Delta[\underline{\mathbf{K}}^{\mathrm{v}}]} \cdot [\mathbf{B}]_\chi + \frac{\mathrm{d}\,[\underline{\mathbf{M}}^{\mathrm{v}}]}{\mathrm{d}\Delta\chi^{\mathrm{v}}} \cdot [\mathbf{N}]_\chi\right)\right.$$
$$\left. + [\mathbf{N}]_\chi{}^{\mathrm{T}} \cdot \left(\frac{\mathrm{d}\tilde{s}_{\mathrm{h}}}{\mathrm{d}\Delta[\underline{\mathbf{K}}^{\mathrm{v}}]} \cdot [\mathbf{B}]_\chi + \frac{\mathrm{d}\tilde{s}_{\mathrm{h}}}{\mathrm{d}\Delta\chi^{\mathrm{v}}} \cdot [\mathbf{N}]_\chi\right) \mathrm{d}V\right] \cdot \Delta\widehat{[\chi^{\mathrm{v}}]}\,. \tag{5.55}$$

The terms in the square brackets constitute the material contributions $[\mathbf{K}]^{\mathrm{t}}_{UU}$, $[\mathbf{K}]^{\mathrm{t}}_{U\chi}$, $[\mathbf{K}]^{\mathrm{t}}_{\chi U}$, $[\mathbf{K}]^{\mathrm{t}}_{\chi\chi}$, respectively, of the tangent stiffness matrix, compare e. g. [58]. Note that certain contributions like $\mathrm{d}\,[\underset{\sim}{\boldsymbol{\Sigma}}]\,/\mathrm{d}\Delta[\underline{\mathbf{K}}^{\mathrm{v}}]$ or $\mathrm{d}\,[\underline{\mathbf{M}}^{\mathrm{v}}]\,/\mathrm{d}\Delta[\underset{\sim}{\mathbf{E}}]$ vanish for isotropic, linear elastic material (4.65). However, when the yield condition (5.45) is active, these coupling terms are necessary. Geometric contributions to the tangent stiffness matrix are neglected.

Element formulation

The (macroscopic) domain $\Omega_{\underline{\mathbf{X}}}$ is divided into elements. The polynomial shape functions of each element are specified with respect to a simply shaped unit domain. Identical shape functions are employed to discretize the displacements $\underline{\mathbf{U}}$ and the location $\underline{\mathbf{X}}$. Note that the aforementioned balances of momenta apply to the current configuration ($\underset{\sim}{\boldsymbol{\Sigma}}$, $\tilde{s}_{\mathrm{h}}$, $\underline{\mathbf{M}}^{\mathrm{v}}$ are Eulerian measures of stress). Consequently, the integrals in Eqs. (5.46)–(5.55) are to be computed over the current configuration. However, the nodes are material points and moved with the deformation corresponding to an updated Lagrangian formulation. As usual, the integrals over the unit domain of each element are computed by Gauss quadrature.

The element was implemented into the commercial FEM code Abaqus/Standard as a user-defined element via the UEL interface [138] using the in-house library [139] based on the microstrain element of the graduate student Rostyslav Skrypnyk [120, 121].

Integration of constitutive equations

The hypoelastic-plastic relations (5.41)–(5.42) are discretized by the Euler-backward method

$$\begin{aligned}
\underset{\sim}{\boldsymbol{\Sigma}} &= \underset{\sim}{\boldsymbol{\Sigma}}_0 - 2\mu^{(\mathrm{eff})}\Delta t\underset{\sim}{\mathbf{D}}_{\mathrm{pl}} - \lambda^{(\mathrm{eff})}\underset{\sim}{\mathbf{I}}\Delta E^{\mathrm{v}}_{\mathrm{pl}} - \beta^{\mathrm{v}}\underset{\sim}{\mathbf{I}}\Delta t\dot{\chi}^{\mathrm{v}}_{\mathrm{pl}},\\
\tilde{s}_{\mathrm{h}} &= \tilde{s}_{\mathrm{h}0} - \xi^{\mathrm{v}}\Delta t\dot{\chi}^{\mathrm{v}}_{\mathrm{pl}} - \beta^{\mathrm{v}}\Delta t\Delta E^{\mathrm{v}}_{\mathrm{pl}},\\
\underline{\mathbf{M}}^{\mathrm{v}} &= \underline{\mathbf{M}}^{\mathrm{v}}_0 - \alpha^{\mathrm{v}}\underline{\mathbf{L}}^{K\mathrm{v}}_{\mathrm{pl}}\Delta t\,.
\end{aligned} \tag{5.56}$$

with elastic predictors

$$\begin{aligned}
\underset{\sim}{\boldsymbol{\Sigma}}_0 &= \underset{\sim}{\boldsymbol{\Sigma}}^m + 2\mu^{(\mathrm{eff})}\Delta\underset{\sim}{\mathbf{E}} + \lambda^{(\mathrm{eff})}\underset{\sim}{\mathbf{I}}\Delta\underset{\sim}{\mathbf{E}} : \underset{\sim}{\mathbf{I}} + \beta^{\mathrm{v}}\underset{\sim}{\mathbf{I}}\Delta\chi^{\mathrm{v}}\\
\tilde{s}_{\mathrm{h}0} &= \tilde{s}^m_{\mathrm{h}} + \xi^{\mathrm{v}}\Delta\chi^{\mathrm{v}} + \beta^{\mathrm{v}}\Delta\underset{\sim}{\mathbf{E}} : \underset{\sim}{\mathbf{I}},\\
\underline{\mathbf{M}}^{\mathrm{v}}_0 &= \underline{\mathbf{M}}^{\mathrm{v}m} + \alpha^{\mathrm{v}}\Delta\underline{\mathbf{K}}^{\mathrm{v}}\,.
\end{aligned} \tag{5.57}$$

Therein, the superscript m refers to the last time increment and updated quantities in the current time increment $m+1$ are written without additional superscript. In addition, the abbreviation $\Delta E^{\mathrm{v}}_{\mathrm{pl}} = \Delta t \underset{\sim}{\mathbf{D}}_{\mathrm{pl}} : \underset{\sim}{\mathbf{I}}$ was introduced for the increment of the plastic dilatation. According to the stress integration algorithm of Hughes and Winget [140], the stresses $\underset{\sim}{\boldsymbol{\Sigma}}^m$ and $\underline{\mathbf{M}}^{\mathrm{v}m}$ have to be incrementally rotated before inserting them to Eq. (5.57) in order to account for the rotation terms of the Jaumann rate in Eq. (5.42). Furthermore, the evolution equation (5.38) for the equivalent plastic strain is discretized as

$$E_{\mathrm{eq}} = E^m_{\mathrm{eq}} + \Delta\tilde{\lambda} \frac{\frac{\partial \Phi}{\partial Q} Q + \frac{\partial \Phi}{\partial P} P}{1-f} \tag{5.58}$$

wherein the abbreviation $\Delta\tilde{\lambda} := \lambda \Delta t / \tilde{\Sigma}$ was introduced for the normalized plastic multiplier (of strain-type). Note that Eq. (5.58) is implicit since the yield function Φ depends on E_{eq} via the matrix hardening law $\tilde{\Sigma}(E_{\mathrm{eq}})$. Nucleation of porosity is not considered in the following which is why the evolution equation (5.39) for the porosity can be integrated exactly as

$$f = 1 - (1 - f^m) \exp\left(-\Delta E^{\mathrm{v}}_{\mathrm{pl}}\right) . \tag{5.59}$$

Compared to an approximate integration by Euler's method, Eq. (5.59) has the advantage that f cannot exceed unity if the time increment is too large. The evolution (5.40) of the intrinsic length R is considered to be of minor importance for the envisaged example and not implemented yet (though this would be no problem in principle).

Together with yield condition (5.45) and flow rule (5.14), Eqs. (5.56)–(5.59) form a system of nonlinear (in-)equalities for the plastic multiplier λ and the plastic parts of all measures of deformation. In view of the isotropic yield condition and the associated flow rule, this system can be reduced dramatically by adopting the method of Aravas [141] to the present microdilatational model. In particular, it turns out that the updated values of the stress deviator $\underset{\sim}{\boldsymbol{\Sigma}}^{\mathrm{d}}$ and of the double stress $\underline{\mathbf{M}}^{\mathrm{v}}$ are co-linear to the respective predictor values

$$\underset{\sim}{\boldsymbol{\Sigma}}^{\mathrm{d}} = \frac{1}{1 + 3\mu^{(\mathrm{eff})} \lambda \Delta t \frac{\Phi_{,Q}}{Q}} \underset{\sim}{\boldsymbol{\Sigma}}^{\mathrm{d}}_0, \qquad \underline{\mathbf{M}}^{\mathrm{v}} = \frac{1}{1 + \frac{\alpha^{\mathrm{v}} q_M}{R^2} \lambda \Delta t \frac{\Phi_{,Q}}{Q}} \underline{\mathbf{M}}^{\mathrm{v}}_0 . \tag{5.60}$$

These relations may be interpreted as a radial return mapping within the space of $\underset{\sim}{\boldsymbol{\Sigma}}^{\mathrm{d}}$ and $\underline{\mathbf{M}}^{\mathrm{v}}$. The first term in the particular yield function (5.45) can thus be expressed as

$$\frac{Q^2}{\tilde{\Sigma}^2} = \frac{\left(\Sigma^{\mathrm{eq}}_0\right)^2}{\left(\tilde{\Sigma} + 6\mu^{(\mathrm{eff})} \Delta\tilde{\lambda}\right)^2} + \frac{q_M}{R^2} \frac{\underline{\mathbf{M}}^{\mathrm{v}}_0 \cdot \underline{\mathbf{M}}^{\mathrm{v}}_0}{\left(\tilde{\Sigma} + \frac{2\alpha^{\mathrm{v}} q_M}{R^2} \Delta\tilde{\lambda}\right)^2} . \tag{5.61}$$

At this point it shall be remarked that the second term on the right-hand side of Eq. (5.61), being related to the double stress $\underline{\mathbf{M}}^{\mathrm{v}}$, is not present in the procedure of Aravas. That is why he could compute the square root and obtained a linear relation between the increment of the equivalent stress Q and $\Delta\tilde{\lambda}$. In contrast, Eq. (5.61) is highly nonlinear.

Furthermore, an update equation for the equivalent hydrostatic stress P is required which appears in the cosh-term in the yield condition (5.45). Firstly, the flow rule is inserted into Eqs. $(5.56)_1$ and $(5.56)_2$:

$$\Sigma^{\mathrm{h}} = \Sigma^{\mathrm{h}}_0 - \left(K^{(\mathrm{eff})}_{\varepsilon} + q_P \beta^{\mathrm{v}}\right) \Delta E^{\mathrm{v}}_{\mathrm{pl}}, \qquad \tilde{s}_{\mathrm{h}} = \tilde{s}_{\mathrm{h}0} - \left(q_P \xi^{\mathrm{v}} + \beta^{\mathrm{v}}\right) \Delta E^{\mathrm{v}}_{\mathrm{pl}} \tag{5.62}$$

wherein $\Sigma^{\mathrm{h}}_0 = \underset{\sim}{\boldsymbol{\Sigma}}_0 : \underset{\sim}{\mathbf{I}}/3$ refers to the elastic predictor of the hydrostatic stress. Furthermore, the abbreviations

$$q_P = \frac{5}{2} \frac{1 - f^{2/3}}{1 - f^{5/3}}, \qquad K^{(\mathrm{eff})}_{\varepsilon} = \frac{2}{3}\mu^{(\mathrm{eff})} + \lambda^{(\mathrm{eff})}$$

were introduced. Subsequently, definition (5.35) yields

$$P = P_0 - \left[\frac{2}{3}\mu^{(\mathrm{eff})} + \lambda^{(\mathrm{eff})} + q_P\left(2\beta^{\mathrm{v}} + q_P\xi^{\mathrm{v}}\right)\right]\Delta E^{\mathrm{v}}_{\mathrm{pl}} \tag{5.63}$$

wherein $P_0 = \Sigma^{\mathrm{h}}_0 + q_P\tilde{s}_{\mathrm{h}0}$ refers to the elastic predictor of P. Note that K_P depends on f and thus on $\Delta E^{\mathrm{v}}_{\mathrm{pl}}$ via Eq. (5.59). In addition, the discretized flow rule (5.14) for $\Delta E^{\mathrm{v}}_{\mathrm{pl}}$ reads

$$\Delta E^{\mathrm{v}}_{\mathrm{pl}} = \Delta\tilde{\lambda}\frac{\partial\Phi}{\partial P/\tilde{\Sigma}}\,. \tag{5.64}$$

Finally, the solution algorithm is as follows: Firstly, the elastic predictors are computed according to Eq. (5.57) and it is checked, whether they lie in the elastic regime $\Phi(\underset{\sim}{\mathbf{\Sigma}}_0, \tilde{s}_{\mathrm{h}0}, \underline{\mathbf{M}}^{\mathrm{v}}_0) \leq 0$ (corresponding to an initial guess $\Delta\tilde{\lambda} = 0$). If so, the predictor values correspond to the actual stresses. Otherwise, a return mapping step is necessary: the *three nonlinear equations* (5.45), (5.58), (5.64)

$$[\mathbf{R}] = \begin{bmatrix} \Phi \\ \Delta E^{\mathrm{v}}_{\mathrm{pl}} - \Delta\tilde{\lambda}\frac{\partial\Phi}{\partial P/\tilde{\Sigma}} \\ E_{\mathrm{eq}} - E^{m}_{\mathrm{eq}} - \frac{\Delta\tilde{\lambda}\frac{\partial\Phi}{\partial Q}Q + \Delta E^{\mathrm{v}}_{\mathrm{pl}}P}{1-f} \end{bmatrix} = 0 \tag{5.65}$$

need to be solved for the three primary unknowns $[\mathbf{r}] = [\Delta\tilde{\lambda}, \Delta E^{\mathrm{v}}_{\mathrm{pl}}, E_{\mathrm{eq}}]^{\mathrm{T}}$. The secondary unknowns f, Q, P and $\tilde{\Sigma}$ can be computed explicitly from Eqs. (5.59), (5.63), (5.61) and a matrix hardening law $\tilde{\Sigma}(E_{\mathrm{eq}})$.

In the present implementation, Eq. (5.65) is solved by a monolithic Newton-Raphson scheme[4] requiring to compute the Jacobian matrix $[\mathbf{J}] = \mathrm{d}\,[\mathbf{R}]\,/\mathrm{d}\,[\mathbf{r}]$. Having solved Eq. (5.65), the stresses STRESS $:= [\underset{\sim}{\mathbf{\Sigma}}, \tilde{s}_{\mathrm{h}}, \underline{\mathbf{M}}^{\mathrm{v}}]$ can be updated by Eqs. (5.60) and (5.62).

Algorithmically consistent tangent stiffness

The algorithmically consistent tangent stiffnesses are thus obtained by derivatives of Eqs. (5.60) and (5.62) with respect to the strain increments ΔSTRAIN $:= [\Delta\underset{\sim}{\mathbf{E}}, \Delta\chi^{\mathrm{v}}, \Delta\underline{\mathbf{K}}^{\mathrm{v}}]^{\mathrm{T}}$ under condition (5.65). Formally, this yields

$$\frac{\mathrm{dSTRESS}}{\mathrm{d}\Delta\mathrm{STRAIN}} = \frac{\partial\mathrm{STRESS}}{\partial\Delta\mathrm{STRAIN}} + \frac{\partial\mathrm{STRESS}}{\partial\,[\mathbf{r}]} \cdot \frac{\partial\,[\mathbf{r}]}{\partial\Delta\mathrm{STRAIN}}\,. \tag{5.66}$$

The explicit derivative of Eqs. (5.60) and (5.62) amounts to

$$\frac{\partial\mathrm{STRESS}}{\partial\Delta\mathrm{STRAIN}} = \begin{bmatrix} K^{(\mathrm{eff})}_{\varepsilon}\underset{\approx}{\mathbf{II}} + \frac{2\mu^{(\mathrm{eff})}}{1+6\Delta\tilde{\lambda}\frac{\mu^{(\mathrm{eff})}}{\tilde{\Sigma}}}\left(\underset{\approx}{\mathbf{I}}_{\mathrm{S}} - \frac{1}{3}\underset{\approx}{\mathbf{II}}\right) & \beta^{\mathrm{v}} & 0 \\ \beta^{\mathrm{v}}\underset{\sim}{\mathbf{I}} & \xi^{\mathrm{v}} & 0 \\ 0 & 0 & \frac{1}{1+\frac{\alpha^{\mathrm{v}}q_M}{R^2}\lambda\Delta t\frac{\Phi_{,Q}}{Q}}\underset{\sim}{\mathbf{I}} \end{bmatrix} \tag{5.67}$$

The required derivative $\partial\,[\mathbf{r}]/\partial\Delta$STRAIN can be gained by implicit differentiation of Eq. (5.65). The derivation of this term can be simplified greatly by taken advantage of the fact that the primary variables $[\mathbf{r}]$ do depend on the strain increments ΔSTRAIN only through the three invariants $[\mathbf{S_0}] := [\Sigma^{\mathrm{eq}}_0, P_0, M^{\mathrm{v}}_0]^{\mathrm{T}}$ of the elastic predictors via the two equivalent stresses

[4] Aravas [141] and many subsequent studies in literature employed a staggered scheme where the evolution equation for E_{eq} is solved separately.

$[\mathbf{Q}] := [P, Q]^{\mathrm{T}}$. Thus, only an implicit differentiation of Eq. (5.65) with respect to $[\mathbf{Q}]$ is necessary yielding

$$\frac{\partial[\mathbf{r}]}{\partial[\mathbf{Q}]} = -[\mathbf{J}]^{-1} \cdot \frac{\partial[\mathbf{R}]}{\partial[\mathbf{Q}]} \tag{5.68}$$

The Jacobian matrix $[\mathbf{J}]$ is available from the Newton-Raphson method anyway. The derivative $\frac{\partial[\mathbf{R}]}{\partial[\mathbf{Q}]}$ can be computed from Eq. (5.65). Finally, the algorithmic tangent stiffness reads

$$\frac{\mathrm{dSTRESS}}{\mathrm{d\Delta STRAIN}} = \frac{\partial\mathrm{STRESS}}{\partial\Delta\mathrm{STRAIN}} - \frac{\partial\mathrm{STRESS}}{\partial\,[\mathbf{r}]} \cdot [\mathbf{J}]^{-1} \cdot \frac{\partial[\mathbf{R}]}{\partial[\mathbf{Q}]} \cdot \frac{\partial[\mathbf{Q}]}{\partial[\mathbf{S_0}]} \cdot \frac{\partial[\mathbf{S_0}]}{\partial\Delta\mathrm{STRAIN}} \tag{5.69}$$

The derivative $\partial\,[\mathbf{Q}]/\partial\,[\mathbf{S_0}]$ is computed from Eqs. (5.61) and (5.63). The particular expressions are listed in Appendix A.2.

5.2.4. Example

As a first example, a tensile test was simulated for an initial void volume fraction $f_0 = 0.01$ and coalescence parameters $f_{\mathrm{c}} = 0.15$ and $f_{\mathrm{f}} = 0.25$ as proposed by Tvergaard and Needleman [136]. Following the latter study, a power-hardening law is employed for the matrix yield stress $\tilde{\Sigma}$ which is given implicitly by

$$\frac{\tilde{\Sigma}}{\tilde{\Sigma}_0} = \left(\frac{\tilde{\Sigma}}{\tilde{\Sigma}_0} + \frac{E^{(\mathrm{m})}}{\tilde{\Sigma}_0} E_{\mathrm{eq}}\right)^m . \tag{5.70}$$

Therein, $E^{(\mathrm{m})}$ denotes Young's modulus of the matrix material. In the numerical implementation, this equation is solved for $\tilde{\Sigma}$ by means of a fixpoint iteration scheme. The hardening exponent of the matrix and its initial yield stress are chosen as $m = 0.1$ and $\tilde{\Sigma}_0 = 0.003\,E^{(\mathrm{m})}$, respectively. These values are representative for medium strength engineering alloys. Furthermore, values $q_M = 36/5$ (corresponding to Eq. (5.30) for small values of f) are used as well as the usual GTN parameters $q_1 = 1.5$ and $q_2 = 1$.

Quadrilateral axisymmetric elements with quadratic shape functions are chosen for the displacements and linear ones for the micro-dilatation χ^{v}, compare e. g. [58, 86]. Nine Gauss points are employed within an element. The specimen has a diameter $D_0 = 100R$ and a length of $L_0 = 3D_0$. Due to symmetry, only a half of the specimen needs to be incorporated in the FEM simulation. In addition to the classical boundary conditions, a natural boundary condition $\underline{\mathbf{M}}^{\mathrm{v}} \cdot \underline{\mathbf{n}} = 0$ is applied for the double tractions at the free surfaces and at lines of symmetry.

The extracted nominal stress-strain curve is depicted in Fig. 5.4a. At the maximum point, the solution bifurcates into a necking mode. The solution shows that the employed irregular mesh is sufficient to trigger the necking. Subsequently, the stress triaxiality increases in the center of the neck and so does the rate of porosity in this region. The macroscopic stress-carrying capacity drops drastically when when critical value of porosity f_{c} is reached. The steep load-drop is troublesome from a numerical point of view.

Figure 5.4b shows the distribution of the porosity at the end of the simulation when the Gauss points of the first elements reached the final value f_{f} (corresponding to $q_1 f^* = 1$). For illustration purposes, the FEM results were extruded according to the exploited symmetries. Firstly, it can be seen that the field remains smooth. Even the region of coalescence $f_{\mathrm{c}} \leq f \leq f_{\mathrm{f}}$ (green to red in Fig. 5.4b) extends over several layers of elements. The developed microdilatational model of ductile damage "regularizes" the problem successfully and prevents spurious mesh dependency, a localisation of damage within a single layer of elements.

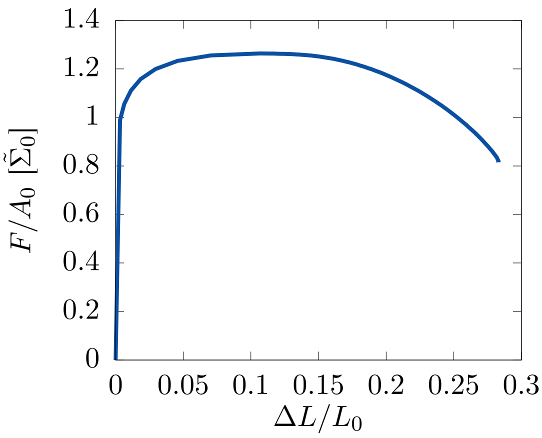

(a)

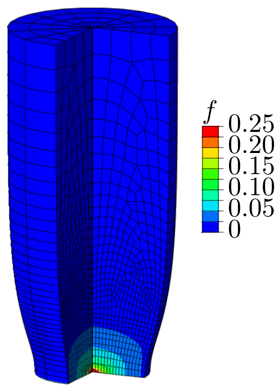

(b)

Fig. 5.4.: Simulation of tensile test: (a) Nominal stress-strain curve, (b) final distribution of porosity

6. Discussion

In literature, there is a controversial debate whether a homogenisation procedure for generalized continuum theory should yield vanishing double stresses in the case of homogeneous material at the microscale ΔV or not, compare e. g. [62, 142]. Obviously, for a homogeneous ΔV neither with the present procedure the higher order terms do vanish, compare Sections 4 and 5.2, nor was it the case in literature [4, 44, 114]. However, to the author's opinion this behavior is reasonable and the double stresses *must not* vanish in this case since, as argued by Mühlich et al. [62], a *locally* homogeneous ΔV can still have an *inhomogeneous neighboring* ΔV whose interaction is still described, in some average sense, by the additional higher order momentum balance equation (2.110). This neighbor might also be a macroscopic boundary at which non-vanishing double tractions are allowed to be prescribed due to (2.110). Consequently, from a mathematical point of view, the macroscopic boundary value problem would even be ill-posed if the macroscopic constitutive relation read $\underset{\sim}{\underline{\mathbf{M}}} = 0$. Whether such boundary conditions are physically reasonable in the case of homogeneous material at the microlevel is of course another question. The explicit definition of the involved generalized stress and deformation quantities derived in the present contribution provides a sound basis for addressing this question.

A similar question is whether for heterogeneous material the obtained macroscopic constitutive relations may depend on the particular choice of the unit cell ΔV. It is obvious in (4.7), that with the present procedure, even in the uniaxial case the non-classical terms (with $s = \Sigma - \bar{\sigma}$ and M) depend on location and size of the chosen unit cell. This is inevitably necessary since also potential generalized boundary conditions on χ or M require an interpretation with respect to the location of the corresponding macroscopic boundary relative to material heterogeneities, see e. g. [80, 143].

However, it is recalled that when the non-classical stresses vanish, either through suitable boundary conditions as described above or in sufficient distance to a boundary, then the classical theory is recovered whose solution does *not* depend on the particular choice of the unit cell.

In this context it is recalled that in Section 4.6, the size effect in an elastic layer of foam was predicted. The micromorphic properties were obtained from a unit cell ΔV where the pore was located at the center, i. e. from a realisation which has the highest stiffness against bending-type modes among all possible realisations of such a microstructure. Consequently, the macroscopic size effect was overestimated compared to discrete numerical simulation with random microstructure. In order to capture the random nature in the micromorphic properties, an ensemble average over different realisations of the microstructure needs to be considered in the future.

Recently, Lurie et al. [104] pointed out the possibility of micromorphic theories to address different realisations of the surface via a mixed boundary condition between double traction and microdeformation. Depending on the sign and amount of the coupling coefficient in the mixed boundary condition, even negative size effects can be reproduced. A similar approach was presented by Javili et al. [144] as "surface elasticity". Although not explicitly considered in the present work, the provided micro-macro relations for all kinetic and kinematic quantities should be helpful in identifying such coupling coefficients from micromechanics considerations.

A further question, which was discussed in literature on homogenisation of a Cauchy continuum on the microscale to a generalized continuum at the macroscale, was how the additional deformation measures of such theories can be prescribed via boundary conditions at the microscale. The kinematic micro-macro relations derived in the present contribution (as well as those in the average field theory of Forest et al., Section 2.2.4) cannot be completely converted to surface integrals. That is why they are prescribed as integral constraints whereby the difference stress $\underset{\sim}{\mathbf{s}}$ in its role as Lagrange multiplier acts as a distributed volume force. Thus, the difference stress can be interpreted as a penalty for the difference between $\underset{\sim}{\chi}$ and the actual gradient of displacements.

In the present thesis, the two possibly most simple situations were considered: the uniaxial case and a spherical or circular volume element. For the latter case it was found that the problem for the hydrostatic and for the skew-symmetric stresses becomes axi-symmetric. In these cases, as well as in the uniaxial case, just the number of potential boundary conditions at the microscale is not sufficient to prescribe the microdeformation $\underset{\sim}{\chi}$ in addition to the classical measures of deformation. From this point of view, the author does not see an alternative to prescribing $\underset{\sim}{\chi}$ via integral constraints.

In this context it is recalled that a weighting function $\mathrm{H}_V\left(\underline{\xi}\right)$ was introduced in Section 3.4 which defines how difference stress $\underset{\sim}{\mathbf{s}}$ is distributed within the volume element or, vice verse, how the local deformations contribute to the microdeformation $\underset{\sim}{\chi}$. In the present work, a uniform distribution of $\mathrm{H}_V\left(\underline{\xi}\right)$ was assumed for the matrix material. However, the presented procedure does not apply any restrictions on the choice of $\mathrm{H}_V\left(\underline{\xi}\right)$. For instance, the local values of mass or stiffness could be identified with $\mathrm{H}_V\left(\underline{\xi}\right)$, or the gradients thereof. In the latter case, internal interfaces would correspond to $\mathrm{H}_V\left(\underline{\xi}\right)$ being the Dirac distribution, i. e. the microdeformation $\underset{\sim}{\chi}$ would be computed from an integral over the internal interface as proposed recently by Biswas and Poh [91] (Similarly, Hlaváćek [73] and Berglund [67] defined $\underset{\sim}{\chi}$ via the displacement field of an inclusion.). This consideration implies the question on the optimal choice of the weighting function $\mathrm{H}_V\left(\underline{\xi}\right)$ which should be addressed in future studies.

Anyway, it was demonstrated in the present work, that the implementation of volume average micro-macro links via Lagrange multipliers is straight forward, both in analytical investigations and numerical implementations. Regarding a potential FE^2 implementation, the volume average leads to a few full rows in the otherwise sparse system of equations for whose solution suitable algorithms are favorable.

In classical homogenisation, it is required that the volume element ΔV should be "representative". The term was introduced by Hill [34] and associated with the conditions that the volume element "(a) is structurally entirely typical of the whole mixture on average, and (b) contains a sufficient number of inclusions for the apparent overall moduli to be effectively independent of the surface values of traction and displacement, so long as these values are 'macroscopically uniform'. That is, they fluctuate about a mean with a wavelength small compared with the dimensions of the sample, and the effects of such fluctuations become insignificant within a few wavelengths of the surface. The contribution of this surface layer to any average can be made negligible by taking the sample large enough". In classical homogenisation, often *periodic boundary conditions* are employed at the microscale to mimic the behavior of an infinite and periodic arrangement of identical volume elements to fulfill condition (b). For this purpose, periodic fluctuations are allowed as deviations from the corresponding kinematic boundary conditions. Regarding micromorphic continua, condition (a) remains reasonable whereas (b) contradicts the intention of most generalized continuum theories (for this reason, the author refrains from using the term "representative" in the context of micromorphic continua). Anyhow, several attempts were made to extend the concept of periodic boundary conditions to the homogenisation of generalized continua in order to have the established classical homogenisation contained as a strict special case, e. g. [45, 47, 49, 50, 145]. For this purpose, Hill's "macroscopically uniform" field was taken as a polynomial field ([49]: "assigned" field, [50]: "projected" field, [145]: "inserted" field) which fulfills the respective kinematic micro-macro relations ad hoc. Besides a certain arbitrariness in such a definition of a macroscopically uniform field for micromorphic continua, the problem is that the kinematic micro-macro relations for such a generalized homogenisation procedure can not completely be transformed to surface integrals. Thus, for performing the homogenisation, the split into a macroscopically uniform field and a fluctuation field does not lead to a simplification since volume average kinematic micro-macro relations then still need to be fulfilled, now with respect to the fluctuation field. In the procedure proposed in [145], the macroscopically uniform ("inserted") field actually serves to define indirectly the macroscopic stress measures.

In contrast, in the present contribution the macroscopic stress measures are defined directly and explicitly and corresponding work-conjugate deformation measures are derived. The boundary value problem at the microscale is completely defined either using static or kinematic boundary conditions, both including the classical and non-classical terms. The author sees no reason why the microscopic fields at the boundary of the volume element should be periodic if the macroscopic field quantities have strong gradient, i. e. if the non-classical terms are active. That is why the approach of Kouznetsova et al. [45] is adopted here, Section 3.5, and fluctuations are incorporated *at the boundary* of ΔV only in such a way that they reduce to classical periodic boundary conditions in the case the non-classical terms are absent.

The proposed micromorphic theory contains the special case of the strain-gradient theory as derived in Section 3.6.1. It was shown that the present theory reduces to the theory of Gologanu, Kouznetsova et al.[44, 45] under two conditions. Firstly, the kinamtic micro-macro relation that the macroscopic displacement corresponds to the *volume average* of its microscopic counterpart is *not* enforced by a Lagrange multiplier. It is recalled that Gologanu et al. [44] defined the macroscopic velocity as *surface average*. In future work, it may be checked whether this approach can be adopted to the present micromorphic theory (though, the definition as volume average is established in the micromorphic community since the pioneering work of Forest and Sab [47]). Secondly, the microdeformation $\underset{\sim}{\chi}$ needs to be identified with *half* of the macroscopic displacement gradient, not with the displacement gradient itself as mostly employed since Mindlin [10]. It was shown that this discrepancy is related solely with a prefactor of $\alpha = 1/2$ in the quadratic term of the kinematic boundary conditions which arose due to the interpretation of the boundary condition as a Taylor expansion. Future numerical benchmarks should elucidate the effect of this constraint factor α on the predictive quality, potentially in comparison to results of asymptotic expansion methods. Anyway, for the unconstrained micromorphic theory, α is not necessary but the ratio between microdeformation $\underset{\sim}{\chi}$ and macroscopic displacement gradient is an outcome of the proposed homogenisation theory.

Furthermore, it is to be recalled that within the present theory, the double stress $\underset{\sim}{\underline{\mathbf{M}}}$, and consequently its work-conjugate deformation measure $\underset{\sim}{\underline{\underline{\mathbf{L}}}}^{K\mathrm{s}}$, are symmetric with respect to its first and last index, Eqs. (3.11) and (3.25), although this symmetry is not required per se in the macroscopic theories of Eringen and Mindlin (but in the strain-gradient theory of Gologanu, Kouznetsova et al.). For the special case of the micropolar theory, this symmetry has the consequence that the polar double stress $\underset{\sim}{\mathbf{M}}^{\mathrm{r}}$ is traceless and consequently, only the deviator of the tensor of the rotation gradient (curvature-twist tensor) appears in the constitutive relations. For a isotropic linear-elastic micropolar, this means that the polar ratio amounts to $\Psi^{\mathrm{r}} = 3/2$. Remarkably, this values was employed in several recent studies [19, 25, 101] for empirical reasons.

A further remark shall be dedicated to the construction of higher order micromorphic theories. Firstly, recall that the classical theory is a first gradient theory and corresponding kinematic boundary conditions at the microscale are thus first order polynomials. The second gradient theory of Gologanu, Kouznetsova et al. involves an additional quadratic term at the boundary. In consequence, N^{th} gradient theories would thus have a polynomial displacement of degree N. The micromorphic theory considered in the present work is a first order micromorphic theory as the approximation of the displacement field with respect to the macroscopic balances is a polynomial of degree one with tensor of microdeformation $\underset{\sim}{\chi}$ as coefficient. This microdeformation of first order can be interpreted as relaxed first gradient. In the present theory, a difference stress $\underset{\sim}{\mathbf{s}}$ penalizes the difference between actual first gradient $\underline{\nabla_{\underline{\mathbf{X}}}\mathbf{U}}$ and relaxed gradient $\underset{\sim}{\chi}$ and acts as linear volume term at the microscale together with quadratic kinematic boundary conditions. Correspondingly, the double stress, i. e. the second-order hyperstress, is the surface average of the tractions weighted by a quadratic polynomial. The extension towards an N^{th} order micromorphic theory is thus straight-forward: it contains hyperstresses up to $(N+1)^{\mathrm{th}}$ order whose kinetic micro-macro relation are the surface averages of the tractions weighted by a polynomial of degree N. Correspondingly, the respective kinematic boundary condition at the microscale is a polynomial of degree N, too. Furthermore, such a theory has N difference stresses which penalize each the difference between the $(I+1)^{\mathrm{th}}$ microdeformation and the gradient of the I^{th} microdeformation. At the microscale, the I^{th} difference stress acts as coefficient of the volume force which is a polynomial of degree I. Though, before developing the homogenisation towards such a N^{th} order micromorphic theory in detail, the possibilities and limitations of the presented first order theory need to be elucidated for more example problems.

7. Summary

In the present contribution, a consistent theory of homogenisation of a classical Cauchy continuum at the microscale towards a micromorphic continuum at the macroscale was presented. Starting point was a critical review of the strain-gradient theory of Gologanu, Kouznetsova et al. and the micromorphic approaches of Eringen, Forest et al. The aforementioned strain-gradient theory is consistent in the sense that a boundary-value problem is formulated at the microscale whose solution yields, together with respective kinetic micro-macro relations, the macroscopic constitutive behavior. To the author's best knowledge, neither kinematic micro-macro relations for the strain-gradient nor correspondingly static boundary conditions have not been formulated yet in explicit form for this theory. Though, this is of minor importance since kinematic and periodic condition are favored anyway for most applications.

In contrast, the micromorphic approaches were not developed up to this stage yet. Eringen derived the governing balance equations by a spatial averaging procedure. Thereby, the flux-like quantities, including the double stress, were defined through a "surface operator". Unfortunately, an explicit definition of this operator was neither given by Eringen nor could the author find it anywhere else in literature. That means that the kinetic micro-macro relations are incomplete. In contrast, Forest et al. developed kinematic micro-macro relations for the micromorphic theory. The non-classical parts thereof contain volume integrals which cannot be transformed into surface integrals and thus not be prescribed solely by boundary conditions.

Within the concept of minimal loading conditions, the kinematic micro-macro relations are prescribed as global constraints at the microscale by means of Lagrange multipliers. These Lagrange multipliers can be identified with the work-conjugate stresses to the respective macroscopic kinematic quantities. It was checked whether the kinetic micro-macro relations of existing theories are suitable for the micromorphic theory. It turned out that external and internal stress could be computed by the volume average and surface integral expressions from classical theory of homogenisation. Though, the kinetic micro-macro relations for the double stress from strain-gradient theory did not work completely.

However, the successful application of the surface integral expressions from classical theory motivated the explicit definition of Eringen's surface operator. Thus having explicit definitions of all macroscopic stress-type quantities of the micromorphic theory, the minimal loading conditions concept could be revised inversely to construct suitable kinematic micro-macro relations. The micro-macro-relations for the gradient of microdeformation could be satisfied by quadratic kinematic boundary conditions. The kinematic micro-macro relation for the microdeformation is identical to Forest's expressions. If it is enforced, the difference stress (between internal and external stress) as corresponding Lagrange multiplier acts like a volume force at the microscale. In the interpretation of the microdeformation as relaxed displacement gradient, the difference stress thus penalizes a difference between actual and relaxed displacement gradient. The application to porous materials required a few minor modifications. Periodic boundary conditions are obtained by amending periodic fluctuations to the kinematic boundary conditions. The corresponding tractions are anti-periodic only in absence of double stresses, thus recovering the classical theory.

In summary, a consistent theory of micromorphic homogenisation was derived. It involves macroscopic balances, micro-macro relations for all kinetic and kinematic quantities and a boundary-value problem at the microscale. The latter can be formulated with static, kinematic or periodic boundary conditions. The same set of equations was formulated for the special cases of strain-gradient theory, micropolar theory (Cosserat theory), microstrain theory and microdilatational theory. With a complete formulation of a boundary-value problem, the developed homogenisation method is well-suited for FE^2 applications.

It turned out that the strain-gradient theory of Gologanu, Kouznetsova et al. is recovered if the microformation is constrained to coincide with *half* the displacement gradient (in contrast to Mindlin's usual assumption to identify with the displacment gradient itself). This point might require further discussion. Nevertheless, the presented theory can thus be interpreted as straight-forward extension of the theory of Gologanu, Kouznetsova et al. towards the unconstrained micromorphic case.

The micromorphic theory of homogenisation was demonstrated for certain examples starting with an uniaxial composite. Furthermore, the boundary-value problem at the microscale was solved approximately by Ritz' method for a porous, isotropic and linear-elastic material yielding all macroscopic constitutive parameters in closed form. The quality of the Ritz estimates was verified by a comparison certain analytical and FEM solutions. Special attention was paid to the special cases of micropolar theory. The predicted micropolar constitutive parameters agree in principle with experimental data from literature. By means of the derived micromorphic constitutive parameters, the size effect for a thin layer of foam in simple shearing could be predicted. It agrees qualitatively with direct numerical simulations from literature, though the absolute value is overestimated for very thin layers. This fact was related to the particular choice of the volume element. Instead, an ensemble average over different realizations should be employed in future investigations.

Furthermore, constitutive models for quasi-brittle and ductile damage were developed. For the quasi-brittle case it was assumed that propagating microcracks lead to an increase of the effective porosity of a material. Considerations on the associated dissipation lead to a rate-independent model.

Gurson's model is established to model the ductile mechanism. In this model, void growth and the associated dilatation drive the macroscopic softening. In order to overcome its spurious mesh sensitivity, Gurson's model was extended towards the microdilatational framework. In particular, additional trial fields, which comply with the derived microdilatational kinematic micro-macro relations, were employed in the limit-load analysis. Consequently, both the double stress as well as the difference stress enter the resulting macroscopic yield condition (in contrast to heuristic gradient-extensions of such damage models). The model was implemented in a FEM code and applied to an example. The results confirm that the microdilatational extension overcomes the spurious mesh dependency of Gurson's original model.

Future work needs to address the quantitative predictive capabilities of the proposed methodology. In this context, ensemble averages over different realizations of the microstructure need to be considered. Furthermore, the effect of the type of boundary conditions at the microscale, i. e. static, kinematic or periodic ones, needs to be investigated quantitatively for a sufficient number of benchmark problems.

Bibliography

[1] Hütter, G. "Micromorphic homogenisation and its application to a model of ductile damage". In: *Proc. Appl. Math. Mech.* 2017:17, pp. 599–600.

[2] Hütter, G. "Homogenization of a Cauchy continuum towards a micromorphic continuum". In: *J. Mech. Phys. Solids* 2017:99, pp. 394–408.

[3] Hütter, G. "A micromechanical gradient extension of Gurson's model of ductile damage within the theory of microdilatational media". In: *Int. J. Solids Struct.* 2017:110–111, pp. 15–23.

[4] Hütter, G., Mühlich, U., and Kuna, M. "Micromorphic homogenization of a porous medium: elastic behavior and quasi-brittle damage". In: *Contin. Mech. Therm.* 2015:27, pp. 1059–1072.

[5] Tekoğlu, C. "Size effects in cellular solids". Proefschrift. Rijksuniversiteit Groningen, 2007.

[6] Hütter, G., Zybell, L., Mühlich, U., and Kuna, M. "Consistent Simulation of Ductile Crack Propagation with Discrete 3D Voids". In: *Comp. Mater. Sci.* 2013:80, pp. 61–70.

[7] Eringen, A. C. "Mechanics of Micromorphic Continua". In: *Mechanics of Generalized Continua: Proceedings of the IUTAM-Symposium on The Generalized Cosserat Continuum and the Continuum Theory of Dislocations with Applications, Freudenstadt and Stuttgart (Germany) 1967.* Berlin, Heidelberg: Springer, 1968, pp. 18–35.

[8] Eringen, A. C. and Kafadar, C. B. "Polar and Nonlocal Field Theories". Ed. by Eringen, A. C. Vol. IV. Continuum Physics. New York: Academic Press, 1976.

[9] Eringen, A. C. and Suhubi, E. S. "Nonlinear theory of simple micro-elastic solids–I". In: *Int. J. Eng. Sci.* 1964:2(2), pp. 189–203.

[10] Mindlin, R. D. "Micro-structure in linear elasticity". In: *Arch. Ration. Mech. An.* 1964:16(1), pp. 51–78.

[11] Forest, S. and Sievert, R. "Nonlinear microstrain theories". In: *Int. J. Solids Struct.* 2006:43(24), pp. 7224–7245.

[12] Maugin, G. A. "Generalized Continuum Mechanics: What Do We Mean By That?" In: *Mechanics of Generalized Continua.* Ed. by Maugin, G. A. and Metrikine, A. V. Vol. 21. Advances in Mechanics and Mathematics. New York: Springer, 2010, pp. 3–13.

[13] Germain, P. "The method of virtual power in continuum mechanics. Part 2: Microstructure". In: *SIAM J. Appl. Math.* 1973:25(3), pp. 556–575.

[14] Forest, S. "Micromorphic Approach for Gradient Elasticity, Viscoplasticity, and Damage". In: *J. Eng. Mech.* 2009:135(3), pp. 117–131.

[15] Dimitrijevic, B. J. and Hackl, K. "A method for gradient enhancement of continuum damage models". In: *Tech. Mech.* 2008:28(1), pp. 43–52.

[16] Hütter, G. "An extended Coleman-Noll procedure for generalized continuum theories". In: *Contin. Mech. Therm.* 2016:28, pp. 1935–1941.

[17] Gauthier, R. D. and Jahsman, W. E. "A Quest for Micropolar Elastic Constants". In: *J. Appl. Mech.* 1975:42(2), pp. 369–374.

[18] Anderson, W. B. and Lakes, R. S. "Size effects due to Cosserat elasticity and surface damage in closed-cell polymethacrylimide foam". In: *J. Mater. Sci.* 1994:29(24), pp. 6413–6419.

[19] Ha, C. S., Plesha, M. E., and Lakes, R. S. "Chiral three-dimensional isotropic lattices with negative Poisson's ratio". In: *Phys. Status Solidi B* 2016:253(7), pp. 1243–1251.

[20] Lakes, R. “Physical meaning of elastic constants in Cosserat, void, and microstretch elasticity”. In: *J. Mech. Mater. Struct.* 2016:11(3), pp. 217–229.

[21] Lakes, R. and Drugan, W. J. “Bending of a Cosserat Elastic Bar of Square Cross Section: Theory and Experiment”. In: *J. Appl. Mech.* 2015:82(9), p. 091002.

[22] Lakes, R. S. “Size effects and micromechanics of a porous solid”. In: *J. Mater. Sci.* 1983:18(9), pp. 2572–2580.

[23] Park, H. C. and Lakes, R. S. “Torsion of a micropolar elastic prism of square cross-section”. In: *Int. J. Solids Struct.* 1987:23(4), pp. 485–503.

[24] Rueger, Z. and Lakes, R. S. “Experimental Cosserat elasticity in open-cell polymer foam”. In: *Philos. Mag.* 2016:96(2), pp. 93–111.

[25] Rueger, Z. and Lakes, R. S. “Strong Cosserat elastic effects in a unidirectional composite”. In: *Z. Angew. Math. Mech.* 2017:68(3), p. 54.

[26] Rueger, Z., Li, D., and Lakes, R. S. “Observation of Cosserat Elastic Effects in a Tetragonal Negative Poisson’s Ratio Lattice”. In: *Phys. Status Solidi B* 2017, p. 1600840.

[27] Liebenstein, S., Sandfeld, S., and Zaiser, M. “Size and disorder effects in elasticity of cellular structures: From discrete models to continuum representations”. In: *Int. J. Solids Struct.* 2018:146, pp. 97–116.

[28] Diebels, S. and Geringer, A. “Micromechanical and macromechanical modelling of foams: Identification of Cosserat parameters”. In: *Z. Angew. Math. Mech.* 2014:94(5), pp. 414–420.

[29] Tekoğlu, C., Gibson, L., Pardoen, T., and Onck, P. “Size effects in foams: Experiments and modeling”. In: *Prog. Mater. Sci.* 2011:56(2), pp. 109–138.

[30] Tekoğlu, C. and Onck, P. R. “Size effects in two-dimensional Voronoi foams: A comparison between generalized continua and discrete models”. In: *J. Mech. Phys. Solids.* 2008:56(12), pp. 3541–3564.

[31] Hütter, G., Linse, T., Mühlich, U., and Kuna, M. “Simulation of Ductile Crack Initiation and Propagation by means of a Non-local GTN-model under Small-Scale Yielding”. In: *Int. J. Solids Struct.* 2013:50, pp. 662–671.

[32] Forest, S. “Nonlinear regularization operators as derived from the micromorphic approach to gradient elasticity, viscoplasticity and damage”. In: *Proc. R. Soc. A* 2016:472, p. 20150755.

[33] Ehlers, W. and Volk, W. “On theoretical and numerical methods in the theory of porous media based on polar and non-polar elasto-plastic solid materials”. In: *Int. J. Solids Struct.* 1998:35(34-35), pp. 4597–4617.

[34] Hill, R. “Elastic properties of reinforced solids: Some theoretical principles”. In: *J. Mech. Phys. Solids* 1963:11(5), pp. 357–372.

[35] Hill, R. “On Constitutive Macro-Variables for Heterogeneous Solids at Finite Strain”. In: *P. Roy. Soc. Lond. A. Math.* 1972:326(1565), pp. 131–147.

[36] Forest, S. “Mechanics of generalized continua: construction by homogenizaton”. In: *J. Phys. IV* 1998:08(PR4), pp. 39–48.

[37] Bouyge, F., Jasiuk, I., and Ostoja-Starzewski, M. “A micromechanically based couple-stress model of an elastic two-phase composite”. In: *Int. J. Solids Struct.* 2001:38(10–13), pp. 1721–1735.

[38] Adomeit, G. “Determination of Elastic Constants of a Structured Material”. In: *Mechanics of Generalized Continua.* Ed. by Kröner, E. Berlin/Heidelberg: Springer-Verlag, 1968, pp. 80–82.

[39] Besdo, D. “Towards a Cosserat-theory describing motion of an originally rectangular structure of blocks”. In: *Arch. Appl. Mech.* 2009:80(1), pp. 25–45.

[40] Ehlers, W., Ramm, E., Diebels, S., and D’Addetta, G. “From particle ensembles to Cosserat continua: homogenization of contact forces towards stresses and couple stresses”. In: *Int. J. Solids Struct.* 2003:40(24), pp. 6681–6702.

[41] Trovalusci, P., De Bellis, M. L., and Masiani, R. “A multiscale description of particle composites: From lattice microstructures to micropolar continua”. In: *Compos. Part. B-Eng.* 2017:128, pp. 164–173.

[42] Chung, J. and Waas, A. M. “The micropolar elasticity constants of circular cell honeycombs”. In: *Proc. R. Soc. A* 2009:465(2101), pp. 25–39.

[43] Segerstad, P. Hård af, Toll, S., and Larsson, R. “A micropolar theory for the finite elasticity of open-cell cellular solids”. In: *Proc. R. Soc. A* 2009:465(2103), pp. 843–865.

[44] Gologanu, M., Leblond, J. B., Perrin, G., and Devaux, J. “Recent extensions of Gurson’s model for porous ductile metals – Part II: A Gurson-like model including the effect of strong gradients of the macroscopic field”. In: *Continuum micromechanics.* Ed. by Suquet, P. CISM Courses And Lectures 377. Springer-Verlag, 1997, pp. 97–130.

[45] Kouznetsova, V., Geers, M. G. D., and Brekelmans, W. A. M. “Multi-scale constitutive modelling of heterogeneous materials with a gradient-enhanced computational homogenization scheme”. In: *Int. J. Numer. Meth. Engng.* 2002:54(8), pp. 1235–1260.

[46] Forest, S. “Homogenization methods and the mechanics of generalized continua - part 2”. In: *Theor. Appl. Mech.* 2002:28-29, pp. 113–143.

[47] Forest, S. and Sab, K. “Cosserat overall modeling of heterogeneous materials”. In: *Mech. Res. Commun.* 1998:25(4), pp. 449–454.

[48] Forest, S. “Aufbau und Identifikation von Stoffgleichungen für höhere Kontinua mittels Homogenisierungsmethoden”. In: *Tech. Mech.* 1999:19(4), pp. 297–306.

[49] De Bellis, M. L. and Addessi, D. “A Cosserat Based Multi-scale Model For Masonry Structures”. In: *Int. J. Multiscale Com.* 2011:9(5), pp. 543–563.

[50] Jänicke, R., Diebels, S., Sehlhorst, H.-G., and Düster, A. “Two-scale modelling of micromorphic continua”. In: *Contin. Mech. Therm.* 2009:21, pp. 297–315.

[51] Toupin, R. A. “Elastic materials with couple-stresses”. In: *Arch. Ration. Mech. An.* 1962:11(1), pp. 385–414.

[52] Mindlin, R. D. and Eshel, N. N. “On first strain-gradient theories in linear elasticity”. In: *Int. J. Solids. Struct.* 1968:4(1), pp. 109–124.

[53] Truesdell, C. and Toupin, R. A. “The Classical Field Theories”. In: *Principles of Classical Mechanics and Field Theories.* Ed. by Flügge, S. Vol. III/1. Encyclopedia of Physics. Berlin, Göttingen, Heidelberg: Springer-Verlag, 1960.

[54] Gudmundson, P. “A unified treatment of strain gradient plasticity”. In: *J. Mech. Phys. Solids* 2004:52(6), pp. 1379–1406.

[55] Gurtin, M. E. and Anand, L. “Thermodynamics applied to gradient theories involving the accumulated plastic strain: The theories of Aifantis and Fleck and Hutchinson and their generalization”. In: *J. Mech. Phys. Solids* 2009:57(3), pp. 405–421.

[56] Kouznetsova, V. G. “Computational homogenization for the multi-scale analysis of multi-phase materials”. PhD thesis. Technische Universiteit Eindhoven, 2002.

[57] Kirchner, N. and Steinmann, P. “A unifying treatise on variational principles for gradient and micromorphic continua”. In: *Philos. Mag.* 2005:85(33–35), pp. 3875–3895.

[58] Hirschberger, B. C., Kuhl, E., and Steinmann, P. “On deformational and configurational mechanics of micromorphic hyperelasticity - Theory and computation”. In: *Comput. Method. Appl. M.* 2007:196(41), pp. 4027–4044.

[59] Maugin, G. A. “The method of virtual power in continuum mechanics: Application to coupled fields”. In: *Acta. Mech.* 1980:35(1), pp. 1–70.

[60] Hellinger, E. “Die allgemeinen Ansätze der Mechanik der Kontinua”. In: *Encyklopädie der mathematischen Wissenschaften.* Ed. by Klein, F. and Wagner, K. Vol. 4. Berlin: Springer, 1913, pp. 602–694.

[61] Storm, J. “Entwicklung und Bewertung von effizienten Berechnungskonzepten für keramische Filter”. Dissertation. TU Bergakademie Freiberg, 2016.

[62] Mühlich, U., Zybell, L., and Kuna, M. “Estimation of material properties for linear elastic strain gradient effective media”. In: *Eur. J. Mech. A-Solid.* 2012:31(1), pp. 117–130.

[63] Forest, S. and Sab, K. “Stress gradient continuum theory”. In: *Mech. Res. Commun.* 2012:40, pp. 16–25.

[64] Kaczmarczyk, L., Pearce, C. J., and Bićanić, N. “Scale transition and enforcement of RVE boundary conditions in second-order computational homogenization”. In: *Int. J. Numer. Meth. Engng.* 2008:74(3), pp. 506–522.

[65] Li, J. “Establishment of strain gradient constitutive relations by homogenization”. In: *C. R. Mécanique* 2011:339(4), pp. 235–244.

[66] Fischer, P., Mergheim, J., and Steinmann, P. “C^1 Discretizations for the Application to Gradient Elasticity”. In: *Mechanics of Generalized Continua – One Hundred Years After the Cosserats.* Ed. by Maugin, G. A. and Metrikine, A. V. New York: Springer, 2010, pp. 279–286.

[67] Berglund, K. “Structural Models of Micropolar Media”. In: *Mechanics of Micropolar Media.* Ed. by Brulin, O. and Hsieh, R. K. T. World Scientific, 1982, pp. 35–86.

[68] Forest, S. and Trinh, D. “Generalized continua and non-homogeneous boundary conditions in homogenisation methods”. In: *Z. Angew. Math. Mech.* 2011:91(2), pp. 90–109.

[69] Kruch, S. and Forest, S. “Computation of coarse grain structures using a homogeneous equivalent medium”. In: *J. Phys. IV France* 1998:08(PR8), pp. 197–205.

[70] Branke, D., Brummund, J., Haasemann, G., and Ulbricht, V. “Obtaining Cosserat material parameters by homogenization of a Cauchy continuum”. In: *Proc. Appl. Math. Mech.* 2009:9(1), pp. 425–426.

[71] Sun, C.-T., Achenbach, J. D., and Herrmann, G. “Continuum Theory for a Laminated Medium”. In: *J. Appl. Mech.* 1968:35(3), pp. 467–475.

[72] Herrmann, G. and Achenbach, J. D. “Applications of Theories of Generalized Cosserat Continua to the Dynamics of Composite Materials”. In: *Mechanics of Generalized Continua: Proceedings of the IUTAM-Symposium on The Generalized Cosserat Continuum and the Continuum Theory of Dislocations with Applications, Freudenstadt and Stuttgart (Germany) 1967.* Ed. by Kröner, E. Springer, 1968, pp. 69–79.

[73] Hlaváček, M. “A continuum theory for isotropic two-phase elastic composites”. In: *Int. J. Solids Struct.* 1975:11(10), pp. 1137–1144.

[74] Achenbach, J. “Generalized Continuum Theories for Directionally Reinforced Solids.” In: *Arch. Mech.* 1976:28(3), pp. 257–278.

[75] Chen, H., Liu, X., Hu, G., and Yuan, H. “Identification of material parameters of micropolar theory for composites by homogenization method”. In: *Comp. Mater. Sci.* 2009:46(3), pp. 733–737.

[76] Jänicke, R. and Steeb, H. “Minimal loading conditions for higher order numerical homogenisation schemes”. In: *Arch. Appl. Mech.* 2012:82(8), pp. 1075–1088.

[77] Forest, S. and Sab, K. “Finite-deformation second-order micromorphic theory and its relations to strain and stress gradient models”. In: *Math. Mech. Solids.* 2017.

[78] Coleman, B. D. and Noll, W. “The thermodynamics of elastic materials with heat conduction and viscosity”. In: *Arch. Ration. Mech. An.* 1963:13(1), pp. 167–178.

[79] Waseem, A., Beveridge, A., Wheel, M., and Nash, D. “The influence of void size on the micropolar constitutive properties of model heterogeneous materials”. In: *Eur. J. Mech. A-Solid.* 2013:40, pp. 148–157.

[80] Wheel, M. A., Frame, J. C., and Riches, P. E. “Is smaller always stiffer? On size effects in supposedly generalised continua”. In: *Int. J. Solids Struct.* 2015:67-68, pp. 84–92.

[81] Dillard, T., Forest, S., and Ienny, P. “Micromorphic continuum modelling of the deformation and fracture behaviour of nickel foams”. In: *Eur. J. Mech. A-Solid.* 2006:25(3), pp. 526–549.

[82] Leblond, J. B., Perrin, G., and Devaux, J. “Bifurcation Effects in Ductile Metals With Nonlocal Damage”. In: *J. Appl. Mech.* 1994:61(2), pp. 236–242.

[83] Needleman, A. and Tvergaard, V. “Dynamic crack growth in a nonlocal progressively cavitating solid”. In: *Eur. J. Mech. A-Solid.* 1998:17(3), pp. 421–438.

[84] Jackiewicz, J. and Kuna, M. “Non-local regularization for FE simulation of damage in ductile materials”. In: *Comp. Mater. Sci.* 2003:28(3–4), pp. 684–695.

[85] Reusch, F., Svendsen, B., and Klingbeil, D. “Local and non-local Gurson-based ductile damage and failure modelling at large deformation”. In: *Eur. J. Mech. A-Solid.* 2003:22(6), pp. 779–792.

[86] Linse, T., Hütter, G., and Kuna, M. “Simulation of crack propagation using a gradient-enriched ductile damage model based on dilatational strain”. In: *Eng. Fract. Mech.* 2012:95, pp. 13–28.

[87] Bargellini, R., Besson, J., Lorentz, E., and Michel-Ponnelle, S. “A non-local finite element based on volumetric strain gradient: Application to ductile fracture”. In: *Comp. Mater. Sci.* 2009:45(3), pp. 762–767.

[88] Kiefer, B., Waffenschmidt, T., Sprave, L., and Menzel, A. “A gradient-enhanced damage model coupled to plasticity — multi-surface formulation and algorithmic concepts”. In: *Int. J. Damage. Mech.* 2018:27(2), pp. 253–295.

[89] Samal, M., Seidenfuss, M., Roos, E., Dutta, B., and Kushwaha, H. “Experimental and numerical investigation of ductile-to-brittle transition in a pressure vessel steel”. In: *Mat. Sci. Eng. A-Struct.* 2008:496(1–2), pp. 25–35.

[90] Seidenfuss, M., Samal, M., and Roos, E. “On critical assessment of the use of local and nonlocal damage models for prediction of ductile crack growth and crack path in various loading and boundary conditions”. In: *Int. J. Solids Struct.* 2011:48(24), pp. 3365–3381.

[91] Biswas, R. and Poh, L. “A micromorphic computational homogenization framework for heterogeneous materials”. In: *J. Mech. Phys. Solids* 2017:102, pp. 187–208.

[92] Schaefer, H. “Das Cosserat-Kontinuum”. In: *Z. Angew. Math. Mech.* 1967:47(8), pp. 485–498.

[93] Jänicke, R. “Micromorphic media: Interpretation by homogenisation”. Dissertation. Saarbrücken: Universität des Saarlandes, 2010.

[94] Branke, D. “Homogenisierungsmethode für den Übergang vom Cauchy- zum Cosserat-Kontinuum”. Dissertation. TU Dresden, 2012.

[95] Benzerga, A. A. and Leblond, J.-B. “Ductile Fracture by Void Growth to Coalescence”. In: *Adv. Appl. Mech.* 2010:44. Ed. by Aref, H. and Giessen, E. van der, pp. 169–305.

[96] Hahn, H. G. “Elastizitätstheorie”. Springer, 1985.

[97] Gross, D. and Seelig, T. “Fracture Mechanics – With an Introduction to Micromechanics”. Berlin Heidelberg: Springer, 2006.

[98] Krajcinovic, D. “Damage Mechanics”. Elsevier, 1996.

[99] Benguigui, L. “Experimental Study of the Elastic Properties of a Percolating System”. In: *Phys. Rev. Lett.* 1984:53(21), pp. 2028–2030.

[100] Eringen, A. C. “Linear theory of micropolar elasticity”. In: *J. Math. Mech.* 1966, pp. 909–923.

[101] Neff, P. “The Cosserat couple modulus for continuous solids is zero viz the linearized Cauchy-stress tensor is symmetric”. In: *Z. Angew. Math. Mech.* 2006:86(11), pp. 892–912.

[102] Kachanov, M., Shafiro, B., and Tsukrov, I. “Handbook of elasticity solutions”. Dordrecht / Boston / London: Kluwer Academic Publishers, 2003.

[103] Cowin, S. C. and Nunziato, J. W. “Linear elastic materials with voids”. In: *J. Elasticity.* 1983:13(2), pp. 125–147.

[104] Lurie, S., Solyaev, Y., Volkov, A., and Volkov-Bogorodskiy, D. “Bending problems in the theory of elastic materials with voids and surface effects”. In: *Math. Mech. Solids.* 2017.

[105] Timoshenko, S. and Goodier, J. N. “Theory Of Elasticity”. McGraw-Hill, 1951.

[106] Aifantis, E. C. “The physics of plastic deformation”. In: *Int. J. Plasticity.* 1987:3(3), pp. 211–247.

[107] Diebels, S. and Steeb, H. “Stress and couple stress in foams”. In: *Comp. Mater. Sci.* 2003:28(3-4), pp. 714–722.

[108] Forest, S. “Questioning size effects as predicted by strain gradient plasticity”. In: *J. Mech. Behav. Mater.* 2013:22, pp. 101–110.

[109] Aifantis, K. E. and Willis, J. R. “The role of interfaces in enhancing the yield strength of composites and polycrystals”. In: *J. Mech. Phys. Solids.* 2005:53(5), pp. 1047–1070.

[110] Mazière, M. and Forest, S. “Strain gradient plasticity modeling and finite element simulation of Lüders band formation and propagation”. In: *Contin. Mech. Therm.* 2013.

[111] Iltchev, A., Marcadon, V., Kruch, S., and Forest, S. “Computational homogenisation of periodic cellular materials: Application to structural modelling”. In: *Int. J. Mech. Sci.* 2015:93(0), pp. 240–255.

[112] Jänicke, R., Sehlhorst, H.-G., Duster, A., and Diebels, S. “Micromorphic two-scale modelling of periodic grid structures”. In: *Int. J. Multiscale Com.* 2013:11, pp. 161–176.

[113] Ameen, M. M., Peerlings, R. H. J., and Geers, M. G. D. “A quantitative assessment of the scale separation limits of classical and higher-order asymptotic homogenization”. In: *Eur. J. Mech. A-Solid.* 2018:71, pp. 89–100.

[114] Mühlich, U., Zybell, L., Hütter, G., and Kuna, M. “A first-order strain gradient damage model for simulating quasi-brittle failure in porous elastic solids”. In: *Arch. Appl. Mech.* 2013:83, pp. 955–967.

[115] Lemaitre, J. and Chaboche, J.-L. “Mechanics of solid materials”. Cambridge University Press, 1994.

[116] Geers, M. G. D., Borst, R. de, Brekelmans, W. A. M., and Peerlings, R. H. J. “Strain-based transient-gradient damage model for failure analyses”. In: *Comput. Method. Appl. M.* 1998:160(1–2), pp. 133–153.

[117] Geers, M. G. D., Peerlings, R. H. J., Brekelmans, W. A. M., and Borst, R. de. “Phenomenological nonlocal approaches based on implicit gradient-enhanced damage”. In: *Acta. Mech.* 2000:144(1), pp. 1–15.

[118] Jirásek, M. “Nonlocal models for damage and fracture: Comparison of approaches”. In: *Int. J. Solids. Struct.* 1998:35(31–32), pp. 4133–4145.

[119] Simone, A., Wells, G. N., and Sluys, L. J. “From continuous to discontinuous failure in a gradient-enhanced continuum damage model”. In: *Comput. Method. Appl. M.* 2003:192(41–42), pp. 4581–4607.

[120] Skrypnyk, R. “Simulation of quasi-brittle damage by means of a micromorphic damage model”. Master Thesis. TU Bergakademie Freiberg, Institute of Mechanics and Fluid Dynamics, 2015.

[121] Hütter, G. and Skrypnyk, R. “Micromorphic Homogenisation of a Porous Medium: Application to Size Effects and Quasi-Brittle Damage”. In: *Proc. Appl. Math. Mech.* 2016:16(1), pp. 347–348.

[122] Gurson, A. L. “Plastic Flow and Fracture Behavior of Ductile Materials Incorporating Void Nucleation, Growth, and Interaction”. Phd thesis. Brown University, 1975.

[123] Gurson, A. L. "Continuum Theory of Ductile Rupture by Void Nucleation and Growth: Part I – Yield Criteria and Flow Rules for Porous Ductile Media". In: *J. Eng. Mater-T. Asme.* 1977:99(1), pp. 2–15.

[124] Besson, J. "Continuum Models of Ductile Fracture: A Review". In: *Int. J. Damage. Mech.* 2010:19(1), pp. 3–52.

[125] Benzerga, A. A., Leblond, J.-B., Needleman, A., and Tvergaard, V. "Ductile Failure Modeling". In: *Int. J. Fracture.* 2016:201, pp. 29–80.

[126] Seidenfuss, M. and Linse, T. "Micromechanical-Based Models for Describing Damage of Ferritic Steels". In: *Recent Trends in Fracture and Damage Mechanics.* Springer, 2016, pp. 353–416.

[127] Enakoutsa, K. and Leblond, J.-B. "Numerical implementation and assessment of the GLPD micromorphic model of ductile rupture". In: *Eur. J. Mech. A-Solid.* 2009:28(3), pp. 445–460.

[128] Bergheau, J.-M., Leblond, J.-B., and Perrin, G. "A new numerical implementation of a second-gradient model for plastic porous solids, with an application to the simulation of ductile rupture tests". In: *Comput. Method. Appl. M.* 2014:268, pp. 105–125.

[129] Rice, J. R. and Tracey, D. M. "On the ductile enlargement of voids in triaxial stress fields". In: *J. Mech. Phys. Solids* 1969:17(3), pp. 201–217.

[130] Monchiet, V., Charkaluk, E., and Kondo, D. "A micromechanics-based modification of the Gurson criterion by using Eshelby-like velocity fields". In: *Eur. J. Mech. A-Solid.* 2011:30(6), pp. 940–949.

[131] Chu, C. C. and Needleman, A. "Void Nucleation Effects In Biaxially Stretched Sheets". In: *J. Eng. Mater-T. Asme.* 1980:102(3), pp. 249–256.

[132] Zhang, Z. L. "A complete Gurson model". In: *Nonlinear Fracture & Damage Mechanics.* Ed. by Aliabadi, M. H. Southhampton, Boston: WITpress, 2001. Chap. 8, pp. 223–248.

[133] Needleman, A and Rice, J. "Limits to Ductility Set by Plastic Flow Localization". In: *Mechanics of Sheet Metal Forming.* Ed. by Koistinen, D. P. and Wang, N.-M. New York: Plenum Publishing Corporation, 1978, pp. 237–267.

[134] Tvergaard, V. "Influence of voids on shear band instabilities under plane strain conditions". In: *Int. J. Fracture.* 1981:17(4), pp. 389–407.

[135] Faleskog, J., Gao, X., and Shih, C. F. "Cell model for nonlinear fracture analysis – I. Micromechanics calibration". In: *Int. J. Fracture.* 1998:89(4), pp. 355–373.

[136] Tvergaard, V. and Needleman, A. "Analysis of the cup-cone fracture in a round tensile bar". In: *Acta. Metall. Mater.* 1984:32(1), pp. 157–169.

[137] Nahshon, K. and Hutchinson, J. W. "Modification of the Gurson Model for shear failure". In: *Eur. J. Mech. A-Solid.* 2008:27(1), pp. 1–17.

[138] *Abaqus v6.12.* Dassault Systèmes. 2012.

[139] Hütter, G., Roth, S., and Skrypnyk, R. *UELlib–A library for user-defined elements in Abaqus.* TU Bergakademie Freiberg, Institute of Mechanics and Fluid Dynamics. 2017.

[140] Hughes, T. J. R. and Winget, J. "Finite rotation effects in numerical integration of rate constitutive equations arising in large-deformation analysis". In: *Int. J. Numer. Meth. Engng.* 1980:15(12), pp. 1862–1867.

[141] Aravas, N. "On the numerical integration of a class of pressure-dependent plasticity models". In: *Int. J. Numer. Meth. Eng.* 1987:24(7), pp. 1395–1416.

[142] Li, J. "A micromechanics-based strain gradient damage model for fracture prediction of brittle materials – Part I: Homogenization methodology and constitutive relations". In: *Int. J. Solids Struct.* 2011:48(24), pp. 3336–3345.

[143] Frame, J. C., Wheel, M. A., and Riches, P. E. "A numerical investigation and experimental verification of size effects in loaded bovine cortical bone". In: *Int. J. Numer. Meth. Biomed. Engng.* 2018:34, e2903.

[144] Javili, A., Chatzigeorgiou, G., McBride, A. T., Steinmann, P., and Linder, C. "Computational homogenization of nano-materials accounting for size effects via surface elasticity". In: *GAMM-Mitteilungen* 2015:38(2), pp. 285–312.

[145] Blanco, P. J., Sánchez, P. J., Souza Neto, E. A. de, and Feijóo, R. A. "Variational Foundations and Generalized Unified Theory of RVE-Based Multiscale Models". In: *Arch. Comput. Method. E.* 2016:23(2), pp. 191–253.

[146] Barber, J. R. "Elasticity". 3rd. Dordrecht: Springer Netherlands, 2010.

A. Appendix

A.1. Exact solution for effective shear modulus in plane case for kinematic and periodic boundary conditions

For obtaining the exact solution for the effective shear modulus under kinematic or periodic boundary conditions, an ansatz

$$F = 2\mu g(r)\underset{\sim}{\mathbf{E}}^{\mathrm{d}} : \underline{\xi\xi}\,. \tag{A.1}$$

for the Airy function is adopted. Equation (A.1) corresponds to ansatz (4.38) for static boundary conditions with $\underset{\sim}{\mathbf{E}}^{\mathrm{d}}$ replaced by the deviator of the macroscopic strain $2\mu\underset{\sim}{\mathbf{E}}^{\mathrm{d}}$ with an additional factor 2μ introduced for convenience. Thus, the radial function $g(r)$ involves the same terms of the Mitchell series as for static boundary conditions, Eq. (4.41). The traction-free void surface still requires

$$g(r = R_{\mathrm{void}}) = 0, \qquad g'(r = R_{\mathrm{void}}) = 0\,. \tag{A.2}$$

In order to apply the kinematic boundary conditions (2.45), it is favorable to switch to a coordinate system $\underline{\mathbf{b}}_1$–$\underline{\mathbf{b}}_2$ which is aligned with the principal axes of $\underset{\sim}{\mathbf{E}}^{\mathrm{d}}$, i. e. $\underset{\sim}{\mathbf{E}}^{\mathrm{d}} = E^{\mathrm{d}}(\underline{\mathbf{b}}_1\underline{\mathbf{b}}_1 - \underline{\mathbf{b}}_2\underline{\mathbf{b}}_2)$. Thus, in polar coordinates the scalar product in Eq. (A.1) becomes $\underset{\sim}{\mathbf{E}}^{\mathrm{d}} : \underline{\xi\xi} = E^{\mathrm{d}} r^2\cos(2\varphi)$. The displacement field which belongs to the Mitchell series can be found in [146]. For the particular ansatz (A.1) with Eq. (4.41) it reads

$$\begin{aligned} u_r &= E^{\mathrm{d}}\left[-4\nu C_1 r^3 + 4(1-\nu)\frac{C_2}{r} + \frac{2C_3}{r^3} - 2C_4 r\right]\cos(2\varphi) \\ u_\varphi &= E^{\mathrm{d}}\left[2(3-2\nu)C_1 r^3 - 2(1-2\nu)\frac{C_2}{r} + \frac{2C_3}{r^3} + 2C_4 r\right]\sin(2\varphi)\,. \end{aligned} \tag{A.3}$$

In polar coordinates, the kinematic boundary conditions (2.45) read

$$u_r(r = R) = E^{\mathrm{d}} R\cos(2\varphi)\,. \qquad u_\varphi(r = R) = -\,E^{\mathrm{d}} R\sin(2\varphi)\,. \tag{A.4}$$

Equating Eqs. (A.3) with (A.4) yields two equations which, together with Eq. (A.2), allow to determine the coefficients C_1–C_4. Finally, the kinetic micro-macro relation (2.40) is evaluated, with stress field (4.39) from Eq. (A.1), as

$$\underset{\sim}{\mathbf{\Sigma}} = 2\mu\left[-2g(r = R) - \frac{1}{2}g'(r = R)\right]\underset{\sim}{\mathbf{E}}^{\mathrm{d}}\,. \tag{A.5}$$

Obviously, the prefactor of $\underset{\sim}{\mathbf{E}}^{\mathrm{d}}$ on the right-hand side corresponds to the macroscopic effective shear modulus

$$\mu^{(\mathrm{eff})} = \mu\frac{\left(3 - 4\nu + f^3 - 3f^2 + 3\,f\right)(1-f)}{3 + 3f^4 + 4f^3 - 6f^2 + 12f - 4f^4\nu - 24\nu f + 16\nu^2 f - 4\nu}\,. \tag{A.6}$$

In polar coordinates, periodic boundary conditions (2.49) read

$$\begin{aligned} u_r(R,\varphi) + u_r(R,\varphi+\pi) &= 2E^{\mathrm{d}} R\cos(2\varphi)\,, \\ u_\varphi(R,\varphi) + u_\varphi(R,\varphi+\pi) &= -\,2E^{\mathrm{d}} R\sin(2\varphi)\,. \end{aligned} \tag{A.7}$$

For the particular displacement field (A.3), the periodic boundary conditions (A.7) coincide with kinematic boundary conditions (A.4). Thus, for the circular volume element under consideration, periodic and kinematic boundary conditions yield the same effective shear modulus, Eq. (A.6).

A.2. Consistent tangent stiffness of microdilatational model of ductile damage

The derivative $\frac{\partial[\mathbf{R}]}{\partial[\mathbf{Q}]}$ can be computed from Eq. (5.65) as

$$\frac{\partial[\mathbf{R}]}{\partial[\mathbf{Q}]} = \begin{bmatrix} 3q_1q_2f^*\sinh\left(\frac{3q_2}{2}\frac{P}{\tilde{\Sigma}}\right) & \frac{2Q}{\tilde{\Sigma}^2} \\ -\frac{9}{2}q_1q_2^2f^*\cosh\left(\frac{3q_2}{2}\frac{P}{\tilde{\Sigma}}\right) & 0 \\ -\frac{2\Delta\tilde{\lambda}}{(1-f)\tilde{\Sigma}} & -\frac{\Delta E^{\mathrm{v}}_{\mathrm{pl}}}{(1-f)\tilde{\Sigma}} \end{bmatrix}. \tag{A.8}$$

The term $\partial\,[\mathbf{Q}]/\partial\,[\mathbf{S_0}]$ is obtained from Eqs. (5.61) and (5.63) as

$$\frac{\partial[\mathbf{Q}]}{\partial[\mathbf{S_0}]} = \begin{bmatrix} 0 & 1 & 0 \\ \frac{\Sigma^{\mathrm{eq}}_0}{Q\left(1+6\Delta\tilde{\lambda}\frac{\mu^{(\mathrm{eff})}}{\tilde{\Sigma}}\right)^2} & 0 & \frac{q_M}{R^2}\frac{M^{\mathrm{v}}_0}{Q\left(1+\frac{2\alpha^{\mathrm{v}}q_M}{R^2\tilde{\Sigma}}\Delta\tilde{\lambda}\right)^2} \end{bmatrix}. \tag{A.9}$$

Equations (5.56) and (5.62) lead to

$$\frac{\partial[\mathbf{S_0}]}{\partial\Delta\mathrm{STRAIN}} = \begin{bmatrix} 3\mu^{(\mathrm{eff})}\frac{\underset{\sim}{\boldsymbol{\Sigma}}^{\mathrm{d}}_0}{\Sigma^{\mathrm{eq}}_0} & (K^{(\mathrm{eff})}_{\varepsilon}+q_P\beta^{\mathrm{v}})\underset{\sim}{\mathbf{I}} & 0 \\ 0 & K^{(\mathrm{eff})}_{\varepsilon}+q_P\beta^{\mathrm{v}} & 0 \\ 0 & 0 & \alpha^{\mathrm{v}}\frac{\underline{\mathbf{M}}^{\mathrm{v}}_0}{M^{\mathrm{v}}_0} \end{bmatrix} \tag{A.10}$$

and Eqs. (5.60) and (5.62) yield

$$\frac{\partial\mathrm{STRESS}}{\partial\,[\mathbf{r}]} = \begin{bmatrix} -\frac{6\frac{\mu^{(\mathrm{eff})}}{\tilde{\Sigma}}}{\left(1+6\Delta\tilde{\lambda}\frac{\mu^{(\mathrm{eff})}}{\tilde{\Sigma}}\right)^2}\underset{\sim}{\boldsymbol{\Sigma}}^{\mathrm{d}}_0 & -(K^{(\mathrm{eff})}_{\varepsilon}+q_P\beta^{\mathrm{v}})\underset{\sim}{\mathbf{I}} & \frac{6\Delta\tilde{\lambda}\frac{\mu^{(\mathrm{eff})}}{\tilde{\Sigma}^2}\frac{\partial\tilde{\Sigma}}{\partial E_{\mathrm{eq}}}}{\left(1+6\Delta\tilde{\lambda}\frac{\mu^{(\mathrm{eff})}}{\tilde{\Sigma}}\right)^2}\underset{\sim}{\boldsymbol{\Sigma}}^{\mathrm{d}}_0 \\ 0 & -(q_P\xi^{\mathrm{v}}+\beta^{\mathrm{v}}) & 0 \\ -\frac{2\frac{\alpha^{\mathrm{v}}q_M}{R^2\tilde{\Sigma}}}{\left(1+2\frac{\alpha^{\mathrm{v}}q_M}{R^2\tilde{\Sigma}}\Delta\tilde{\lambda}\right)^2}\underline{\mathbf{M}}^{\mathrm{v}}_0 & 0 & \frac{2\frac{\alpha^{\mathrm{v}}q_M}{R^2\tilde{\Sigma}^2}\frac{\partial\tilde{\Sigma}}{\partial E_{\mathrm{eq}}}}{\left(1+2\frac{\alpha^{\mathrm{v}}q_M}{R^2\tilde{\Sigma}}\Delta\tilde{\lambda}\right)^2}\underline{\mathbf{M}}^{\mathrm{v}}_0 \end{bmatrix}. \tag{A.11}$$